Final Report

# PERFORMANCE-RELATED SPECIFICATIONS OF CONCRETE BRIDGE SUPERSTRUCTURES

**FHWA/IN/JTRP-2001/8**

**Volume 2**
**High Performance Concrete**

By

Jan Olek
Principal Investigator
Professor of Civil Engineering
Aiping Lu
Graduate Research Assistant
Xiuping Feng
Post Doctoral Research Associate
Bryan Magee
Post Doctoral Research Associate

School of Civil Engineering
Purdue University

Joint Transportation Research Program
Project No. C-36-56WW
File No. 7-4-48
SPR-2325

Conducted in Cooperation with the
Indiana Department of Transportation
and the
Federal Highway Administration



Purdue University
West Lafayette, IN 47907
October 2002

**ACKNOWLEDGEMENTS**

The work described in this report was funded by the Joint Transportation Research Program at Purdue University through SPR contract 2325. The Support of Indiana Department of Transportation (INDOT) and Federal Highway Administration (FHWA) is thankfully acknowledged.

The authors would like to extend sincere thanks to Dr. Tommy Nantung from the Division of Research of INDOT for his guidance and support throughout this project. The authors would also like to thank all the members of the Study Advisory Committee, but especially Mr. Tony Zander from the Division of Materials and Test of INDOT, for helpful technical discussions and suggestions offered in the course of this project.

The efforts of Ms. Ayesha Shah, Dr. Manu Santhanam, and Mr. Amir Elsharief in editing of this report are gratefully acknowledged

INDOT Research

# TECHNICAL *Summary*

Technology Transfer and Project Implementation Information

*TRB Subject Code: 25-01 Bridge Design and Performance* *October 2002*
*Publication No.: FHWA/IN/JTRP-2001/8, SPR-2325* *Final Report*

# *Performance Related Specifications (PRS) for Concrete Bridge Superstructures- A Four Volume Report*

## Introduction

The development of Performance Related Specifications (PRS) requires the identification of key performance levels for a given structural system. The first attempt to develop a methodology for PRS can be traced to 1980 when the Federal Highway administration (FHWA) instituted a new research program category. The main two objectives of the program were:

1) To provide a more rational basis for payment reduction plans.
2) To develop additional specifications related to the performance of flexible and rigid pavement structures.

In the early and mid-1980s, the FHWA, the National Cooperative Highway Research Program (NCHRP), and the American Association of State Highway and Transportation Officials (AASHTO) began a cooperative effort searching for supporting data needed for the development of PRS. The idea was to develop performance models that would allow relating the material and construction testing parameters collected at the time of construction to the future performance of the complete project. However, it was concluded that the existing databases were inadequate to derive the needed performance models. A known example of a PRS is the one developed for Portland Cement Concrete (PCC) pavements by Eres Consultants, Inc. and the FHWA (Darter et. al., 1998) in a cooperative effort. In this study, the overall objectives of a methodology for PRS were not completely fulfilled due to the lack of adequate supporting information in the existent databases to construct accurate performance predictive models. As a result, the proposed PRS was presented only as a methodology providing a more rational basis for payment plans.

The objective of the research study was to develop the essential components of a PRS for concrete bridge superstructures for application in the state of Indiana. The work conducted in this research project is presented in four volumes. Volume 1 summarizes the work conducted on the identification of performance levels and key parameters, and the development of acceptance criteria are addressed in Volume 1. The main objective of this volume is to present a proposed methodology for a PRS for concrete bridge superstructures. Volume 2 presents the research findings dealing with development of High-Performance Concrete (HPC) for applications in the bridge structures in the state of Indiana. The objective of the study presented in Volume 2 was to identify and develop concrete mixtures with adequate performance characteristics in terms of durability for the purpose of using these characteristics in performance-related specifications. Volume 3 summarizes the work conducted to investigate the behavior of fiber reinforced polymer (FRP) reinforced concrete structures with an emphasis on bond and shear. The main objective of this volume is to provide design guidelines for the use of FRP reinforcement in bridge superstructures. Volume 4 summarizes the results of an evaluation of the bond performance of epoxy-coated bars with a coating thickness up to 18 mils.

## Findings

In this study emphasis has been placed on the development of a methodology for a Performance Related Specification, PRS, for concrete bridge superstructures. The implementation of the methodology, presented in the form of a user-friendly computer program in Volume 1 of this report, is project specific. It requires the mean and standard deviation (or definition of a probability distribution) of the input parameters for the performance predictive models. This is done for both the as-designed condition and the as-built condition of the structure. The contractor is expected to achieve certain level of compliance during the construction as dictated by the as-designed condition (which is defined based on the submitted design in compliance with agency specifications).

Based on performance predictive models, cost models, and statistical simulation, the methodology reports a relative as-built/as-designed Life-Cycle Cost (LCC). This relative LCC measures the level of compliance of the as-built structure with the design. The agency (INDOT) implementing the methodology could then consider the relative LCC in the form of a pay factor modifying the contractor's bid price. Statistical simulation is conducted to evaluate the effects of the variations in the input parameters for the performance predictive models. The differences in the LCC for the as-designed and as-built elements come from the differences in the input parameters that are under the control of the contractor (referred to as quality characteristics). The framework of the proposed methodology has been fully developed and illustrated with four numerical examples in an initial case study of a simply supported reinforced bridge deck or slab.

The research effort described in Volume 2 of this report was divided in two phases. Phase I was focused on development of concrete mixtures optimized with respect to selected performance-related parameters. During this phase, ten optimum concrete mixes have been identified from 45 mixes in terms of compressive strength, Young's modulus of elasticity, rapid chloride penetration and chloride conductivity using a statistical design procedure. Through surface response methodology, 27 statistical models were developed for each of four parameters. Based on the models developed, 81 contour maps were generated, which indicated how performance of concrete varied in response to the change of dosages of binders at constant water-binder ratio. Based on the overlaid contour maps and the threshold values chosen for the properties of concrete, optimum concrete mixtures including Portland cement and the combinations with fly ash, silica fume and slag were identified.

In Phase II of the HPC study, the ten optimum mixtures were further evaluated with respect to mechanical properties and durability characteristics. Several different tests related to the evaluation of the resistance of concrete to chloride permeability were used: rapid chloride permeability test, chloride conductivity test, test for the resistance of concrete under DC electrical field, ponding test for the determination of the resistance of concrete to chloride penetration, and rapid test for the determination of diffusion coefficient from chloride migration. Tests related to the resistance of concrete to freezing & thawing, and scaling were also investigated. Other tests such as, the determination of drying shrinkage, and test for curing effects on the properties of high performance concrete were also evaluated in this research. Special emphasis was placed on determining and quantifying these parameters that control the ingress of the chloride ions.

Based on the results generated during this research, models have been developed that allow for prediction of certain mechanical and durability-related parameters related to the mixture composition. The parameters that can be predicted include strength, rapid chloride permeability (RCP) values, and chloride diffusion coefficient. Limited validation of these models was performed using field data provided by INDOT. The strength and chloride diffusion coefficient values generated by these models can serve as an input for the life-cycle costing (LCC) model described in Vol. 1 of this report

As summarized in Volume 3, experimental investigations were performed to specifically investigate the behavior of FRP reinforced concrete structures in both bond and shear. For the bond investigation, three series of beam splice tests were performed on specimens reinforced with steel, glass FRP, and aramid FRP to determine the effect of the different types of reinforcement on bond, cracking, and deflections. The test results indicate that the use of FRP reinforcement leads to lower bond strengths and, therefore, require longer development lengths. The specimen crack widths and deflections were substantially larger for FRP specimens than steel specimens due to

the significantly lower modulus of elasticity. Analysis of the test results resulted in recommendations for modifying the empirical development length equation of ACI 318-99 design code for use with FRP reinforcement.

For the shear investigation, two series of beam tests were conducted on specimens reinforced with steel, glass FRP, and aramid FRP to determine the effect of the different types of reinforcement on the concrete shear strength. All specimens did not contain transverse reinforcement. The test results show that the use of FRP reinforcement leads to lower concrete shear strengths than steel reinforcement for equal reinforcement cross-sectional areas (longitudinal reinforcement percentages). In addition, the test results point that the shear strength is a direct function of the longitudinal reinforcement stiffness. The test results further substantiated the findings that larger crack widths and deflections are achieved by FRP specimens relative to steel specimens due to the lower modulus of elasticity. Analysis of the test results resulted in recommendations for the calculation of concrete shear strength.

The experimental work on the bond performance of epoxy-coated bars with thickness up to 18 mils summarized in Volume 4 of the final report indicates that the current AASHTO requirements for development length of epoxy-coated bars could be extended to coating thickness of up to 18 mils.

## Implementation

Based on the results from the research conducted on the framework for a PRS, it was concluded that the most practical implementation of the methodology had to consider the corrosion deterioration problem as the only distress determining/affecting the LCC of the structure. It was concluded that other distress indicators applied at "a section level" should be included in the framework of a PRS to give more integrity to the process of quality control. The needed software for the implementation of the proposed PRS has been provided to INDOT as part of this report. It must be noted that corrosion deterioration represents almost 50% of the problems of the current bridge infrastructure in Indiana.

As part of the implementation efforts for the part of the research dealing with HPC, a series of mathematical models were constructed that allow for the prediction of strength, rapid chloride permeability and chloride diffusion coefficient values based on the binder composition of the mixture.

The data generated using these models have been arranged in an Excel sheet, which allows the user to input desired minimum and maximum values of strength (at 28 days) and/or RCP values (at 56 days) and obtain binder combinations which yield/satisfy the desired input values. Binder system 1 refers to mixtures, which contain PC, SF and GGBS. Binder system 2 refers to mixtures, which contain PC, SF and FA. Binder system 3 refers to mixtures, which contain PC, GGBS and FA. The percentage increments of SF represented in the Excel worksheet are 0, 5 and 7.5 %. The percentage increments of FA and GGBS represented are 0, 20, 25 and 30 %.

The strength and chloride diffusion coefficient values determined for the 10 concrete mixtures tested in Phase II of the study were also used as input values for the LCC model described in Vol. 1 of this report. The LCC model was run for a single, simply supported span. The same type of data was also obtained form three existing Indiana bridges and the LCC model was re-run for these structures. The results indicate that LCC for all laboratory mixtures was lower than the LCC for standard INDOT class C concrete mixture. Furthermore, the LCC of the actual field mixtures was slightly higher than the LCC of standard class C mixture.

Currently, the ability of the models developed as a part of the HPC study to predict the actual properties of a field concrete is being validated on several QC/QA bridge jobs and a supplementary report summarizing the results of these evaluations is expected by June 2003.

Based on the research conducted on the use of FRP reinforcement, design and construction recommendations are provided that can be used in the design and construction of FRP reinforced bridge decks. These recommendations will be implemented in a JTRP study "Implementation of a Non-Metallic Reinforced Bridge Deck." This study will evaluate the design and construction recommendations in a prototype laboratory deck specimen as well as through a pilot field study that incorporates nonmetallic reinforcement in a bridge deck.

No change of the bond specifications is required to implement the use of up to #8 diameter deformed bars with epoxy-coating thickness up to 18 mils.

## Contact

*For more information*:

**Prof. Julio A. Ramirez**
Principal Investigator
School of Civil Engineering
Purdue University
West Lafayette IN 47907
Phone: (765) 494-2716
Fax: (765) 496-1105

**Prof. Jan Olek**
Co-Principal Investigator
School of Civil Engineering
Purdue University
West Lafayette IN 47907
Phone: (765) 494-5015

**Prof. Robert J. Frosch**
Co-Principal Investigator
School of Civil Engineering
Purdue University
West Lafayette IN 47907
Phone: (765) 494-5904

Division of Research
1205 Montgomery Street
P.O. Box 2279
West Lafayette, IN 47906
Phone: (765) 463-1521
Fax: (765) 497-1665

**Purdue University**
Joint Transportation Research Program
School of Civil Engineering
West Lafayette, IN 47907-1284
Phone: (765) 494-9310
Fax: (765) 496-1105

**Indiana Department of Transportation**

TECHNICAL REPORT STANDARD TITLE PAGE

| 1. Report No. | 2. Government Accession No. | 3. Recipient's Catalog No. |
|---|---|---|
| FHWA/IN/JTRP-2001/8 | | |

| 4. Title and Subtitle | 5. Report Date |
|---|---|
| Performance Related Specifications for Concrete Bridge Superstructures<br>*Volume 2: High Performance Concrete* | October 2002 |
| | 6. Performing Organization Code |

| 7. Author(s) | 8. Performing Organization Report No. |
|---|---|
| J. Olek, A. Lu, X. Feng, and B. Magee | FHWA/IN/JTRP-2001/8 |

| 9. Performing Organization Name and Address | 10. Work Unit No. |
|---|---|
| Joint Transportation Research Program<br>1284 Civil Engineering Building<br>Purdue University<br>West Lafayette, Indiana 47907-1284 | |
| | 11. Contract or Grant No.<br>SPR-2325 |

| 12. Sponsoring Agency Name and Address | 13. Type of Report and Period Covered |
|---|---|
| Indiana Department of Transportation<br>State Office Building<br>100 North Senate Avenue<br>Indianapolis, IN 46204 | Final Report |
| | 14. Sponsoring Agency Code |

**15. Supplementary Notes**

Prepared in cooperation with the Indiana Department of Transportation and Federal Highway Administration.

**16. Abstract**

This is Volume 2 of the Final Report for the project titled "Performance-Related Specifications for Concrete-Bridge Superstructures" dealing with the topic of High-Performance Concrete (HPC). The investigation of high-performance concrete included the development of optimized concrete mixtures and identifying their performance characteristics related to durability for the purpose of using these characteristics in performance–related specifications in the state of Indiana.

The research effort described in this report was divided in two phases. Phase I was focused on development of concrete mixtures optimized with respect to selected performance-related parameters. During this phase, ten optimum concrete mixes have been identified from 45 mixes in terms of compressive strength, Young's modulus of elasticity, rapid chloride penetration and chloride conductivity using a statistical design procedure. Through surface response methodology, 27 statistical models were developed for each of four parameters. Based on the models developed, 81 contour maps were generated, which indicated how performance of concrete varied in response to the change of dosages of binders at constant water-binder ratio. Based on the overlaid contour maps and the threshold values chosen for the properties of concrete, optimum concrete mixtures including Portland cement and the combinations with fly ash, silica fume and slag were identified.

In Phase II of this study, the ten optimum mixtures were further evaluated with respect to mechanical properties and durability characteristics. Several different tests related to the evaluation of the resistance of concrete to chloride permeability were used: rapid chloride permeability test, chloride conductivity test, test for the resistance of concrete under DC electrical field, ponding test for the determination of the resistance of concrete to chloride penetration, and rapid test for the determination of diffusion coefficient from chloride migration. Tests related to the resistance of concrete to freezing & thawing, and scaling were also investigated. Other tests such as, the determination of drying shrinkage, and test for curing effects on the properties of high performance concrete were also evaluated in this research. Special emphasis was placed on determining and quantifying these parameters that control the ingress of the chloride ions.

Based on the results generated during this research, models have been developed that allow for prediction of certain mechanical and durability-related parameters related to the mixture composition. The parameters that can be predicted include strength, rapid chloride permeability (RCP) values, and chloride diffusion coefficient. Limited validation of these models was performed using field data provided by INDOT. The strength and chloride diffusion coefficient values generated by these models can serve as an input for the life-cycle costing (LCC) model described in Vol. 1 of this report.

| 17. Key Words | 18. Distribution Statement |
|---|---|
| High-performance concrete, chloride diffusion coefficient, supplementary cementitious materials, binary and ternary cementitious systems, shrinkage, rapid chloride permeability, conductivity, chloride migration test, freezing-thawing resistance, absorption, chloride concentration. | No restrictions. This document is available to the public through the National Technical Information Service, Springfield, VA 22161 |

| 19. Security Classif. (of this report) | 20. Security Classif. (of this page) | 21. No. of Pages | 22. Price |
|---|---|---|---|
| Unclassified | Unclassified | 192 | |

Form DOT F 1700.7 (8-69)

**TABLE OF CONTENTS**

**LIST OF TABLES**

**LIST OF FIGURES**

# 1 INTRODUCTION

High performance concrete (HPC) is generally defined [Russell, 1999] as "concrete meeting special combination of performance and uniformity requirements that cannot always be achieved routinely using conventional constituents and normal mixing, placing and curing practices".

In the commentary to the above definition, Russell further states that "high performance concrete is a concrete in which certain specific characteristics are developed for a particular application or environment". He also lists examples of specific performance characteristics that include:

- Ease of placement
- Compaction without segregation
- Early age strength
- Long term mechanical properties
- Permeability
- Density
- Heat of hydration
- Toughness
- Volume stability
- Long service life in severe environments

As implied by the above definition, the required performance characteristics of HPC could be quite diverse and could strongly depend on the specific service environment. In addition, many of these performance characteristics are interrelated and a change in one of them usually results in changes in one or more of the other. As a result, if several characteristics are taken into account when producing concrete for the intended application, each of these characteristics must be clearly specified in the contract documents [Russell, 1999].

For many years, high-performance concrete has been synonymous with high strength concrete, and was mostly specified and used in columns of high-rise buildings. Lately, however, the Federal Highway Administration (FWHA), in cooperation with state highway departments, started promoting the application of HPC in bridges in order to improve economy of construction and long-term performance. In such applications, in addition to strength, durability also becomes an important parameter that needs to be specified [Russell 1997].

## 1.1 Problem Statement

In general, specifying certain material characteristics and mix composition limits that are needed for desired durability is not easy and in most cases the concrete industry was not very successful in their attempts to do so [Priest, 1995]. This is mostly due to the fact that no single parameter uniquely defines durability and, as already mentioned, change in one parameter often leads to change in other property of the material. For example, specifying water to cement ratio does not always ensure the same quality of cement paste as more than 100 types and classes of cements are now available, each with its unique properties. Similarly, specifying requirements for air content in fresh concrete does not necessarily result in a hardened concrete that is resistant to freeze/thaw action as the size and distribution of the air voids plays an import role in protecting the concrete. In addition, no widely accepted criterions currently exist for specifying when the design life of a structure has been exceeded and how it is to be measured.

Recently, a more generalized approach to defining and specifying high-performance concrete seems to have been accepted by the engineering community. This approach is based on concrete achieving certain performance characteristics that are desirable for a given application rather than specifying the material and mix composition limits [Goodspeed et al., 1996].

Against this background, Indiana Department of Transportation, in collaboration with Purdue University, has initiated this research study to develop performance-related specifications focusing on concrete bridge superstructures in Indiana [Ramirez et al., 1998]. One part of this research program (Task 3.2.1) involves

development of HPC for use in construction of Indiana bridges designed and built using performance-related specification.

### 1.2 Objectives and Scope of the Work in Task 3.2.1

The objectives of the research activities undertaken in this Task are as follows:

- To identify performance characteristics of high performance concrete mixtures related to durability and service life of hardened concrete;
- To develop proportioning methods of high performance concrete for desired performance;
- To identify the optimum mixtures in terms of key performance characteristics identified in the above step;
- To evaluate the mechanical properties and long term durability performance of the optimum mixtures;
- *To evaluate the effects of different curing methods on performance of HPC, and identify the curing method for achieving the desired performance;
- To evaluate a possible testing regime which can be used for quality assurance purposes at the work site;
- To develop guidelines for material selection, mixing procedure, sampling, consolidation, and testing to achieve the desired performance;

*The focus of the curing task is on determination of the cracking tendency of selected mixtures using the AASHTO PP 34 test method (restraining ring test). In addition, the influence of curing conditions on rapid chloride permeability and drying shrinkage of concrete is also evaluated. It is expected that the minimum moist curing time in the moist room needed to ensure the desired properties would be established for selected mixtures.

The flowchart that summarizes the entire test plan for Task 3.2.1 is shown in Figure 1.1. As indicated in this Figure, the experimental plan for this research task has been divided into two Phases. The focus of Phase I is on identification of mixes with optimum binder combinations in terms of selected performance characteristics. The focus of Phase II is on evaluation of mechanical properties and durability parameters related to long-term performance of optimized concrete mixtures identified in Phase I. Durability parameters evaluated during Phase II will include freezing and thawing resistance, scaling resistance, resistance to chloride ion penetration, and determination of the coefficient of diffusion. In addition, the influence of curing conditions on durability of HPC will also be evaluated.

This report presents the results obtained in Phase I of the research and provides detailed plans for experiments to be conducted in Phase II.

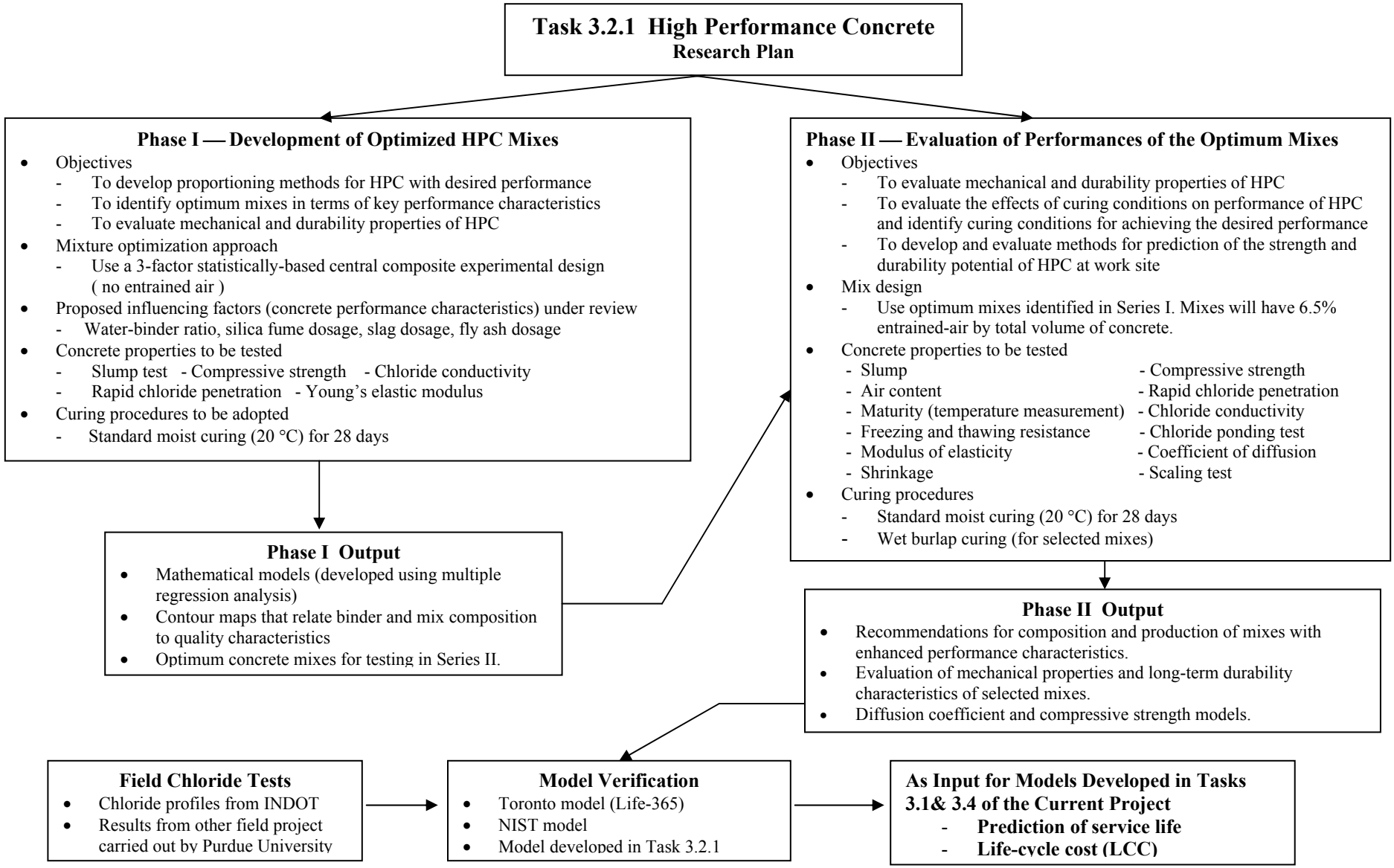


Figure 1.1: Flowchart of the Test Plan for Task 3.2.1- High Performance Concrete

## 2. LITERATURE REVIEW

### 2.1 Introduction

At present, the durability of concrete is controlled almost exclusively by specifying certain requirements for concrete composition, properties and composition of concrete constituents, casting and compaction procedures, curing and sometimes compressive strength. This approach frequently yields unsatisfactory results, and it is a common objective of concrete researchers and engineers to develop performance criteria that would allow more reliable estimates of the potential durability of a given concrete mix and of the probable durability of a concrete structure [Hilsdorf, 1989].

Indeed, it has been suggested [Priest, 1995] that the concrete industry has, for years, been unhappy with the way that durability is specified to give intended performance. For example:

- Limiting water - cement ratio does not give a measure of concrete durability because more than 100 types and classes of cements are now available with various material characteristics.

- Specifying air entrainment in fresh concrete as a quantity of air by volume of concrete does not necessarily result in a hardened concrete that is resistant to freeze-thaw action as it is the size and distribution of the air voids that are the governing factors.

- There is currently no criterion specifying when the notional design life of a structure has been exceeded and how it is measured.

For these reasons, the concrete industry must look into ways of overcoming these problems by moving away from specifying materials and mix limitations to specifying performance, thereby leaving the producer to decide how performance is achieved [Priest, 1995]. It is proposed that this will lead to clients receiving the performance levels they intended, effective use of available resources and durable, cost effective concrete [Priest, 1995].

Against this background, Indiana Department of Transportation, in collaboration with Purdue University, has initiated the current research study to conduct the core work necessary to develop performance-related specifications for concrete bridge superstructures. The purpose of this section of the document is to provide a state-of-the-art review of existing materials-related literature pertaining to the scope of the overall research project. Reviewed in detail is the potential of using high performance concrete and potential test methods for inclusion in PRS. Based on this review of the literature, potential routes for developing material-related PRS for Indiana's bridge superstructures are proposed.

### 2.2 Objectives

The objectives of this section of the document are as follows.

- To discuss the potential use of high-performance concrete as a route to complying with performance-related specifications

- To review performance testing methods

- To propose, based on the literature review carried out, potential routes for the development of a performance-related specification suitable for the design of concrete bridge superstructures in Indiana

## 2.3 Proportioning Concrete to Meet Requirements Specified in PRS

The overall focus of the current research project is to develop original specifications that are capable of producing concrete bridge superstructures with improved performance. In order to comply with the stipulations of such specifications, the adoption of novel construction materials is likely to be mandatory. For this reason, an evaluation of new materials such as high-performance concrete, glass and carbon fiber reinforced polymers and steel bars with thicker epoxy-coatings is central to the success of the project. Of immediate relevance to the current document is high-performance concrete (HPC). It has been stated [Ramirez et al., 1998] that as highway agencies across the country continue to expand the process of development and implementation of PRS, there is a growing need for additional refinements in both design methods and construction practices associated with the use of HPC in bridges.

### 2.3.1 Definition of High-Performance Concrete

It should be realized at the outset that considerable controversy exists concerning the definition of HPC. In the proposal document for the current project [Ramirez et al., 1998], high-performance concrete was defined as concrete meeting special performance provisions that cannot always be achieved using conventional methods and normal mixing, placing and curing procedures. This definition implies that required performance provisions may vary, depending on the nature of structure in question. For instance, provisions for given concrete may be given in terms of mechanical properties, durability properties, or a combination of these. Concrete will be considered 'high-performance', therefore, providing that the concrete used meets the required performance provisions.

In many cases, however, concrete is classified as having 'high-performance' exclusively because its strength is much greater than that of typically specified concrete. High-strength concrete is usually achieved by using very low water - binder ratios (w/b). Indeed, in a recent publication [Aitcin, 1998] the author defined HPC as essentially all concrete having a low water - binder ratio (i.e., $\leq 0.40$). Only in more recent times has recognition been given to the fact that 'high-strength' concrete commonly offers other improvements in performance, such as higher flowability, higher elastic modulus, higher flexural strength, lower permeability, improved abrasion resistance and better durability [Aitcin, 1998]. In spite of this, the term HPC continues to be used primarily for concrete suitable for high-strength applications.

Obtaining very high values of concrete strength is not likely to be the principal design criteria for concrete bridge superstructures in Indiana. For this reason, the term high-performance concrete in this document is used to define concrete meeting any special performance provisions. Special provisions relevant to the current project are likely to include various durability-related concrete properties.

### 2.3.2 Typical Properties of High-Performance Concrete

It has been reported that some engineers are reluctant to implement HPC in bridge construction, mainly due to a lack of understanding for the material and a lack of sufficient data related to performance issues. In addition, higher initial bid prices (to be expected with the use of any new technology) and higher quality assurance demands are common drawbacks linked to the use of HPC. Although it is impossible to characterize the absolute performance of HPC (as many types of HPC exist, through the use of many different materials, etc.), the following sections summarize the typical performance of HPC in a more general manner and review some of the special provisions required.

<u>Mixture Proportions</u>
It has been reported [Neville, 1995] that high-performance concrete generally contains the following ingredients:

- common, albeit good quality aggregate
- ordinary, or rapid hardening Portland cement at a very high content (i.e., 450 to 550 kg/m$^3$)
- silica fume, generally at a dosage of 5 to 15 % by mass of the total binder content
- sometimes, other cementitious replacement materials such as fly ash, or ground granulated slag
- superplasticizer, at high dosages of 5 to 15 litres / m$^3$ of concrete
- sometimes other admixtures

- the use of a low water - binder ratio (i.e., always below 0.35)

A more detailed review of mixture proportions used for numerous high-performance concretes in research and construction projects to date is given below in section 3.4.

Construction practices

Great care is generally required when placing and finishing high-performance concrete, and in many cases conventional construction methods may not be suitable [Aitcin, 1998]. In spite of the usually high slump of such concrete, it still must be internally or externally vibrated to facilitate placement and performance. In flat slabs, vibrators should not be used to displace the concrete into place. Generally, high-performance concrete should not be over-vibrated to avoid segregation and local bleeding. With regard to finishing techniques, the use of vibrating screeds immediately followed by troweling has produced excellent results [Blais et al., 1996].

Curing provisions

Some controversy exists over curing requirements of high-performance concrete. It has been stated that if water curing is essential to usual concrete, then it is crucial to high-performance concrete [Aitcin, 1998]. However, owing to its very dense microstructure, others are of the opinion that HPC does not need any curing at all. In order to eliminate autogenous shrinkage, it is advised that water curing should be applied to HPC as soon as its temperature begins to rise [Aitcin, 1998]. To avoid plastic shrinkage of HPC, temporary-curing membranes, mist fogging or ponding should be applied as soon as it has been finished. It is additionally reported that at least 7-days of continued moist curing is essential to drastically reduce HPC shrinkage [Aitcin, 1998].

Mechanical properties

In order to be classified as high-performance it has been stated that concrete should possess a certain level of dimensional stability [Mehta and Aitcin, 1990]. A high elastic modulus (i.e., 40 to 45 GPa), low drying shrinkage and creep (i.e., less than 0.04 % at 90-days), and low thermal strain are some of the key factors contributing to high-dimensional stability. These properties are essential for counteracting any undesirable stress effects produced as a result of volume changes under conditions of restraint. Although high strength is not necessary criterion for high-performance concrete, many high-performance mixes do exhibit superior strength development [Roy et al., 1998]. Neville [1995] defines high-performance, in terms of strength, as compressive strength in excess of 80 MPa, although values of around 60 MPa are often used.

Durability properties

One of the typical main features of high-performance concrete is its very low penetrability, resulting from a usually dense structure of the hydrated cement paste. HPC has been shown to provide high levels of resistance to durability phenomena such as chloride attack, alkali-silica reaction, freezing and thawing, and abrasion [Neville, 1995]. With regard to the chloride-ion permeability test (AASHTO 227 [1990] test), concrete mixtures resulting in a current flow of 500 Coulombs or less in a 6-hour period have been classified as being virtually impermeable and, therefore, high-performance concrete [Mehta and Aitcin, 1990].

### 2.3.3 Review of Existing Proportioning Methods for HPC

A potential drawback to the use of high-performance concrete in Indiana may be the lack of an established mixture proportioning method. Against this background, a review of the literature was undertaken to identify any existing proportioning methods for high-performance concrete that may be applicable to the current project. No established design methods capable of proportioning HPC for desired levels of durability performance were found in the literature.

Due to the inconsistency of HPC definition (see section 3.1 above), the majority of existing methods [e.g., ACI Committee 363, 1984, Mehta and Aitcin, 1990, Gutierrez and Canovas, 1996, Aitcin, 1998] for HPC have been developed exclusively to proportion concrete achieving high levels of compressive strength. To illustrate the general format of these proportioning methods, a summary of the main stages included in each is given in Table 2.1. Each model requires an initial input in the form of a required value of compressive strength, at a given age. Although each method summarized in Table 2.1 uses varying approaches and assumptions, intermediate design

steps include the selection of (i) workability levels, (ii) binder contents, (iii) binder combinations, (iv) water contents, (v) aggregate contents, (vi) aggregate combinations and (vii) admixture dosages. The outputs from these HPC proportioning methods are mixture quantities likely to provide the required level of strength development.

As in the case of conventional mix design methods, HPC methodologies give initial proportions for trial mix purposes only. Particular adjustments for individual material characteristics and qualities are required thereafter.

Three HPC proportioning methods making reference to durability performance were located in the literature. A computerized method exists which, after receiving inputs such as material properties, performance requirements etc., designs complete mixture proportions for required levels of strength, workability and durability [Dehuai et al., 1997]. Durability is specified in terms of severity of exposure and is controlled by selecting an appropriate water / binder ratio at the outset. It is stated by Denhuai et al., [1997], that permeability of concrete is the most predominant factor influencing durability, and that the use of a low water / binder ratio is essential for improving this.

A recent research study examining the use of HPC for bridge decks in New York State [Bajorski et al., 1996], focused on proportioning binder combinations for optimum durability performance. However, a methodology for arriving at complete concrete mixture proportions is not included. Durability-related properties tested included chloride permeability, plastic-shrinkage cracking and spalling. With respect to chloride permeability, contour maps were developed so that concrete may be proportioned for various performance levels. Optimum chloride permeability is achieved by selecting appropriate ternary combinations of binder materials. An abridged example of a contour map for concrete containing Portland cement, silica fume (both at varying quantities) and fly ash at a constant dosage of 30 % by mass of total binder, is given in Figure 2.1. Using a limited number of experimental mixes these contour maps were fully developed using statistical modeling. The model best suited to the data was as follows:

$$\begin{aligned}\text{Permeability (Coulombs)} = {} & 1970 + 204(Tot - 223)(FA - 1386)(SF) + 736(SF)^2 + 330(SF)^3 - 174(SF)^4 \\ & - 187(Tot)(FA) + 466(Tot)(SF) + 140(FA)(SF) - 457(Tot)(SF)^2 + \beta \quad \text{.....(2.1)}\end{aligned}$$

where,

| | | |
|---|---|---|
| *Tot* | = | [mass of binder materials (kg/m$^3$) – 660] ÷ 30 |
| *FA* | = | [fly ash content (%) – 20] ÷ 5 |
| *SF* | = | [silica fume content (%) -10] ÷ 2 |
| β | = | random error with the normal distribution |

The main purpose of using this model was not to provide exact predictions of concrete performance with respect to chloride permeability, but rather to give a smooth description of the experimental data. Clearly, however, the methodology used could easily be included into a more conventional mixture proportioning method.

The work carried out by Roy et al., [1998] similarly does not provide a methodology for arriving at complete concrete mixture proportions, but instead focuses on achieving improved durability performance by optimizing particle packing. The use of ternary packing diagrams is proposed in order to proportion binder and aggregate combinations for HPC in such a way as to improve long-term durability.

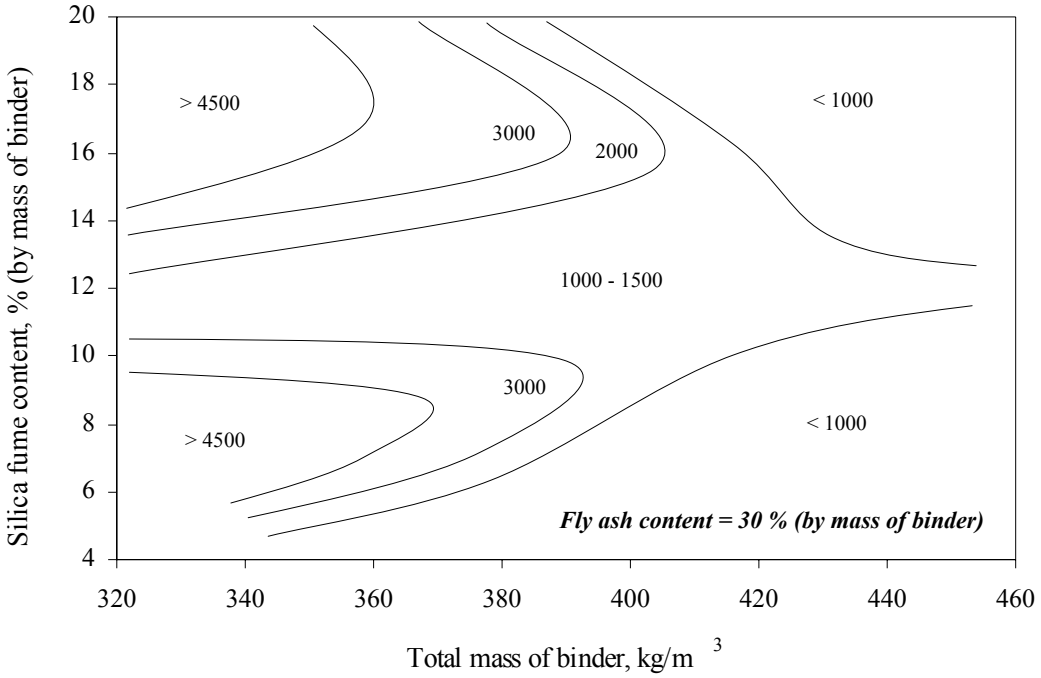


Figure 2.1: Contour Map of Chloride Permeability (Coulombs) For HPC [Bajorski et al., 1996]

Table 2.1: Main Steps Included in Selected HPC Mixture Proportioning Methods (Principal Design Criterion is Strength Development)

| STEP | DESIGN STEPS INCLUDED IN LITERATURE REFERENCE; | | | |
|---|---|---|---|---|
| | [Aitcin, 1998] | [Mehta and Aitcin, 1990] | [ACI Committee 363, 1984] | [Gutierrez and Canovas, 1996] |
| *INPUT* | *Strength requirement (40-160 MPa)* | *Strength requirement (60-120 MPa)* | *Strength requirement (≤ 85 MPa)* | *Strength requirement (60-110 MPa)* |
| 1 | • Select w/b ratio (based on established w/b ratio versus strength curve) | • Select water content (based on MSA in range 12-19 mm and use of superplasticizer) | • Select slump requirement (limits: 20-50 mm, before superplasticizer addition) | • Select w/b ratio (based on curves provided for specific binder combinations) |
| 2 | • Select water content (based on saturation point of superplasticizer) | • Calculate volume fractions of cement paste components (based on fixed binder combinations and assumption that volume of total binder paste is 0.35 $m^3$) | • Select maximum size of coarse aggregate (MSA) (limits: 19-25 mm) | • Select water content (based on binder combination, aggregate absorption and superplasticizer type/dosage) |
| 3 | • Calculate binder content | • Estimate aggregate contents (based on assumption that total aggregate volume is 0.65 $m^3$ and the volumetric ratio between fine and coarse aggregate is 2:3) | • Select coarse aggregate content (based on MSA) | • Calculate binder content |
| 4 | • Select superplasticizer dosage (based on dosage at saturation point) | • Calculate batch weights (based on specific gravity of each material) | • Estimate free water and air contents (based on MSA) | • Calculate aggregate proportions (based on established gradation curves) |
| 5 | • Select coarse aggregate content (based on aggregate shape) | • Select superplasticizer dosage (based on trial mixing) | • Select w/b ratio from table (based on MSA and required strength value) | |
| 6 | • Select desired air content | • Calculate moisture correction (based on moisture content of aggregates and superplasticizer) | • Calculate binder content | |
| 7 | | | • Calculate fine aggregate content | |
| *OUTPUT* | ***Mixture proportions that will produce concrete with a desired level of compressive strength at a given age*** | | | |
| 8 | • Trial mixing stage | • Trial mixing stage | • Trial mixing stages using cement and then replacement materials | • Trial mixing stage |

### 2.3.4 Review of Materials/Material Combinations Used for HPC

It has been stated that high-performance concrete is not a revolutionary material, nor does it contain ingredients that are not used in the concrete industry to date [Neville, 1995]. However, owing to the lack of both a universally accepted definition of the material, and information regarding proportioning methods, particularly with respect to durability, HPC continues to be something of an enigma. For this reason, the intention of the work carried in this section is to demystify HPC, by examining typical constituent materials used and performance levels achieved.

An extensive review of the literature was carried out [see references denoted by +], concentrating solely on construction or research projects claiming to utilize HPC. By extracting the relevant information available in each literature source, a database of 254 high-performance concrete mixes was compiled. Data collected in each instance included the mixture proportions used and any performance level achieved. The range of data properties that were collected from the literature are as listed below:

- Water - binder ratio
- Total binder content
- Portland cement content
- Fly ash content
- Silica fume content
- GGBS content
- Water content
- Aggregate contents
- Admixture dosages
- Workability level
- Air content
- Strength development
- Modulus of elasticity
- Coefficient of diffusion
- Chloride permeability

It should be realized that not all of these properties were reported for every high-performance concrete mix found in the literature.

Constituent material contents used for HPC

From the database of 254 HPC mixes developed, histograms summarizing frequently used quantities of constituent materials have been produced, see Figure 2.2. Illustrated in Figures 2.2(a)-(d) are the most commonly used water, total binder, air, fine and coarse aggregate contents for HPC, respectively. Included in Figure 2.2(f) is a histogram detailing water - binder ratios most frequently used.

Given below is a summary of data reported in Figure 2.2. For each of the main constituent materials (and water - binder ratio), the content range most frequently used for HPC is given. In addition, the overall range of contents used and a mean value is given for each material.

| | *Most common range* | *Overall range* | *Mean* | *See Figure* |
|---|---|---|---|---|
| • Water, kg/m$^3$ | 150 – 175 | 56 – 221 | 144 | 4 (a) |
| • Total binder, kg/m$^3$ | 350 – 400 | 222 – 675 | 443 | 4 (b) |
| • Air (entrapped / entrained), % | 1 – 2 / 5 – 6 | 0.8 – 9.8 | 4.0 | 4 (c) |
| • Fine aggregate, kg/m$^3$ | 700 – 800 | 318 – 1205 | 720 | 4 (d) |
| • Coarse aggregate, kg/m$^3$ | 1000 – 1100 | 561 – 1608 | 1081 | 4 (e) |
| • Water-binder ratio | 0.35 – 0.40 | 0.19 – 0.70 | 0.34 | 4 (f) |

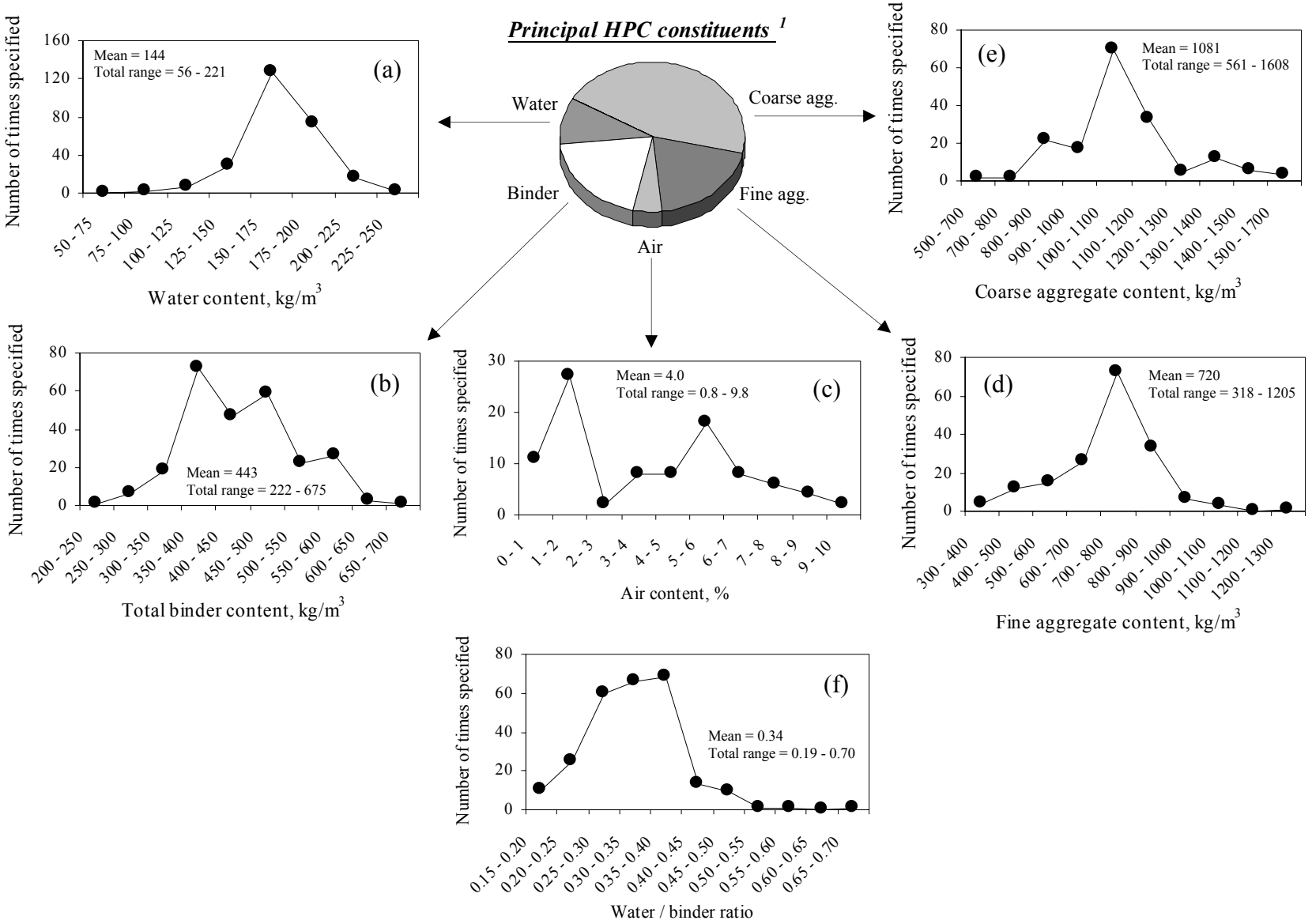


Figure 2.2: Summary of Material Quantities (and w-b Ratios) Most Frequently Used for HPC (Information Taken from Database of 254 Mixes)
1. Chemical Admixtures Not Included in Figure for Clarity

Clearly, water - binder ratios used for HPC (typically in the range 0.35 – 0.40) are much lower than those used for conventional concrete, with values as low as 0.19 specified. In order to achieve this, relatively high total binder contents and low water contents are used. In the case of air content, it can be seen from Figure 2.2(c) that the curve contains two peaks. It is likely that the 1-2 % air content peak corresponds to concrete prepared without the use of air-entraining admixtures (i.e., entrapped air measured only). On the other hand, the 5-6 % air content peak is likely to correspond to concrete inclusive of air-entraining admixture (i.e., entrapped and entrained air contents measured).

Information regarding chemical admixture types and quantities typically used for HPC has not been included in Figure 2.2. These have been omitted both for clarity and due to fact that dosage nomenclature varied widely in the literature. Chemical admixtures most frequently used for HPC include (i) air entraining admixtures, (ii) retarding admixtures, (iii) water-reducing admixtures and (iv) superplasticizing admixtures. Superplasticizers are by far the most frequently used group of admixtures for HPC, with dosages specified for more than 50 % of the mixes located in the current review of the literature. Dosages of superplasticizer were typically high, ranging from around 5 to 15 litres / $m^3$ of concrete.

Binder materials used for HPC

As illustrated in Figure 2.3, four binder materials have been utilized in the production of high-performance concrete; namely, Portland cement (PC), silica fume (SF), fly ash (FA) and ground granulated-blastfurnace slag (GGBS). Of the HPC mixes reviewed, silica fume was the most common Portland cement replacement material, being incorporated in 69 % of all mixes (see Figure 2.3(a)). In comparison, fly ash and GGBS were used in 24 and 12 % of all HPC mixes, respectively.

Using the four binder materials listed above, six different binder combinations have been used for HPC as shown in Figure 2.3(b). These binder combinations are additionally listed below, given in descending order with respect to the percentage of mixes, from the 254 considered, using each combination.

- PC/SF: 46 %
- PC/SF/FA: 17 %
- PC only: 15 %
- PC/FA: 8 %
- PC/SF/GGBS: 7 %
- PC/GGBS: 7 %

Being used for 46 % of all mixes, clearly PC/SF binder combinations are by far the most commonly used for HPC. Silica fume has also been used in ternary blends with both PC/FA and PC/GGBS combinations. These ternary combinations have been used for 17 and 7 % of the reviewed HPC mixes, respectively. Silica fume is most likely used for its beneficial influence on strength development, particularly at early ages, and durability performance. PC only, PC/FA and PC/GGBS binder combinations account for remaining 15, 8 and 7 % of HPC mixes, respectively.

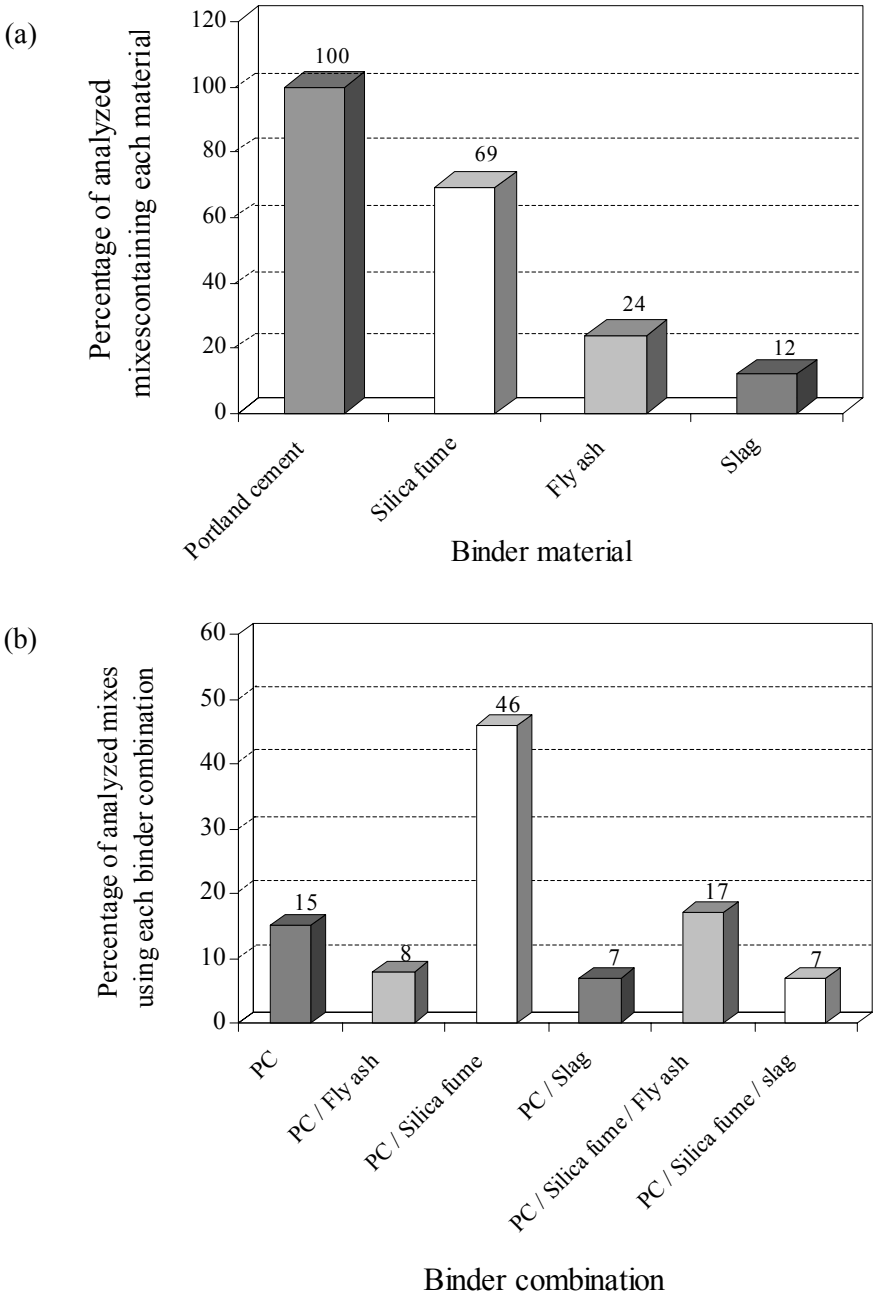


Figure 2.3: Frequency of (a) Binder Material Use, and (b) Binder Combination Use for HPC (Information Taken from Database of 254 Mixes)

Binder material contents used for HPC

Histograms detailing binder material contents used for HPC have been produced, as shown in Figure 2.4. Shown in Figures 2.4(a)-(d) are the most commonly used contents of Portland cement, silica fume, GGBS and fly ash for HPC, respectively.

A summary of data reported in Figure 2.4 is given below, which includes the content range most frequently used for each binder material. In addition, the overall range of contents used and a mean value is given for each binder material.

| | *Most common range* | *Overall range* | *Mean* | *See Figure* |
|---|---|---|---|---|
| • Portland cement, kg/m$^3$ | 400 – 500 | 81 – 600 | 376 | 6 (a) |
| • Silica fume, kg/m$^3$ | 25 – 50 | 9 – 175 | 42 | 6 (b) |
| • GGBS, kg/m$^3$ | 50 – 75 | 10 – 325 | 150 | 6 (c) |
| • Fly ash, kg/m$^3$ | 150 – 200 | 9 – 215 | 80 | 6 (d) |

Due to the use of relatively low water - binder ratios, individual binder contents typical for HPC are somewhat higher than in conventional mixes. For example, Portland cement contents used for conventional concrete are typically in the range of 250 – 400 kg/m$^3$ [Neville, 1995].

Properties of HPC reported in the literature

Only a limited number of concrete properties have been reported in the literature for HPC. As shown in Figure 2.5, properties available for inclusion in the current database include workability measurement, air content, 28-day strength, modulus of elasticity, chloride permeability and coefficient of diffusion. The intention of Figure 2.5 is to provide an indication of how frequently each of these concrete properties was available in the literature. Each property is listed below, given in descending order with respect to the percentage of mixes, from the 254 considered, for which each property was reported.

- 28-day strength: 89 %
- Slump: 51 %
- Air content: 37 %
- Chloride permeability: 33 %
- Elastic modulus: 10 %
- Vebe time: 9 %
- Coefficient of diffusion: 4 %

Perhaps not surprisingly, compressive strength was the most frequently reported property of HPC, with 89 % of reviewed mixes having a result reported. Workability, in terms of slump, and air content were the next most frequently reported HPC properties. Encouragingly, 33 % of mixes had durability performance attached in the form of chloride permeability. Despite being the least commonly reported HPC property, coefficients of diffusion were available for a further 4 % of mixes. Elastic modulus results and Vebe times were additionally reported for 10 and 9 % of HPC mixes, respectively.

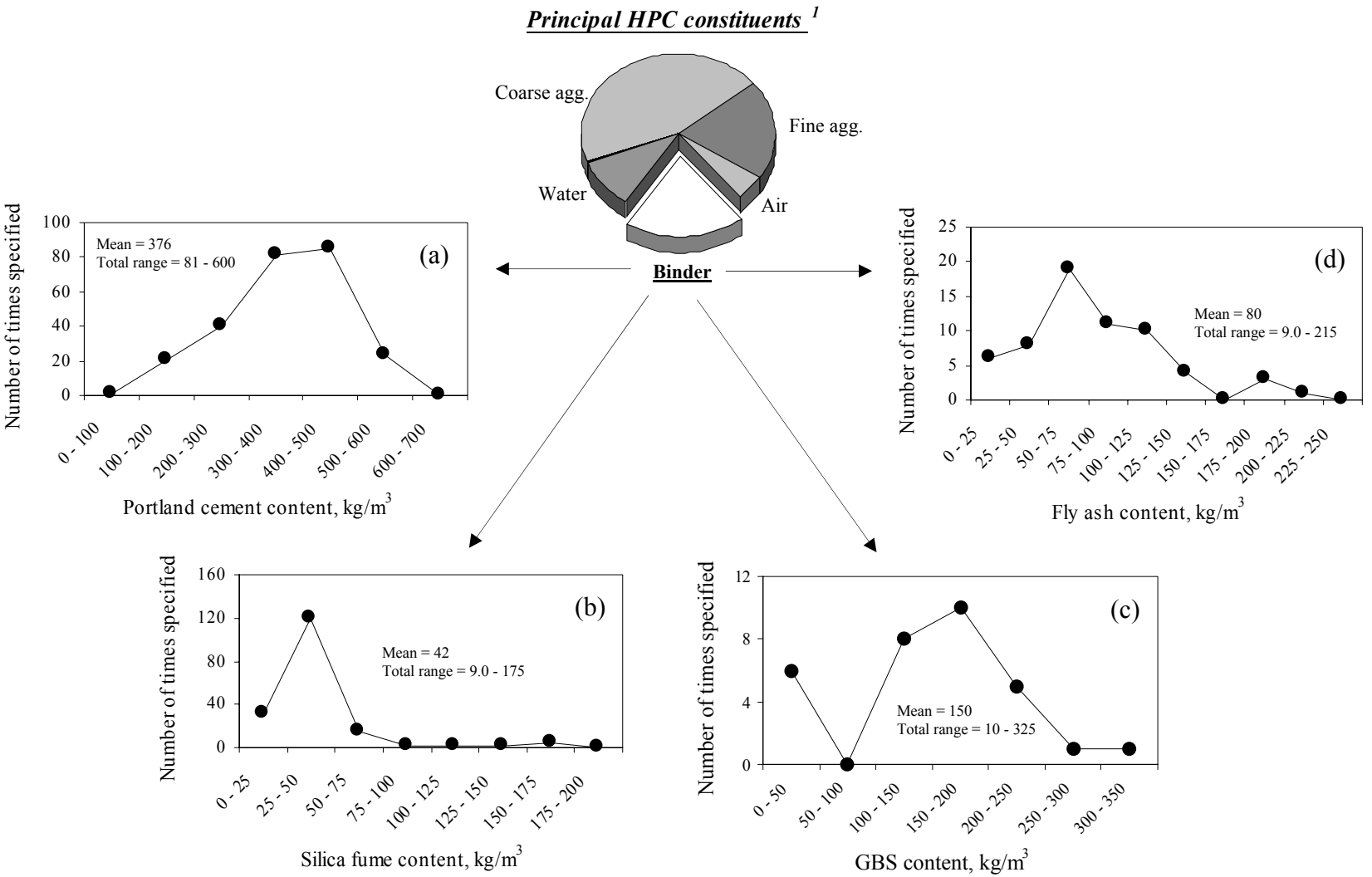


Figure 2.4: Summary of Binder Material Quantities Most Frequently Used for HPC (Information Taken from Database of 254 Mixes)
1. Chemical Admixtures Not Included In Figure for Clarity

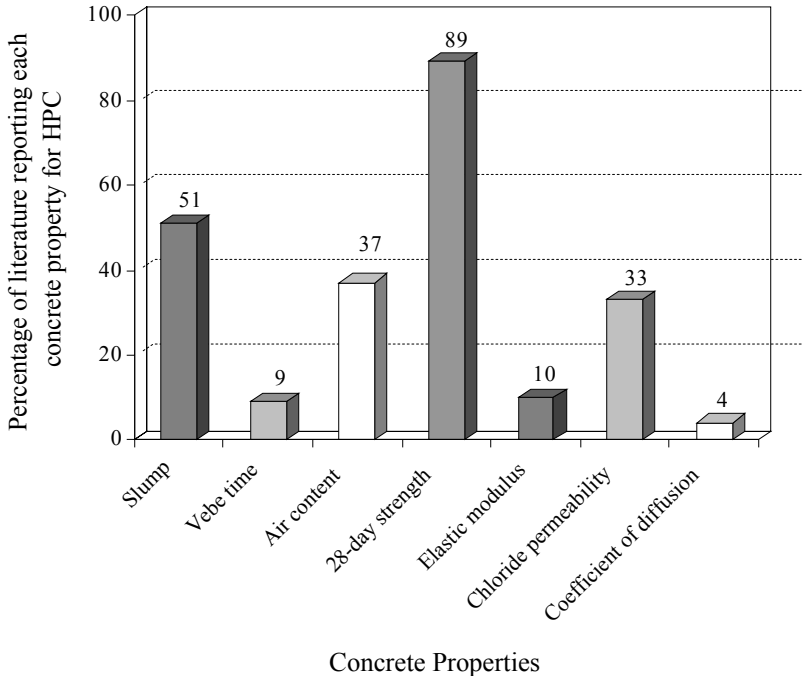


Figure 2.5: Frequency of Concrete Properties being Reported in the Literature for HPC
(Information Taken from Database of 254 Mixes)

HPC performance

Histograms were prepared to highlight the typical performance of HPC, see Figure 2.6. Shown in Figures 2.6(a)-(d) are the most commonly achieved HPC values of slump, Vebe time, 28-day strength, modulus of elasticity, chloride permeability and coefficient of diffusion, respectively.

A summary of data reported in Figure 2.6 is included in the text below, which includes the performance levels most frequently achieved by HPC. In addition, the overall range of values reported and a mean value is given for each performance parameter.

| | *Most common range* | *Overall range* | *Mean* | *See Figure* |
|---|---|---|---|---|
| • Slump, mm | 150 – 200 | 6.0 – 270 | 147 | 8 (a) |
| • Vebe time, sec. | 10 – 15 | 3.5 – 34.0 | 13.0 | 8 (b) |
| • 28-day strength, MPa | 75 – 100 | 30 – 143 | 74 | 8 (c) |
| • Elastic modulus, GPa | 35 – 40 | 24 – 51 | 38 | 8 (d) |
| • Chloride permeability, Coulombs | 500 – 1000 | 115 – 7460 | 1522 | 8 (e) |
| • Diffusion coefficient, $m^2/sec.(x10^{-12})$ | 0.5 – 1.0 | 0.2 – 3.8 | 1.4 | 8 (f) |

Usually achieved by using high dosages of superplasticizer, slump values for HPC are generally high, most commonly falling within the range 150 to 200 mm. Vebe times most commonly reported for HPC were in the range 10 to 15 seconds. The thixotropic nature of concrete containing high quantities of fine material may explain why HPC mixes (with typically high slumps), do not yield a lower range of Vebe times. In terms of mechanical properties, the HPC mixes reviewed achieved 28-day strength and elastic modulus values in the ranges 75 to 100 MPa and 35 to 40 GPa. This strength range highlights the congruence between high-performance and high-strength concrete. In terms of chloride resistance, HPC mixes exhibited excellent performance, with chloride permeability

and diffusion values most commonly falling within the ranges 500 to 1000 Coulombs and 0.5 to 1.0 $m^2/s$ ($x10^{-12}$), respectively.

With respect to rapid-chloride permeability testing (using AASHTO T277-86 method [1990]), it should be noted that considerable controversy currently exists with regards to results obtained for mixes using replacement materials such as PFA, GGBS and SF. It is recognised [e.g., Streicher and Alexander, 1994, Shi et al., 1998] that for such concrete pore solution modification, rather than microstructural improvement, has the dominant influence on the test result obtained. The low results obtained in such cases often reflect the concrete's electrical conductivity and have little to do with its chloride ion transport characteristics. This effect may potentially be exacerbated for HPC where high binder material quantities are often used.

Correlations between HPC constitution and resulting performance

Due to a lack of design methods capable of proportioning HPC with respect to performance (other than strength), the intention of the work reported in this section was to establish the potential for correlations existing between HPC constituents and resulting performance. Against this background, a series of graphs plotting concrete characteristics versus performance properties was methodically prepared, as shown in Figures 2.7 to 2.16. Considered were relationships between performance (including 28-day strength, modulus of elasticity, diffusion coefficients and chloride permeability) and the following HPC characteristics:

- water - binder ratio (see Figure 2.7)
- total binder content, by mass (see Figure 2.8)
- Portland cement content, by mass (see Figure 2.9)
- Portland cement content, as percentage of total binder content (see Figure 2.10)
- Fly ash content, by mass (see Figure 2.11)
- Fly ash content, as percentage of total binder content (see Figure 2.12)
- Silica fume content, by mass (see Figure 2.13)
- Silica fume content, as percentage of total binder content (see Figure 2.14)
- GGBS content, by mass (see Figure 2.15)
- GGBS content, as percentage of total binder content (see Figure 2.16)

Included in Figure 2.17, are relationships between the following parameters:

- 28-day strength versus modulus of elasticity
- 28-day strength versus chloride permeability
- water content versus slump

Most likely due to the very wide range of data sources used and the inherent variability of concrete, strong correlations existing between the various HPC characteristics were limited. However, numerous relationships were evident as discussed below.

- As would be expected, a correlation between water - binder ratio and 28-day strength was found, with strength results increasing with reducing water - binder ratio. The correlation coefficient calculated for this relationship was 0.55, see Figure 2.7(a).

- Recognising the limited amount of data points available, a correlation was apparent between water - binder ratio and diffusion coefficients was found, with diffusion rates increasing with water - binder ratio. The correlation coefficient calculated for this relationship was 0.46, see Figure 2.7(c).

- In agreement with the trend noted above, a correlation, albeit a weak one ($R^2 = 0.28$), was apparent between water - binder ratio and chloride permeability. Permeability results generally increased with water - binder ratio, see Figure 2.7(d). A lack of sensitivity between chloride permeability and changes in water - binder ratio has been noted in a previous study of concrete containing SF [Mackechnie, 1998]. Reiterating the controversy

associated with the rapid chloride permeability test, this trend was attributed to the modified pore solution chemistry of these mixes dominating over microstructural improvements.

- Again as would be expected, a correlation between total binder content and 28-day strength was found, with strength results increasing with the binder content used. The correlation coefficient calculated for this relationship was 0.55, see Figure 2.8(a).

- Correlations were noted between total binder content and both diffusion coefficient and chloride permeability, with both of these durability parameters decreasing with increasing binder content. Correlation coefficients calculated for these relationships were 0.46 and 0.28, respectively, see Figures 2.8(c) and (d).

- Relationships between Portland cement content (expressed both by mass and as a percentage by mass of total binder) and 28-day strength existed. The correlation coefficients calculated for these relationships was 0.38, see Figure 2.9(a) and 2.10(a).

- Again recognising the limited amount of data points available, a relatively strong correlation between Portland cement content (as percentage by mass of total binder content) and diffusion coefficient was found for HPC. Most likely reflecting the beneficial influence of PC replacement materials on chloride resistance, diffusion rates increased with the percentage of PC used. The correlation coefficient calculated for this relationship was 0.78, see Figure 2.10(c).

- For a limited range of silica fume contents (i.e., around 0-50 kg/m$^3$ or 0-15 % by mass of binder), a loose correlation was evident with 28-day strength. In this range, 28-day strengths were found to increase dramatically with the silica fume dosage used, see Figures 2.13(a) and 2.14(a).

- Although plotted using only 5 available data points, a very positive correlation was found between the silica fume content used for HPC and the resulting diffusion coefficients achieved. With calculated correlation coefficients of 0.94 and 0.61, Figures 2.13(c) and 2.14(c) indicate linearly decreasing diffusion coefficients with increasing silica fume dosage (by mass and percentage, respectively).

- Only a very loose correlation was evident between 28-day strength and modulus of elasticity. This trend is in disagreement with many independent research studies where strong correlations between these parameters have been reported [e.g., SHRP, 1996]. The very wide range of data sources used to compile the current database most likely justifies the trend shown in Figure 2.17(a).

- With calculated correlation coefficients of 0.53, a weak correlation between 28-day strength and chloride permeability existed as shown in Figure 2.17(b). Most likely reflecting microstructural improvements, values of chloride permeability were found to decrease with increasing concrete strength.

For the remainder of the relationships explored no particular correlations were found, and in most instances a wide scatter of the data points existed. However, all relationships considered have been included for reference within Figures 2.7 to 2.17.

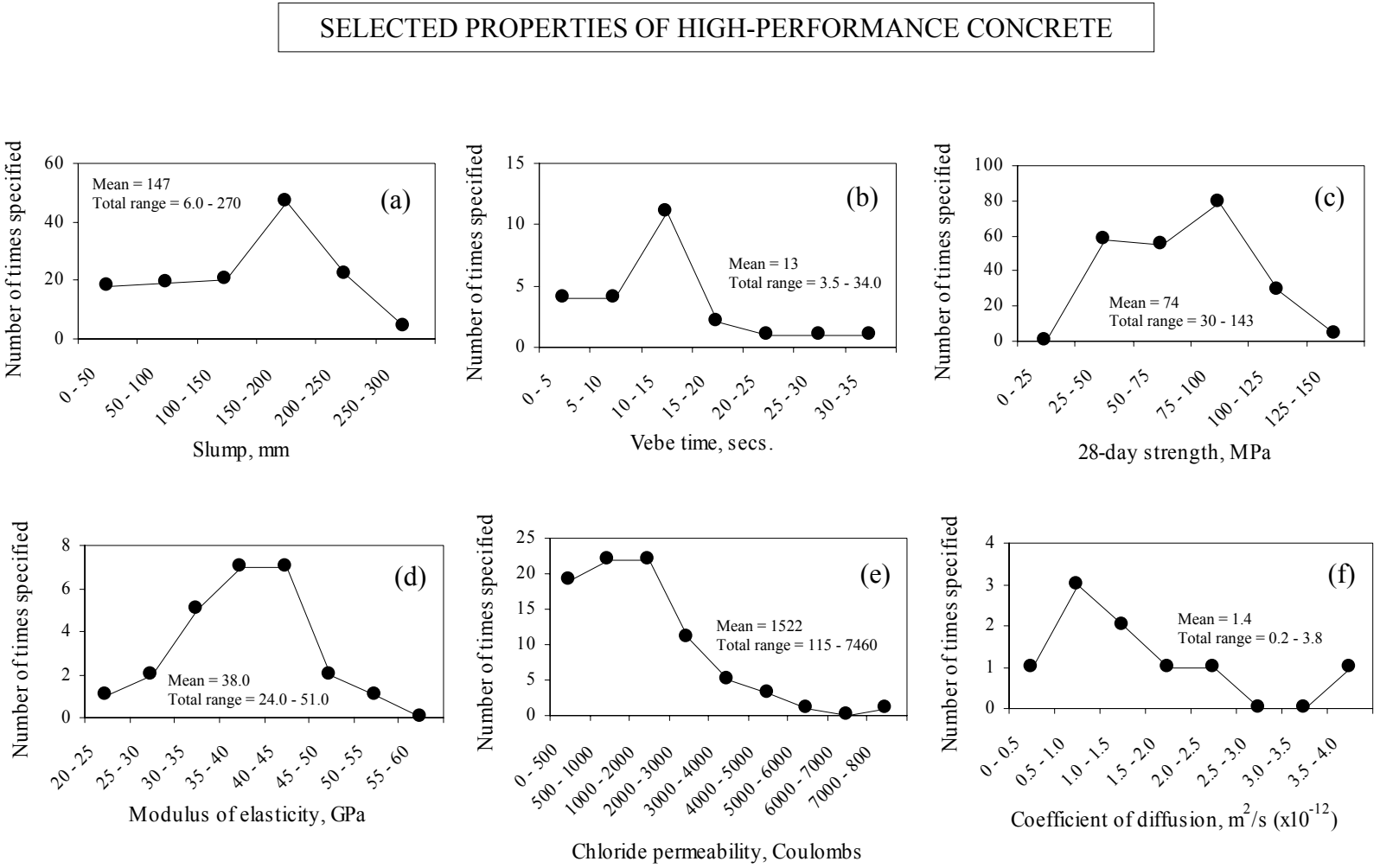


Figure 2.6: Summary of Typical HPC Properties (Information Taken from Database of 254 Mixes)

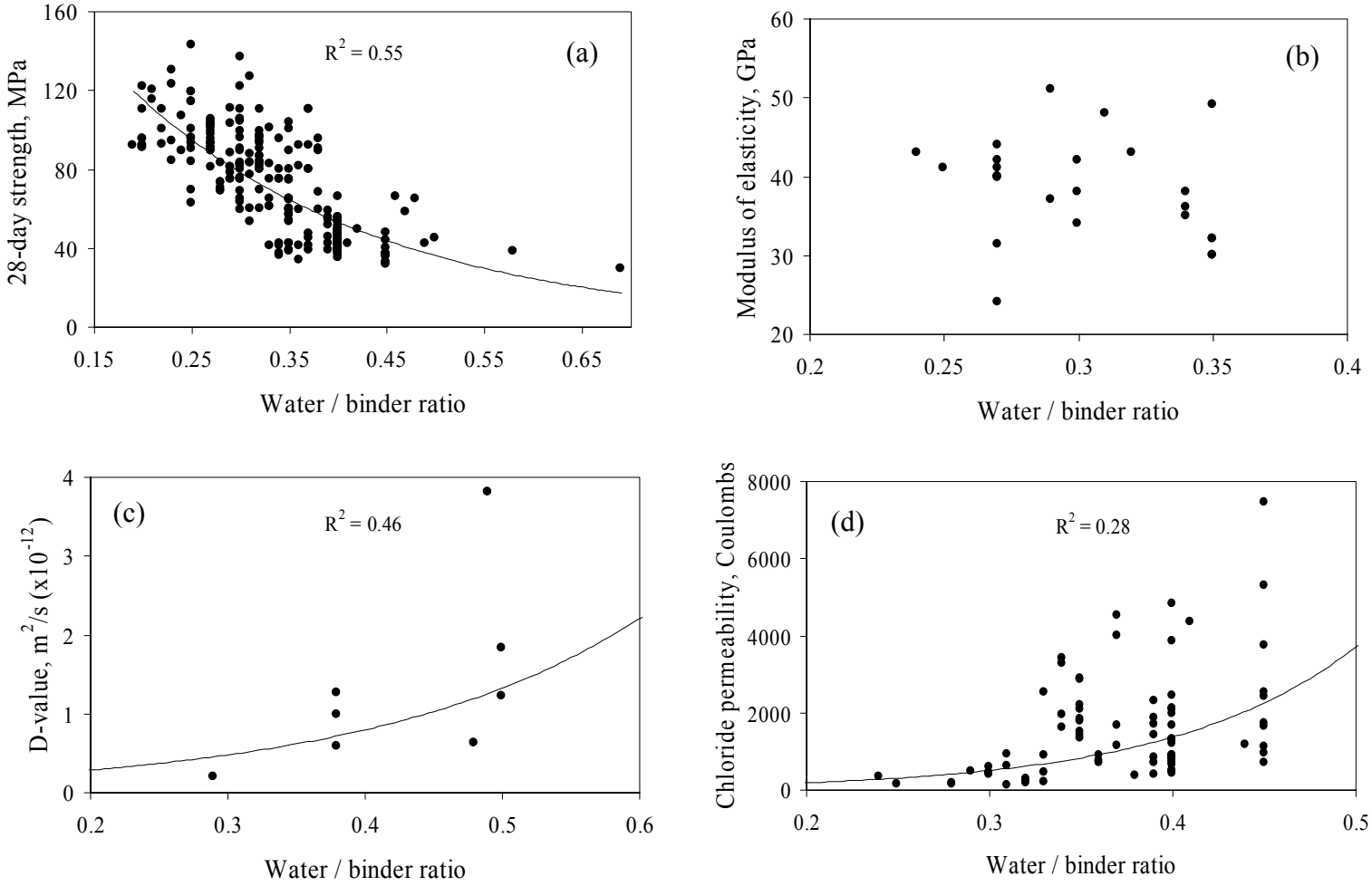


Figure 2.7: Relationship between Water - binder Ratio and Selected HPC Properties

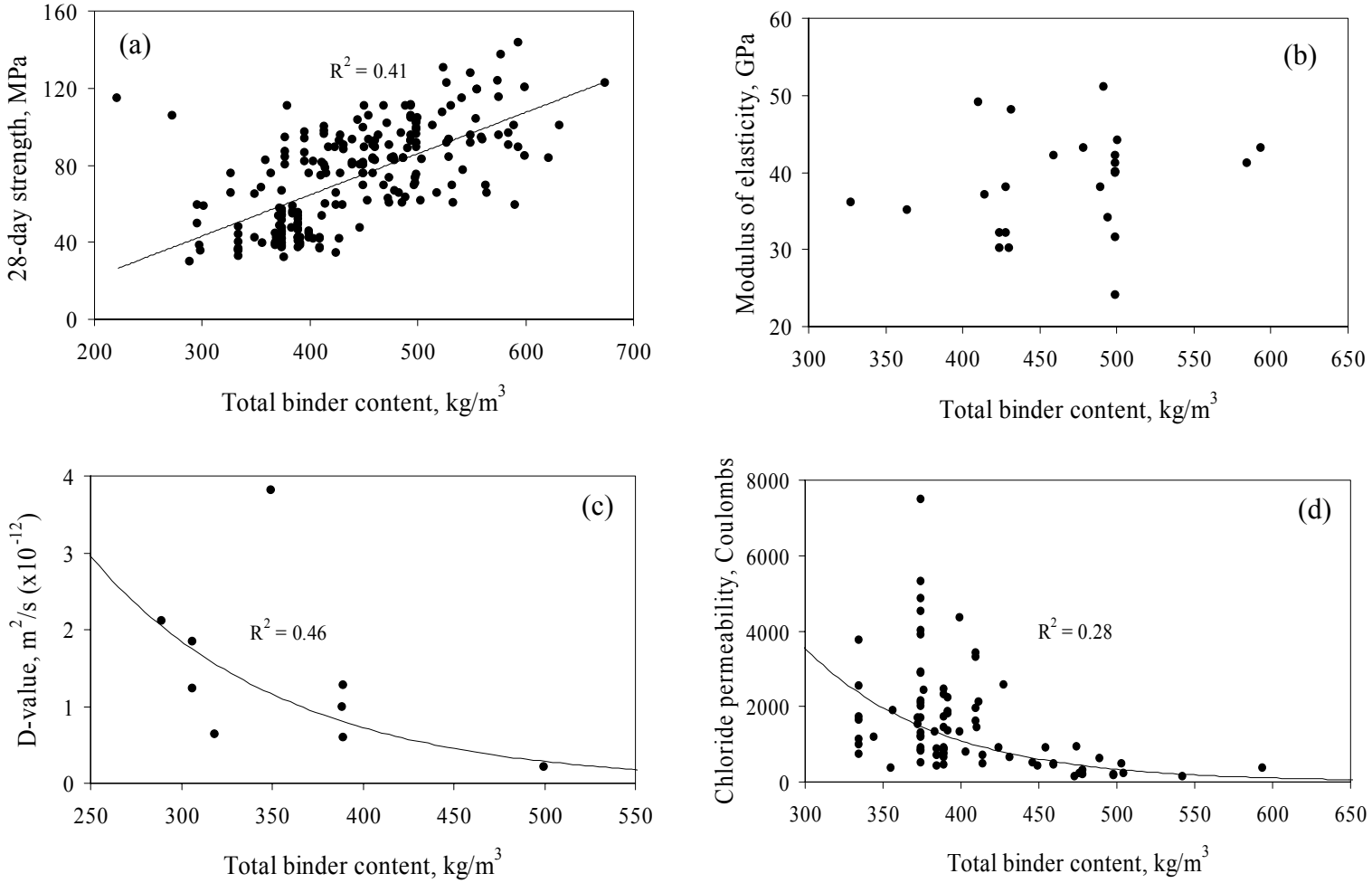


Figure 2.8: Relationship between Total Binder Content and Selected HPC Properties

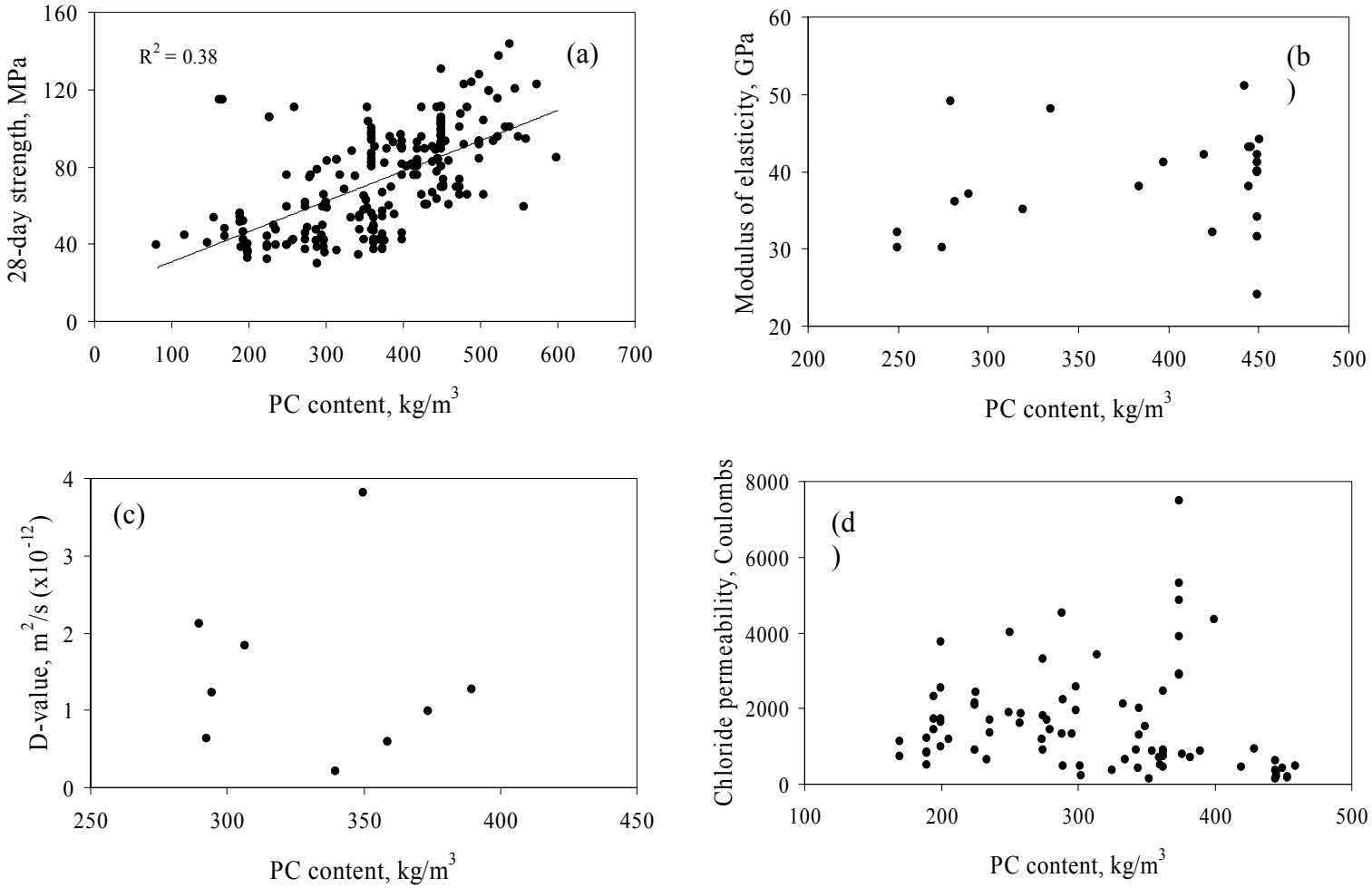


Figure 2.9: Relationship between Portland Cement Content (by Mass) and Selected HPC Properties

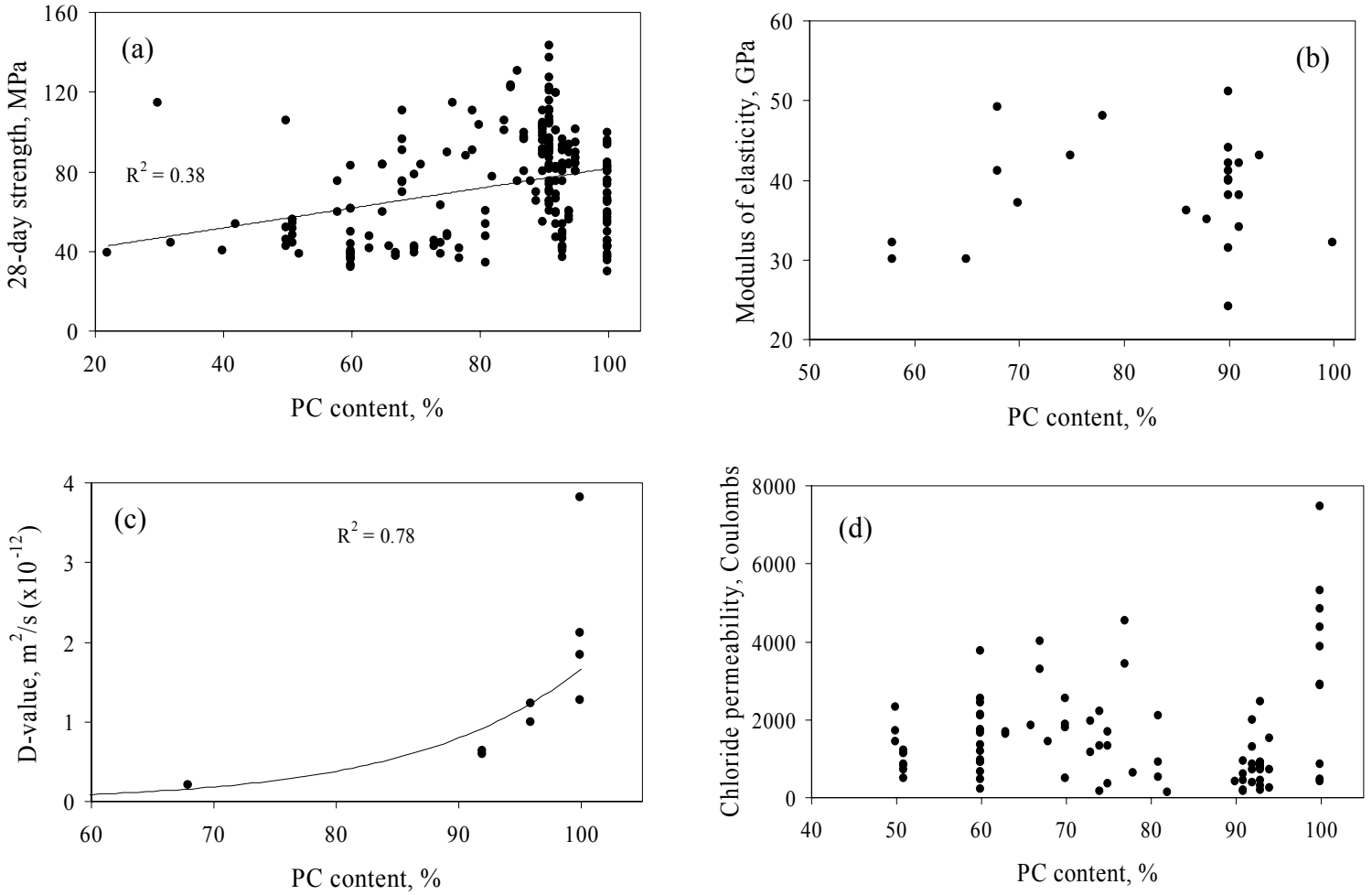


Figure 2.10: Relationship between Portland Cement Content (as % by Mass of Total Binder Content) and Selected HPC Properties

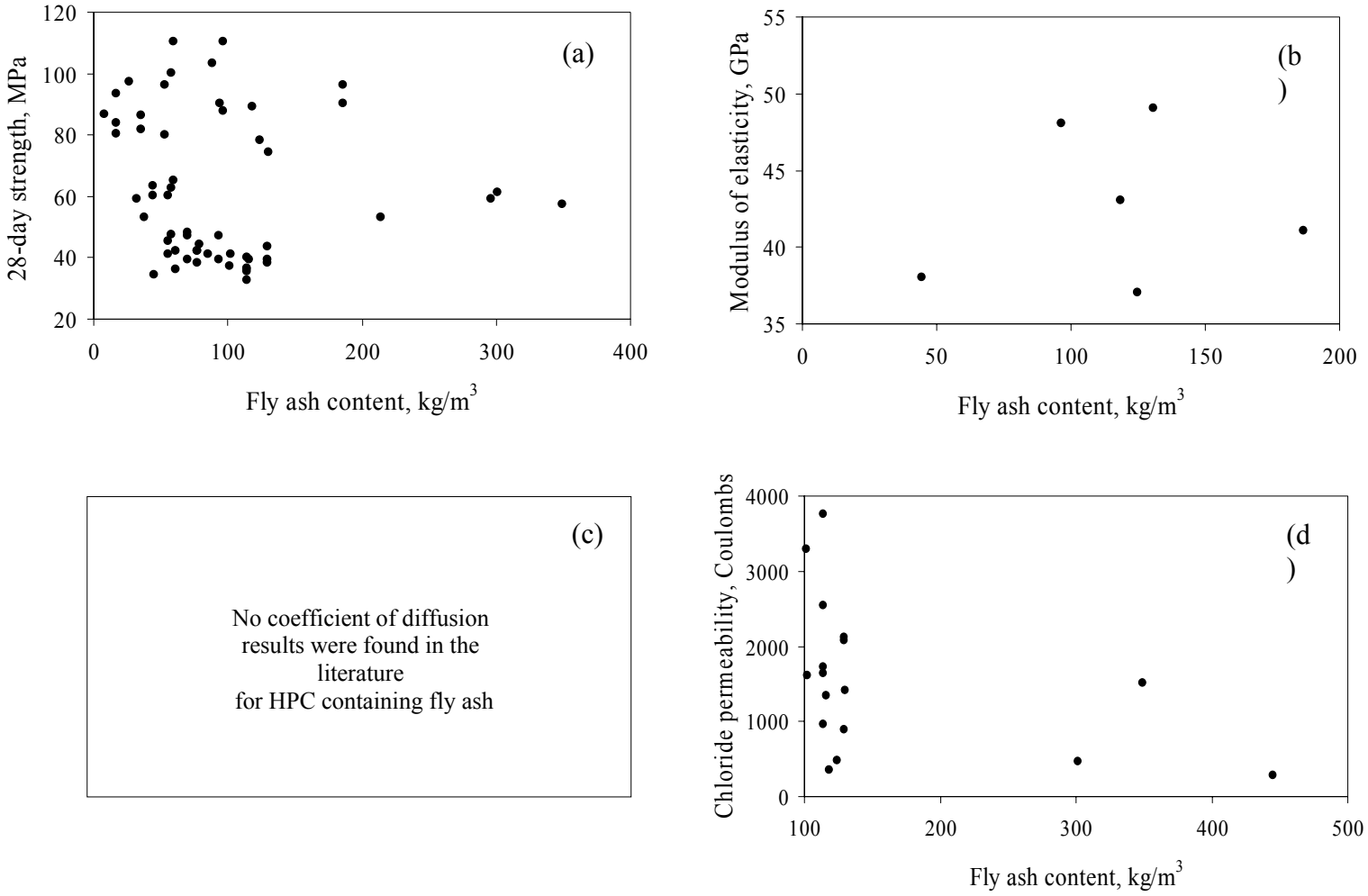


Figure 2.11: Relationship between Fly Ash Content (by Mass) And Selected HPC Properties

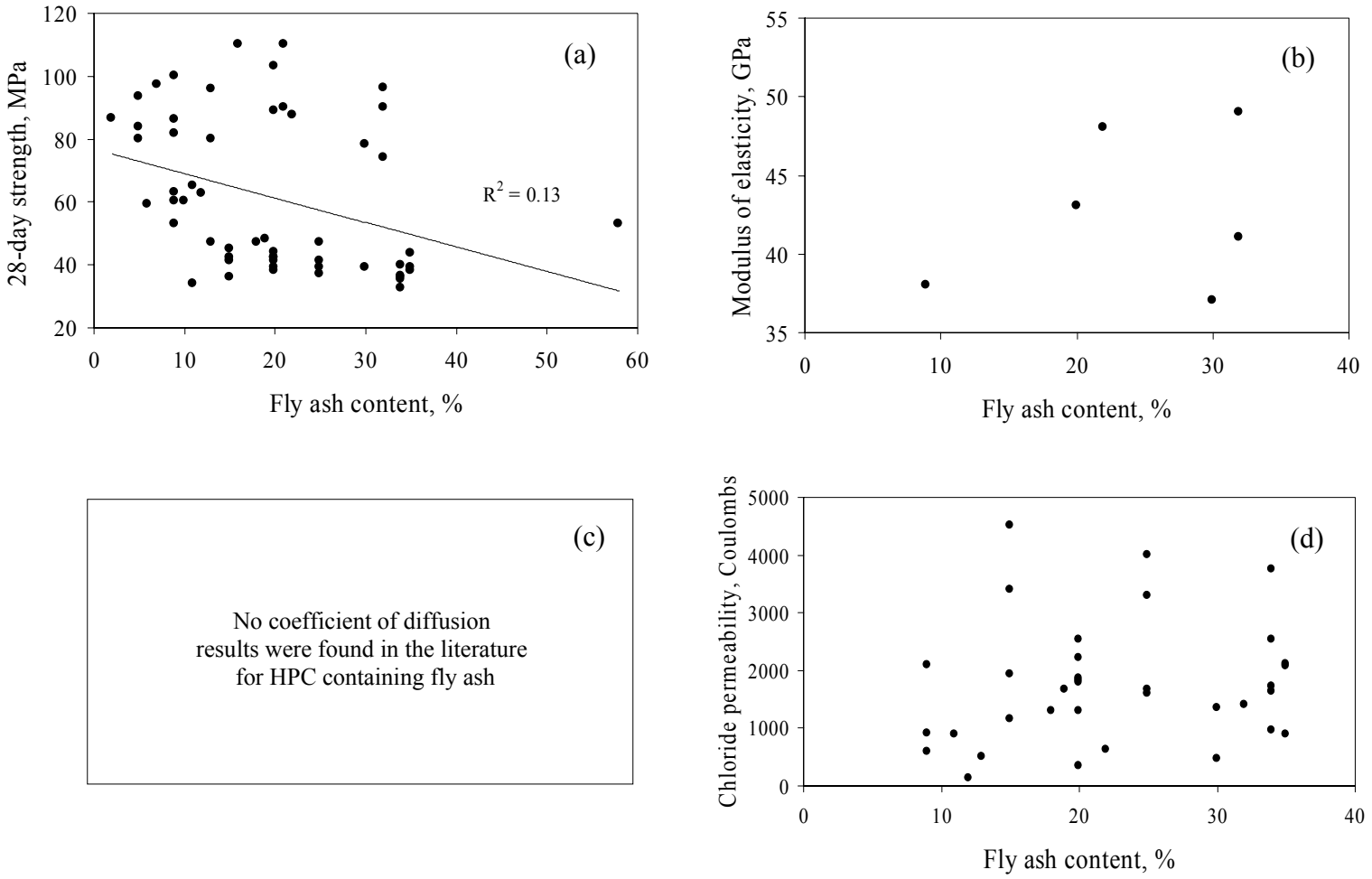


Figure 2.12: Relationship between Fly Ash Content (as % by Mass of Total Binder Content) and Selected HPC Properties

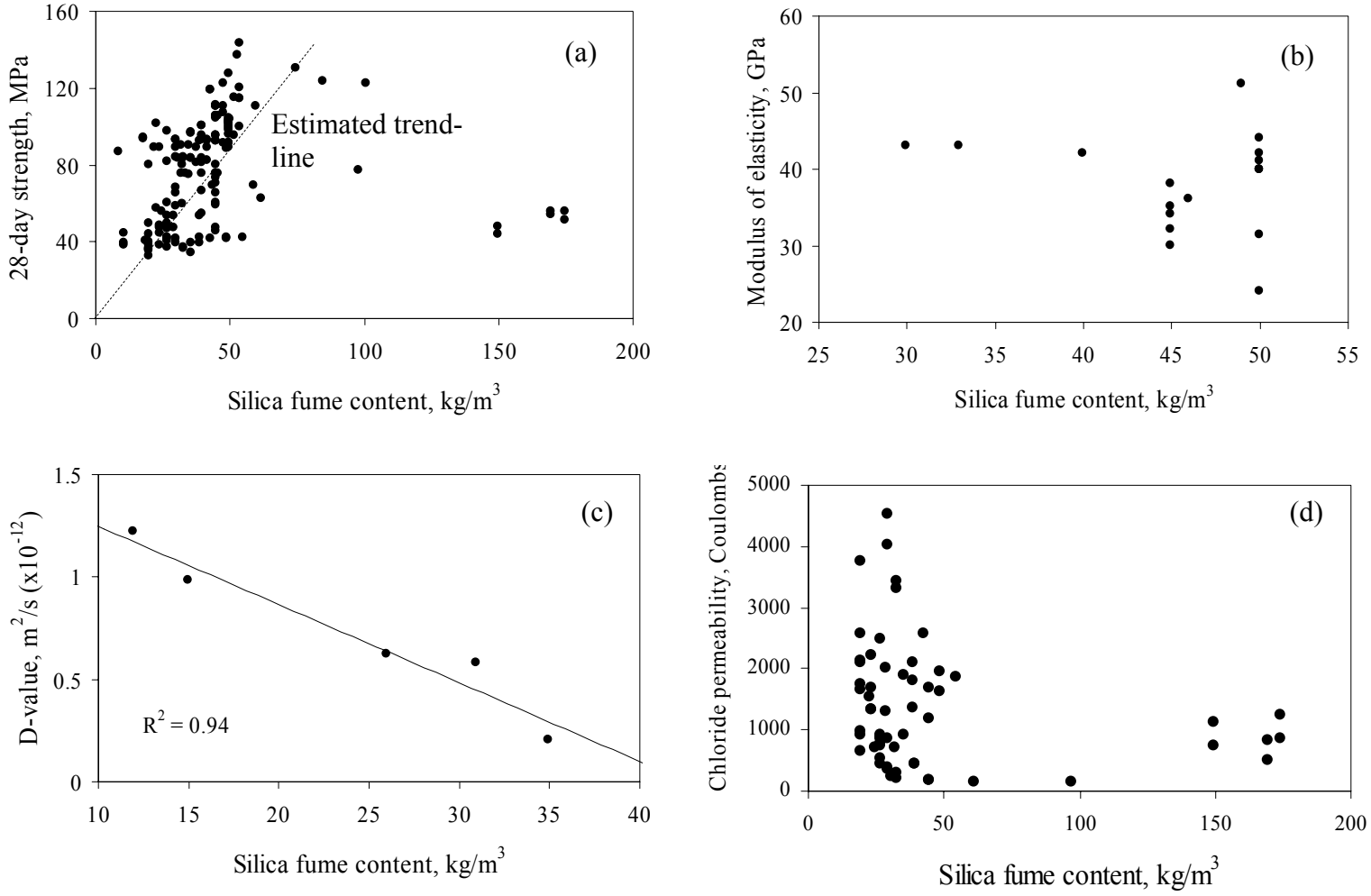


Figure 2.13: Relationship between Silica Fume Content (by Mass) and Selected HPC Properties

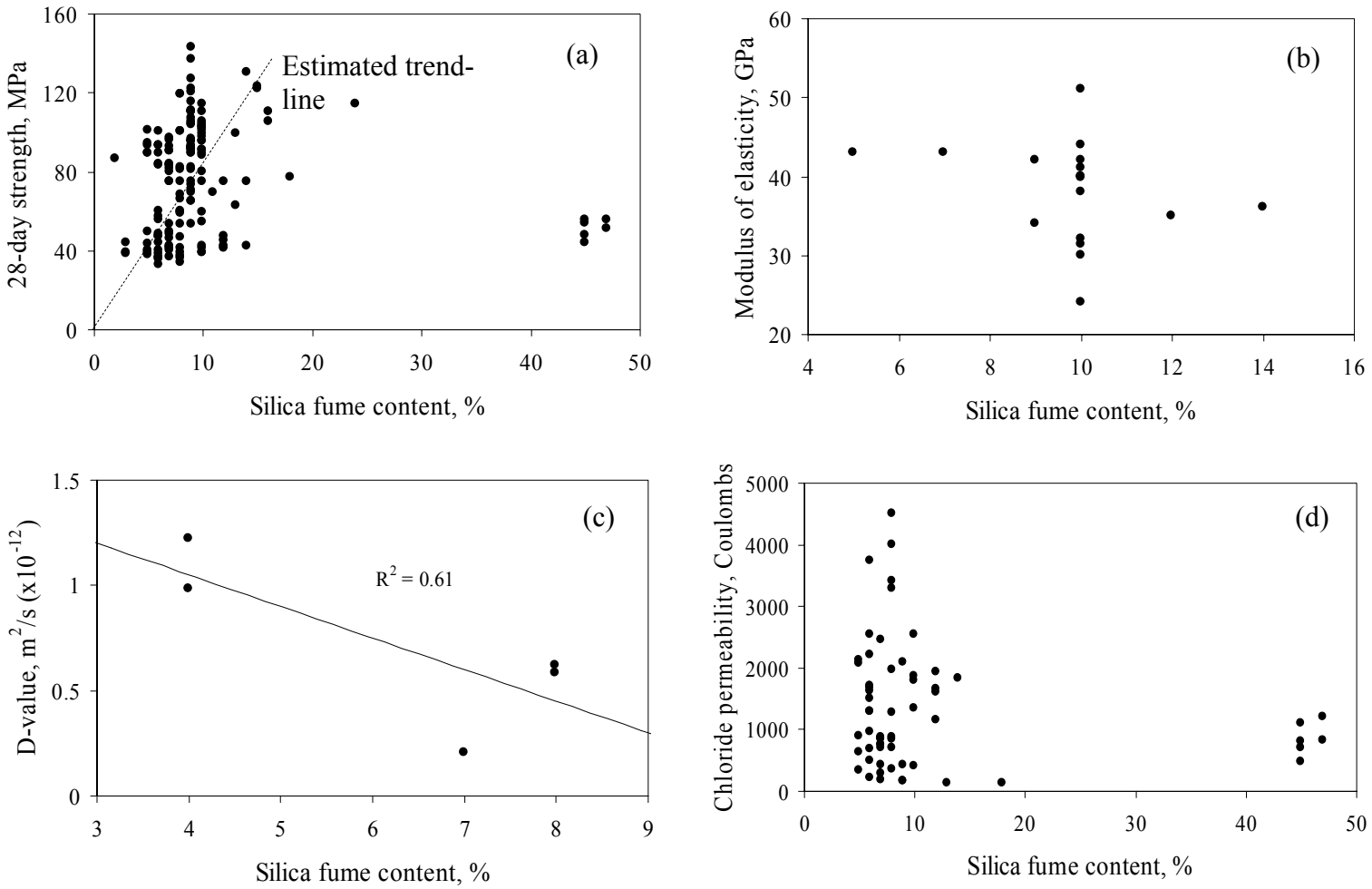


Figure 2.14: Relationship between Silica Fume Content (as % by Mass of Total Binder Content) and Selected HPC Properties

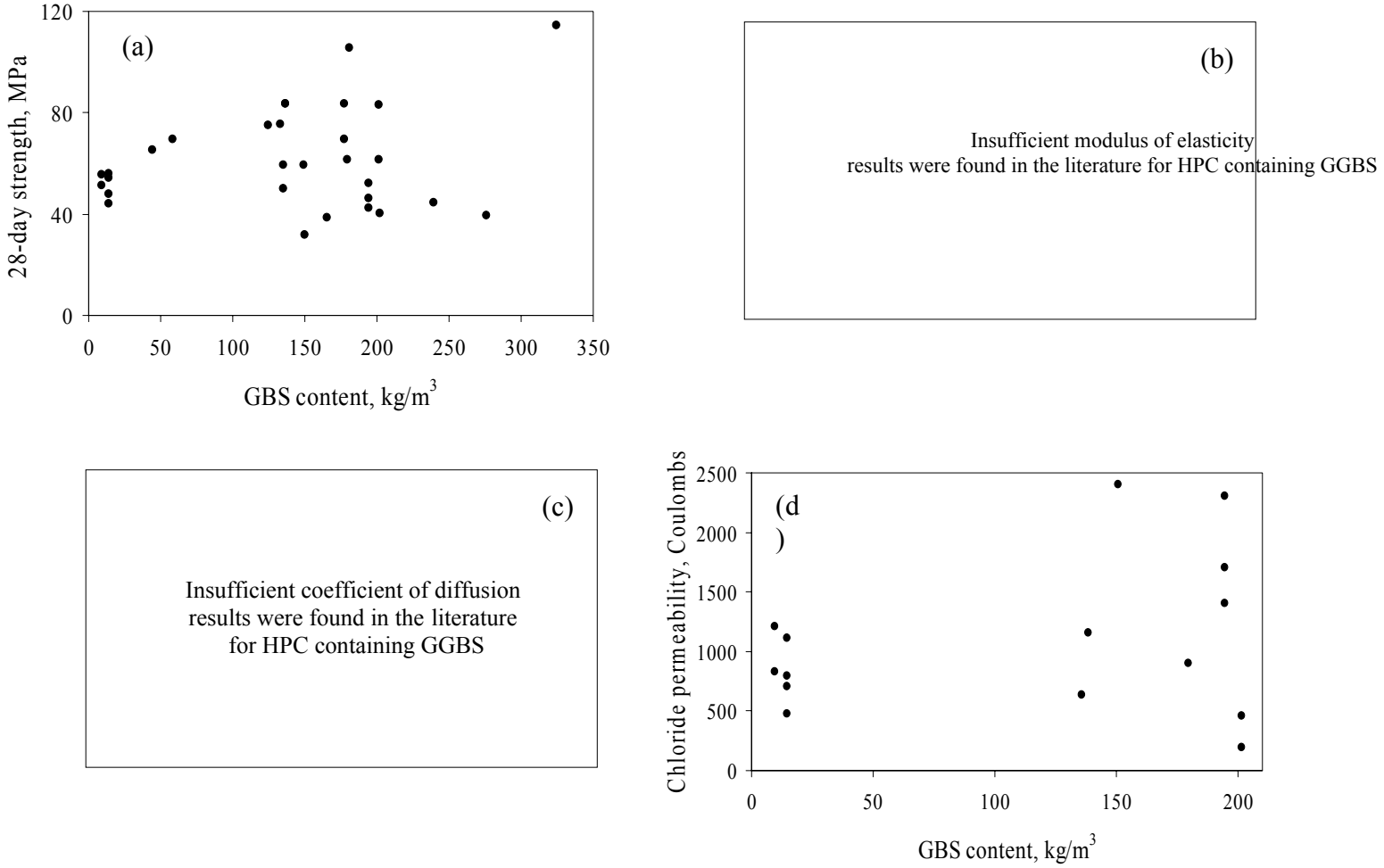


Figure 2.15: Relationship between Ground Granulated Blast Furnace Slag Content (by Mass) And Selected HPC Properties

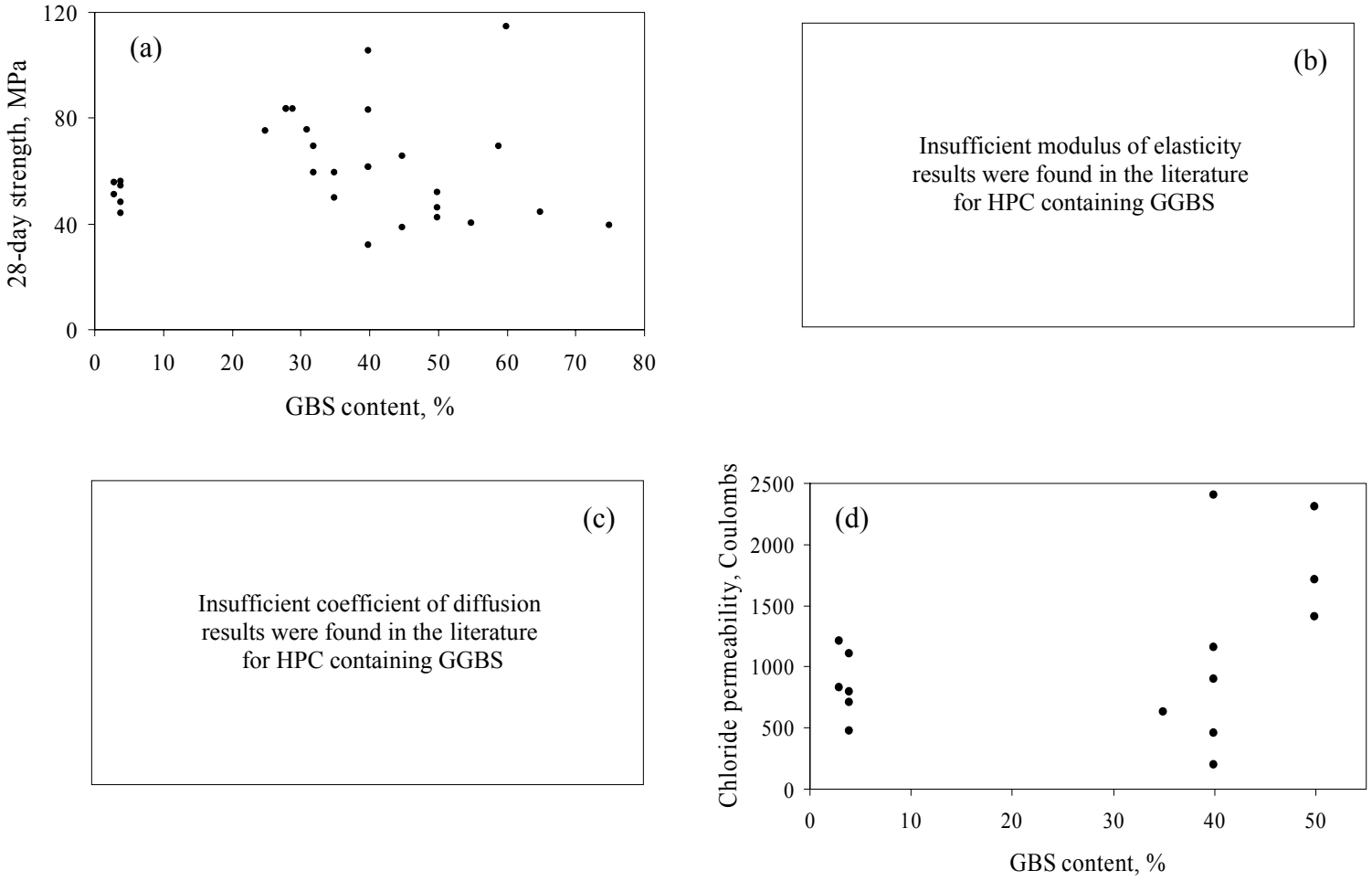


Figure 2.16: Relationship between Ground Granulated Blast Furnace Slag Content (as % by Mass of Total Binder Content) and Selected HPC Properties

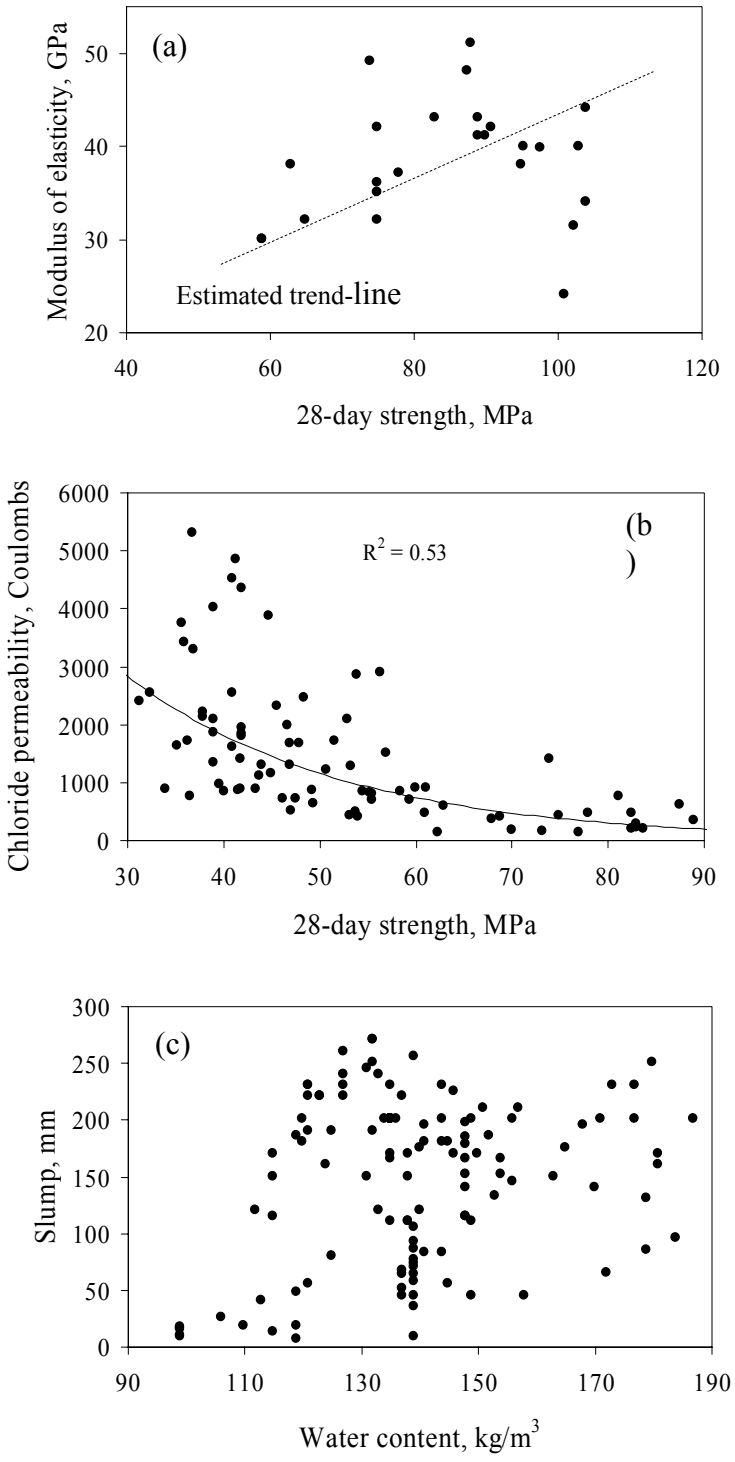


Figure 2.17: Additional Relationships for HPC

## 2.4 Performance Testing

Performance testing is the cornerstone of any performance-related specification. As discussed in the sections covering Task 3.1.1, testing regimes typically make up the third step of existing concrete-related specifications. Other principal PRS features such as assessing compliance to specified performance levels, the calculation of pay adjustment factors and life cycle cost analysis are all directly based on results obtained from performance testing. Due to a necessity to develop or select existing test methods for use in the current project, the following sections include a review of the principal features of performance testing methods. In addition, test methods incorporated in existing performance-related specifications are reviewed and their relevance to estimating durability performance is discussed.

### 2.4.1 Definition of Performance-Related Tests

At present there is no universally agreed definition for performance-related test methods. However, one report [Concrete Society, 1996] has defined performance-related tests as:

- tests that directly assess the resistance of concrete to a standardized deterioration process (e.g., freeze-thaw tests), or
- tests that directly assess the resistance to one of the phases of a deterioration process (e.g., carbonation tests), or
- tests that directly assess a performance-related parameter (e.g., measurement of cover or adiabatic temperature rise).

### 2.4.2 Key Attributes of Performance Tests

Performance-based specifications are intended as replacements for existing method-based or end-result specifications. Confidence in test methods proposed for use is essential, therefore, before any PRS is adopted. It has been reported [FHWA, 1997] that any test procedure selected to measure performance should, if possible, be timely (i.e., less than 30-days), economical, non-destructive, reliable and reproducible. Factors likely to be critical to the suitability of a test method for inclusion in PRS have additionally been proposed [Concrete Society, 1996] and these are summarised in the following sections.

Nature of test method

Two main categories of testing methods suitable for PRS exist, including initial type approval and routine control tests.

Initial type approval tests have been defined as those conducted prior to production, to establish a mix that gives the specified performance, or those used to establish equal or better relative performance from an unproven concrete or constituent material to a concrete or constituent material with established performance. As some initial type approval tests may be long-term (e.g., 1-year carbonation tests), they may only be suitable for established concrete producers with experience of their constituent materials etc. However, for a site plant using unproven materials, alternative options will be required to allow production to commence without significant delay.

Routine control tests have been defined as those used for production / compliance / acceptance purposes to ensure that specified performance is achieved or the performance established by an initial type approval test is maintained or the performance translated to mix limitations is maintained. It should be realised that routine control tests need not be durability performance tests and may, in fact, be simple indicators of fluctuating quality (e.g., a concrete strength test). It is likely that tests taking a long time to complete will be unsuitable for use as routine control tests. However, routine tests that are directly linked to initial type approval tests may be adopted. For example, consider the case where a long-term freeze-thaw test is adopted as an initial type approval test. In situ testing for air content and air spacing factor may then be used to routinely control performance.

Absolute or relative criteria

Durability performance tests can be either absolute (i.e., based on quantified requirements) or relative (i.e., using a control material or concrete with a known good track record) tests. Relative tests provide straightforward links with concretes of established performance and avoids the need to establish quantified criteria. Using relative tests may be the only solution when the reproducibility of a test used in an absolute way is poor. Difficulty for the user exists, however, in the selection of suitable reference concrete if this is not fully defined in the specification. The selection of reference mix used (e.g., based on equal water - binder ratio mixes, equal binder content mixes, equal strength mixes, etc.) will obviously affect the conclusions drawn from the test.

Due to the potential problems when choosing reference mixes for relative tests, the absolute test criteria should be adopted wherever possible [Concrete Society, 1996]. Absolute criteria may be established form concretes with a successful track record, or by proven explicit durability design methods [Concrete Society, 1996]. Based on the review of existing concrete-related PRS, two basic approaches to absolute durability testing through tests on concrete specimens have been identified as follows:

- The first approach determines performance of an average concrete sample and this is compared against a requirement that has also been based on average concrete quality. This approach assumes a fixed margin between average performance level and the characteristic level.

- The second approach requires the performance to be achieved in a concrete sample with a strength of $f_{ck}/\alpha_d$, where $\alpha_d$ is a partial factor of safety that takes account of possible difference between the test specimens and the structure. This assumes that concretes made using the same set of materials, but with higher strengths, will have a higher durability performance. Normal production control should ensure that at least 95 % of batches have a performance higher than that required [Concrete Society, 1996].

To work in practice, the second system would require at least two samples to be tested with, say, estimated strengths of ($f_{ck}/\alpha_d \pm 5$ MPa). The specified durability-related performance requirement would then be interpolated and the resulting $f_{ck}/\alpha_d$ obtained. It would have to be established that linear interpolation was suitable, and if not, then more samples would have to be tested to establish a relationship for interpolation. Such a system would also provide an indication of the sensitivity of the performance requirement to changes in concrete strength.

Severity of method

Many durability tests are designed to reproduce conditions that give maximum deterioration. When undertaking a suite of independent tests, what must be avoided is assuming the worst at every stage and finishing up with unobtainable or uneconomic requirements.

Point of testing

The point of testing involves two main considerations, namely where to test and when to test. The main choices of where to test include the actual structure / pre-cast unit, specially cast test specimens or the constituent materials used. The suggested main advantages and disadvantages of these choices are as listed below:

- Testing of structure / pre-cast unit
  - takes actual reinforcement position into account
  - measures actual structure quality at point of testing
  - tests reflect influence of actual exposure condition
  - moisture history will seriously affect results obtained
  - not all structure location will be available for testing
  - non-compliance of an in situ test is difficult to remedy (in comparison to non-compliance prior to concrete placing)

- Testing specially cast test specimens
  - actual structure is not tested
  - tests do not take construction factors such as workmanship into account

- testing is better controlled giving higher precision levels
- suitability of potential mix proportions may be assessed

- Testing constituent materials
  - when appropriate, renders testing of specimens and the structure unnecessary
  - nature of tests may reduce time, cost etc.
  - tests often must be backed up by additional tests or mix limitations

With regard to when testing should be carried out, it is stated that testing should be completed as soon as possible and at least prior to handing the structure over to the client. Once a structure is in use, remedial works are likely to result in high disruption costs. Although many in situ tests may be completed relatively quickly (e.g., cover depths, abrasion resistance), many take a long time to complete and this may be a major disadvantage. If such tests use specially cast test specimens, then the concrete producer may establish performance well in advance of construction. If testing must be of the actual structure, it is unlikely that concreting operations could wait for long periods of time for compliance results. Such considerations favour tests that can be completed quickly, even though the results may not be as ideal as those obtained from longer-term tests.

Precision of method

Test precision is mandatory and is measurable in terms of 'repeatability' and 'reproducibility'. Repeatability is a measure of within laboratory variability between successive tests using identical specimens of the same concrete, whilst reproducibility is a measure of between laboratory variability of single tests using identical specimens of the concrete. Directly linked to test precision is purchaser risk (i.e., the purchaser accepts concrete that was below the acceptable quality level) and producer risk (i.e., the producer has concrete rejected that reached the acceptable quality level). It is suggested that test precision, purchaser risk and producer risk be considered when selecting testing methods for use in PRS.

Moisture condition

In most aspects of durability performance the moisture-state is an important factor. For this reason, moisture conditioning of specimens may be necessary and this should be carried out to match the particular aspect of durability being tested. Careful control of moisture-states prior to and during testing will be necessary to obtain acceptable levels of precision. When interpreting in situ performance, or estimating longer-term performance from test results, allowance will be required for differences in moisture condition.

### 2.4.3 Test Methods Used in Existing Concrete-Related PS

As shown in Task 3.1.1, existing concrete-related PS has made use of a wide range of testing methods. Given below is a summary of the concrete properties tested in these PS and an indication of those likely to be of relevance to the current project:

| *Concrete property tested* | *Relevant to current project?* | *PS reference* |
|---|---|---|
| • Workability | ✓ | - Schell et al[1997] |
| • Compressive strength | ✓ | - Darter et al.[1996]<br>- Goodspeed et al.[1996]<br>- Schell et al.[1997] |
| • Modulus of elasticity | ✓ | - Goodspeed et al.[1996] |
| • Shrinkage | ✓ | - Goodspeed et al.[1996] |
| • Creep | ✓ | - Goodspeed et al.[1996] |
| • Concrete temperature rise | ✓ | - Schell et al[1997] |
| • Freeze-thaw resistance | ✓ | - Concrete Society [1996]<br>- Goodspeed et al.[1996] |
| • Scaling resistance | ✓ | - Goodspeed et al.[1996] |
| • Air content / air void system | ✓ | - Darter et al.[1996]<br>- Schell et al.[1997] |
| • Carbonation | ✗ | - Concrete Society [1996]<br>- Ho et al. [1988] |
| • Chloride resistance | ✓ | - Concrete Society [1996]<br>- Goodspeed et al.[1996]<br>- Armaghani and Bloomquist [1998]<br>- Ozyildirim [1998]<br>- Schell et al[1997] |
| • Sulfate resistance | ✗ | - Concrete Society [1996] |
| • Abrasion resistance | ✗ | - Concrete Society [1996]<br>- Goodspeed et al.[1996] |
| • Permeability | ✓ | - Armaghani and Bloomquist [1998] |
| • Water sorptivity | ✓ | - Ho et al. [1988] |

In the following sections, the concrete properties marked as having potential relevance to the current project are discussed in more detail. In particular, the significance of the tested property to predicting the durability performance of concrete in bridge superstructures and the nature of test method required is considered.

Workability

Although a property of concrete while in its fresh state, inappropriate workability (most commonly measured using the slump test) may have significant bearing on the performance of hardened concrete due to compaction difficulties. It has been stated that the long-term performance of concrete is very seriously affected by the degree of its compaction [Neville, 1995].

Compressive strength

The most common of all test methods on hardened concrete is the compressive strength test, partly because it is easy to perform and partly because many, though not all, of the desirable characteristics of concrete are qualitatively related to its strength [Neville, 1995]. In the majority of current specifications compressive strength is used not only as a basis of structural design and as a criterion of structural performance, but also as a criterion for the durability of a concrete structure. This approach may be justified by the observation that both strength and transport characteristics are to a large extent linked to the pore structure of the concrete: low porosity results in high strength and also in a high resistance to the penetration of aggressive media [Rilem Report 12, 1995]. For instance, in one

publication it has been shown that strong correlations exist between concrete strength and durability-related properties such as gas permeability, water permeability, carbonation and abrasion [Rilem Report 12, 1995].

Mechanical concrete properties

Deformations of modern concrete structures due to elastic strains, creep and shrinkage are becoming increasingly important for a number of reasons (e.g., improved materials giving larger spans, mingling of in situ and precast elements, use of increasing working stresses etc.). With regard to serviceability, the main effects of deformations are deflections and cracking [Portland Cement Institute, 1994]. Data directly linking mechanical concrete properties to durability-related properties is very limited in the literature. Clearly, however, the occurrence of cracking is central to the durability performance of any concrete structure. For this reason, tests for elasticity, shrinkage and creep may be relevant to the current PRS. Standard test methods are currently available for testing modulus of elasticity, shrinkage and creep of concrete.

Concrete temperature

Thermal properties of concrete are of vital importance during construction when heat of hydration is generated and later when thermal movements occur due to temperature changes [Concrete Society, 1996]. As a result, performance requirements may be specified to prevent or limit early-age thermal cracking and, to a lesser extent, reductions in long-term strength. Clearly, both cracking and strength loss play a roll in the overall durability of a structure. Limits imposed may be on maximum adiabatic temperature rise and/or maximum in situ temperature rise and difference. Testing may be carried out on individual test specimens (using isothermal conduction calorimetry) or insitu (using thermocouples or thermistors probes placed at various section depths).

Freeze-thaw / scaling resistance

There exists no standard test method for determining the resistance of concrete to cycles of freezing and thawing as may occur in service. However, there is a large of number of accelerated tests using rapidly repeated freeze-thaw cycles, many of which are standardized. The most widely used tests are the ASTM C 666 [1992] and ASTM C 672 [1992] methods. These are relative test methods and may be used to compare the performance of various mixes. Control mixes used may be those with a proven track record of performance in service.

Air content / air void system

As discussed in the previous section, freeze-thaw tests are initial type approval tests, used most constructively to assess the performance of new or unknown materials, or as part of routine testing of a structure [Concrete Society, 1996]. For this reason, freeze-thaw tests should be considered in conjunction with other means of assessing the freeze-thaw resistance of concrete. These include (i) measuring the air content of the fresh concrete, (ii) measuring the spacing factor of the fresh concrete and (iii) measuring the spacing factor of the hardened concrete. Standard test methods are currently available for testing these properties.

Chloride resistance

Chloride ions, when present at the surface of reinforcing steel in sufficient quantities, result in the occurrence of corrosion by acting as catalysts in the disruption of the passive oxide layer. For this reason, much research has concentrated on chloride diffusion mechanisms, with specifications often written in terms of chloride diffusion coefficients. There are a number of diffusion test methods and models for determining chloride diffusion coefficients. Some tests rely on the achievement of steady state conditions, while others use electrical current to accelerate the time taken to achieve an answer. Other methods measure a chloride profile, which also gives information on chloride distribution. Measured values of diffusion coefficient depend on the test method, initial chloride content of the concrete, subsequent chloride binding and the maturity of the test specimens [Concrete Society, 1996]. The most commonly adopted chloride-related test in North America is the rapid method to AASHTO T277 [1990] requirements. Due to the previously discussed drawbacks associated with this test, careful consideration will be required concerning its adoption for use in the current project.

Permeability / sorptivity

Some aspects of concrete durability are governed to a large extent by the resistance of concrete to penetration of aggressive media. Performance testing based on such resistance may, therefore, be a reliable approach to ensuring durable concrete. As discussed previously, aggressive media may be transported by various mechanisms, including

permeation, absorption and capillary suction. Whilst it is questionable whether any single such property of concrete is sufficient to predict its overall durability performance, some correlations exist between selected transport and durability characteristics. For instance, research as indicated that the following durability characteristics correlate strongly to various transport mechanisms (as shown in brackets) [RILEM Report 12, 1995]:

- Carbonation (air permeability, water sorptivity)
- Freeze-thaw resistance of non-air entrained concrete (air permeability, water sorptivity)
- Sulfate resistance (water sorptivity)
- Abrasion resistance (air permeability, capillary suction)
- Chloride ingress (air permeability, capillary suction)

Numerous test methods for testing concrete permeability and sorptivity exist, developed for use both in the laboratory and insitu, at least two of which are commercially available. A review of many of these test methods is included in reference [RILEM Report 12, 1995]. Potentially, some of these test methods are suitable as a type approval test for a proposed concrete mix, or alternatively for use as a routine control test on the quality of the concrete supply [Concrete Society, 1996].

## 2.5 Development of Initial PS Stages

### 2.5.1 Identification of Parameters Influencing Performance

It is proposed that the specification to be developed in the current project be structured similarly to existing concrete-related PS (see Task 3.1.1). Against this background, the initial action required is to identify parameters considered critical to the overall performance of concrete.

As is the case in the PRS developed for PCC pavements [Darter et al., 1996], it is proposed that the parameters driving the current specification should be in the form of distress indicators. Based on information reported in the literature and an extensive survey carried out among 38 state DOTs (see Task 3.1.1 for details), a provisional list of material-related distress indicators for the current project is given below:

- degree of cracking
- degree of spalling / potholing
- degree of delamination
- degree of scaling
- degree of leaching
- percentage of chlorides at steel
- partial or complete loss of cross-section

The ultimate goal of this part of the project is to attach numerical limits to chosen distress levels. By doing this, the 'end-of-service-life' for bridge superstructures (as determined by materials-related failure) will be clearly defined at the outset of design. The challenge will be to ensure that these proposed limits are not exceeded prematurely by testing concrete at the mix design and/or construction stages. The 'end-of-service-life' is likely to trigger the need for rehabilitation or repair of the concrete structure in some way. This task may require a further review of INDOT's bridge inspection database and any other relevant information sources available.

### 2.5.2 Specification of Concrete Quality Characteristics and Their Target Values

On confirming the distress indicators / performance levels that influence performance, the next step is to develop a suite of specifications capable of producing serviceable concrete. In short, specifications must be such that the concrete produced has a 'design-life' greater than or equal to its 'end-of-service-life'.

Based on the materials-related distress indicators proposed above, given below is a list of provisional quality characteristics that may be specified in the proposed PRS. Based on existing specifications and literature sources reviewed, also given for each property is a proposed specification target value for discussion purposes:

- workability (175 mm slump)
- compressive strength (55 MPa, 28-days)
- modulus of elasticity (45 GPa, 28-days)
- shrinkage (500 microstrain)
- creep (60, microstrain / MPa)
- heat of hydration ($20^{o}$C, maximum differential)
- cover depth to reinforcement (70 mm)
- chloride resistance (≤ 1000 Coulombs)
- freeze-thaw resistance (70 %, dynamic modulus - 300 cycles)
- air content and air void system parameters (≥ 6.0 %)
- air permeability ($10\ m^2$, $x10^{-16}$)
- sorptivity ($6.0\ mm/year^{0.5}$)

These quality characteristics have initially been proposed due to their potential influence on the occurrence of the distress indicators listed in section 5.1 above. It is very important to recognize that in the majority of cases, target values for these quality characteristics do not exist in current specifications, nor are they determined during structural design. It is for this reason, therefore, that provisional target values have been attached at this time. It is recognized that this is in contrast to the PCC pavement PRS [Darter et al., 1996], where no target values are specified for quality characteristics. The members of the Focus Group for Task 3.2.1 have approved the above list.

Using the target values shown as a starting point, the ultimate goal in this task is to attach acceptable numerical values to those properties chosen. In order to verify specification values, positive correlations between each specified concrete property and corresponding performance levels must be established. Correlations may be established using either accelerated testing methods or mathematical modeling.

## 2.6 Potential Novel Materials for Concrete Bridge Superstrucutres

At the time of preparing the project proposal, high-performance concrete was exclusively proposed as a new / improved material to be investigated in Task 3.2.1. While HPC continues to command the main focus of the research, the literature review has disclosed alternative technologies with potential applicability to the current project. Potential materials to be considered for the design and construction of concrete bridge superstructures in Indiana are discussed below:

### 2.6.1 High-Performance Concrete

Section 3 provides a good synopsis of conventional HPC, covering both the constituent materials typically used and performance levels commonly achieved. In summary, HPC is generally proportioned using low water - binder ratios (most commonly in the range 0.25 to 0.40) and high total binder contents (values as high as 675 $kg/m^3$ have been used to date). Silica fume is frequently used, most commonly in binary blends with Portland cement, although the use of ternary blends with fly ash and GGBS have also been used.

HPC usually requires very stringent control of construction techniques such as placing, finishing and in particular curing. In terms of reported performance, HPC is distinguished mainly by its high compressive strength (mainly in the range 75 to 100 MPa, with results as high as 143 MPa noted). Owing mainly to the use of very low water - binder ratios, HPC also tends to exhibit good durability performance. For example, chloride permeability values for HPC are typically very low, most often falling within the range 500 to 1000 Coulombs, with values as low as 115 Coulombs reported.

### 2.6.2 Ternary-Binder Concrete

From the list of distress indicators identified in Section 5.1, durability-related performance (rather than strength development) appears to be the principal design criterion for concrete bridges. In terms of strength development

requirements, therefore, the use of conventional HPC in bridge deck construction may be uneconomical and/or over-conservative.

A potential route to achieving durable concrete without yielding excessive strength values is through binder optimisation. Indeed, research has been carried out to investigate the practicality and performance of concrete containing ternary blended binders [e.g., Jones et al., 1997, Jones et al., 1998, Magee and Alexander, 1998]. Ternary binder concrete (TBC) has been found to exhibit no visual dissimilarity to good quality PC concrete. In fact with regards to fresh concrete properties, TBC was generally of a higher quality than the PC and PC / FA control concrete. Of practical significance, TBC was easily compacted, exhibited no visible bleeding and produced an excellent surface finish [Jones et al., 1998]. For typical structural strength grades, research has additionally led to the development of a simple mix design method for TBC.

A major potential benefit associated with using ternary binders is enhanced concrete durability, particularly with regards to chloride ingress. Research has been undertaken to examine the chloride resistance of TBC relative to more conventional mixes. For instance, given in Figures 2.18(a) and (b) are results obtained from accelerated electrochemical chloride transmission tests and chloride conductivity tests, respectively [Jones et al., 1997, Magee and Alexander, 1998].

The results shown in Figure 2.18(a) are for concrete prepared using equal water - binder ratios. Clearly, TBC mixes out-performed PC, PC/GGBS and PC/SF controls over the range of water - binder ratios considered (0.49, 0.56 and 0.66). It should be noted that due to the competitive nature of the pozzolanic reactions, the 28-day strength of these TBC mixes was around 33 % lower than that of the PC/SF binary controls. Interestingly, TBC prepared with a water - binder ratio of 0.66 exhibited higher chloride resistance than PC and PC/FA and PC/SF concrete with a water - binder ratio of 0.49.

In contrast, Figure 2.18(b) shows results for concrete prepared with equal 28-day strength. In agreement with the trends discussed above, the chloride resistance of TBC was markedly higher than the PC and PC/FA controls over the range of strengths considered (20, 40 and 60 MPa). Indeed, no chloride transmission was measured for either of the 60 MPa TBC mixes by the conclusion of the 14-day test period. Levels of improvement were such that the 20 MPa TBC mixes generally out-performed the 60 MPa controls.

For most practising engineers the concept of using multiple binder combinations, whilst still rarely used in many countries, is now an option which can be seriously considered for conventional structural concrete. Indeed, examples of major infrastructure projects that have used TBC include the Stoerbelt bridge/tunnel link in Denmark [Vincensten and Henrikson, 1992] and the Chek Lap Kok bridge at the new Hong Kong airport [New Civil Engineer, 1995].

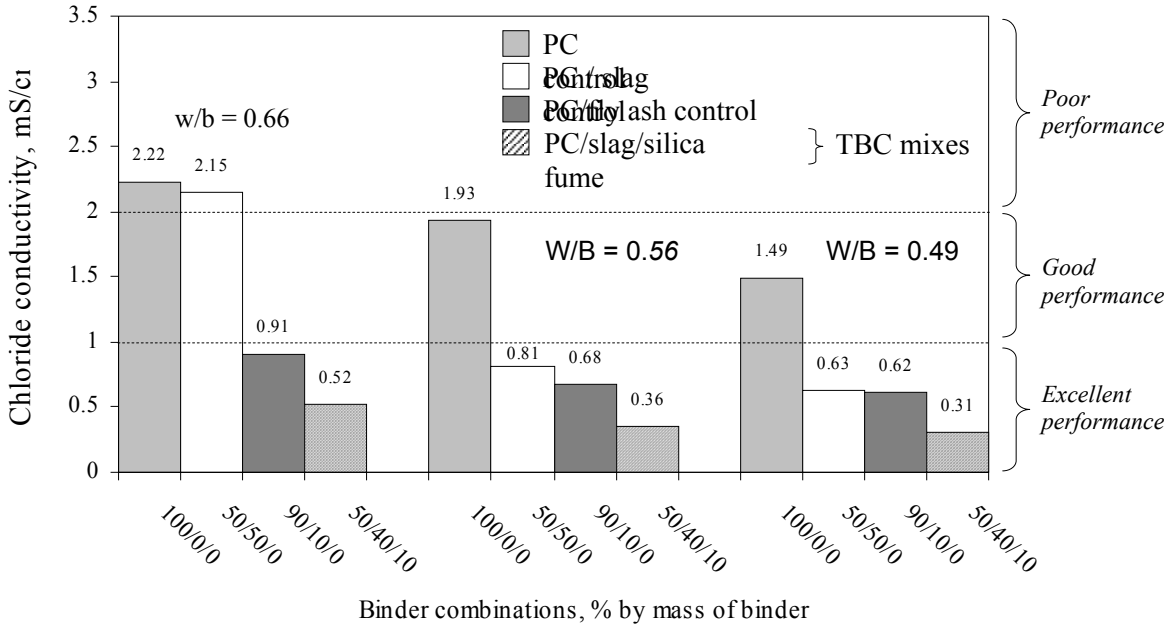


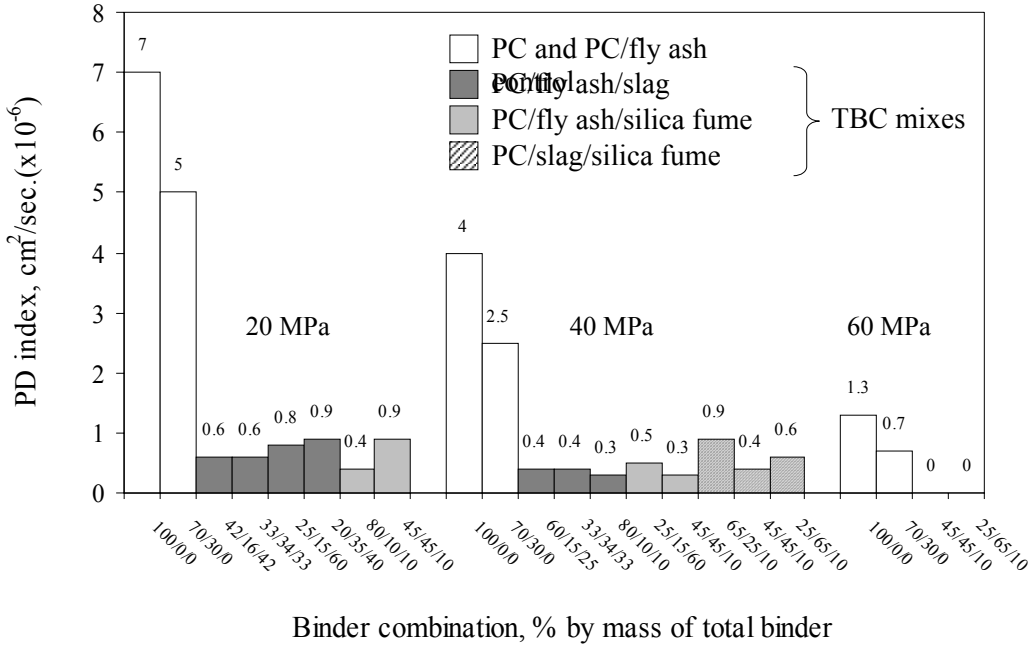


Figure 2.18: Chloride Resistance of Control and TBC Mixes Designed with:
(a) Equal Water - binder Ratio [Magee And Alexander, 1998]
(b) Equal 28-day Strength [Jones Et Al., 1997]

### 2.6.3 Concrete Designed Using Porosity Transformation Approach

A further material worthy of consideration for the design and construction of concrete bridge superstructures is concrete prepared using the porosity transformation approach [Rangaraju, 1997]. The main principles of porosity transformation are summarized in Figure 2.19.

Figure 2.19(a) represents the composition of a unit volume of paste as typically used in a conventional concrete mix. In this example, the paste has been prepared with a water - binder ratio of 0.5. In comparison, the composition of a typical HPC paste is given in Figure 2.19(b), prepared in this case with a water - binder ratio of 0.25. In accordance with current concrete technology, this reduction in w/b ratio was achieved by lowering the free water content. In order to maintain a constant unit volume, the reduced water content in Figure 2.19(b) was compensated by increasing the amount of binder material (assuming that both conventional and HPC will have similar air content). While increased binder contents enhance strength and other mechanical properties, their use can adversely influence other properties such as workability, shrinkage, creep and heat of hydration etc. In addition, concrete with high cementitious contents are more expensive to produce.

Against this background, the proposed alternative approach to achieving concrete with high performance is illustrated in Figure 2.19(c). In this case, the porosity-transformed paste has been prepared with a w/b equal to that of the HPC (i.e., 0.25), while maintaining a binder content equal to that of the conventional concrete. In order to achieve unit volume, increasing the entrained air content compensates for the reduced water content. In this way, the porosity-transformed paste provides concrete with similar performance to HPC while overcoming the drawbacks inherent with the use of high binder contents. As entrained air bubbles are empty and discontinuous, they participate in transport phenomenon only when the concrete is subjected to hydraulic pressure gradients. In addition, even though the diameter of entrained air bubbles are in the range of 50 to 500 μm, the pore entrances to the air bubble are much smaller (typically < 1 μm).

Further advantages of porosity transformation through air entrainment include an obvious contribution to freeze-thaw resistance and reduced unit weights of concrete to levels comparable to semi-light weight concrete. Through the use of adequate superplasticizer dosages, the thixotropic behaviour commonly exhibited by HPC (using low w/b , high dosages of superplasticizer and materials such as silica fume and slag), is greatly minimized, thus allowing for easier handling and placement. Indeed, experimental work [Rangaraju, 1995] indicated no practical difficulties of the air-entrained mixes in their fresh state. Mixes achieved satisfactory workability (75–125 mm slump) and were easily compacted under vibration.

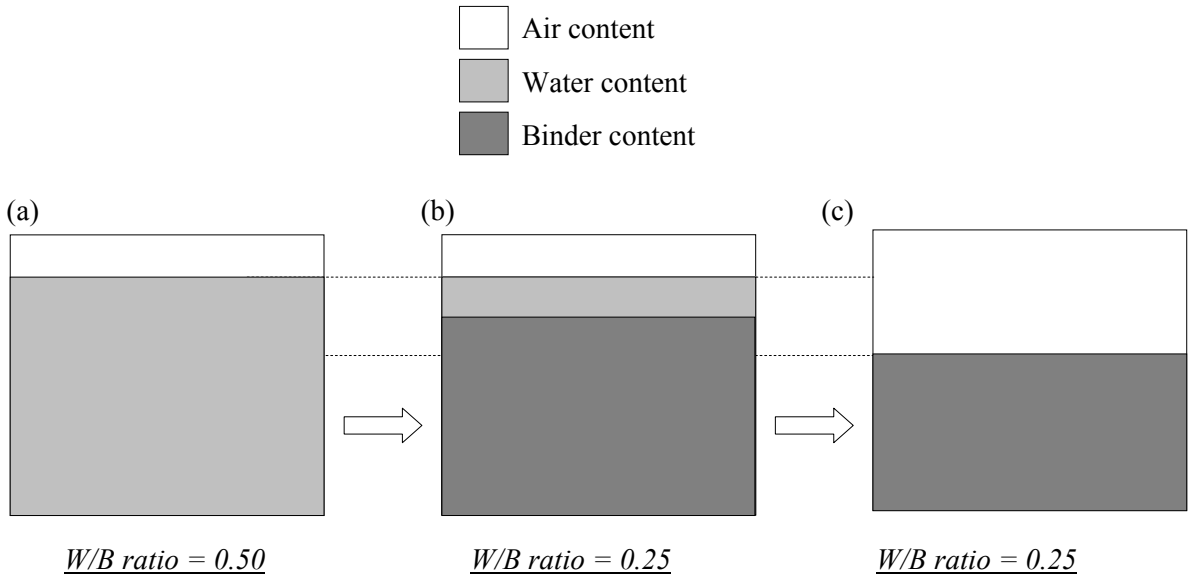


Figure 2.19: Schematic Representation of A Unit Volume of Paste for:
(a) A Conventional Concrete Mix,
(b) A Typical High-Performance Concrete Mix,
(c) A Porosity Transformed Concrete Mix [Rangaraju, 1997].

## 2.7 Summary of Findings

PART I

1. To comply with PRS, the adoption of novel construction materials is likely to be necessary. High-performance concrete has been identified as a potential material for use in bridge design and construction.

2. High-performance concrete has been defined as concrete meeting special performance provisions that cannot always be achieved using conventional methods and normal mixing, placing and curing procedures. Controversy exists concerning this definition, however, and in many cases concrete is classified as having 'high-performance' exclusively because it has high compressive strength.

3. No design methods capable of proportioning HPC for required levels of durability performance were found in the literature. Due to the inconsistency of HPC definition, the majority of existing methods for HPC have been developed to proportion concrete to achieve high levels of compressive strength.

4. Analysis of 254 HPC mixes indicated that HPC is generally prepared using w/b ratios in the range 0.25 to 0.40 and total binder contents in the range 350 to 500 kg/m$^3$. Water contents in the range 150 to 175 kg/m$^3$ are typically used in conjunction with superplasticizing chemical admixtures. Silica fume is the most popular replacement material for HPC, with binary PC/SF blends those most commonly used. In terms of performance and recognising the controversy surrounding the AASHTO T277-86 test method, HPC is best distinguished by high workability (150 to 200 mm slump), high strength (75 to 100 MPa at 28-days) and low chloride permeability (500 to 1000 Coulombs).

5. Most likely due to the wide range of data sources used and the inherent variability of concrete, strong correlations between HPC characteristics and performance were limited. However, relationships were evident

between the following. Water - binder ratio and (i) 28-day strength, (ii) diffusion coefficient, (iii) chloride permeability. Total binder content and (i) 28-day strength, (ii) diffusion coefficient, (iii) chloride permeability. PC content and (i) 28-day strength, (ii) diffusion coefficient. Silica fume content and (i) 28-day strength, (ii) diffusion coefficient.

6. The key properties of performance-related test methods have been discussed. In addition, the test methods included in current concrete-related PRS have been reviewed and their relevance to the current project discussed.

PART II

7. Based on information reported in the literature and an extensive survey carried out among 38 state DOTs, a list of potential key distress indicators (with respect to material performance) for Task 3.2.1 of the current project has been given. Based on these, a list of properties that may be specified in the proposed PRS has additionally been proposed.

8. In addition to HPC, the literature review has disclosed alternative materials to be considered for the design and construction of concrete bridge superstructures in Indiana; namely ternary binder concrete (TBC) and porosity-transformed concrete containing high dosages of air-entraining admixture. A brief review of the properties of these materials is given.

# 3 PHASE I: DEVELOPMENT OF OPTIMIZED HPC MIXES

## 3.1 Optimization Process - Statistical Design of the Experiment

Traditionally, many experimental programs that focus on evaluation of concrete properties are designed to hold all but one variable (factor under examination) constant. In this way, the variables are tested in sequence rather than in combination. While relatively simple, this approach may obscure interactions among variables, and is typically inefficient, requiring large numbers of concrete mixes to be prepared to obtain information on the effects of a single independent variable on the property of interest [Mason et al., 1989].

HPC mixes are typically composed of more ingredients than the traditional concrete mixes and therefore, one-component-at-a-time experiments would be extremely inefficient when trying to develop an optimized mixture. In order to properly account for interactions among various components of HPC, and to determine the influence of mixture composition on various performance parameters, a multiple-variable experiment must be carefully *designed* and statistically evaluated. Statistically designed experiment allows for a more systematic approach to the task of evaluation of the effects of multiple variables/factors on product/process performance by providing a structured design matrix.

During the current research program, a statistical experimental design procedure was adopted for the purposes of identifying the optimum concrete mixes in terms of several performance-related parameters. Using statistical principles to design the plan for the experimental work maximized the efficiency of the concrete preparation phase (by minimizing the number of mixes) and afforded the use of the test results in development of mathematical models to predict expected performance.

As presented in the first Interim Report [Ramirez et al., 1999], the production of HPC typically involves blending of Portland cement with two or three supplementary cementitious materials. In order to determine an optimum combination of the ingredients, a 3-factor central composite experimental design approach, as shown in Figure 3.1, was used in the current research program. Central composite experimental designs have been reported [Simon et al., 1999] to provide data that can be efficiently used to fit a full quadratic response-surface model.

### 3.1.1 Selection of Binder Combinations

Although the current INDOT specifications [Book of Standard Specifications, 1999] for Class C concrete allow the use of fly ash or ground granulated blast furnace slag as a partial replacement for Portland cement, they also stipulate that these pozzolanic materials can only be used individually. In fact, section 702.05 of these specifications explicitly prohibits the use of pozzolanic materials with blended cements. However, as indicated in the literature review presented in the previous Interim Report [Ramirez et al., 1999], a significant improvement in performance characteristics of concrete can be achieved by using a ternary binder system in which two (rather than one) pozzolanic materials are used as partial substitution for Portland cement. These improvements are typically attributed to the synergistic effects generated by interaction of the individual components of the blended binder during the hydration process. The supplementary cementitious materials most commonly used in ternary blends include silica fume, fly ash and slag. In order to develop concrete mixes that can offer enhanced performance, both binary and ternary blends were considered in the current research.

In compliance with the proposed research plan (Figure 1.1), the principal responses of interest selected for the experimental design were in the form of concrete performance characteristics (i.e., mechanical and durability properties). The independent factors influencing these responses were in the form of water-binder ratio and dosages of supplementary cementitious materials such as fly ash, silica fume and slag. Using only 15 factor combinations, the statistical approach allows the effect of all combinations of any three factors on a given response to be examined.

As illustrated in Figure 3.1, which shows the proposed experimental region geometrically, each of the 15 factor combinations to be considered in the experiment is represented by a point in a three-dimensional space. It is proposed to consider three separate composite designs using the following factor combinations:

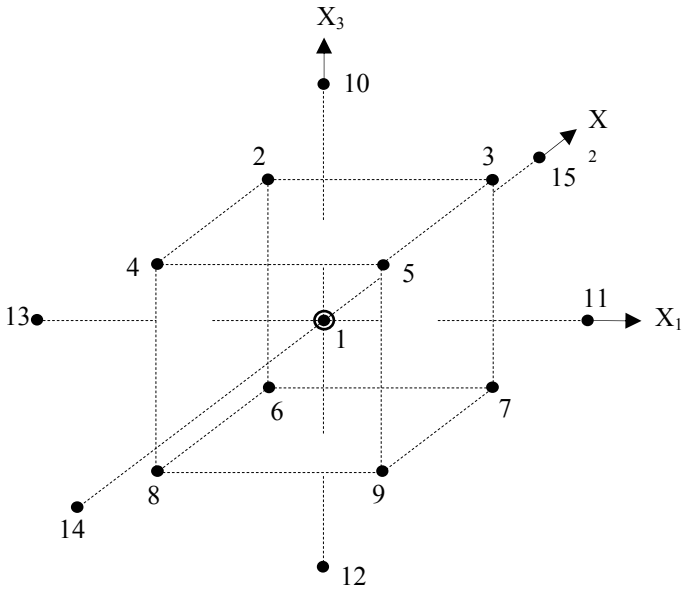


| EXPERIMENTAL DESIGN | FACTOR TO BE PLOTTED ON AXIS: | | |
|---|---|---|---|
| | $X_1$ | $X_2$ | $X_3$ |
| 1 | Fly ash (0-40%) | Silica fume (0-10%) | Water / binder ratio (0.30-0.50) |
| 2 | Slag (0-40%) | Silica fume | Water / binder ratio |
| 3 | Fly ash | Slag | Water / binder ratio |

By adopting experimental designs 1-3, as shown above, all possible combinations of silica fume, fly ash and slag will be accounted for over a given range of water-binder ratio:

- Portland cement only *(e.g. Design 1: silica fume dosage = 0, fly ash dosage = 0)*
- Portland cement + silica fume *(e.g. Design 2: fly ash dosage = 0)*
- Portland cement + fly ash *(e.g. Design 3: slag dosage = 0)*
- Portland cement + slag *(e.g. Design 2: silica fume dosage = 0)*
- Portland cement + silica fume + fly ash *(i.e. Design 1)*
- Portland cement + silica fume + slag *(i.e. Design 2)*
- Portland cement + fly ash + slag *(i.e. Design 3)*

Figure 3.1: Proposed 3-factor Composite Experimental Design **Procedure Figure 1:** 3-factor Central Composite Experimental Design Procedure

The mixture proportions for each factor combination are given in Tables 3.1 (a) – 3.3 (b).

- Silica fume dosage/fly ash dosage/water-binder ratio
- Silica fume dosage/slag dosage/water-binder ratio
- Fly ash dosage/slag dosage/water-binder ratio

In this way, and requiring a total of 45 (i.e., 15 × 3) concrete mixes, all possible combinations of silica fume, fly ash and slag will be considered over a range of water-binder ratios. Ranges of each factor (at five different levels) were determined based on literature review. For water-binder ratio, the range is from 0.30 to 0.50; for fly ash from 0% to 40% by weight of total binder; for silica fume from 0% to 10% by weight of total binder; and for slag from 0% to 40% by weight of total binder. The summary of all factor combinations to be considered in the current research is given in Tables 3.1 (a) – 3.3 (b).

### 3.1.2 Mix Design Parameters, Mix Proportions, and Testing Program

In order to simplify the experimental process, no air-entraining admixture (AEA) was used in any of the mixes prepared in Phase I. When developing the mixes for Phase I of the study, the following design parameters were also specified:

- Target slump: 5.5 inches with a tolerance of ±1.5 inches
- A total binder content: 390 kg/m$^3$ (657 lbs/yd $^3$) for all mixes
- The amount of coarse aggregate: 1100 kg/m$^3$ (1854 lbs/yd$^3$) for all mixes.

For each of the 45 mixes prepared in Phase I of this study, the following concrete properties were evaluated:

- Compressive Strength
- Modulus of Elasticity
- Rapid Chloride Penetration (RCP)
- Chloride Conductivity (CT).

The resulting data were used to prepare mathematical models (as described in Section 3.2 below) that were, in turn, used to select a set of representative (optimized) mixes for Phase II of the study.

Table 3.1(a): Factor Combinations to be Considered for PC/FA/SF Concrete Mixtures

| FACTOR COMBINATION | FACTORS CONSIDERED | | |
|---|---|---|---|
| | Fly ash dosage, % By mass of binder | Silica fume dosage, % By mass of binder | Water-binder ratio |
| ***1. PC/FA/SF mixes*** | | | |
| 1 | 20 | 5 | 0.40 |
| 2 | 10 | 7.5 | 0.45 |
| 3 | 30 | 7.5 | 0.45 |
| 4 | 10 | 2.5 | 0.45 |
| 5 | 30 | 2.5 | 0.45 |
| 6 | 10 | 7.5 | 0.35 |
| 7 | 30 | 7.5 | 0.35 |
| 8 | 10 | 2.5 | 0.35 |
| 9 | 30 | 2.5 | 0.35 |
| 10 | 20 | 5 | 0.50 |
| 11 | 40 | 5 | 0.40 |
| 12 | 20 | 5 | 0.30 |
| 13 | 0 | 5 | 0.40 |
| 14 | 20 | 0 | 0.40 |
| 15 | 20 | 10 | 0.40 |

Table 3.1(b): Concrete Mixture Proportions for PC/FA/SF Concrete Mixtures

| MIX NO. | CONSTITUENT MATERIAL, kg/m$^3$ | | | | | | | Water-binder ratio | ADMIXTURE DOSAGES, ml/m$^3$ |
|---|---|---|---|---|---|---|---|---|---|
| | Binder materials | | | | Water | Aggregate | | | |
| | PC | FA | SF | Total | | Fine | Coarse | | Superplasticizer [1, 2] |
| • ***Class C control mix*** | | | | | | | | | |
| | 390 | - | - | 390 | 170 | 735 | 1100 | 0.435 | - |
| • ***PC/FA/SF mixes*** | | | | | | | | | |
| 1 | 293 | 78 | 20 | 390 | 156 | 740 | 1100 | 0.40 | 761 |
| 2 | 322 | 39 | 29 | 390 | 175.5 | 697 | 1100 | 0.45 | 264 |
| 3 | 244 | 117 | 29 | 390 | 175.5 | 673 | 1100 | 0.45 | 466 |
| 4 | 341 | 39 | 10 | 390 | 175.5 | 705 | 1100 | 0.45 | 231 |
| 5 | 263 | 117 | 10 | 390 | 175.5 | 681 | 1100 | 0.45 | 245 |
| 6 | 322 | 39 | 29 | 390 | 136.5 | 798 | 1100 | 0.35 | 1203 |
| 7 | 244 | 117 | 29 | 390 | 136.5 | 775 | 1100 | 0.35 | 1694 |
| 8 | 341 | 39 | 10 | 390 | 136.5 | 806 | 1100 | 0.35 | 1537 |
| 9 | 263 | 117 | 10 | 390 | 136.5 | 783 | 1100 | 0.35 | 1162 |
| 10 | 293 | 78 | 20 | 390 | 195 | 638 | 1100 | 0.50 | 0 |
| 11 | 215 | 156 | 20 | 390 | 156 | 716 | 1100 | 0.40 | 778 |
| 12 | 293 | 78 | 20 | 390 | 117 | 841 | 1100 | 0.30 | 2269 |
| 13 | 371 | 0 | 20 | 390 | 156 | 763 | 1100 | 0.40 | 741 |
| 14 | 312 | 78 | 0 | 390 | 156 | 748 | 1100 | 0.40 | 394 |
| 15 | 273 | 78 | 39 | 390 | 156 | 732 | 1100 | 0.40 | 1042 |

[1] Quantities were established at time of mixing based on slump (5.5 ± 1.5 in).
[2] High Range Water Reducer (RHEOBUILD 3000FC from Master Builders, Inc.) to be used as required. The actual amount of the mixing water was reduced by the weight of admixtures used.

Table 3.2(a): Factor Combinations to be Considered for PC/GGBS/SF Concrete Mixtures

| FACTOR COMBINATION | FACTORS CONSIDERED | | |
|---|---|---|---|
| | Slag dosage, % By mass of binder | Silica fume dosage, % By mass of binder | Water-binder ratio |
| ***2. PC/GGBS/SF mixes*** | | | |
| 1 | 20 | 5 | 0.40 |
| 2 | 10 | 7.5 | 0.45 |
| 3 | 30 | 7.5 | 0.45 |
| 4 | 10 | 2.5 | 0.45 |
| 5 | 30 | 2.5 | 0.45 |
| 6 | 10 | 7.5 | 0.35 |
| 7 | 30 | 7.5 | 0.35 |
| 8 | 10 | 2.5 | 0.35 |
| 9 | 30 | 2.5 | 0.35 |
| 10 | 20 | 5 | 0.50 |
| 11 | 40 | 5 | 0.40 |
| 12 | 20 | 5 | 0.30 |
| 13 | 0 | 5 | 0.40 |
| 14 | 20 | 0 | 0.40 |
| 15 | 20 | 10 | 0.40 |

Table 3.2(b): Concrete Mixture Proportions for PC/GGBS/SF Concrete Mixtures

| MIX NO. | CONSTITUENT MATERIAL, kg/m$^3$ | | | | | | | Water-binder ratio | ADMIXTURE DOSAGES, ml/m$^3$ |
|---|---|---|---|---|---|---|---|---|---|
| | Binder materials | | | | Water | Aggregate | | | |
| | PC | Slag | SF | Total | | Fine | Coarse | | Superplasticizer [1, 2] |
| • ***Class C control mix*** | | | | | | | | | |
| | 390 | - | - | 390 | 170 | 735 | 1100 | 0.435 | - |
| • ***PC/Slag/SF mixtures*** | | | | | | | | | |
| 1 | 293 | 78 | 20 | 390 | 156 | 758 | 1100 | 0.40 | 806 |
| 2 | 322 | 39 | 29 | 390 | 175.5 | 706 | 1100 | 0.45 | 264 |
| 3 | 244 | 117 | 29 | 390 | 175.5 | 701 | 1100 | 0.45 | 241 |
| 4 | 341 | 39 | 10 | 390 | 175.5 | 714 | 1100 | 0.45 | 250 |
| 5 | 263 | 117 | 10 | 390 | 175.5 | 709 | 1100 | 0.45 | 185 |
| 6 | 322 | 39 | 29 | 390 | 136.5 | 808 | 1100 | 0.35 | 1685 |
| 7 | 244 | 117 | 29 | 390 | 136.5 | 802 | 1100 | 0.35 | 1653 |
| 8 | 341 | 39 | 10 | 390 | 136.5 | 815 | 1100 | 0.35 | 1565 |
| 9 | 263 | 117 | 10 | 390 | 136.5 | 810 | 1100 | 0.35 | 1533 |
| 10 | 293 | 78 | 20 | 390 | 195 | 657 | 1100 | 0.50 | 0 |
| 11 | 215 | 156 | 20 | 390 | 156 | 753 | 1100 | 0.40 | 1236 |
| 12 | 293 | 78 | 20 | 390 | 117 | 860 | 1100 | 0.30 | 2833 |
| 13 | 371 | 0 | 20 | 390 | 156 | 763 | 1100 | 0.40 | 1088 |
| 14 | 312 | 78 | 0 | 390 | 156 | 766 | 1100 | 0.40 | 907 |
| 15 | 273 | 78 | 39 | 390 | 156 | 750 | 1100 | 0.40 | 1120 |

[1] Quantities were established at time of mixing based on slump (5.5 ± 1.5 in)
[2] High Range Water Reducer (RHEOBUILD 3000FC from Master Builder, Inc.) to be used as required. The actual amount of the mixing water was reduced by the weight of admixtures used

Table 3.3(a): Factor Combinations to be Considered for PC/FA/GGBS Concrete Mixtures

| FACTOR COMBINATION | FACTORS CONSIDERED | | |
|---|---|---|---|
| | Fly ash, % By mass of binder | Slag, % By mass of binder | Water-binder ratio |
| ***3. PC/FA/GGBS mixes*** | | | |
| 1 | 20 | 20 | 0.40 |
| 2 | 10 | 30 | 0.45 |
| 3 | 30 | 30 | 0.45 |
| 4 | 10 | 10 | 0.45 |
| 5 | 30 | 10 | 0.45 |
| 6 | 10 | 30 | 0.35 |
| 7 | 30 | 30 | 0.35 |
| 8 | 10 | 10 | 0.35 |
| 9 | 30 | 10 | 0.35 |
| 10 | 20 | 20 | 0.50 |
| 11 | 40 | 20 | 0.40 |
| 12 | 20 | 20 | 0.30 |
| 13 | 0 | 20 | 0.40 |
| 14 | 20 | 0 | 0.40 |
| 15 | 20 | 40 | 0.40 |

Table 3.3(b): Concrete Mixture Proportions for PC/FA/GGBS Concrete Mixtures

| MIX NO. | CONSTITUENT MATERIAL, kg/m$^3$ | | | | | | | Water-binder ratio | ADMIXTURE DOSAGES, ml/m$^3$ |
|---|---|---|---|---|---|---|---|---|---|
| | Binder materials | | | | Water | Aggregate | | | |
| | PC | FA | Slag | Total | | Fine | Coarse | | Superplasticizer [1, 2] |
| • ***Class C control mix*** | | | | | | | | | |
| | 390 | - | - | 390 | 170 | 735 | 1100 | 0.435 | - |
| • ***PC/FA/Slag mixtures*** | | | | | | | | | |
| 1 | 234 | 78 | 78 | 390 | 156 | 743 | 1100 | 0.40 | 694 |
| 2 | 234 | 39 | 117 | 390 | 175.5 | 701 | 1100 | 0.45 | 0 |
| 3 | 156 | 117 | 117 | 390 | 175.5 | 677 | 1100 | 0.45 | 0 |
| 4 | 312 | 39 | 39 | 390 | 175.5 | 706 | 1100 | 0.45 | 0 |
| 5 | 234 | 117 | 39 | 390 | 175.5 | 683 | 1100 | 0.45 | 0 |
| 6 | 234 | 39 | 117 | 390 | 136.5 | 802 | 1100 | 0.35 | 1074 |
| 7 | 156 | 117 | 117 | 390 | 136.5 | 779 | 1100 | 0.35 | 1208 |
| 8 | 312 | 39 | 39 | 390 | 136.5 | 808 | 1100 | 0.35 | 1120 |
| 9 | 234 | 117 | 39 | 390 | 136.5 | 784 | 1100 | 0.35 | 1060 |
| 10 | 234 | 78 | 78 | 390 | 195 | 641 | 1100 | 0.50 | 0 |
| 11 | 156 | 156 | 78 | 390 | 156 | 719 | 1100 | 0.40 | 315 |
| 12 | 234 | 78 | 78 | 390 | 117 | 844 | 1100 | 0.30 | 1713 |
| 13 | 312 | 0 | 78 | 390 | 156 | 766 | 1100 | 0.40 | 537 |
| 14 | 312 | 78 | 0 | 390 | 156 | 748 | 1100 | 0.40 | 310 |
| 15 | 156 | 78 | 156 | 390 | 156 | 737 | 1100 | 0.40 | 278 |

[1] Quantities were established at time of mixing based on slump (5.5 ± 1.5 in).
[2] High Range Water Reducer (RHEOBUILD 3000FC from Master Builders, Inc.) to be used as required. The actual amount of the mixing water was reduced by the weight of admixtures used

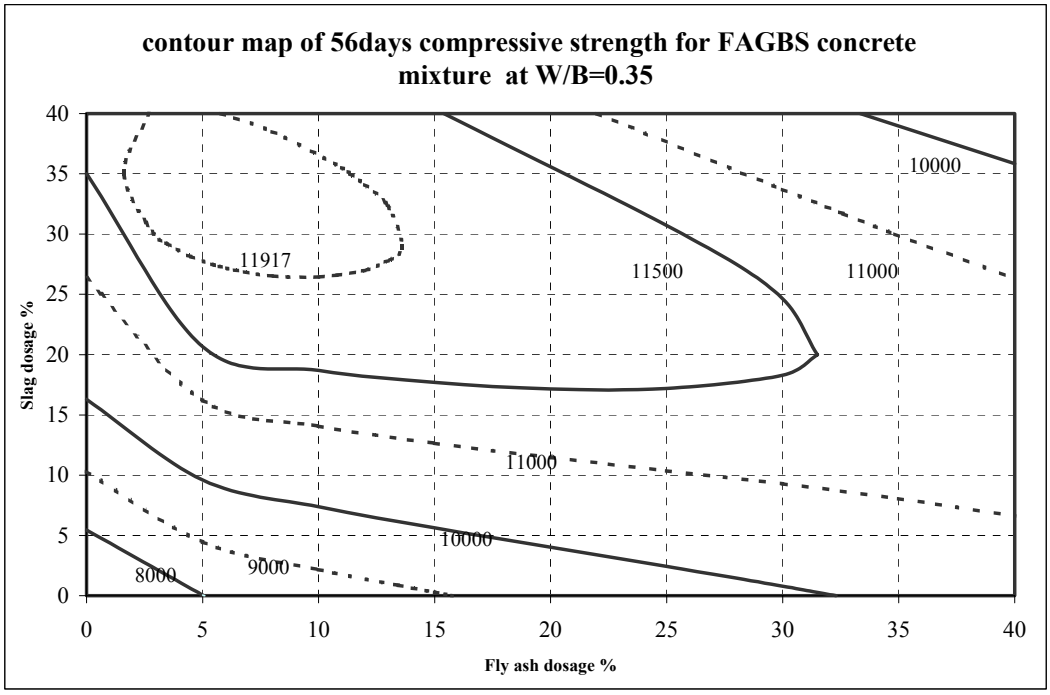


Figure 3.2: Example Contour Map for 56-day Compressive Strength (in psi) (FAGBS System, w/b=0.35)

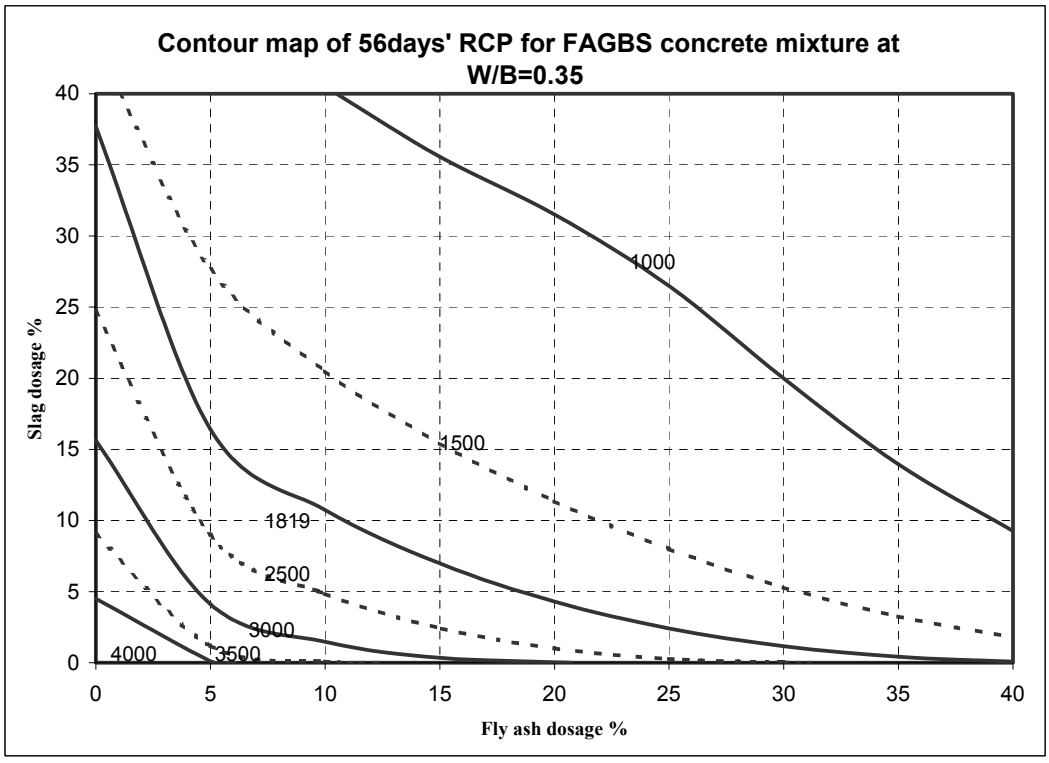


Figure 3.3: Example Contour Map for 56-day RCP Value (in Coulombs) (FAGBS System, w/b=0.35)

### 3.2 Response Surface Method and Model Development

The data generated from the previously described 3-factor central composite experimental design can be conveniently evaluated using response-surface methodology. Response-surface methods are especially useful in the situations where one or more measured responses (that need to be optimized) are influenced by several factors as they help to identify and characterize relationships existing between each response and various combinations of the influencing factors. This is often achieved by constructing models that describe each response over applicable ranges of the factors of interest. In order to construct appropriate models, a statistical procedure such as multiple regression analysis is often used to develop multivariate relationships linking measured characteristics and performance levels achieved. In many cases the relationships between response function and measured characteristic are best characterized by polynomial models. Polynomial models are well suited to engineering problems where the underlying mechanism generating data is not well understood due to the complexity of the problem and the lack of sufficient theory. In such cases, polynomial models can often provide adequate approximations to the known functional relationship.

When using multiple regression analysis to construct models various combinations of variables are used until the accuracy (in terms of an $R^2$ value) of the models developed is optimized. After that goal is accomplished, the results are displayed graphically using contour maps. These contour maps (also referred to as response surfaces) are then analyzed to determine factor combinations for which each response variable is an optimum. Figures 3.2 and 3.3 give examples of the typical forms of contour maps obtained from the experimental data. By overlaying the contour maps produced for each response, optimum variables in terms of more than one response may be potentially identified. In the current research, the procedures undertaken to construct appropriate models included the following steps:

Step 1: Performing a simple statistical analyses of the raw results obtained from the experiment. This analysis included calculation of result means, standard deviations and coefficients of variance. The objective of this step was to identify and remove any erroneous results. It was felt that in this way, the accuracy of the model would be improved.

Step 2: Performing regression analysis using the test results obtained from Step 1. In each instance, regression analysis was initially carried out using a confidence level of 95% and the following equation;

$$Y = m_1X_1 + m_2X_2 + m_3X_3 + m_4X_1^2 + m_5X_2^2 + m_6X_3^2 + m_7X_1X_2 + m_8X_1X_2 + m_9X_2X_3 + m_{10}X_1X_3 + m_{11}X_1^{0.5} + m_{12}X_2^{0.5} + m_{13}X_3^{0.5} \quad (3.1)$$

where:
Y is the desired performance characteristic (e.g., compressive strength or chloride permeability)
$X_1$, $X_2$ and $X_3$ are the variables being considered (e.g., $X_1$ = fly ash content, $X_2$ = silica fume content and $X_3$ = water-binder ratio)
$m_i$, $m_{ij}$ are the regression parameter

Step 3: Checking the F-value of the equation. The F-value is a measure of the potential existence of a relationship between the response and the independent variables. If the F-value is larger than a standard value of $F_{\alpha, k, n-k-1}$ (where $\alpha$ is the confidence level chosen in the analysis, k is the number of variables in the equation, n is the number of data points modeled), then it can be stated with certain confidence that the relationship does indeed exist.

Step 4: Checking the t-value of each variable in the equation. If the t-value of any variable is larger than the standard $T_{\alpha/2, n-1}$ (where $\alpha$ is the confidence level chosen in the analysis, n is the number of data points modeled), it can be concluded that the variable is significant to the response. Variables exhibiting t-values less than $T_{\alpha/2, n-1}$ were omitted from the equation. At the same time, the standard deviation of the equation and the adjusted $R^2$ should be also checked. Smaller standard deviations and higher adjusted $R^2$ values represent more accurate models.

Step 5 Repeating regression analyses after deletion of some of the terms involving certain combinations of variables. The checks described in step 4 were then repeated. The objective of the fifth step was to delete all insignificant variables from the equation and to check again that all remaining variables are significant.

Step 6 If required, additional variables were added to the equation in step six to improve the accuracy of the equation (i.e., to lower standard deviation and to increase adjusted value of $R^2$).

Step 7 If some variables in the equation were found to be significant, but not very significant, the power of the variable was changed in step seven to improve the degree of significance of the variable.

Step 8: If the accuracy of the final equation is still not very good after the previous steps (e.g., $R^2$ is lower than 0.90, or the coefficient of variation is too large or too small), the response variable was mathematically transformed (e.g., by applying the log function) and the previous steps were repeated.

## 3.3 Materials and Experimental Procedures

This section describes the materials used for production of concrete mixtures used in Phase I of this study. In addition, the experimental procedures used for production and testing of concrete are also presented.

### 3.3.1 Materials

Portland Cement
An ASTM Type I Portland cement produced by Lone Star Industries plant at Greencastle, IN was used throughout this study. This cement is widely used in the northwestern part of Indiana. The composition and physical characteristics of this cement are presented in Table 3.4.

Aggregates
The coarse aggregate used in this study was No. 8 crushed stone (in accordance with Section 904.02 of the 1999 Book of Standards of the Indiana Department of Transportation) and was supplied by the Martin Marietta plant in Indianapolis. The selected physical properties and sieve analysis data for the coarse aggregate are given in Table 3.5. The fine aggregate used in this study was No. 23 (in accordance with Section 904.01 of the 1999 Book of Standards of the Indiana Department of Transportation) natural sand supplied by the IMI plant in Greenwood, Indiana. The selected physical properties and sieve analysis data for fine aggregate are given in Table 3.6. The aggregate correction factor for the air content determination was 0.3%.

Mineral Admixtures
Mineral admixtures used in this study included fly ash, silica fume and ground granulated blast furnace slag. The fly ash was Class C, supplied by American FlyAsh Company. Bulk specific gravity of this fly ash was 2.700. The silica fume used was EMSAC, Type F-100, in powder form supplied by W. R. Grace & Co. The bulk specific gravity of this silica fume was 2.167. Holnam Inc., in Chicago supplied the slag. The bulk specific gravity of the slag was 2.924.

Chemical Admixtures
RHEOBUILD 3000FC superplasticizer produced by Master Builders, Inc. was used in Phase I of this study. This superplasticizer meets requirements of ASTM C494 for Type A, water-reducing, and Type F, high range water-reducing admixture. The normal dosage rate range recommended by manufacturer is 4 - 6 fl oz. per 100 lbs of cement (260 - 390 ml per 100 kg) of cement.

### 3.3.2 Batching, Mixing, and Curing Procedures

The standard laboratory batching and mixing procedures were used in the current study. All batches were mixed in the capacity the pan mixer with capacity of 2-$ft^3$. After casting, the specimens remained in the molds (covered with wet burlap) for a period of 24 hours. The specimens were then demolded and stored in a moist room (100% RH) until tested.

### 3.3.3 Compressive Strength

Compressive strength tests were performed in accordance with the Standard Method of Test for Compressive Strength of Cylindrical Concrete Specimens (AASHTO T22-97). Compressive strength determinations were performed using 4” x 8” concrete cylinders.

### 3.3.4 Rapid Chloride Penetration Test (RCPT)

Rapid chloride penetration test was performed in accordance with the Standard Test Method for Electrical Indication of Concrete's Ability to Resist Chloride Ion Penetration (AASHTO T 277-96). It is a quick test method that gives an indication of concrete resistance to the penetration of chloride ions. However, for poor quality concrete the results of this test can be influenced by temperature and by the fact that the ionic strength of the pore solution in hardened concrete could be quite variable depending on cement and admixture type and content. In addition, some research results suggest [Zia and Hansen, 1993] that the validity of RCPT as a measure of chloride penetration should be reevaluated, particularly in terms of its application to HPC, as high performance concrete may contain additional ions resulting from the use of various admixtures.

### 3.3.5 Chloride Conductivity Test (CT)

In order to avoid some of the difficulties associated with the use of RCP test for HPC, a chloride conductivity test developed at the University of Cape Town, South Africa [Streicher and Alexander, 1995], was adopted in this study. The schematic of the conduction cell is shown in Figure 3.4. The specimens used for this test were in the form of concrete discs that were 25-mm thick and had a diameter of 68 mm. Before the conductivity test was performed, the specimens were pre-conditioned by drying in an oven for a minimum of 7 days at the temperature of 50 ± 2°C. After the drying period, the specimens were cooled to room temperature by placing them for 1 hour on a dry steel plate and than placed in a desiccator and subjected to a vacuum for 3 hours to remove air from concrete pores. Immediately after 3 hours, a 5M NaCl solution was allowed to enter the vacuum chamber, and the specimens and solution were kept under vacuum for additional 5 hours. After vacuum saturation, the samples were left to soak in the NaCl solution for additional period of 18 ± 1hrs. After the conditioning was completed, the samples were subjected to a potential of 10V applied across the end of each specimens using a conduction cell filled with a 5M NaCl solution and the electrical current passing through each specimen was measured.

To determine the conductivity value the measured current and applied voltage were substituted into equation show below:

$$\sigma = \frac{it}{VA} \qquad \text{.....(3.2)}$$

where:
$\sigma$ = conductivity of sample (mS/cm)
i = electrical current (mA)
V = potential difference (V)
t = thickness of the sample (cm)
A = Cross sectional area of sample ($cm^2$)

It should be noted that in general lower conductivity values are more desirable as they indicate that concrete is more resistant to chloride ion penetration.

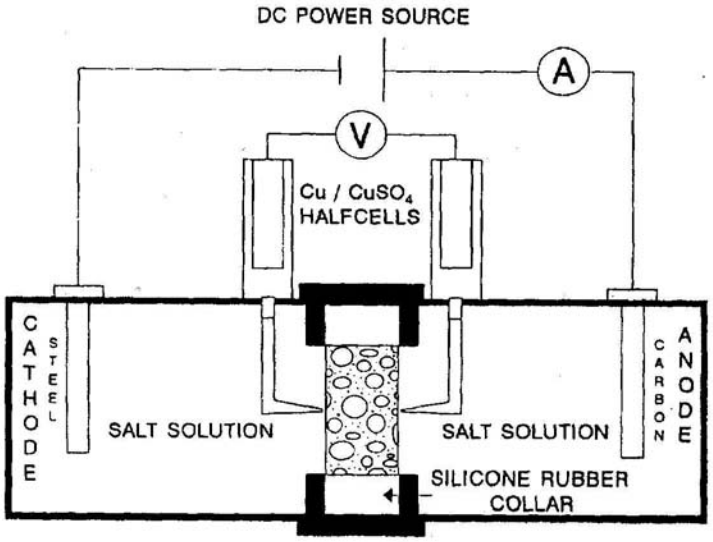


Figure 3.4: Schematic of the Cell Used for the Chloride Conductivity Test [Streicher and Alexander, 1995]

Table 3.4: Composition and Physical Characteristics of Cement Used in Phase I

| Chemical Composition (%) | | Physical Data | |
|---|---|---|---|
| CaO | 65.11 | Expansion, % | 0.01 |
| $SiO_2$ | 20.03 | Air Entrainment, % | 7 |
| $Al_2O_3$ | 5.28 | Setting Time: | |
| $Fe_2O_3$ | 2.50 | Vicat, min | 85 |
| MgO | 1.21 | Wagner, $m^2/kg$ | 192 |
| $SO_3$ | 2.36 | | |
| $Na_2O$ | 0.12 | | |
| $K_2O$ | 0.43 | | |
| Total Alkali as $Na_2O$ | 0.40 | | |
| Loss on Ignition | 2.65 | | |
| Potential Compound Composition, % | | Compressive Strength, psi | |
| $C_3S$ | 67 | | |
| $C_2S$ | 7 | 3 day | 3200 |
| $C_3A$ | 10 | 7 day | 4600 |
| $C_4AF$ | 8 | | |

Table 3.5: Physical Properties and Gradation of Coarse Aggregate (Phase I mixtures)

| Bulk Specific Gravity (saturated surface-dry) $BSG_{SSD}$=2.676<br>Absorption =1.18% | | | INDOT #8<br>Passing Percent |
|---|---|---|---|
| Sieve Designation | Cumulative Weight Percent | | |
| | Retained | Passing | |
| 1” | 0.2 | 99.8 | 100 |
| 3/4” | 5.2 | 94.8 | 75-95 |
| 1/2” | 34.7 | 65.3 | 40-70 |
| 3/8” | 54.7 | 45.3 | 20-50 |
| No.4 | 81.4 | 18.6 | 0-15 |
| Less than No.4 | 99.9 | | 0-10 |

Table 3.6: Physical Properties and Gradation of Fine Aggregate (Phase I Mixtures)

| Fineness Modulus FM=2.71<br>Bulk Specific Gravity (saturated surface-dry) $BSG_{SSD}$=2.63<br>Absorption =1.63% | | | INDOT #23<br>Passing Percent |
|---|---|---|---|
| Sieve Designation | Cumulative Weight Percent | | |
| | Retained | Passing | |
| No.4 | 0.04 | 99.96 | 95-100 |
| No.8 | 4.73 | 95.27 | 80-100 |
| No.16 | 27.33 | 72.67 | 50-85 |
| No.30 | 52.73 | 47.27 | 25-60 |
| No.50 | 87.9 | 12.10 | 5-30 |
| No.100 | 98.46 | 1.54 | 0-10 |
| Dust | 100 | | 0-3 |

### 3.3.6 Static Modulus of Elasticity

The test for static modulus of elasticity was conducted in compliance with the Standard Test Method for Static Modulus of Elasticity and Poisson's Ratio of Concrete Compression (ASTM C469-94). Static modulus of elasticity of hardened concrete was determined by testing 100 mm x 200 mm (4" x 8") cylinders. These cylinders were axially loaded in a universal testing machine with the load capacity of 100000 lbs. The strain of the cylinder was measured through a compressometer. The specimen was loaded up to 40% of the ultimate load of cylinders achieved from compressive strength testing. The slope of the secant from the resulting stress-strain curve was used to determine the static modulus of elasticity.

$$E = \frac{(\sigma_2 - \sigma_1)}{\varepsilon_2 - 50 \times 10^{-6}} \quad \text{.....(3.3)}$$

where:
$\sigma_1$ and $\sigma_2$ are the stress corresponding to the initial strain (50 microstrains) and a final strain at 40% of the ultimate load, respectively.

## 3.4 Results and Discussion

### 3.4.1 Statistical Evaluation of the Test Results and Model Development

Performance results, including compressive strength results (7, 28 and 56 days), modulus of elasticity data (28 and 56 days), rapid chloride penetration results (8 and 56 days) and chloride conductivity results (28 and 56 days), for PC/FA/SF, PC/GGBS/SF and PC/FA/GGBS concrete mixes produced in Phase I of the study are given in Tables 3.7 - 3.9. As can be seen from these tables, a wide range of results was obtained reflecting the broad range of mix compositions used in this study. In order to establish a relationship between mixture parameters (namely, water-binder ratio and dosages of supplementary cementitious materials) and performance, the multiple regression analysis was used to analyze the data generated. For each group of three components mixes a total of 9 mathematical models were developed, including three compressive strength models (7, 28, 56 days); two rapid chloride penetration models (28 and 56 days); two chloride conductivity models (28 and 56 days); and two static modulus of elasticity models (28 and 56 days). In all, 27 mathematical models were generated from the 45 mixes. The details of the models are shown in Tables 3.10 - 3.12.

### 3.4.2 Contour Maps

The best way to quickly evaluate the results produced by the model is to create a contour map of the response function. All 27 of the previously developed models were used to perform simulations at 3 different water-binder ratios (w/b = 0.45, 0.40, 0.35). As a result, 81 contour maps that relate the binder and mix composition to various concrete parameters (quality characteristics/performance indictors) were generated. Each of these contour maps gives an indication of how performance varies in response to changes in relative proportions of mineral admixtures when water-binder ratio is held constant. By adding the measured values of a given parameter to the corresponding contour map, the degree of accuracy with which the developed models predict performance can also be evaluated.

In order to determine the optimum mixture composition as a function of more than one parameter (performance indicator) the contour maps produced for selected values (threshold values defined in Table 3.13) of individual parameters were superimposed on each other. The overlaid contour maps for each mix system at different water-binder ratio are shown in Figures 3.5 - 3.13. Each of these Figures contains four individual contour maps that were developed for one of the following four parameters: i) compressive strength at 28, ii) compressive strength at 56 days, iii) resistance to chloride ions penetration at 56 days, and iv) conductivity at 56 days. Based on literature review, these properties (with the exception of conductivity at 56 days) have been frequently specified and measured on other projects involving HPC. They are related to long-term performance of concrete, and are relatively easy to measure and as such are often monitored for QC/QA purposes. After these parameters were selected, a threshold value was assigned to each of them (see Table 3.13) and used to select the composition of an optimum binder.

When selecting the threshold values for strength the overall goal was to ensure that the concrete used in bridge construction will achieve a strength in the range 5,000 - 8,000 psi at an average air content of about 6%. Since none of the mixes prepared in Phase I was air-entrained, an allowance was made for strength decrease with the increase in the air content of the mix. It was assumed that the average strength reduction would be about 500 psi for 1% of entrained air. The threshold values for RCP test were selected based on the goal of achieving concrete with low and very low permeability using the scale included in AASHTO T 277-96. The threshold values selected for chloride conductivity (CT) were also based on the desire to achieve concrete with excellent performance. Due to a lack of standard limits for this property, guidelines developed in one of the earlier studies [Alexander and Magee, 1999] were adopted in the current investigation. These guidelines stipulate that concrete can be expected to give an excellent performance if the chloride conductivity value of concrete at 56 days is smaller than 0.75 mS/cm. The good performance can be expected from concrete at 56 days with the chloride conductivity value in the range of 0.75 - 1.5 mS/cm.

Table 3.7: Test Results for Concrete Mixtures Containing PC/FA/SF

| CONCRETE MIXTURE DETAILS | | | | PERFORMANCE RESULTS | | | | | | | | |
|---|---|---|---|---|---|---|---|---|---|---|---|---|
| Mix No. | FA dosage % by mass | SF dosage % by mass | w/b ratio | Modulus of Elasticity (ksi)[1] 28days | 56days | Compressive Strength[2] (psi) 7days | 28days | 56days | RCPT[3] results (Coulombs) 28days | 56days | CT[4] (mS/cm) 28days | 56days |
| 01 | 20 | 5 | 0.4 | 4524 | 4959 | 6406 | 8694 | 9191 | 2415 | 1605 | 1.07 | 0.99 |
| 02 | 10 | 7.5 | 0.45 | 4800 | 4945 | 6048 | 9112 | 8674 | 2097 | 1621 | 1.01 | 0.90 |
| 03 | 30 | 7.5 | 0.45 | 4988 | 5351 | 7003 | 8594 | 9569 | 1294 | 820 | 0.74 | 1.00 |
| 04 | 10 | 2.5 | 0.45 | 4858 | 5336 | 6685 | 7600 | 8574 | 2774 | 2610 | 1.00 | 0.65 |
| 05 | 30 | 2.5 | 0.45 | 4771 | 5336 | 6366 | 9589 | 9510 | 2406 | 1617 | 0.77 | 0.80 |
| 06 | 10 | 7.5 | 0.35 | 4901 | 4988 | 10086 | 12056 | 12772 | 677 | 511 | 0.41 | 0.33 |
| 07 | 30 | 7.5 | 0.35 | 4988 | 5844 | 9410 | 12195 | 12255 | 831 | 587 | 0.45 | 0.37 |
| 08 | 10 | 2.5 | 0.35 | 5206 | 5539 | 9927 | 12275 | 12215 | 1596 | 1391 | 0.80 | 0.74 |
| 09 | 30 | 2.5 | 0.35 | 5641 | 5945 | 8415 | 11260 | 12136 | 1800 | 1222 | 0.60 | 0.66 |
| 10 | 20 | 5 | 0.5 | 4553 | 4582 | 5909 | 8097 | 8117 | 3547 | 2404 | 1.16 | 1.07 |
| 11 | 40 | 5 | 0.4 | 5148 | 5597 | 6844 | 9490 | 9828 | 1449 | 973 | 0.61 | 0.55 |
| 12 | 20 | 5 | 0.3 | 5757 | 6003 | 10624 | 13429 | 14006 | 747 | 536 | 0.37 | 0.34 |
| 13 | 0 | 5 | 0.4 | 5162 | 5568 | 8117 | 9271 | 10285 | 1485 | 1330 | 0.70 | 0.90 |
| 14 | 20 | 0 | 0.4 | 5032 | 5481 | 7142 | 8972 | 9569 | 4091 | 3021 | 0.93 | 0.99 |
| 15 | 20 | 10 | 0.4 | 5032 | 5409 | 7600 | 9947 | 10325 | 1206 | 723 | 0.49 | 0.43 |

1 Conversion Factor: 1 GPa = 145 ksi.
2 Concrete tested here was non-air entrained concrete
3 Rapid Chloride Ion Permeability Test (RCPT)
4 Chloride Conductivity test (CT)

Table 3.8: Test Results for Concrete Mixtures Containing PC/GGBS/SF

| CONCRETE MIXTURE DETAILS | | | | PERFORMANCE RESULTS | | | | | | | | |
|---|---|---|---|---|---|---|---|---|---|---|---|---|
| Mix | FA dosage | GGBS dosage | w/b | Modulus of Elasticity (ksi)[1] | | Compressive Strength[2] (psi) | | | RCPT[3] results (Coulombs) | | CT[4] (mS/cm) | |
| No. | % by mass | % by mass | ratio | 28days | 56days | 7days | 28days | 56days | 28days | 56days | 28days | 56days |
| 01 | 20 | 5 | 0.4 | 5467 | 5597 | 6406 | 10126 | 9888 | 1024 | 715 | 0.54 | 0.41 |
| 02 | 10 | 7.5 | 0.45 | 4959 | 5423 | 6048 | 8594 | 8933 | 1229 | 798 | 0.74 | 0.67 |
| 03 | 30 | 7.5 | 0.45 | 4814 | 5481 | 7003 | 8773 | 9510 | 1037 | 604 | 0.67 | 0.57 |
| 04 | 10 | 2.5 | 0.45 | 4785 | 5162 | 6685 | 7022 | 8256 | 2899 | 2416 | 1.17 | 0.95 |
| 05 | 30 | 2.5 | 0.45 | 5133 | 5191 | 6366 | 7997 | 8455 | 2255 | 1509 | 0.98 | 0.80 |
| 06 | 10 | 7.5 | 0.35 | 5684 | 5873 | 10086 | 11260 | 12036 | 795 | 534 | 1.04 | 0.44 |
| 07 | 30 | 7.5 | 0.35 | 5728 | 5960 | 9410 | 12513 | 12096 | 667 | 417 | 1.08 | 0.29 |
| 08 | 10 | 2.5 | 0.35 | 4655 | 5409 | 9927 | 10106 | 10504 | 1668 | 1312 | 0.84 | 0.71 |
| 09 | 30 | 2.5 | 0.35 | 5829 | 6061 | 8415 | 10743 | 10624 | 1312 | 953 | 0.60 | 0.52 |
| 10 | 20 | 5 | 0.5 | 4423 | 4887 | 5909 | 6724 | 6923 | 2843 | 2483 | 1.49 | 1.32 |
| 11 | 40 | 5 | 0.4 | 5525 | 5438 | 6844 | 10026 | 10186 | 864 | 550 | 0.66 | 0.44 |
| 12 | 20 | 5 | 0.3 | 6134 | 5873 | 10624 | 12831 | 14264 | 692 | 456 | 0.27 | 0.28 |
| 13 | 0 | 5 | 0.4 | 5090 | 5539 | 8117 | 9609 | 9470 | 1991 | 1483 | 1.09 | 0.89 |
| 14 | 20 | 0 | 0.4 | 5336 | 5742 | 7142 | 8116 | 9211 | 3447 | 2618 | 1.08 | 0.76 |
| 15 | 20 | 10 | 0.4 | 4916 | 5249 | 7600 | 8853 | 7998 | 833 | 519 | 0.79 | 0.79 |

1 Conversion Factor: 1 GPa = 145 ksi.
2 Concrete tested here was non-air entrained concrete
3 Rapid Chloride Ion Permeability Test (RCPT)
4 Chloride Conductivity test (CT)

Table 3.9: Test Results for Concrete Mixtures Containing PC/FA/GGBS

| CONCRETE MIXTURE DETAILS | | | | PERFORMANCE RESULTS | | | | | | | | |
|---|---|---|---|---|---|---|---|---|---|---|---|---|
| Mix No. | FA dosage % by mass | GGBS dosage % by mass | w/b ratio | Modulus of Elasticity (ksi)[1] 28days | Modulus of Elasticity (ksi)[1] 56days | Compressive Strength[2] (psi) 7days | Compressive Strength[2] (psi) 28days | Compressive Strength[2] (psi) 56days | RCPT[3] results (Coulombs) 28days | RCPT[3] results (Coulombs) 56days | CT[4] (mS/cm) 28days | CT[4] (mS/cm) 56days |
| 01 | 20 | 5 | 0.4 | 5351 | 5322 | 6386 | 8594 | 9967 | 2744 | 1548 | 1.93 | 0.71 |
| 02 | 10 | 7.5 | 0.45 | 4901 | 5162 | 5232 | 7361 | 8256 | 3262 | 2054 | 1.20 | 0.85 |
| 03 | 30 | 7.5 | 0.45 | ---- | 4988 | 4357 | 7719 | 7162 | 3765 | 1954 | 1.18 | 0.80 |
| 04 | 10 | 2.5 | 0.45 | 5104 | 5133 | 6446 | 8336 | 9171 | 5169 | 3109 | 1.49 | 1.07 |
| 05 | 30 | 2.5 | 0.45 | 5133 | 5061 | 5232 | 8395 | 9907 | 4187 | 2191 | 1.36 | 0.78 |
| 06 | 10 | 7.5 | 0.35 | 5568 | 5858 | 7759 | 10564 | 11917 | 1707 | 1279 | 0.96 | 0.60 |
| 07 | 30 | 7.5 | 0.35 | 5945 | 5612 | 6565 | 9888 | 10942 | 1409 | 930 | 0.60 | 0.37 |
| 08 | 10 | 2.5 | 0.35 | 5525 | 5626 | 6824 | 9251 | 10723 | 2358 | 1819 | 0.84 | 0.81 |
| 09 | 30 | 2.5 | 0.35 | 5510 | 5742 | 6784 | 9072 | 10643 | 2395 | 1451 | 0.85 | 0.56 |
| 10 | 20 | 5 | 0.5 | 4959 | 4916 | 5113 | 7958 | 9370 | 4117 | 2235 | 1.32 | 1.31 |
| 11 | 40 | 5 | 0.4 | 5046 | 5452 | 5570 | 8952 | 10763 | 3038 | 1427 | 0.90 | 0.47 |
| 12 | 20 | 5 | 0.3 | 6177 | 5684 | 10504 | 12474 | 14980 | 1555 | 944 | 0.65 | 0.32 |
| 13 | 0 | 5 | 0.4 | 4916 | 5568 | 6326 | 7918 | 8614 | 3719 | 3352 | 1.13 | 0.62 |
| 14 | 20 | 0 | 0.4 | 5032 | 5293 | 6147 | 8077 | 8714 | 5741 | 3534 | 1.33 | 0.81 |
| 15 | 20 | 10 | 0.4 | 5148 | 5119 | 4556 | 7301 | 8356 | 2730 | 1518 | 0.95 | 1.38 |

1 Conversion Factor: 1 GPa = 145 ksi.
2 Concrete tested here was non-air entrained concrete
3 Rapid Chloride Ion Permeability Test (RCPT)
4 Chloride Conductivity test (CT)

Table 3.10: Mathematical Models for Concrete Mixtures Containing PC/FA/SF

| SUMMARY OF MODEL EQUATIONS[2] ( in the form, $y_n = m_1x_1 + m_2x_2 + m_3x_3 + \ldots. + m_{18}x_{18} + C$) | | | | | | | | | | |
|---|---|---|---|---|---|---|---|---|---|---|
| **Variable Number** | **Description of Variable[1] ($x_n$)** | **Equation constants ($m_n$)** | | | | | | | | |
| | | **Compressive Strength (psi)** | | | **Modulus of Elasticity (ksi)** | | **Rapid chloride Ion Permeability (Coulombs)** | | **Chloride Conductivity (mS/cm)** | |
| | | **7 days** | **28days** | **56days** | **28days** | **56days** | **28days** | **56days** | **28days** | **56days** |
| 01 | XC | -25.614 | ---- | ---- | ---- | 10.79 | ---- | -16.259 | -0.0053 | -0.003 |
| 02 | YC | ---- | 93.005 | 70.622 | ---- | -30.09 | -236.14 | -197.41 | -0.0359 | -0.0326 |
| 03 | ZC | -26460 | -28772 | -30438 | -4667.12 | -5245.38 | 11582 | 8369.4 | 3.5525 | 3.3738 |
| 04 | XC^2 | ---- | ---- | ---- | 1.52 | 0.73 | -2.223 | ---- | -0.001 | ---- |
| 05 | YC^2 | ---- | ---- | ---- | 19.49 | ---- | ---- | 20.844 | -0.013 | ---- |
| 06 | ZC^2 | 99700 | 143030 | 116310 | 60884.05 | ---- | ---- | ---- | -27.044 | ---- |
| 07 | XCYC | 10.544 | -9.449 | ---- | ---- | 4.19 | ---- | ---- | ---- | ---- |
| 08 | XCZC | 706.27 | 452.6 | 487.43 | ---- | -213.15 | -382.12 | -425.12 | ---- | ---- |
| 09 | YCZC | ---- | ---- | ---- | 1106.35 | ---- | ---- | ---- | 0.518 | 1.157 |
| 10 | Intercept, D | 7506.2 | 9621.5 | 10190 | 4572.14 | 5315.27 | 2131.2 | 1258.9 | 1.0009 | 0.7162 |
| | $R^2$ | 0.923 | 0.915 | 0.945 | 0.828 | 0.761 | 0.875 | 0.932 | 0.913 | 0.791 |

1 X = Fly ash dosage, % by mass; Y = Silica fume dosage, % by mass; Z = Water – binder ratio;
XC = X – 20, YC = Y –5, ZC = Z – 0.40;

2 All the models are constructed at 95% confidence levels.

3 Conversion Factor: 1 GPa = 145 ksi.

Table 3.11: Mathematical Models for Concrete Mixtures Containing PC/GGBS/SF

| SUMMARY OF PREDICTION MODEL EQUATIONS[2] ( in the form, $y_n = m_1x_1 + m_2x_2 + m_3x_3 + \ldots + m_{18}x_{18} + C$) | | | | | | | | | | |
|---|---|---|---|---|---|---|---|---|---|---|
| **Variable Number** | **Description of Variable[1] ($x_n$)** | **Equation constants ($m_n$)** | | | | | | | | |
| | | **Compressive Strength (psi)** | | | **Modulus of Elasticity (ksi)** | | **Rapid chloride Ion Permeability (Coulombs)** | | **Chloride Conductivity (mS/cm)** | |
| | | **7 days** | **28days** | **56days** | **28days** | **56days** | **28days** | **56days** | **28days** | **56days** |
| 01 | XC | ---- | 24.247 | ---- | 14.31 | ---- | -22.334 | -21.515 | -0.0083 | -0.0093 |
| 02 | YC | 64.655 | 168.61 | ---- | ---- | ---- | -240.84 | -200.9 | ---- | -0.0238 |
| 03 | ZC | -27802 | -30563 | -30985 | -7045.26 | -5042.38 | 9099.4 | 7707 | 3.05 | 3.8875 |
| 04 | XC^2 | ---- | ---- | -1.4275 | ---- | ---- | ---- | 0.8925 | ---- | 0.0007 |
| 05 | YC^2 | -39.843 | -55.546 | -71.781 | ---- | ---- | 34.736 | 36.374 | ---- | 0.0154 |
| 06 | ZC^2 | ---- | ---- | ---- | ---- | ---- | 49589 | 81046 | ---- | 40.944 |
| 07 | XCYC | ---- | ---- | ---- | -8.00 | -2.70 | ---- | 4.78 | ---- | ---- |
| 08 | XCZC | 547.1 | ---- | ---- | -257.74 | -161.68 | ---- | ---- | ---- | ---- |
| 09 | YCZC | ---- | ---- | ---- | -1059.95 | ---- | -1370.5 | -1209 | -1.42 | ---- |
| 10 | Intercept, D | 7468.7 | 9923.6 | 10521 | 5231.60 | 5524.50 | 1206.9 | 604.28 | 0.8693 | 0.3711 |
| | $R^2$ | 0.960 | 0.963 | 0.874 | 0.871 | 0.720 | 0.960 | 0.960 | 0.563 | 0.858 |

1 X = Slag dosage, % by mass; Y = Silica fume dosage, % by mass; Z = Water – binder ratio;
XC = X – 20, YC = Y –5, ZC = Z – 0.40;
2 All the models are constructed at 95% confidence levels.
3 Conversion Factor: 1 GPa = 145 ksi.

Table 3.12: Mathematical Models for Concrete Mixtures Containing PC/FA/GGBS

| SUMMARY OF PREDICTION MODEL EQUATIONS[2] ( in the form, $y_n = m_1x_1 + m_2x_2 + m_3x_3 + \ldots. + m_{18}x_{18} + C$) | | | | | | | | | | |
|---|---|---|---|---|---|---|---|---|---|---|
| **Variable Number** | **Description of Variable[1] ($x_n$)** | **Equation constants ($m_n$)** | | | | | | | | |
| | | **Compressive Strength (psi)** | | | **Modulus of Elasticity (ksi)** | | **Rapid chloride Ion Permeability (Coulombs)** | | **Chloride Conductivity (mS/cm)** | |
| | | **7 days** | **28days** | **56days** | **28days** | **56days** | **28days** | **56days** | **28days** | **56days** |
| 01 | XC | -30.219 | ---- | 18.031 | 4.19 | -3.73 | -13.138 | -34.906 | ---- | ---- |
| 02 | YC | -28.469 | ---- | -18.019 | ---- | ---- | -62.425 | -39.906 | -0.0085 | 0.0034 |
| 03 | ZC | -21809 | -19995 | -26186 | -6142.49 | -5037.01 | 17048 | 8013.8 | 4.15 | 3.925 |
| 04 | XC^2 | ---- | ---- | ---- | -1.29 | 0.59 | 1.5386 | 2.0993 | -0.0021 | -0.0006 |
| 05 | YC^2 | -1.7843 | -2.0371 | -3.0281 | -1.03 | ---- | 3.6811 | 2.4406 | -0.0017 | -0.0008 |
| 06 | ZC^2 | 174329 | 171215 | 242875 | ---- | ---- | ---- | ---- | -85.278 | ---- |
| 07 | XCYC | ---- | ---- | -3.4063 | ---- | -0.58 | ---- | 1.0463 | ---- | ---- |
| 08 | XCZC | ---- | 318 | ---- | ---- | ---- | ---- | ---- | ---- | ---- |
| 09 | YCZC | -701.25 | -945 | -1288.3 | -220.76 | ---- | ---- | ---- | ---- | ---- |
| 10 | Intercept, D | 5978.8 | 8551.4 | 9641 | 5533.49 | 5304.10 | 2636.3 | 1472.1 | 1.7456 | 0.7369 |
| | $R^2$ | 0.931 | 0.950 | 0.945 | 4.19 | -3.73 | 0.9147 | 0.919 | 0.826 | 0.716 |

1 X = Slag dosage, % by mass; Y = Slag dosage, % by mass; Z = Water – binder ratio;
XC = X – 20, YC = Y –20, ZC = Z – 0.40;

2 All the models are constructed at 95% confidence levels.

3 Conversion Factor: 1 GPa = 145 ksi.

Table 3.13: Threshold values for Performance Indicators Used in Phase I of the Study

| w/b | Performance Indicators (Quality Characteristic) - Phase I Mixes | | | |
|---|---|---|---|---|
| | Compressive. Strength[1] @28 days, psi | Compressive. Strength[1] @56 days, psi | Rapid chloride penetration value @ 56 days, C | Conductivity value @ 56 days, ms/cm |
| 0.45 | >8,500 | >9,000 | <1,000-2,000 | <0.65-0.85 |
| 0.40 | >8,500-9,500 | >9,000-10,000 | <1,000-1,500 | <0.55-0.65 |
| 0.35 | >11,000 | >11,000-11,500 | <1,000 | <0.45-0.50 |

1 Concrete for the determination of compressive strength was non-air entrained concrete

Table 3.14: Proposed Binder Composition of Mixtures for Phase II

| Mix No. | w/b | FA (%)* | SF (%)* | Slag (%)* |
|---|---|---|---|---|
| 1 | 0.4 | 0 | 6 | 0 |
| 2 | 0.4 | 25 | 6 | 0 |
| 3 | 0.4 | 40 | 6 | 0 |
| 4 | 0.4 | 25 | 0 | 0 |
| 5 | 0.35 | 40 | 0 | 0 |
| 6 | 0.4 | 0 | 6 | 25 |
| 7 | 0.35 | 0 | 0 | 0 |
| 8 | 0.4 | 0 | 0 | 0 |
| 9 | 0.35 | 0 | 0 | 25 |
| 10 | 0.35 | 25 | 0 | 25 |

* All the contents are by weight of total binder

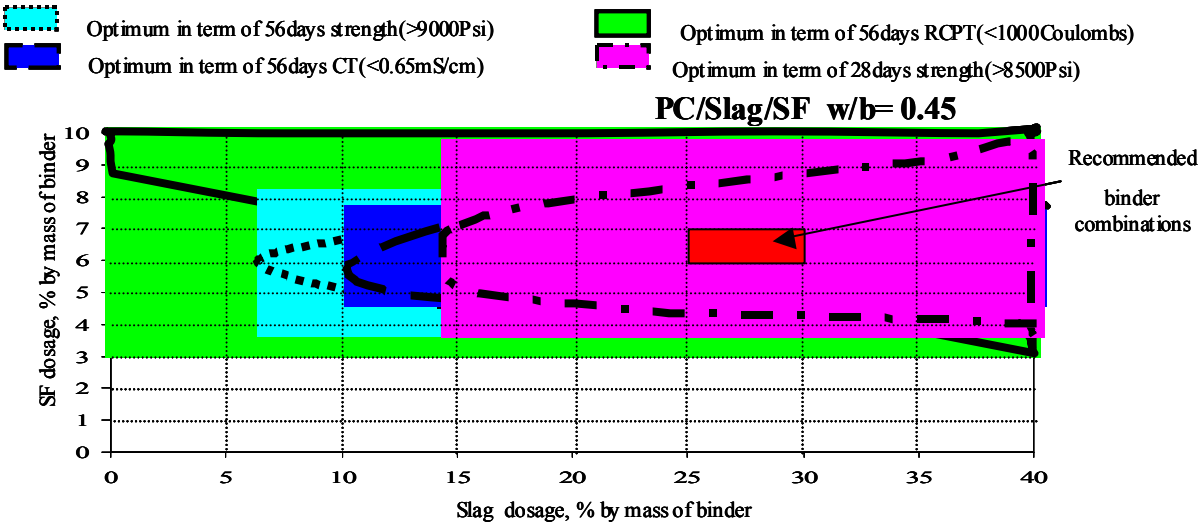


Figure 3.5: Optimum Binder Combinations for PC/Slag/SF with w/b=0.45

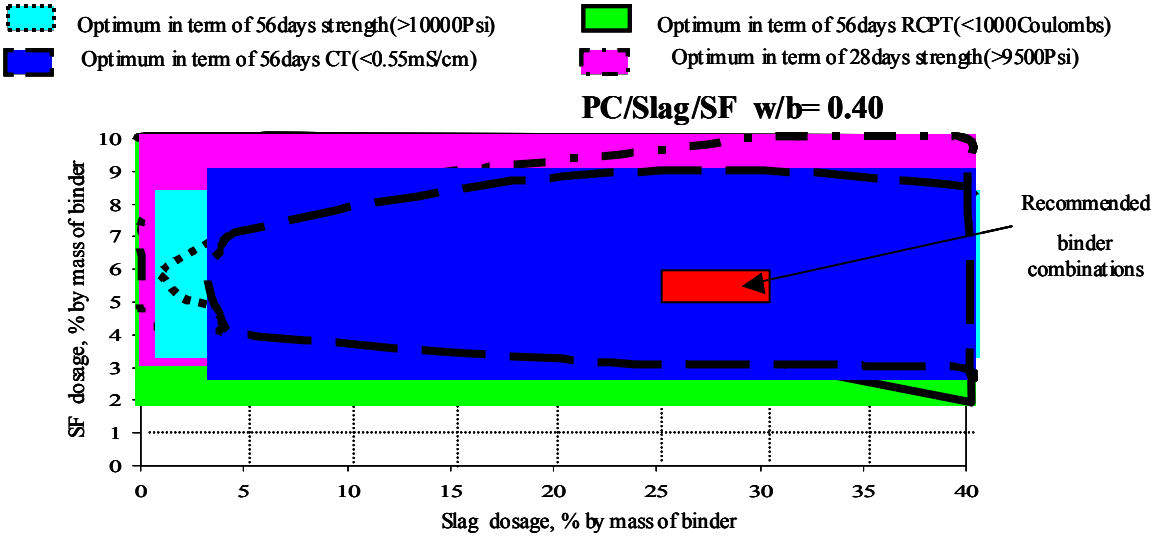


Figure 3.6: Optimum Binder Combinations for PC/Slag/SF with w/b=0.40

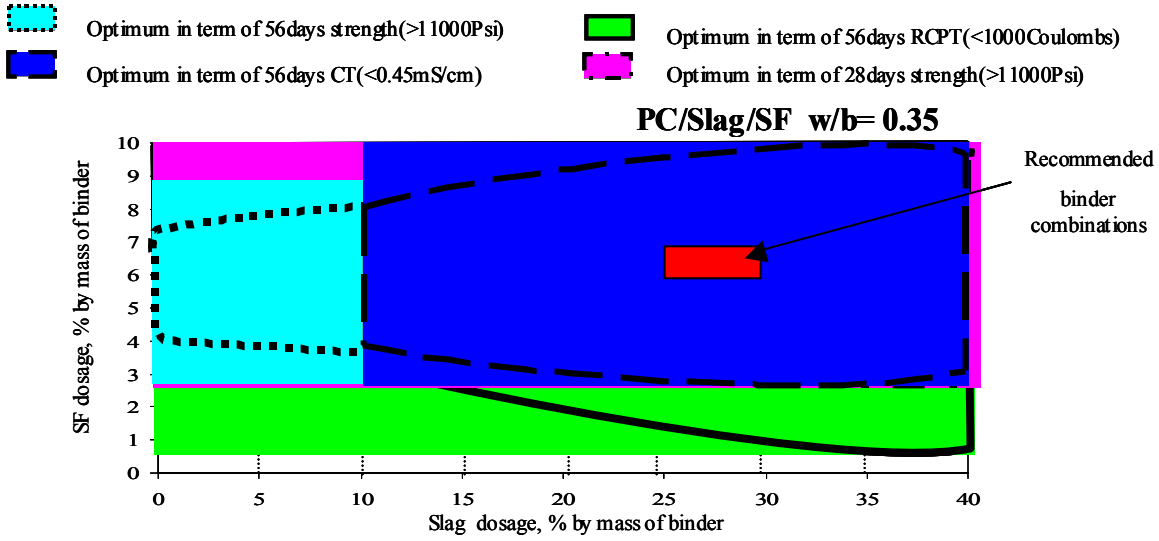


Figure 3.7: Optimum Binder Combinations for PC/Slag/SF with w/b=0.35

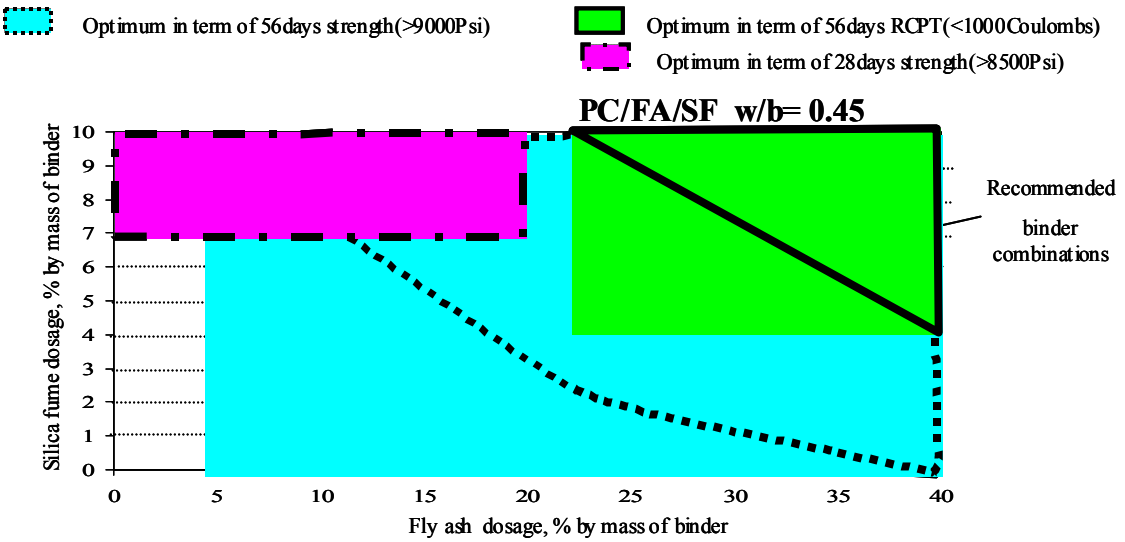


Figure 3.8: Optimum Binder Combinations for PC/FA/SF with w/b=0.45

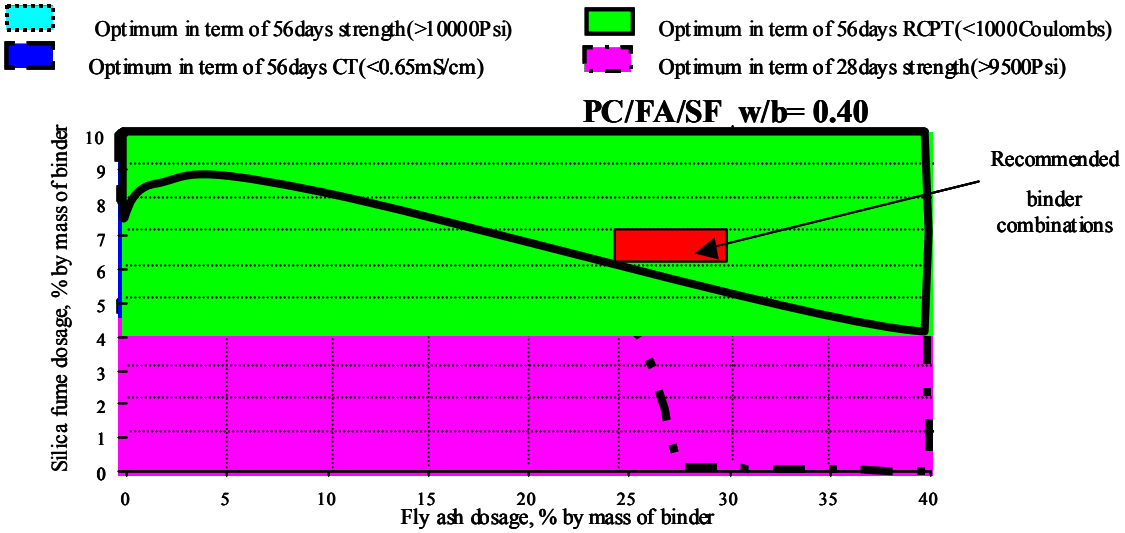


Figure 3.9: Optimum Binder Combinations for PC/FA/SF with w/b=0.40

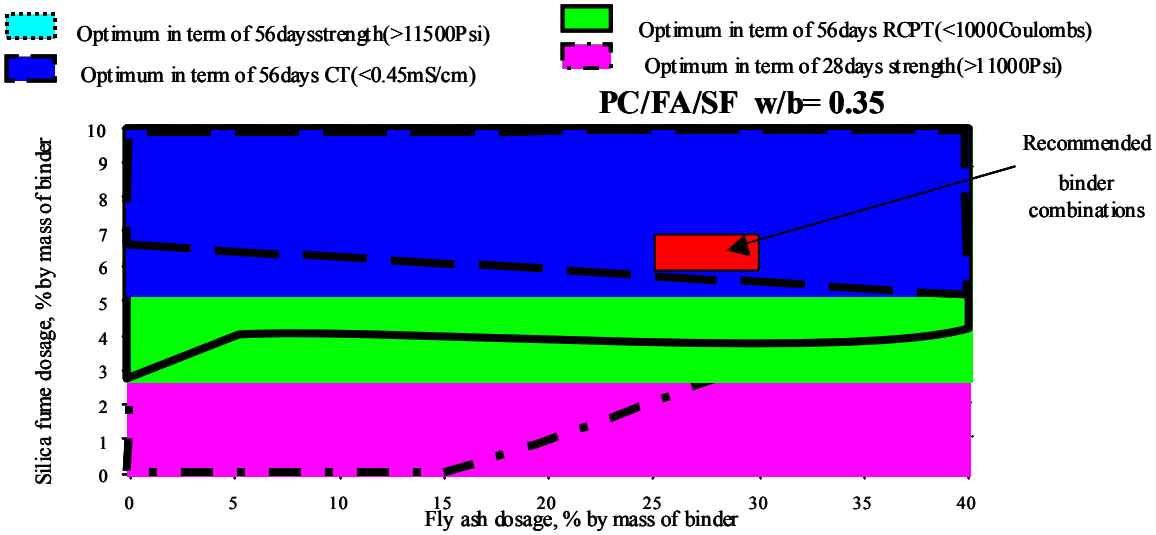


Figure 3.10: Optimum Binder Combinations for PC/FA/SF with w/b=0.35

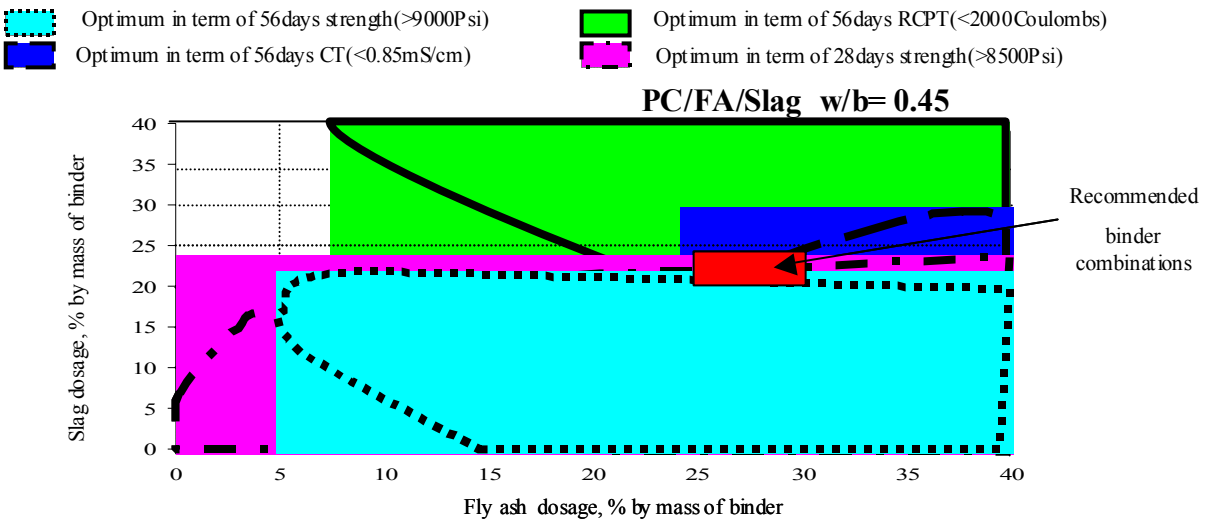


Figure 3.11: Optimum Binder Combinations for PC/FA/Slag with w/b=0.45

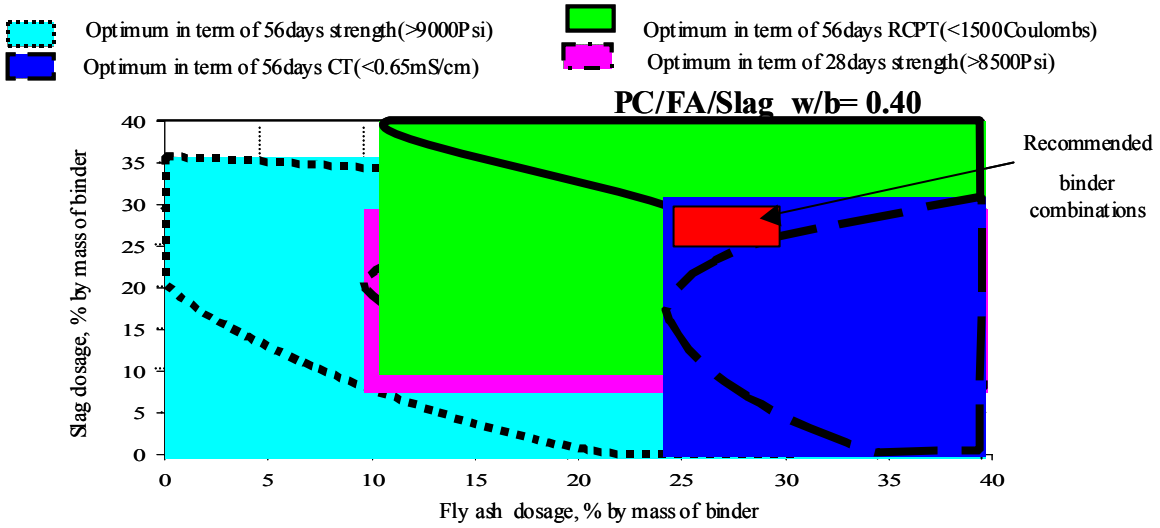


Figure 3.12: Optimum Binder Combinations for PC/FA/Slag with w/b=0.40

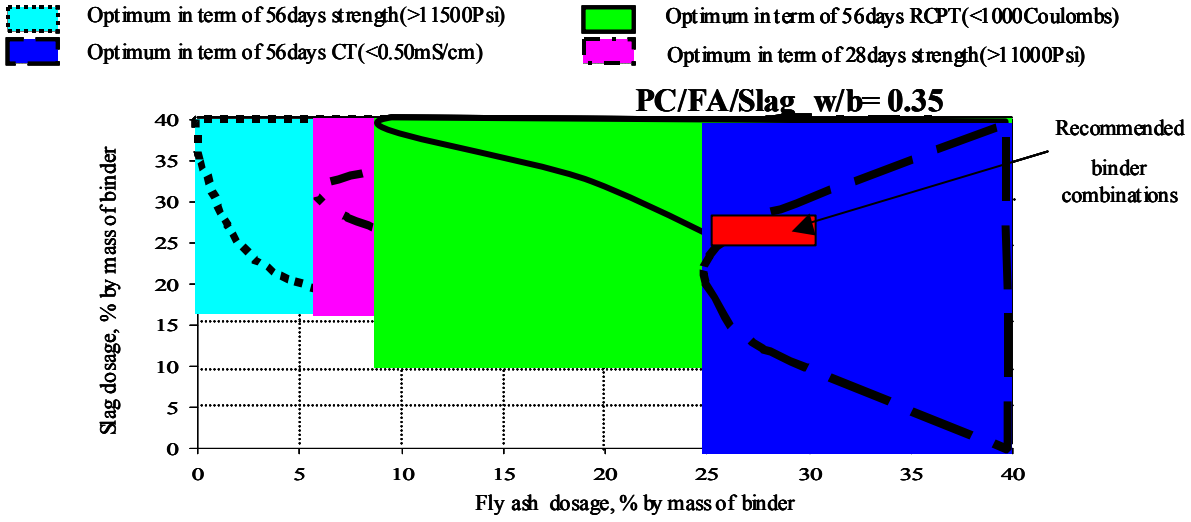


Figure 3.13: Optimum Binder Combinations for PC/FA/Slag with w/b=0.35

A quick examination of Figures 3.5 - 3.13 indicates that there is a broad range of binder compositions that will produce mixes that satisfy all four performance criteria used in Phase I of the study. However, closer examination of these possible binder compositions reveals that some of them will not be practical and that a further refinement is needed. This refinement was achieved by performing additional analysis of general trends between binder composition and a given property as indicated by individual contour maps. The result of this analysis was a common area called "*Recommended binder combinations*" that is identified on each of the Figures 3.5 - 3.13. As all mixtures with binder composition within this common area will satisfy each of the individual performance criteria, these mixtures can be considered as having the optimized composition. Since it was not practical to include the detailed discussion of all of the 81 individual contour maps in this report, only the summary of the analysis is presented in section 3.4.3 below.

### 3.4.3 Selection of Optimum Binder Combinations

The analysis of individual contour maps (Note: these maps are not included in this report) reveals some general trends as discussed below. These trends, along with the summary maps presented in Figures 3.5 - 3.13 were used to select the range of optimum binder combinations.

PC/Slag/SF system

The contour maps prepared for this series of mixes indicate that increasing the content of silica fume results in reduced chloride permeability at 28 days and 56 days. The influence of slag on chloride permeability is similar but less pronounced. For the range of slag content used in this study (0 – 40%), only limited enhancement of compressive strength was observed at 28 and 56 days. Addition of up to 6% of silica fume results in strength enhancement, but when larger percentage of silica fume was added, slight reduction in compressive strength was observed. From the above analysis, the optimum binder combinations recommended for this series of mixes are as follows: silica fume 5 - 7%, slag 25 - 30%.

PC/FA/SF system

The compressive strength of concrete mixtures at 28 days or 56 days will increase when the content of silica fume added to the system increases, providing fly ash addition is kept below 30% of total binder. The chloride permeability at 28 days or 56 days decreases with increased content of silica fume. Addition of fly ash further reduces chloride permeability of concrete mixtures at 28 days and 56 days except for mixes with water-binder ratio of 0.35. Fly ash is also beneficial for the 56-day compressive strength of concrete mixtures; however, the influence of fly ash on 28-day compressive strength depends on the amount of silica fume added to the concrete mixes. The recommended optimum binder combinations for PC/FA/SF series are as follows: silica fume 5 ~ 7%, fly ash 25 ~ 30%.

PC/FA/Slag system

The chloride permeability at 28 days and 56 days is reduced greatly with increase in the amount of fly ash or slag added to the concrete mixes. However, the resistance to chloride penetration at 28 days will decrease when the dosages of slag and fly ash added to the concrete mixes exceed 30% each. The compressive strength of concrete mixture at 28days will increase when the dosage of fly ash is increased. In general, the same trend is observed for mixes containing slag; however, the total amount of slag leading to the increase of compressive strength appears to be a function of water-binder ratio. For water-binder ratio of 0.35, as much as 30% of slag can be added. This value drops to about 20% for mixes with water-binder ratio of 0.40, and to 6% for mixes with water-binder ratio of 0.45. The trends for compressive strength of concrete mixture at 56 days was not very clear; however, when the total content of fly ash and slag is too low or too high, the compressive strength tends to decrease. From the above analysis, using RCPT, compressive strength and CT results as performance indicators, the following binder combinations are suggested: fly ash 20 ~ 30%, slag 20 ~ 30%. In addition, water-binder ratio should be kept as low as practical.

Based on the above analysis, the optimum binder combinations for each of the binder combinations used in this study can be summarized as follows:

- PC/FA/SF system: FA 25 - 30% SF 5 - 7%
- PC/Slag/SF system: Slag 25 - 30% SF 5 - 7%
- PC/FA/Slag system: FA 20 - 30% Slag 20 - 30%.

Based on the analysis prescribed above, ten potential optimum concrete mixes (as presented in Table 3.14) were recommended for further evaluation in Phase II of this study.

# 4 PHASE II: PERFORMANCE EVALUATION OF THE OPTIMUM MIXTURES FROM PHASE I

## 4.1 Mixture Design Parameters and Composition

As already discussed, the experiments performed in Phase I of this study resulted in 10 optimum concrete mixtures that were selected for further evaluation in Phase II. The design parameters used for mixtures produced in Phase II were very similar to those used for mixtures produced in Phase I, with the exception that all mixtures in Phase II were air-entrained. The specific design parameters selected for mixtures in Phase II were as follows:

- Target slump: 5.5 inches with a tolerance of ± 1.5 inches, (the same as used for mixtures in Phase I).
- Target total air content in fresh concrete: 6.5% with a tolerance of ± 0.5%.
- A total binder content of 390 kg/m$^3$ (657 lbs/yd$^3$) for all mixtures (the same as used for mixtures in Phase I).
- Although the basic composition of mixtures selected for Phase II was very similar to that used in Phase I of this study, some adjustments were necessary to accommodate the yield changes resulting from the increase in total air content. These adjustments involved changing the quantities of coarse and fine aggregates while keeping the water-cementitious materials ratio and the total volume ratio of mortar (excluding volume of entrained air) in the Phase II mixtures at the same levels as these used in Phase I. The compositions of all mixtures used in Phase II of the study are given in Table 4.1.

Table 4.1: Proposed Binder Composition of Mixtures for Phase II of this Study

| Mix No. | w/b | FA (%)* | SF (%)* | Slag (%)* |
|---|---|---|---|---|
| 1 | 0.4 | 0 | 6 | 0 |
| 2 | 0.4 | 25 | 6 | 0 |
| 3 | 0.4 | 40 | 6 | 0 |
| 4 | 0.4 | 25 | 0 | 0 |
| 5 | 0.35 | 40 | 0 | 0 |
| 6 | 0.4 | 0 | 6 | 25 |
| 7 | 0.35 | 0 | 0 | 0 |
| 8 | 0.4 | 0 | 0 | 0 |
| 9 | 0.35 | 0 | 0 | 25 |
| 10 | 0.35 | 25 | 0 | 25 |

* All the contents of cementitious materials are by the weight of total binder

## 4.2 Materials

### 4.2.1 Binder

ASTM Type I Portland cement produced by the Lone Star Industries plant at Greencastle, IN was used throughout the study. The composition and physical characteristics of this cement are presented in Table 4.2, and all of the reported values were determined by the manufacturer.

Table 4.2: Composition and Physical Characteristics of Cement Used in Phase II

| Chemical Composition (%) | | Physical Data | |
|---|---|---|---|
| CaO | 64.87 | Expansion, % | 0.037 |
| $SiO_2$ | 20.93 | Air Entrainment, % | 5.6 |
| $Al_2O_3$ | 5.16 | Setting Time: | |
| $Fe_2O_3$ | 2.87 | Vicat, min | 85 |
| MgO | 1.68 | Blaine Surface, $cm^2/g$ | 3600 |
| $SO_3$ | 2.37 | Wagner, $m^2/kg$ | 189 |
| $Na_2O$ | 0.13 | | |
| $K_2O$ | 0.47 | | |
| Total Alkali as $Na_2O$ | 0.44 | | |
| Loss on Ignition | 1.45 | | |
| Potential Compound Composition, % | | Compressive Strength, psi | |
| $C_3S$ | 59 | | |
| $C_2S$ | 15 | 3 day | 3500 |
| $C_3A$ | 9 | 7 day | 4330 |
| $C_4AF$ | 9 | | |

### 4.2.2 Aggregate

No. 8 crushed limestone with a maximum size of 25 mm was used as coarse aggregate in Phase II concrete mixtures of this study, and the coarse aggregate was supplied by the Martin Marietta plant in Indianapolis. The properties of the sample from coarse aggregate used in this study are given in Table 4.3.

No. 23 river sand from the IMI plant in Greenwood, Indiana, was used as the fine aggregate in Phase II concrete mixtures of this study (in accordance with Section 904.01 of the 1999 Book of Standards of the Indiana Department of Transportation). The properties of the sample from fine aggregate used in this study are given in Table 4.4. The correction factor for the air content determination was 0.3%.

Table 4.3: Properties of Coarse Aggregate Used in Phase II Concrete Mixtures

| Bulk Specific Gravity (saturated surface-dry) $BSG_{SSD}$=2.671<br>Absorption =1.21% | | | INDOT #8<br>Passing Percent |
|---|---|---|---|
| Sieve Designation | Cumulative Weight Percent | | |
| | Retained | Passing | |
| 1” | 0.6 | 99.4 | 100 |
| 3/4” | 12.8 | 87.2 | 75-95 |
| 1/2” | 48.5 | 51.5 | 40-70 |
| 3/8” | 76.9 | 23.1 | 20-50 |
| No.4 | 91.6 | 8.4 | 0-15 |
| Less than No.4 | 99.9 | | 0-10 |

Table 4.4: Properties of Fine Aggregate Used in Phase II Concrete Mixtures

| Fineness Modulus, FM=2.71<br>Bulk Specific Gravity (saturated surface-dry), $BSG_{SSD}$=2.63<br>Absorption = 1.63% | | | INDOT #23<br>Passing Percent |
|---|---|---|---|
| Sieve Designation | Cumulative Weight Percent | | |
| | Retained | Passing | |
| No.4 | 0.1 | 99.9 | 95-100 |
| No.8 | 5.1 | 94.9 | 80-100 |
| No.16 | 28.7 | 71.3 | 50-85 |
| No.30 | 52.9 | 47.1 | 25-60 |
| No.50 | 88.5 | 11.5 | 5-30 |
| No.100 | 98.7 | 1.3 | 0-10 |
| Dust | 100 | | 0-3 |

### 4.2.3 High Range Water Reducer

All the chemical admixtures for Phase II concrete mixtures of this study were provided by W. R. Grace and Co. An ASTM Type A and Type F high range water reducer (DARACEM 19) meeting ASTM C 494 standard was used to satisfy the requirements for fresh concrete in Phase II of this study.

The high range water reducer used in this study was an aqueous solution of a modified naphthalene sulfonate with a specific gravity of 1.2. The recommended addition rate to the concrete ranges from 390 to 1300 ml/100kg (6 to 20 fl oz/100lb) of cement.

### 4.2.4 Air-Entraining Agent

An air entraining agent (DARAVAIR 1400) meeting ASTM C 260 standard was used to achieve 6.5 ±1.5 % air content in the fresh concrete in this study. The aggregate correction factor for the air content determination was 0.3%.

The air entraining agent (DARAVAIR 1400) was based on a high-grade saponified rosin formulation. It is chemically similar to vinsol-based formulation, but with increased purity. The recommended addition rates range from 30 to 200 ml/100 kg (½ to 3 fl oz /100 lb) of cement to achieve 5 to 8% of total air content in concrete.

## 4.3 Experimental Approach

Based on the research done in Phase I of this study, 10 concrete mixtures were recommended for the further evaluation of concrete properties in Phase II of this study. The details of these 10 concrete mixture proportions are shown in Table 4.1. Four concrete mixtures (No. 2, No. 3, No. 6, and No. 10) are the optimized concrete mixtures with enhanced performance, which were selected from the three different binder systems in Phase I. Other concrete mixtures were chosen as control mixtures (No. 7 & 8) or mixtures that can achieve properties comparable to the control mixtures (No. 1, No.4, No. 5, No. 9). The purpose of the testing is to further verify the validity of the concrete proportioning methods developed in Phase I and develop a final recommendation for composition and production of concrete mixtures with enhanced performance characteristics. In order to investigate the overall properties of optimum concrete mixtures suggested in Phase I of the study, the following performance properties are proposed to be tested in Phase II of this study.

- Maturity (ASTM C 1074)
- Compressive strength (ASTM C 39, or AASHTO T 22)
- Static modulus of elasticity (ASTM C 469)
- Drying Shrinkage (ASTM C 157, or AASHTO T 160)
- Freezing and thawing resistance (ASTM C666, or AASHTO T 161)
- Scaling resistance (ASTM C 672)
- Coefficient of diffusion

- Resistance of concrete to chloride ion penetration - ponding test (AASHTO T 259)
- Resistance to the penetration of chloride ions - accelerated test (ASTM C 1202, or AASHTO T 277)
- Chloride conductivity test
- Electrical resistance under 60 volts DC

All mixtures tested in Phase II are prepared and cured in the same way as mixes tested in Phase I. However, in addition to the tests conducted for Phase I concrete mixtures, more testing related to the durability of Phase II mixtures were used.

The detailed test plan for mixtures prepared in Phase II of this study is given in Table 4.5.

## 4.4 Experimental Procedures

### 4.4.1 Fresh Concrete Properties

Slump of concrete in fresh state was determined according to ASTM C 143-90a (Standard Test Method for Slump of Hydraulic Cement Concrete). The total air content in the fresh concrete was determined in accordance with ASTM C 231 using the Type B pressure meter.

### 4.4.2 Compressive Strength

The compressive strength of concrete was determined by testing 100 mm x 200 mm (4" x 8") cylinders. ASTM C 39-94 (Standard Test Method for Compressive Strength of Cylindrical Concrete Specimens) was followed during the testing. A high rate of loading was applied on the specimens up to one third of the anticipated ultimate load, and then a loading rate of 35 psi/sec (14.4 MPa/min) was used until the specimen failed.

### 4.4.3 Flexural Strength

The flexural strength of concrete was determined using simple beam with third point loading, which was in accordance with ASTM C 78-94 standard (Standard Test Method for Flexural Strength of Concrete). The beam size was 3" x 3" x 15". A constant loading rate of 150 psi /min (1.05 MPa/min) was applied on the test specimen until failure in a universal testing machine with a capacity of 100,000 lbs.

The following equation can be used to calculate the flexural strength of the specimen if fracture initiates in the tension surface within the middle third of the span length:

$$R = \frac{PL}{bd^2} \quad \text{.....(4.1)}$$

where:
R = flexural strength, psi;
P = maximum applied load, lbs;
L = span length, in;
b = average width of specimen, in;
d = average depth of specimen, in;

### 4.4.4 Static Modulus of Elasticity

The static modulus of elasticity of concrete was determined in accordance with ASTM C 469 – 94 (Standard Test Method for Static Modulus of Elasticity and Poisson's Ratio of Concrete in Compression). 100 mm x 200 mm concrete cylinders were used for the testing. The cylindrical specimens were loaded axially in a universal testing machine with the capacity of 100000 lbs. A constant loading rate of 35 psi/sec (241 kPa/sec) was applied on the specimen. The applied load related to a longitudinal strain of 50 $x10^{-6}$ and a longitudinal strain related to 40% of the ultimate load was recorded.

Table 4.5: Proposed Testing Plan for Phase II Concrete Mixtures

| Mix No. | w/b | FA (%) | SF (%) | Slag (%) | Fresh concrete | | |
|---|---|---|---|---|---|---|---|
| | | | | | Slump and slump loss | Air content and air loss | Maturity measurement |
| **1** | 0.4 | 0 | 6 | 0 | √ | √ | |
| **2** | 0.4 | 25 | 6 | 0 | √ | √ | √ |
| **3** | 0.4 | 40 | 6 | 0 | √ | √ | √ |
| **4** | 0.4 | 25 | 0 | 0 | √ | √ | |
| **5** | 0.35 | 40 | 0 | 0 | √ | √ | |
| **6** | 0.4 | 0 | 6 | 25 | √ | √ | √ |
| **7** | 0.4 | 0 | 0 | 0 | √ | √ | √ |
| **8** | 0.35 | 0 | 0 | 0 | √ | √ | √ |
| **9** | 0.35 | 0 | 0 | 25 | √ | √ | |
| **10** | 0.35 | 25 | 0 | 25 | √ | √ | √ |

Table 4.5: Proposed Testing Plan for Phase II Concrete Mixtures (Continuation)

| Mix No. | Hardened concrete | | | | | | | | | | |
|---|---|---|---|---|---|---|---|---|---|---|---|
| | Maturity measurement | Compressive strength | | | | | | Elastic modulus | | Freezing and thawing | Scaling |
| | up to7days | 1 days | 3days | 7days | 28days | 56days | 180days | 28 days | 56 days | 28days | 28days |
| 1 | | √ | √ | √ | √ | √ | √ | √ | √ | | |
| 2 | √ | √ | √ | √ | √ | √ | √ | √ | √ | √ | √ |
| 3 | √ | √ | √ | √ | √ | √ | √ | √ | √ | √ | √ |
| 4 | | √ | √ | √ | √ | √ | √ | √ | √ | | |
| 5 | | √ | √ | √ | √ | √ | √ | √ | √ | | |
| 6 | √ | √ | √ | √ | √ | √ | √ | √ | √ | √ | √ |
| 7 | √ | √ | √ | √ | √ | √ | √ | √ | √ | √ | √ |
| 8 | √ | √ | √ | √ | √ | √ | √ | √ | √ | | |
| 9 | | √ | √ | √ | √ | √ | √ | √ | √ | | |
| 10 | √ | √ | √ | √ | √ | √ | √ | √ | √ | √ | √ |

Table 4.5: Proposed Testing Plan for Phase II Concrete Mixtures (Continuation)

| Mix No. | Hardened concrete | | | | | | | | | | | | | | | |
|---|---|---|---|---|---|---|---|---|---|---|---|---|---|---|---|---|
| | Diffusion coefficient | | | Rapid chloride penetration | | | Chloride ponding | Chloride conductivity | | Drying Shrinkage | | | | | | |
| | 28days | 56days | 180days | 28days | 56days | 180days | 90days | 28days | 56days | 1day | 3 days | 7days | 28days | 56days | 90days | 180days |
| 1 | √ | √ | √ | √ | √ | √ | √ | √ | √ | √ | √ | √ | √ | √ | √ | √ |
| 2 | √ | √ | √ | √ | √ | √ | √ | √ | √ | √ | √ | √ | √ | √ | √ | √ |
| 3 | √ | √ | √ | √ | √ | √ | √ | √ | √ | √ | √ | √ | √ | √ | √ | √ |
| 4 | √ | √ | √ | √ | √ | √ | √ | √ | √ | √ | √ | √ | √ | √ | √ | √ |
| 5 | √ | √ | √ | √ | √ | √ | √ | √ | √ | √ | √ | √ | √ | √ | √ | √ |
| 6 | √ | √ | √ | √ | √ | √ | √ | √ | √ | √ | √ | √ | √ | √ | √ | √ |
| 7 | √ | √ | √ | √ | √ | √ | √ | √ | √ | √ | √ | √ | √ | √ | √ | √ |
| 8 | √ | √ | √ | √ | √ | √ | √ | √ | √ | √ | √ | √ | √ | √ | √ | √ |
| 9 | √ | √ | √ | √ | √ | √ | √ | √ | √ | √ | √ | √ | √ | √ | √ | √ |
| 10 | √ | √ | √ | √ | √ | √ | √ | √ | √ | √ | √ | √ | √ | √ | √ | √ |

The instrument parameters included:
Gage length of the apparatus 5.5 inches;
The sensitivity of the dial gage: 0.0001 inch;
The strain of the specimen under 40 % load of the ultimate load is:

$\varepsilon_2$ = x * 0.0001 / ( 5.5 /2 );

where:
x is the final dial reading indicating the deformation;
$\varepsilon_2$ is the longitudinal strain related to 40% of the ultimate load;
Static modulus of elasticity of the concrete specimen can be calculated by the following equation:

$$E = \frac{\sigma_2 - \sigma_1}{\varepsilon_2 - 50 * 10^{-6}} \quad \text{.....(4.2)}$$

where:
E = chord modulus of elasticity, psi;
$\sigma_2$ = stress corresponding to 40% of ultimate load, psi;
$\sigma_1$ = stress corresponding to a longitudinal strain of 50 millionth, psi;
$\varepsilon_2$ = the longitudinal strain produced by stress $\sigma_2$.

### 4.4.5 Dynamic Modulus of Elasticity

Dynamic modulus of elasticity of concrete was determined in accordance with ASTM E 1876-99 (Standard Test Method for Dynamic Young's Modulus, Shear Modulus, and Poisson's Ratio by Impulse Excitation of Vibration). Fundamental flexural resonance frequency (out-of plane flexure) was determined for each concrete mixture on prismatic specimens with a size of 3 in. x 3 in. x 15 in. The beam specimen was simply supported at a distance of 0.224L from each end of the specimen, where L is the length of the beam. Grindosonic MK4 Sonometer was used to determine the resonance frequency when the specimen was tapped gently at the middle point of the beam using an impulse hammer.

In flexural mode, the dynamic Young's modulus of a rectangular concrete bar can be calculated by the following equation:

$$E = 0.9465 \frac{m f_f^{\,2}}{b} * \frac{L^3}{t^3} * T_1 \quad \text{.....(4.3)}$$

where:
E = Dynamic Young's modulus, Pa;
m = mass of the bar, g;
$f_f$ = fundamental resonant frequency of bar in flexure, Hz;
L = length of the bar, mm;
b = width of the bar, mm;
t = thickness of the bar, mm,
$T_1$ = correction factor for fundamental flexural mode to account for finite thickness of bar, Poisson's ratio, and so forth, which is given by the following equation:

$$T_1 = 1 + 6.585(1 + 0.0752\mu + 0.8109\mu^2) * (\frac{t}{L})^2 - 0.868(\frac{t}{l})^4 - \frac{(8.340(1 + 0.2023\mu + 2.173\mu^2)(t/L)^4}{1.0 + 6.338(1 + 0.1408\mu + 1.536\mu^2)(t/L)^2}$$

……..…….(4.4)

where:
$\mu$ = Poisson's ratio.

### 4.4.6 Chloride Conductivity

Based on the research by Streicher and Alexander [1995], chloride conductivity of concrete specimen was determined in Phase II concrete mixtures of this study. Conductivity test of concrete specimens saturated with 5M sodium chloride solution was carried out under 10 volts DC, and the electrical current passing through the specimen

was recorded during the test. Cylinder specimen with the thickness of 25 mm and a diameter of 68 mm was used during the conductivity test. This test provided a rapid indication of the resistance of concrete to the penetration of chloride ions.

The conductivity of the specimen can be calculated using the following equation:

$$\sigma = \frac{it}{VA} \quad \text{.....(4.5)}$$

where:
σ = conductivity of specimen, mS/cm;
i = electrical current, mA;
V = potential difference, V;
t = thickness of the specimen, cm;
A = cross sectional area of specimen, $cm^2$;

### 4.4.7 Rapid Chloride Ion Permeability

Rapid chloride ion permeability was determined in accordance with Standard Test Method for Electrical Indication of Concrete's Ability to Resist Chloride Ion Penetration (AASHTO T 277-96). A model 164 apparatus from RLC Instruments Co was used during the rapid chloride ion permeability test in this study. The specimen disc with a diameter of 3.75 inches and a thickness of 2 inches was used for RCP test, and the total amount of electrical current (Coulombs) passing through the specimen under 60 DC volts during 6 hours was recorded as the indication of the resistance of the specimen to chloride ion penetration.

Three cylinders for each test age per concrete mixture were used (3.73 inch in inner diameter x 8 inch high), and total 9 cylinders were cast for each different mixture during RCP test, and all the cylinders were covered with the plastic caps immediately after casting and consolidating. The cylinders were demolded 24 hours later after casting and concrete cylinders were stored in the fog room until the test age prescribed in the test plan. Concrete cylinders were subjected to three different curing lengths, and these were 28 days, 56 days, and 180 days at the fog room.

When the test time was due, a 50 ±3 mm slice from the top of the cylinder was cut through water cooled diamond saw, with the cut parallel to the top of surface. Use blush to remove any burrs on the end of the disc. Allow the discs surface dry in the laboratory environment, and prepare the rapid set coating and brush the coating onto the side surface of disc, and check the side surface free from any apparent holes, place the specimens on a metal cylinder support during coating preventing coating from the end surface of the specimen. Cure the coating for about 5 hours based on the manufacturer's instruction. Place the specimens into the vacuum desiccator and start to vacuum for 3 hours, and drain sufficient de-air water into the desiccator until the water cover all the portion of the specimens with the pump still running, and the vacuum keeps on running for additional one hour. Soak the specimen under water for 18 hours under normal air pressure.

The positive reservoir of the cell was filled with 0.30N sodium hydroxide solution, and the negative part of the cell was filled with 3.0% by mass of sodium chloride solution. A 60-volt electrical potential was applied across the two sides of the disc, and the DC current and the accumulated coulombs across the disc was recorded every half hour covering a total period of 6 hours. The permeability of concrete mixture was expressed as the average coulomb value of three 50 ± 3 mm thick discs under 60-volt electrical potential applied on the two sides of each disc for 6 hours, and these three discs should come from the same position of the cylinders, and the top portion of 51 mm thickness of concrete disc near to the casting surface was used at this study.

### 4.4.8 DC Resistance

Three copper rods were imbedded in some concrete cylinders during casting, at a distance of 2 inches from each other, and at a depth of 2 inches into the concrete. The electrical current passing through the specimen in between the copper rods was determined under an applied potential of 60 volts DC. The electrical current was recorded as an indication of the resistance to ionic movement within the concrete. This is a very quick test, and does not require any preconditioning. It is also a non-destructive test, and can be performed reproducibly in the lab.

### 4.4.9 Absorption

Absorption of concrete specimens was determined in accordance with ASTM C 642-90 (Standard Test Method for Specific Gravity, Absorption, and Voids in Hardened Concrete). The absorption value obtained from this test was used as an indication of the total volume of permeable capillary pores in the concrete. The specimen used for this test was a concrete disc with a diameter of 4 inches and a thickness of 2 inches, and was obtained by saw-cutting from a concrete cylinder (4 in. x 8 in.).

### 4.4.10 Resistance of Concrete to Chloride Ion Penetration by the Ponding test

The resistance of concrete to chloride ion penetration was evaluated for each concrete mixture in Phase II of this study in accordance with AASHTO T 259-80 and AASHTO T 260-84. Two concrete slabs (10 x 15 x 3 inch) were cast for each concrete mixture. These concrete slabs were moist cured for 14 days, and then air-dried for 28 days. They were then ponded with 3% sodium chloride solution for 90 days. Upon completion of ponding, 2 in diameter cylindrical cores were removed from the center of the slab. Specimens for the determination of chloride ion concentration at each half-inch slice along the depth of the cylinder were obtained from these cores. These specimens were pulverized and the acid-soluble chloride ion content was determined according to AASHTO T 260-84 (Standard Test Method of Sampling and Testing for Total Chloride Ion in Concrete and Concrete Raw Materials). The chloride ion concentration of concrete in the top two layers (each ½ inch thick) was used as an indication of the resistance of concrete to chloride ion penetration. The diffusion coefficient of concrete mixtures was then calculated from the chloride profiles. The method used in this study is discussed later in Chapter 5.

### 4.4.11 Drying Shrinkage

Drying shrinkage of concrete specimens was determined in accordance with ASTM C 157-93 (Standard Test Method for Length Change of Hardened Hydraulic-Cement Mortar and Concrete). Prismatic specimens were used for the test, having a cross section of 3 inch x 3 inch and a length of 11 1/4 inches. The specimens were first cured for 28 days in lime water and then moved to a drying room with a temperature of 20°C and 50% relative humidity. Length of the specimens was monitored during the drying period. A comparator with an accuracy of 0.0001 inch was used to determine the length of the specimen, and 10 inches was used as the effective gage length of concrete during the calculation of drying shrinkage.

Length change of concrete specimens can be calculated using the following equation:

$$\Delta L_x = \frac{CRD - CRD_i}{G} \times 100 \quad \text{.....(4.6)}$$

where:
$\Delta L_x$ = length change of specimen at any age, %,
CRD = the comparator reading of the specimen at any time,
$CRD_i$ =the reading of the reference bar at any time,
G = the gage length (= 10 inches).

### 4.4.12 CTH Electrical Migration Test

4.4.12.1 Chloride Diffusion Coefficient from Electrical Migration Test: The transport of chloride ions through concrete can be accelerated by applying a potential gradient across the specimen mounted in the so-called migration cell. The rapid chloride permeability test (RCPT) described in Section 4.4.7 of this report is an example of the electric field migration test. However, the RCPT measures only the total charge passed through the specimen, resulting from the movement of all ions present in the pore solution, and therefore, does not provide direct information on the chloride ion diffusion.

In order to overcome the difficulties related to calculating chloride diffusion coefficient from RCP test, the CTH Rapid Migration Test [Tang and Wilson, 1992] was utilized in this study to determine the chloride diffusion coefficient.

4.4.12.2 CTH Test Procedure: The set-up for this test is presented in Figure 4.1. The test specimen is a 100-mm diameter disc that is 50-mm thick. The specimen is kept under vacuum (1 to 5 KPa) for 3 hours and is then flooded (with vacuum pump still running) with a saturated solution of $Ca(OH)_2$. The vacuum is maintained for an additional 1 hour after which time the air is allowed to enter the container. The specimen is inserted in a tight-fitting rubber sleeve, and placed in a container filled with 10% NaCl solution. The bottom of the specimen is set on a stainless steel plate (cathode) that rests on a plastic support. The specimen is tilted on the support to make it easy for gas bubbles to escape the cathodic plate. The rubber sleeve is filled with 0.3N NaOH solution that covers the top of the specimen. The cathode plate is connected to the negative pole of the power supply. The anode stainless plate is inserted on the top of the specimen, which is exposed to NaOH solution, and connected to the positive pole. A voltage of 30 V is applied across the specimen and the initial current is measured to estimate the required test duration. The duration of the test can vary from 6 to 96 hours depending on the quality of concrete.

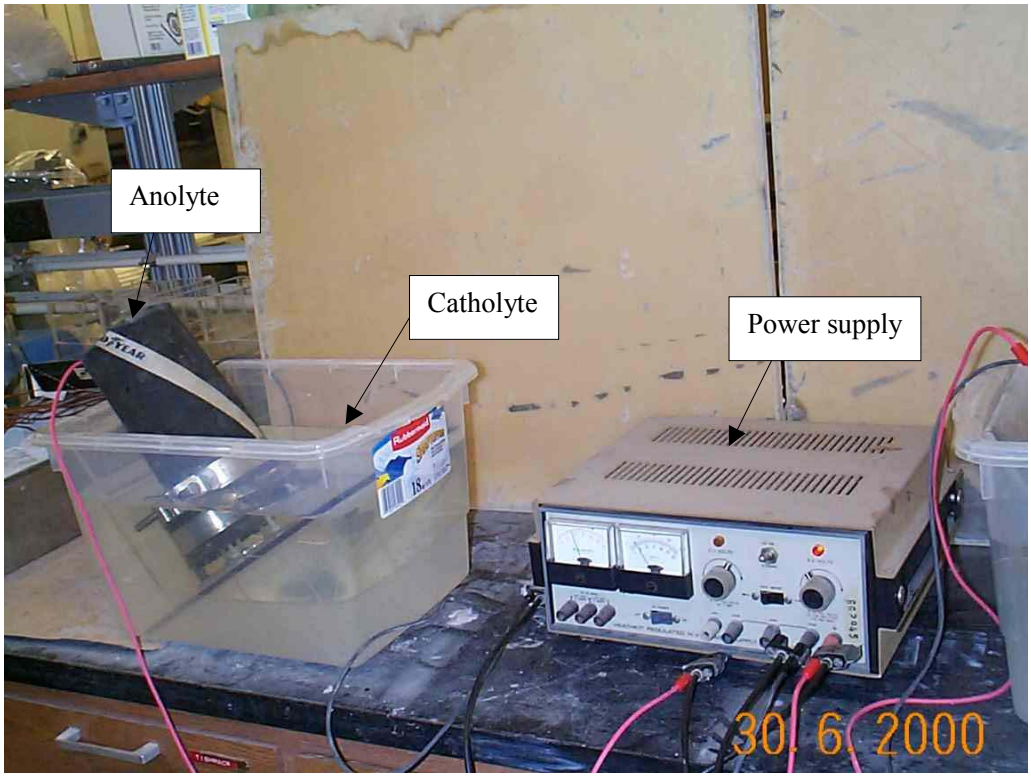


Figure 4.1: Set-up of the Test for Determination of Diffusion Coefficient from Migration

After the test is complete, the specimen is split into two pieces and the fractured surface is sprayed with 0.1M $AgNO_3$ solution. After about 15 minutes, AgCl precipitate will form on the area where the chlorides are present , as shown in Figure 4.2. The depth of chloride penetration is determined by measuring the location of the AgCl front from the center of specimen to both edges at 10-mm intervals (to within 10 mm from the edge).

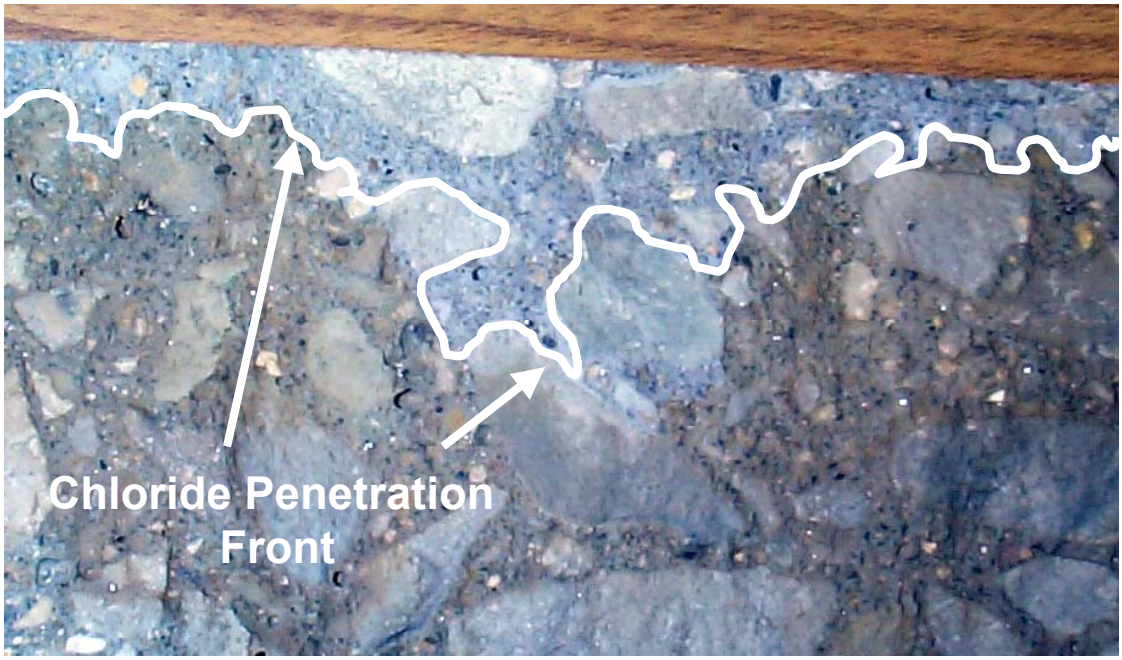


Figure 4.2: Chloride Penetration Front on the Fracture of Concrete Specimen after Migration Test

The depth of chloride penetration is used to calculate the chloride diffusion coefficient using Equation 4.7 shown below:

$$D_{nssm} = \frac{0.0239(273+T)L}{(U-2)t}(x_d - 0.0238\sqrt{\frac{(273+T)x_d}{U-2}}) \quad \text{.....(4.7)}$$

where:

T = average value of the initial and final temperature in the anolyte solution, °C;

L = thickness of the concrete specimen, m;

U = absolute value of the applied potential, V;

$D_{nssm}$ = non-steady state migration coefficient, $m^2/s$;

$x_d$ = average value of the penetration depths, m;

t = test durations, hour;

### 4.4.13 Resistance to Freezing and Thawing

The test for resistance of concrete to freezing and thawing cycles was performed in this study in accordance with ASTM C 666 –92 (Standard Test Method for Resistance of Concrete to Rapid Freezing and Thawing). Procedure A: rapid freezing and thawing in water was chosen in this study. The nominal freezing and thawing cycle for Procedure A consists of alternately lowering the temperature of the specimens from 40 to 0°F (4.4 to –17.8°C) and raising the temperature from 0 to 40°F (–17.8 to 4.4°C) in not less than 2 and not more than 5 hours. For Procedure A, not less than 25% of the time is required for thawing. There are 18 specimen chambers in the freezing and thawing instrument. One specimen was placed in the middle of the chamber, and a temperature sensor was inserted into the specimen to control the temperature in the chamber. The concrete beams were rotated from the right end to the left end after about every 30 freezing and thawing cycle. Grindosonic MK4 Sonometer was used to determine the resonant frequency of concrete specimens during the freezing and thawing cycles. The freezing and thawing cycles were continued until the specimen was subjected to 300 cycles, or until its relative dynamic modulus of elasticity reached 60% of the initial modulus, whichever occurred first.

The relative dynamic modulus of elasticity of concrete specimens can be calculated by the following equation:

$$P_N = (\frac{n_1^{\ 2}}{n^2}) \times 100 \quad \text{.....(4.8)}$$

$P_N$ = relative dynamic modulus of elasticity after N cycles of freezing and thawing, %,
n = fundamental transverse frequency at the beginning of the freezing and thawing cycles, and
$n_1$ = fundamental transverse frequency after N cycles of freezing and thawing.

### 4.4.14 Scaling Resistance to Deicing Salts

The resistance of concrete mixtures to deicer salt scaling was evaluated for Phase II concrete mixtures of this study. ASTM C 672(Standard Test Method for Scaling Resistance of Concrete Surfaces Exposed to Deicing Chemicals) was followed during the scaling test. This test covers the determination of the resistance to scaling of a horizontal concrete surface subjected to freezing and thawing cycles in the presence of deicing chemicals. The horizontal surface of slabs used for scaling resistance test was 10" x 7", and the thickness of the slab was 3".

A solution containing 4% anhydrous calcium chloride by weight was used during this test. The slabs were stored in a chamber where the temperature was alternately lowered to 0°F and maintained this temperature for 16 hours and then raised up to 23°C and maintained for 6 hours. This cycle was repeated daily, and the surface of concrete slab was flushed off every five cycles. The visual evaluation was made after flushing off, and the test was continued until 50 cycles.

# 5 RESULTS AND DISCUSSION FOR PHASE II MIXTURES

## 5.1 Properties of Concrete Mixtures in Fresh State

### 5.1.1 Compatibility of Chemical Admixtures

Since the 10 concrete mixtures selected in Phase II of this study were air-entrained concrete, it was necessary to use two types of chemical admixtures during the production of air-entrained concrete. One of the admixtures used was a high range water reducer and the other admixture used was an air-entraining agent.

RHEOBUILD 3000FC superplasticizer produced by Master Builders, Inc. was used at the beginning of Phase II of this study. However the compatibility of RHEOBUILD 3000FC with the air-entraining admixture DARAVAIR 1400 (produced by W. R. Grace & Co.) was not good, due to an unstable air bubble system. For No. 9 concrete mixture with 25% slag and w/b=0.35, a small change in the dosage of air-entraining admixtures caused large changes in the air content of the fresh concrete, as shown in Table 5.1. The aggregate correction factor for the air content was 0.3% in this study.

Table 5.1: Compatibility of RHEOBUILD 3000FC and DARAVAIR 1400

| Mixing No. | Dosage of RHEOBUILD 3000FC (ml) | Dosage of DARAVAIR 1400 (ml) | Slump (inches) | Air content (%) |
|---|---|---|---|---|
| 1 | 27 | 1.8 | 8.25 | 5.4 |
| 2 | 23 | 2.2 | 7.50 | 9.7 |
| 3 | 23 | 1.6 | 7.50 | 8.2 |
| 4 | 20 | 1.5 | 2.00 | 3.5 |
| 5 | 30 | 1.5 | 4.75 | 8.3 |
| 6 | 33 | 1.2 | 6.25 | 6.7 |

After consulting with the manufacturers (Master Builders, Inc., and W. R Grace & Co.), another type of high range water reducer DARACEM 19 was used to replace RHEOBUILD 3000FC. The air bubble system of No. 9 fresh concrete with DARACEM 19 and DARAVAIR 1400 was relatively stable, and the results showed good repeatability, as shown in Table 5.2.

Table 5.2: Compatibility of DARACEM 19 and DARAVAIR 1400

| Mixing No. | Dosage of DARACEM 19 (ml) | Dosage of DARAVAIR 1400 (ml) | Slump value (inch) | Air content (%) |
|---|---|---|---|---|
| 1 | 140 | 5.5 | 5.75 | 6.4 |
| 2 | 140 | 5.5 | 6.00 | 6.0 |
| 3 | 130 | 6.0 | 5.00 | 6.1 |

### 5.1.2 Design Parameters for Phase II Concrete Mixtures

As already discussed, the experiments performed in Phase I of this study resulted in 10 optimum concrete mixtures that were selected for further evaluation in Phase II. The design parameters used for mixtures produced in Phase II were similar to those used for mixtures produced in Phase I, with the exception that all mixtures in Phase II were air-entrained. The specific design parameters selected for mixtures in Phase II were as follows:

- Target slump: 5.5 inches with a tolerance of ±1.5 inches, (the same as used for mixtures in Phase I)
- Target total air content in fresh concrete: 6.5% with a tolerance of ±0.5%.
- A total binder content of 390 kg/m$^3$ (657 lbs/yd$^{3)}$ for all mixtures (the same as used for mixtures in Phase I).
- Although the basic composition of mixtures selected for Phase II of this study was similar to that used in Phase I of this study, some adjustments were necessary to accommodate the yield changes resulting from the increase in total air content. These adjustments involved changing the quantities of coarse and fine aggregates while keeping the water-cementitious material ratio and the total volume ratio of mortar (excluding volume of entrained air) in the Phase II mixtures at the same levels as these used in Phase I.

The process of mixture composition selection was as follows:

1. First the water content was calculated, based on the total binder content (fixed at 390 kg/m$^3$ of concrete) and water-binder ratio;
2. The next step involved calculation of the content of supplementary cementitious materials per cubic meter of concrete. This calculation was done using 1:1 weight replacement of cement;
3. Using volume fraction of mortar from Phase I concretes (0.582) and volume of cementitious materials (based on weight from step 2 above) the volume content of fine aggregate was calculated.
4. The coarse aggregate was determined by subtracting the volume of mortar and total air from the unit volume.

### 5.1.3 Proportioning of Concrete Mixtures

All concrete mixtures in Phase II of this study were air-entrained. Their design air content was 6.5% of total concrete volume. Since Phase I mixtures were not air-entrained, it was necessary while converting Phase I mixture composition into Phase II mixture composition to maintain the same yield. As the result of these adjustments, the coarse aggregate content changed from 1100 to 1049 kg/m$^3$ of concrete. The fine aggregate content also changed slightly in order to maintain the same mortar ratio by volume for concrete mixtures in these two parts of the study. The proportions of 10 concrete mixtures used in Phase II of this study are shown in Table 5.3. Additional details (mortar and paste volumes) are shown in Table 5.4.

### 5.1.4 Determination of Dosage of Chemical Admixtures

Under certain conditions, chemical admixtures, whose performance when used separately is satisfactory, may become incompatible when used in combination with other admixtures. Therefore, it is necessary to use trial mixtures for any combinations of admixtures. Since the 10 concrete mixtures in Phase II used different types of cementitious materials and variable water-binder ratios, trial mixtures were prepared for each of the 10 mixtures to determine optimum dosage of chemical admixtures. Since the order in which the materials are introduced to the mixer and the mixing time will influence the air content of fresh concrete, these factors were held constant during mixing.

The mixing procedure used in the production of Phase II concrete mixtures was as follows:

1. The inner-surface of the mixer was wetted;
2. Sand and coarse aggregate were added into the mixer and mixed for about 3 minutes. If needed, a small amount of water was added into the aggregate to keep it in the saturated surface-dry state;
3. All cementitious materials were added into the mixer, and mixed for 5 minutes to ensure uniform distribution of supplementary materials in the mixture;
4. The air-entraining admixture diluted with one liter of mixing water was added into the mixture and all ingredients were mixed for about 2 minutes;
5. Half of the water was added into the mixture and all ingredients were mixed for about 2 minutes;

Table 5.3: Mixture Proportions and Fresh Concrete Properties of 10 Concrete Mixtures Selected for Phase II Study

| Mix No. | W/B | Binder | | | | | Aggregate | | | HRWR* | AEA** | Slump | Air content |
|---|---|---|---|---|---|---|---|---|---|---|---|---|---|
| | | FA | SF | Slag | Portland cement | Total binder | Coarse | Fine | water | | | | |
| | | (%) | (%) | (%) | (kg/m$^3$) | (kg/m$^3$) | (kg/m$^3$) | (kg/m$^3$) | (kg/m$^3$) | (l/m$^3$) | (ml/m$^3$) | (mm) | (%) |
| 1 | 0.4 | 0 | 6 | 0 | 366.6 | 390 | 1049 | 683 | 156 | 2.9 | 195 | 165 | 6.50 |
| 2 | 0.4 | 25 | 6 | 0 | 269.1 | 390 | 1049 | 669 | 156 | 2.9 | 238 | 152 | 6.30 |
| 3 | 0.4 | 40 | 6 | 0 | 210.6 | 390 | 1049 | 661 | 156 | 2.4 | 238 | 165 | 6.40 |
| 4 | 0.4 | 25 | 0 | 0 | 292.5 | 390 | 1049 | 678 | 156 | 1.2 | 226 | 171 | 6.10 |
| 5 | 0.35 | 40 | 0 | 0 | 234.0 | 390 | 1049 | 721 | 137 | 2.4 | 191 | 165 | 6.50 |
| 6 | 0.4 | 0 | 6 | 25 | 269.1 | 390 | 1049 | 677 | 156 | 3 | 215 | 171 | 6.20 |
| 7 | 0.35 | 0 | 0 | 0 | 390.0 | 390 | 1049 | 743 | 137 | 3.1 | 133 | 165 | 6.50 |
| 8 | 0.4 | 0 | 0 | 0 | 390.0 | 390 | 1049 | 692 | 156 | 1.8 | 238 | 140 | 6.30 |
| 9 | 0.35 | 0 | 0 | 25 | 292.5 | 390 | 1049 | 737 | 137 | 3.3 | 133 | 146 | 6.40 |
| 10 | 0.35 | 25 | 0 | 25 | 195.0 | 390 | 1049 | 723 | 137 | 2.9 | 191 | 152 | 6.30 |

* DARACEM 19 (W. R. Grace & Co.) was used as high range water reducer (HRWR)

** DARAVAIR 1400 (W. R. Grace & Co.) was used as air entraining agent (AEA)

The quantities of HRWR and AEA were adjusted during mixing to obtain the target slump of 5.5 ± 1.5 in and air content of 6.5 ± 0.5%

Table 5.4: Mortar and Paste Volumes of Phase II Concrete Mixtures

| Mix No. | W/B | Binder | | | Sand/total aggregate | Paste volume ($yd^3$) | Paste Percent | Mortar volume ($yd^3$) | mortar ratio by volume |
|---|---|---|---|---|---|---|---|---|---|
| | | FA (%) | SF (%) | Slag (%) | | | | | |
| 1 | 0.4 | 0 | 6 | 0 | 0.404 | 0.285 | 101.2 | 0.569 | 0.581 |
| 2 | 0.4 | 25 | 6 | 0 | 0.400 | 0.290 | 102.8 | 0.569 | 0.581 |
| 3 | 0.4 | 40 | 6 | 0 | 0.398 | 0.293 | 103.8 | 0.569 | 0.581 |
| 4 | 0.4 | 25 | 0 | 0 | 0.403 | 0.286 | 101.7 | 0.569 | 0.581 |
| 5 | 0.35 | 40 | 0 | 0 | 0.417 | 0.270 | 95.7 | 0.569 | 0.581 |
| 6 | 0.4 | 0 | 6 | 25 | 0.403 | 0.287 | 101.8 | 0.569 | 0.581 |
| 7 | 0.35 | 0 | 0 | 0 | 0.423 | 0.262 | 93.1 | 0.569 | 0.581 |
| 8 | 0.4 | 0 | 0 | 0 | 0.407 | 0.282 | 100.0 | 0.569 | 0.581 |
| 9 | 0.35 | 0 | 0 | 25 | 0.421 | 0.264 | 93.8 | 0.569 | 0.581 |
| 10 | 0.35 | 25 | 0 | 25 | 0.418 | 0.269 | 95.4 | 0.569 | 0.581 |

6. High range water reducer (diluted with mixing water) and the remaining portion of the mix water were added into the mixture;
7. All ingredients were mixed for 3 minutes after all the water was added into the mixture;
8. The mixer was stopped for 3 minutes;
9. Mixing was resumed for additional 2 minutes;

Production of trial mixes continued until the desired slump and air content of fresh concrete were achieved. In general, it was much easier to achieve the desired slump than the target value of air content. After the slump value was achieved, the dosage of air entraining admixture was adjusted based on the results of the previous trial mixture until the desired value of air content was obtained.

### 5.1.5. Slump Loss and Air Loss

Fresh concrete will experience slump loss with time due to cement hydration, water evaporation, absorption of water by the aggregate and loss of entrained air. Addition of regular or high-range water reducer to concrete mixture initially increases the workability of fresh concrete. However, the addition of water reducer increases the degree of dispersion of cement particles in the water system, and could cause higher slump loss due to the increase in the rate of chemical reaction between cement particle and water. Therefore, concrete mixture with the addition of water reducer is expected to have relatively higher amount of slump loss compared with concrete without water reducer.

Concrete mixtures containing high range water reducers (HRWR) may experience relatively high rate of slump loss and loss of entrained air. Therefore, a series of tests was performed on all 10 Phase II mixtures to develop information on their relative susceptibility to slump and air losses. These tests were performed using the following procedure:

- After initial slump and air content testing, the portion of the concrete used for air content determination was discarded. The concrete mixture used for slump test was put back in the mixer;
- The concrete mixture was kept in mixer pan for 20 minutes;
- After 20 minutes of rest, the concrete was remixed for 45 seconds;
- Second readings for slump and air content were obtained. Again, concrete used for air content test was discarded and the concrete used for slump test was placed back into the mixer and reused;
- Concrete mixture was kept in mixer pan for additional 20 minutes and was then remixed for 45 seconds;
- After remixing, the third set of slump and air content data was collected;

The results obtained during the tests for slump loss and air content loss are summarized in Table 5.5. Most concrete mixtures experienced slump loss in the range from 0.75 inch to 1.75 inch, and the total air loss in the range from 0.6% to 1.8% during the first 20 minutes of rest. The slump loss after 40 minutes of rest varied from 1.5 to 3.25 inches (depending on the mixture proportion) with plain concrete mixtures (No. 7 & 8) experiencing higher slump loss than other concrete mixtures. At the same time, the values of air loss varied from 1.0 to 3.1%. Figure 5.1 shows the correlation between air loss and slump loss for concrete mixtures after 20 and 40 minutes' rest. In general, it appears that higher amount of air loss of concrete results in higher amount of slump loss for both rest periods. The increase in the amount of fly ash or slag in concrete mixture leads to smaller losses of slump and air content, as shown by the results obtained from mixtures No. 3, No. 4, No. 5 and No. 10.

Table 5.5: Results of Slump Loss and Air Loss for Phase II Mixtures

| Mix No. | Water Reducer * | Air entraining agent ** | Initial Readings | | Reading after rest period of 20 minutes | | Reading after rest period of 40 minutes | | Relative loss after rest period of 20 minutes | | relative loss after rest period of 40 minutes | |
|---|---|---|---|---|---|---|---|---|---|---|---|---|
| | | | slump | air content | slump | air content | slump | air content | slump loss | air loss | slump loss | air loss |
| | ($l/m^3$) | ($ml/m^3$) | (inch) | (%) | (inch) | (%) | (inch) | (%) | (inch) | (%) | (inch) | (%) |
| 1 | 2.7 | 193 | 7.00 | 6.7 | 6.00 | 5.8 | 4.75 | 4.7 | 1.00 | 0.9 | 2.25 | 2.0 |
| 2 | 2.4 | 262 | 6.50 | 6.2 | 5.25 | 4.7 | 4.00 | 4.1 | 1.25 | 1.5 | 2.50 | 2.1 |
| 3 | 1.4 | 262 | 6.50 | 5.9 | 5.50 | 5.3 | 5.00 | 4.9 | 1.00 | 0.6 | 1.50 | 1.0 |
| 4 | 1.2 | 238 | 6.75 | 6.5 | 6.00 | 5.7 | 4.75 | 5 | 0.75 | 0.8 | 2.00 | 1.5 |
| 5 | 2.4 | 193 | 6.50 | 6.7 | 5.75 | 5.9 | 4.50 | 4.8 | 0.75 | 0.8 | 2.00 | 1.9 |
| 6 | 3.1 | 238 | 5.50 | 5.2 | 4.00 | 3.7 | 2.75 | 2.6 | 1.50 | 1.5 | 2.75 | 2.6 |
| 7 | 2.4 | 167 | 6.50 | 6.0 | 5.00 | 4.2 | 3.25 | 3.5 | 1.50 | 1.8 | 3.25 | 2.5 |
| 8 | 1.9 | 262 | 5.25 | 6.5 | 3.50 | 4.9 | 2.00 | 3.5 | 1.75 | 1.6 | 3.25 | 3.0 |
| 9 | 3.3 | 131 | 5.75 | 6.4 | 4.25 | 4.8 | 2.75 | 3.3 | 1.50 | 1.6 | 3.00 | 3.1 |
| 10 | 2.9 | 190 | 6.00 | 6.2 | 5.00 | 5.5 | 3.75 | 4.7 | 1.00 | 0.7 | 2.25 | 1.5 |

* DARACEM 19 produced by W. R. Grace was used as high range water reducer (HRWR);

** DARAVAIR 1400 produced by W. R. Grace was used as air entraining agent (AEA);

The quantities of HRWR and AEA were adjusted during mixing to obtain the target slump of 5.5 ± 1.5 inch and air content of 6.5 ± 0.5%.

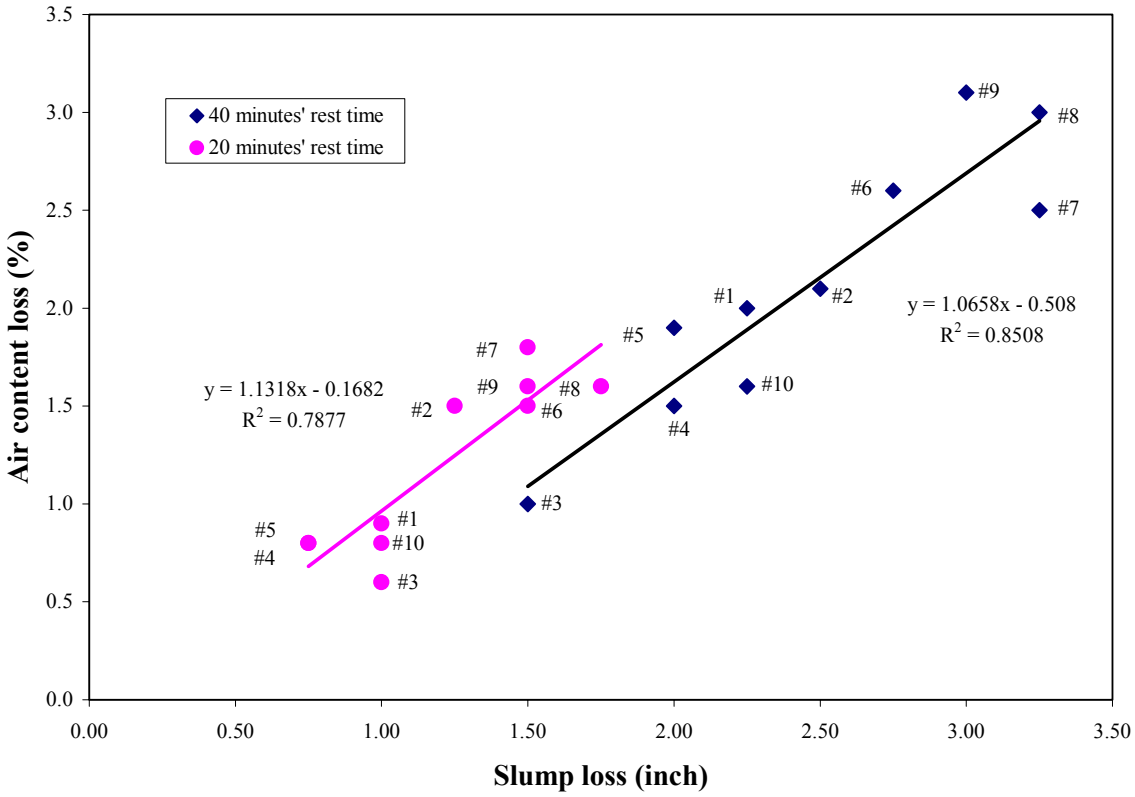


Figure 5.1: Slump Loss versus Air Content Loss for Phase II Concrete Mixtures

## 5.2 Compressive Strength

10 concrete mixtures were prepared in Phase II of this study and were used to investigate the gain of compressive strength with time. Specimens were cured continuously in a standard moist room at the temperature of 23°C and relative humidity of 100% RH until the designed test ages of 1, 3, 7, 28, 56, and 180 days. Three cylinders were tested at each age for each concrete mixture. In order to avoid the effects of type of coarse aggregate on the compressive strength of concrete, only one type of crushed limestone coarse aggregate was used in this research, and the maximum size of coarse aggregate was 1 inch. The summary of compressive strength results is shown in Table 5.6.

Table 5.6: Compressive Strength of Phase II Concrete Mixtures

| Mix No. | W/B | Binder | | | Compressive strength (psi) | | | | | |
|---|---|---|---|---|---|---|---|---|---|---|
| | | FA | SF | Slag | | | | | | |
| | | % | % | % | 1 day | 3 days | 7 days | 28 days | 56 days | 180 days |
| 1 | 0.4 | 0 | 6 | 0 | 2334 | 4960 | 6167 | 8143 | 8714 | 9098 |
| 2 | 0.4 | 25 | 6 | 0 | 1273 | 3860 | 5411 | 7401 | 8873 | 9059 |
| 3 | 0.4 | 40 | 6 | 0 | ------ | 3090 | 4390 | 6817 | 7865 | 9191 |
| 4 | 0.4 | 25 | 0 | 0 | 1651 | 3926 | 5385 | 7056 | 7931 | 9204 |
| 5 | 0.35 | 40 | 0 | 0 | ------ | 3833 | 5226 | 7520 | 8356 | 9708 |
| 6 | 0.4 | 0 | 6 | 25 | 2202 | 4257 | 5730 | 8223 | 8502 | 9059 |
| 7 | 0.35 | 0 | 0 | 0 | 3004 | 5769 | 6897 | 8754 | 8846 | 10133 |
| 8 | 0.4 | 0 | 0 | 0 | 2507 | 4536 | 4874 | 6990 | 7334 | 8369 |
| 9 | 0.35 | 0 | 0 | 25 | 3263 | 5836 | 7162 | 8966 | 10040 | 10730 |
| 10 | 0.35 | 25 | 0 | 25 | ------ | 4072 | 5637 | 8342 | 9801 | 10677 |

When compared with plain concrete mixture having the same w/b (mixture 8) the addition of 6% silica fume to No. 1 concrete improved the compressive strength at ages of 3 days and higher. The average improvement was about 1000 psi. When used at the same replacement level (25%) as fly ash, slag did not hinder the development of early age compressive strength. For example, mixture No. 6 had a 1-day strength comparable to the strength of No. 1 mixture. Although addition of fly ash reduced the development of early age strength, at later ages fly ash mixtures achieved strengths comparable to the strength of mixtures without fly ash (compare mixtures No. 2 and No. 6).

### 5.2.1 Early-age Compressive Strength of HPC

In general, the addition of supplementary cementitious materials reduced the 1-day strength for all concretes except for mixture No. 9 that contained 25% of slag, as shown in Table 5.6. The relative strength reduction increased with the increase in the amount of fly ash. Water-binder ratio has a significant effect on the 1-day strength, and the decrease of w/b will increase the early age strength. As to the 3-day strength, concrete with 6% silica fume (No. 1) showed higher compressive strength than that of No. 8. Other concrete mixtures at 0.40 w/b with the addition of fly ash still showed a little lower 3-day strength than No. 8. After 6 days of moist curing, only one mixture (No. 3) showed a lower strength than No. 8, and the others achieved higher 7-day strength than No. 8. The degree of 7-day strength increase varied from 7% to 47% depending on the mixture, as shown in Table 5.7.

Table 5.7: Development of Relative Compressive Strength of Phase II Mixtures

| Mix No. | W/B | Binder | | | Relative Compressive Strength* (%) | | | | | |
|---|---|---|---|---|---|---|---|---|---|---|
| | | FA | SF | Slag | | | | | | |
| | | % | % | % | 1 day | 3 days | 7 days | 28 days | 56 days | 180 days |
| 1 | 0.4 | 0 | 6 | 0 | 93.1 | 109.3 | 126.5 | 116.5 | 118.8 | 108.7 |
| 2 | 0.4 | 25 | 6 | 0 | 50.8 | 85.1 | 111.0 | 105.9 | 121.0 | 108.2 |
| 3 | 0.4 | 40 | 6 | 0 | ------ | 68.1 | 90.1 | 97.5 | 107.2 | 109.8 |
| 4 | 0.4 | 25 | 0 | 0 | 65.9 | 86.6 | 110.5 | 100.9 | 108.1 | 110.0 |
| 5 | 0.35 | 40 | 0 | 0 | ------ | 84.5 | 107.2 | 107.6 | 113.9 | 116.0 |
| 6 | 0.4 | 0 | 6 | 25 | 87.8 | 93.8 | 117.6 | 117.6 | 115.9 | 108.2 |
| 7 | 0.35 | 0 | 0 | 0 | 119.8 | 127.2 | 141.5 | 125.2 | 120.6 | 121.1 |
| 8 | 0.4 | 0 | 0 | 0 | 100.0 | 100.0 | 100.0 | 100.0 | 100.0 | 100.0 |
| 9 | 0.35 | 0 | 0 | 25 | 130.1 | 128.7 | 146.9 | 128.3 | 136.9 | 128.2 |
| 10 | 0.35 | 25 | 0 | 25 | ------ | 89.8 | 115.7 | 119.3 | 133.6 | 127.6 |

* The relative compressive strength at each age is calculated with respect to concrete mixture No. 8.

The data from Table 5.8 indicate that at 7 days most concrete mixtures had achieved about 70% of 28-day compressive strength except for mixture No. 3. Mixtures No. 2, 6, and 10 have a similar 7-day strength development rate as mixture No. 8. Based on the results obtained in this study, replacing part of cement with fly ash, silica fume, slag or combination of any two of these admixtures will generally lead to reduction of early age (up to 7 days) strength.

Table 5.8: Compressive Strength Gain of Phase II Concrete Mixtures with Time*

| Mix No. | W/B | Binder | | | Relative compressive strength (%) | | | | | |
|---|---|---|---|---|---|---|---|---|---|---|
| | | FA | SF | Slag | | | | | | |
| | | % | % | % | 1 day | 3 days | 7 days | 28 days | 56 days | 180 days |
| 1 | 0.4 | 0 | 6 | 0 | 28.7 | 60.9 | 75.7 | 100.0 | 107.0 | 111.7 |
| 2 | 0.4 | 25 | 6 | 0 | 17.2 | 52.2 | 73.1 | 100.0 | 119.9 | 122.4 |
| 3 | 0.4 | 40 | 6 | 0 | ---- | 45.3 | 64.4 | 100.0 | 115.4 | 134.8 |
| 4 | 0.4 | 25 | 0 | 0 | 23.4 | 55.6 | 76.3 | 100.0 | 112.4 | 130.4 |
| 5 | 0.35 | 40 | 0 | 0 | ---- | 51.0 | 69.5 | 100.0 | 111.1 | 129.1 |
| 6 | 0.4 | 0 | 6 | 25 | 26.8 | 51.8 | 69.7 | 100.0 | 103.4 | 110.2 |
| 7 | 0.35 | 0 | 0 | 0 | 34.3 | 65.9 | 78.8 | 100.0 | 101.1 | 115.8 |
| 8 | 0.4 | 0 | 0 | 0 | 35.9 | 64.9 | 69.7 | 100.0 | 104.9 | 119.7 |
| 9 | 0.35 | 0 | 0 | 25 | 36.4 | 65.1 | 79.9 | 100.0 | 112.0 | 119.7 |
| 10 | 0.35 | 25 | 0 | 25 | ---- | 48.8 | 67.6 | 100.0 | 117.5 | 128.0 |

* The compressive strength gain of concrete is expressed as the percent of compressive strength at any age to that at 28 days.

### 5.2.2 Long-term Compressive Strength of Concrete Mixtures

Continuous moist curing resulted in an increase of the compressive strength and at 180 days all mixtures showed higher strength than at 56 days. Concrete with higher content of supplementary cementitious materials showed higher increase rate of compressive strength with prolonged moist curing. For example, at 180 days the compressive strength of mixtures No. 3, No. 4, No. 5 and No. 10 was about 30% higher than the 28-day compressive strength. Other concrete mixtures showed 10 to 20% increase of 180-day compressive strength compared to 28-day strength.

### 5.2.3 Verification of Semi-empirical Models for Compressive Strength

Based on compressive strength data obtained from 45 concrete mixtures from three different binder systems tested during Phase I of this study, statistically best fitting quadratic models were developed for each binder system.

For Portland cement/fly ash/silica fume binder system, the best fitting model for 28-day compressive strength is given by:

$$\text{Compressive strength (psi) at 28 days} = 9621.5 + 93.0*(SF - 5) - 28772*(w/b - 0.40) - 143030*(w/b - 0.40)^2 - 9.5*(FA - 20)*(SF - 5) + 452.6*(FA - 20)*(w/b - 0.40) \quad (5.1)$$

$$\text{Compressive strength (psi) at 56 days} = 10190 + 70.6*(SF - 5) - 30438*(w/b - 0.40) + 116310*(w/b - 0.4)^2 + 487.4*(FA - 20)*(w/b - 0.40) \quad (5.2)$$

For Portland cement/slag/silica fume binder system, the best fitting model for compressive strength is given by:

$$\text{Compressive strength (psi) at 28 days} = 9923.6 + 24.2*(slag - 20) + 168.6*(SF - 5) - 30563*(w/b - 0.40) - 55.5*(SF - 5)^2 \quad (5.3)$$

$$\text{Compressive strength (psi) at 56 days} = 10521 - 30985*(w/b - 0.40) - 1.43*(slag - 20)^2 - 71.8*(SF - 5)^2 \quad (5.4)$$

For Portland cement/ fly ash/ slag binder system, the best fitting models for compressive strength are:

$$\text{Compressive strength (psi) at 28 days} = 8551.4 - 19995*(w/b - 0.40) - 2.04*(Slag - 20)^2 + 171215*(w/b - 0.40)^2 + 318*(FA - 20)*(w/b - 0.40) - 945*(Slag - 20)*(w/b - 0.40) \quad (5.5)$$

$$\text{Compressive strength (psi) at 56 days} = 9641 + 18.0*(FA - 20) - 18.0*(slag - 20) - 26186*(w/b - 0.40) - 3.0*(Slag - 20)^2 + 242875*(w/b - 0.40)^2 - 3.41*(FA - 20)*(Slag - 20) - 1288.3*(Slag - 2)*(w/b - 0.40) \quad (5.6)$$

As discussed at the beginning of this chapter, all the concrete mixtures in Phase II were air-entrained with a design air content of 6.5%. However, the models constructed for compressive strength are based on Phase I mixtures that only had about 2% of entrapped air. Therefore, the strength decrease due to increased air content should be considered while applying these models to Phase II mixtures. This was done by assuming that 1% difference in the air content will result in 500 psi compressive strength reduction.

Due to the variations in the type of binders used to produce Phase II mixtures, theoretically more than one model can be used for strength prediction. For example, in order to predict the compressive strength of No. 1 concrete, two different models (one developed for Portland cement/fly ash/silica fume binder system and the other developed for Portland cement/slag /silica fume binder system) can be applied. The summary of predicted results is shown in Table 5.9. The short dashed line shown in the cells of the table indicates that the compressive strength cannot be predicted by the specific models. For example, the compressive strength of No. 1 concrete can not be predicted by the model developed for FAGBS binder system, as shown by the two short dashed line in the cells related to No. 1 mixture.

In general, FAGBS models are not effective for the prediction of the compressive strength of plain concrete or concrete mixtures only with fly ash. When using this model, about 2000 psi differences between the test value and predicted values have been observed, especially for 56-day compressive strength of No. 7 and No. 8 mixtures. In addition, the predicted 56-day compressive strength values were lower than the 28-day predicted values, contrary to the trends observed for actual test data. Based on FAGBS models, the predicted values for No. 9 and No. 10 concrete mixtures matched the laboratory values for both 28-day and 56-day compressive strength. The match was particularly good for No. 10 mixture. The effectiveness of the FAGBS model is closely related to the actual binder combination used during its development. As most mixtures used in Phase I of this study contained both fly ash and slag, it is not surprising that FAGBS model will be more accurate in predicting the strength of mixtures containing both fly ash and slag additions.

Table 5.9: Summary of Test and Predicted Values of Compressive Strength for Phase II Concrete Mixtures

| Mix No. | W/B | Binder | | | Test Value | | Predicted Value | | | | | |
|---|---|---|---|---|---|---|---|---|---|---|---|---|
| | | | | | Compressive Strength (psi) | | By FASF model | | By GBSF model | | By FAGBS model | |
| | | FA | SF | Slag | | | | | | | | |
| | | % | % | % | 28days | 56days | 28days | 56days | 28days | 56days | 28days | 56days |
| 1 | 0.4 | 0 | 6 | 0 | 8143 | 8714 | 7503 | 7861 | 7152 | 7478 | ---- | ---- |
| 2 | 0.4 | 25 | 6 | 0 | 7401 | 8873 | 7367 | 7961 | ---- | ---- | ---- | ---- |
| 3 | 0.4 | 40 | 6 | 0 | 6817 | 7865 | 7176 | 7911 | ---- | ---- | ---- | ---- |
| 4 | 0.4 | 25 | 0 | 0 | 7056 | 7931 | 7193 | 7637 | ---- | ---- | 5330 | 6384 |
| 5 | 0.35 | 40 | 0 | 0 | 7520 | 8356 | 9045 | 8762 | ---- | ---- | 4858 | 2569 |
| 6 | 0.4 | 0 | 6 | 25 | 8223 | 8502 | ---- | ---- | 7908 | 8164 | ---- | ---- |
| 7 | 0.35 | 0 | 0 | 0 | 8754 | 8846 | 8060 | 9737 | 6335 | 7305 | 5437 | 4767 |
| 8 | 0.4 | 0 | 0 | 0 | 6990 | 7334 | 5912 | 7537 | 4907 | 5855 | 6137 | 5295 |
| 9 | 0.35 | 0 | 0 | 25 | 8966 | 10040 | ---- | ---- | 6991 | 7890 | 8133 | 9344 |
| 10 | 0.35 | 25 | 0 | 25 | 8342 | 9801 | ---- | ---- | ---- | ---- | 7785 | 9419 |

The GBSF models can predict the compressive strength of No. 6 concrete mixture quite accurately. The difference between the predicted and laboratory results was less than 350 psi. Again, this model is not well suited to predict the strength of a plain concrete mixture as it gives values that are about 1500 to 2000 psi different from measured values.

The FASF models gave good strength prediction for concrete mixtures (including No. 1, No. 2, No. 3 and No. 4) for both 28-day and 56-day compressive strength. In most cases the difference between the predicted and laboratory results varied from 100 psi to 800 psi. In addition, these models also gave a fair prediction of strength for plain concrete (mixtures No. 7 and No. 8), compared with the models developed for other two binder systems. The FASF models also give a fair prediction of strength for concrete containing just silica fume or fly ash.

### 5.2.4 Factors Affecting Compressive Strength of HPC

Porosity of concrete is one of the most important factors affecting the compressive strength of concrete. Thus, other factors that can influence the porosity of concrete will affect the compressive strength. The porosity of concrete includes porosity existing in both cement paste matrix and the transition zone between the cement paste and aggregate. Therefore, water-binder ratio is the obvious factor that will influence strength because as the water-binder ratio increases, the porosity of concrete also increases. This is illustrated by data in Table 5.6 where No. 7 with 0.35 w/b developed (as expected) higher strength than No. 8 with 0.40 w/b.

When air voids are entrained or entrapped in concrete, reduction of compressive strength can be expected because of the higher porosity of the concrete. During this study, the assumption was made that a 1% difference in the air content of concrete results in a change of 500 psi in compressive strength.

The characteristics of aggregate such as the size, shape, surface texture, grading and mineralogy also affect concrete strength [Cetin et al., 1998, Kjellsen, 1998, and Zhou, 1995]. These characteristics affect the water demand in the mixture or change the quality of transition zone between cement paste and aggregate, and therefore, affect the strength.

The effect of mixture composition on the strength is mainly related to the change in the quality of paste matrix and the transition zone. From test results shown in this study, different binder combinations resulted in development of different ultimate strength and different rate of strength gain. With the increase in curing time, the compressive strength of concrete will also increase. However, different concrete mixtures have their own rate of strength development. For example, mixtures with fly ash or slag need more time to achieve a given level of strength than mixtures with silica fume. Type of cement will also influence the compressive strength and the rate of gain of strength. As the temperature can influence the cement hydration rate, it is expected that temperature will influence both ultimate strength and the rate of strength development. As a result, concrete will achieve lower early age strength during colder parts of the year than during summer even if the same composition is used.

## 5.3 Modulus of Elasticity

### 5.3.1 Introduction

The modulus of elasticity is one of the most important mechanical properties of concrete. In spite of the nonlinear behavior of concrete, an estimate of the elastic modulus is necessary to determine the stresses induced by the strain associated with environmental effects. During this study, ASTM C 469 standard was used to determine the modulus of elasticity.

Based on the literature review [NCHRP 380], adjusted for creep, the concrete modulus of elasticity affects both the thermal and shrinkage stresses more than other physical concrete properties. Low modulus of elasticity would help to decrease the stress due to the thermal and shrinkage strain. The modulus of elasticity of concrete is mainly determined by the modulus of elasticity of the aggregates used, and concrete containing aggregate with low modulus will also have low modulus. In addition, the elastic modulus of concrete also depends on the other properties of aggregate such as the mineralogy, surface texture, and particle size [Cetin et al., 1998]. In general, concrete with crushed limestone achieves higher modulus of elasticity than that with crushed gravel or trap rock at a given aggregate content. . Low modulus of elasticity of aggregate may be needed to achieve low modulus of elasticity of concrete. Also, concrete with higher aggregate content will have higher modulus.

However, high modulus of elasticity, low drying shrinkage and creep, and low thermal strain are the key factors contributing to high dimensional stability of concrete, which is essential for counteracting any undesirable stress effects produced as a result of volume changes under conditions of restraint [Mehta et al., 1990]. Certain level of modulus of elasticity is needed for high performance concrete to provide adequate stiffness to avoid excessive deformation and to provide satisfactory serviceability of structures.

Based on the research by French et al.[1999], restraint of concrete deck shrinkage was believed to be the primary cause of transverse cracks. In order to reduce the stress produced due to the volume changes of restrained concrete, lower modulus of elasticity is also needed, for Lower modulus of elasticity enables the concrete structure to undergo larger shrinkage deformation before cracking. Through using low modulus of elasticity of aggregate, and high water binder ratio, and increasing paste content can reduce the concrete modulus of elasticity. However, the total amount of shrinkage would increase significantly.

According to high performance concrete defined for highway structures [Goodspeed, et al., 1996], three grades have been specified for modulus of elasticity of concrete. The range of the first grade of the modulus of elasticity is from 28 to 40 GPa. Other grades of HPC require higher amount of modulus of elasticity (higher than 40 GPa). As

discussed later in this section, the modulus of elasticity of Phase II concrete achieved in this test was in the range of 25 to 34 GPa, which was generally in the first grade of modulus of elasticity specified for HPC.

### 5.3.2 Review of Existing Models for Modulus of Elasticity

The modulus of elasticity of concrete is determined by the properties of cement paste, the characteristics of aggregate, and the interface between the cement paste and aggregate.

Usually, the elasticity modulus of concrete is expressed as the function of compressive strength of concrete. The most common equations that relate modulus of elasticity to compressive strength are summarized in Table 5.10.

Table 5.10: Models for Modulus of Elasticity of Concrete

| Reference | Equation | Units | Notes |
|---|---|---|---|
| ACI 363R-92 | $E_c = 3320 (f_c')^{1/2} + 6900$ | Ec, $fc'$: MPa | $21MPa < f_c' < 83MPa$ |
| ACI 318M-89 | $E_c = 4700 (f_c')^{1/2}$ | Ec, $f_c'$: MPa | $f_c' < 41MPa$ |
| CAN A23.3-M90 | $E_c = 5000 (f_c')^{1/2}$ | Ec, $fc'$: MPa | |
| CEB-FIP-90 | $E_c = 10 (f_c' + 8)^{1/3}$ | Ec: GPa; $fc'$: MPa | $f_c' < 80MPa$ |
| Parrott (1979) | $E_c = K_0 + 0.2\ fc'$ | Ec: GPa; $fc'$: MPa | $K_0$: a factor depending on the type of aggregate $20MPa < f_c' < 70MPa$ |

Only the model proposed by Parrott [1979] includes the effect of coarse aggregate on elastic modulus of concrete. Each model has its own valid range of compressive strength and the transition zone is not considered when calculating the elastic modulus of concrete. It has been reported [Mehta, 1993] that the strength and elastic modulus of concrete are not influenced to the same degree by curing age. With different concrete mixtures of varying strength, it was found that at later ages, (3 months to 1 year) the elastic modulus increases at a higher rate than the compressive strength. This was attributed to beneficial effect of improvement in the density of the transition zone.

It has been reported [Cetin et al, 1995] that: although modulus of elasticity can be expressed as a function of compressive strength, whenever possible, the measured value should be used in analysis instead of any predicted value. This conclusion was reinforced by the results from this study, as shown in Figure 5.2. The lines shown in Figure 5.2 are based on the five models for elastic modulus of concrete given in Table 5.10. The diamond points (and rectangle points) are the results obtained from laboratory test.

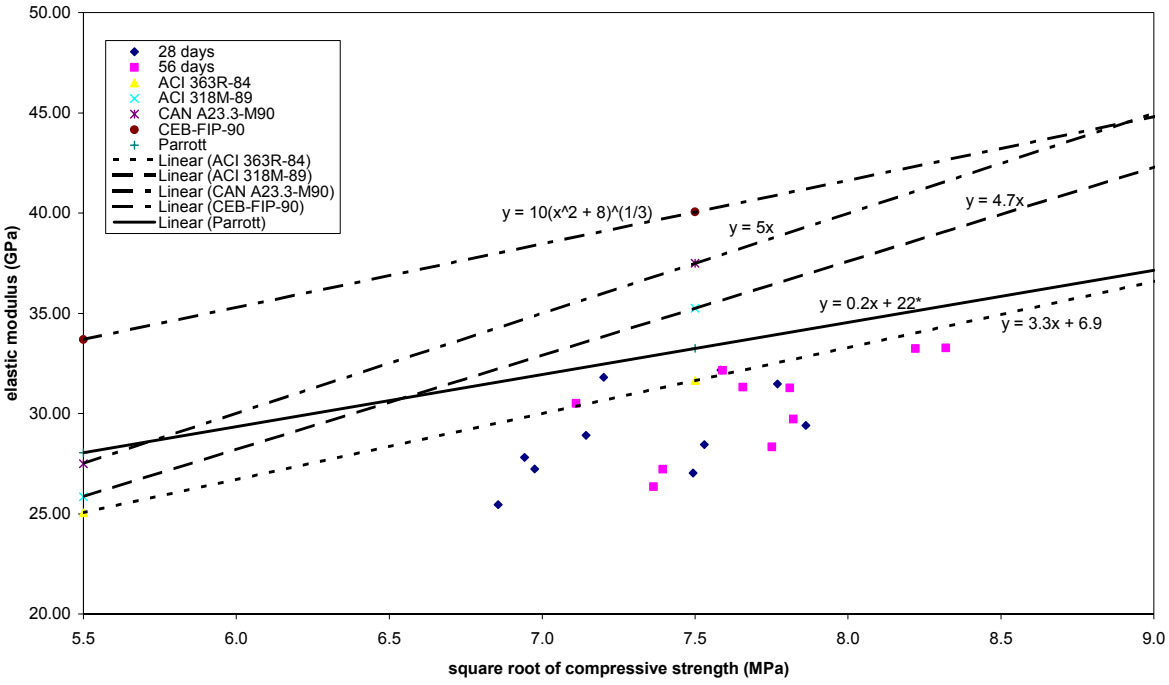


Figure 5.2: Relationships between Compressive Strength and Elastic Modulus

### 5.3.3. Results and Discussion

This section presents the results and analysis of static modulus and dynamic modulus of elasticity of Phase II concrete mixtures. The static modulus of elasticity of concrete was determined in accordance to ASTM C 469 (Standard Test Method for Static Modulus of Elasticity and Poisson's Ratio of Concrete in Compression). 100 mm x 200 mm concrete cylinders were used for this test. The summary results of the static modulus of elasticity of Phase II concrete mixtures are shown in Table 5.11.

As shown in Table 5.11, the static modulus of elasticity of concrete was in the range of 25 to 34 GPa for Phase II concrete. The static modulus of elasticity of concrete increases with the test age, and the amount of increase in the static modulus of concrete was very limited (less than 15%) from 28 days to 56 days. In general, concrete mixtures (No. 5, No.7, No. 9, and No. 10) with low water-binder ratio (= 0.35) achieved higher static modulus of elasticity than concrete mixtures (No. 1, No. 2, No. 3, No. 4, No. 6 and No. 8) with high water-binder ratio (= 0.40).

Table 5.11: Summary Results of Dynamic and Static Moduli of Elasticity for Phase II Mixtures

| Mix No. | W/B | Binder | | | Static Modulus Ec (GPa) | | Dynamic Modulus Ed (GPa) | (Ed - Ec)/Ec |
|---|---|---|---|---|---|---|---|---|
| | | FA (%) | SF (%) | Slag (%) | 28 days | 56 days | 56days | Percent (%) |
| 1 | 0.4 | 0 | 6 | 0 | 27.04 | 28.33 | 34.83 | 18.7 |
| 2 | 0.4 | 25 | 6 | 0 | 28.92 | 29.73 | 33.15 | 10.3 |
| 3 | 0.4 | 40 | 6 | 0 | 25.46 | 26.35 | 32.90 | 19.9 |
| 4 | 0.4 | 25 | 0 | 0 | 27.23 | 27.22 | 33.40 | 18.5 |
| 5 | 0.35 | 40 | 0 | 0 | 31.81 | 32.15 | 35.82 | 10.2 |
| 6 | 0.4 | 0 | 6 | 25 | 28.45 | 31.31 | 35.52 | 11.9 |
| 7 | 0.35 | 0 | 0 | 0 | 31.47 | 31.27 | 40.57 | 22.9 |
| 8 | 0.4 | 0 | 0 | 0 | 27.81 | 30.50 | 38.68 | 21.1 |
| 9 | 0.35 | 0 | 0 | 25 | 29.40 | 33.27 | 36.46 | 8.8 |
| 10 | 0.35 | 25 | 0 | 25 | 32.18 | 33.24 | 38.58 | 13.8 |

The dynamic modulus of concrete prisms was determined in accordance with ASTM E 1876 (Standard Test Method for Dynamic Young's Modulus, and Poisson's Ratio by Impulse Excitation of Vibration). The Grindo-sonic Mk4x manufactured by J. M. Lemmens, St. Louis, Missouri, was used in the flexural mode to determine the resonant frequencies. Prismatic specimens with a size of 3" x 3" x 15" were used in this test. The dynamic modulus of elasticity of concrete was tested at 56 days.

The results of dynamic modulus of elasticity of concrete were shown in Table 5.11. In general, concrete with low water binder ratio had relatively higher dynamic modulus of elasticity than concrete with high water-binder ratio. As shown in Table 5.11, the dynamic modulus of concrete was higher than static modulus, and the difference between the dynamic and static modulus of elasticity of Phase II concrete was in the range of 8.8% to 22.9%, depending on the concrete mixture proportions. In general, dynamic modulus is higher by 20, 30 and 40% than the static modulus of elasticity for high, medium, and low-strength concretes, respectively [Mehta, 1993]. Therefore, the results achieved in this study coincided with the literature.

Because the ratio of static modulus of elasticity to the dynamic modulus always varies, no simple relationship exists between these two parameters, although some equations relating them have been reported in the literature [Neville, 1996].

### 5.3.4. Verification of Semi-empirical Elastic Modulus Models Built in This Study

The elastic modulus models constructed for mixtures from Phase I of the study are based on the results from non-air entrained concrete. The nominal difference in the air content between Phase I and Phase II mixtures is about 4.5%. Assuming the unit weight of Phase I concrete to be 2400 kg/m$^3$, 4.5% increase in air content will lead to about 18% reduction in elastic modulus as shown below:

According to the equation relating unit weight and compressive strength to the modulus [ACI 318M]:

$$E_c = 0.043 \times W_c^{1.5} \times (f_c)^{0.5} \quad \text{.....(5.7)}$$

% Reduction of $E_c$ = $100-(0.955*/1.0)^{1.5}*(1-5*4.5/100)^{1/2}*100 = 18$ (%).....(5.7)

.

As shown in Table 5.12, the predicted values of elastic modulus show generally that the models constructed work effectively. In most cases, the difference between the laboratory results and predicted values is less than 3 GPa, or about 10% of the test result. However, there are some abnormal mixtures. For example, some predicted 28-day values are larger than predicted 56-day values, i.e., values for mixtures No. 5, No. 7 predicted by FASF model, and values for mixtures No. 10 by FAGBS model based on Phase I mixtures.

Table 5.12: Actual and Predicted Value of Elastic Modulus of Air-entrained Concrete

| Mix No. | W/B | Actual value | | Predicted Value (ksi) | | | | | |
|---|---|---|---|---|---|---|---|---|---|
| | | elsatic modulus (ksi) | | By FASF model | | By GBSF model | | By FAGBS model | |
| | | 28days | 56days | 28days | 56days | 28days | 56days | 28days | 56days |
| 1 | 0.4 | 3920 | 4108 | 4264 | 4325 | | | | |
| 2 | 0.4 | 4193 | 4310 | 4325 | 4409 | | | | |
| 3 | 0.4 | 3691 | 3821 | 4264 | 4817 | | | | |
| 4 | 0.4 | 3949 | 3947 | 4180 | 4454 | | | 4191 | 4394 |
| 5 | 0.35 | 4612 | 4662 | 5191 | 4943 | | | 3916 | 4881 |
| 6 | 0.4 | 4125 | 4540 | | | 4315 | 4520 | | |
| 7 | 0.35 | 4564 | 4534 | 5191 | 4927 | 3260 | 4383 | 3779 | 4621 |
| 8 | 0.4 | 4033 | 4423 | 4649 | 4887 | 3399 | 4309 | 3708 | 4415 |
| 9 | 0.35 | 4263 | 4824 | | | 4637 | 4826 | 4321 | 4859 |
| 10 | 0.35 | 4666 | 4820 | | | | | 4804 | 4541 |

## 5.4 Rapid Chloride permeability

### 5.4.1 Introduction

Compressive strength and water binder ratio are conventionally used to describe the quality of concrete mixtures, and they have been extensively used for formulating technical specifications and guidelines for concrete mixture design, and quality control of the construction process. In this study, attempts were made to identify the performance characteristics of concrete that essentially influence the long-term durability and service life of concrete structure under certain environmental exposure. Efforts were also made to evaluate these performance characteristics of concrete in the laboratory and relate the data to values that can be obtained from the field measurement. New criteria (performance characteristics rather than compressive strength) are used to design the concrete mixture proportions with enhanced properties.

Chloride induced corrosion of reinforcing bars in concrete is one of main causes of premature deterioration and degradation of bridge deck structures located in the state of Indiana. In this region, bridge decks are exposed to de-icing salts. In order to prevent or delay the occurrence of corrosion of steel bars in bridge decks, one of the effective approaches is to design more impermeable concrete to hinder the penetration of chloride ion into concrete. Therefore, chlorides permeability of concrete mixtures is treated as an intrinsic property of concrete. Several test methods related to chloride permeability of concrete are now available, and one of them is Rapid Chloride Ion Permeability Test (RCPT), covered by the ASTM C 1202 specification.

Chloride ion permeability was determined for all concrete mixtures in this study using ASTM C 1202 test method. Concrete mixtures containing fly ash, ground granulated blast furnace slag, and silica fume, at various percentages,

were examined. Water-binder ratio in the experimental study varied from 0.30 to 0.50. Curing period of concrete specimens varied from 28 days to 180 days in the moist room.

Modeling efforts were also made not only to simulate the RCP values of concrete mixtures achieved in the laboratory, but also to predict RCP values of concrete mixtures with other different binder combinations.

The experimental results of rapid chloride ion permeability for 10 concrete mixtures after 28 days and 56 days of curing are shown in Table 5.13. RCP values of concrete mixtures decreased with an increase in curing time. The rate of decrease in RCP value of concrete mixtures after the 56-day curing period varies from 8% to 60% compared with the 28-day curing period.

Compared with No. 1 concrete with 6% silica fume, No. 2 concrete with 25% fly ash and 6% silica fume showed lower coulomb value after both 28-day and 56-day curing periods. These two concrete mixtures have the same water binder ratio (0.40), which indicates that combination of fly ash and silica fume in No. 2 concrete enhanced the impermeability of hardened concrete even after 28-day curing period. However, as fly ash dosage in concrete increased from 25% to 40% (No. 2 and No. 3 mixtures), much lower decrease in 56-day RCP value was observed for mixture No. 3 than for mixture No. 2 relative to the 28-day value.

Addition of 6% silica fume to concrete resulted in significant improvement in the impermeability of hardened concrete not only at 28 days, but also at 56 days. A major enhancement is seen in the impermeability at 28 days. As shown in Table 5.13, all the RCP value of concrete mixtures with addition of 6% silica fume at 28 days are less than 2000 Coulombs, which is the threshold value for low chloride ion penetrability of concrete, according to ASTM C 1202.

No. 6 concrete mixture with 25% slag and 6% silica fume showed much lower coulomb values at both 28 days and 56 days than that of No. 2 concrete. These two mixtures had the same water-binder ratio and silica fume content, and the only difference between these two concrete mixtures was the addition of 25% fly ash by mass of total binder in No. 2 instead of 25% slag used in No. 6. The results here show that slag is more effective in reducing chloride ion permeability than fly ash with the combination of 6% silica fume in the binder system after both 28 and 56 days of curing.

### 5.4.2. Results and Discussion

Table 5.13 shows the summary results of 28-day and 56 day RCP values for Phase II concrete mixtures. Compared with 28-day RCP value, the decrease rate of 56-day RCP value of concrete mixtures is also shown in Table 5.13.

Table 5.13: Summary of RCP Values for Phase II Concrete Mixtures

| Mix No. | W/B | Binder | | | Laboratary Results | | |
|---|---|---|---|---|---|---|---|
| | | FA | SF | Slag | RCPT(Coulomb) | | Decrease rate |
| | | % | % | % | 28days | 56days | (%) |
| 1 | 0.40 | 0 | 6 | 0 | 1987 | 1378 | **30.7** |
| 2 | 0.40 | 25 | 6 | 0 | 1851 | 1252 | **32.3** |
| 3 | 0.40 | 40 | 6 | 0 | 1651 | 1494 | **9.5** |
| 4 | 0.40 | 25 | 0 | 0 | 4313 | 2612 | **39.4** |
| 5 | 0.35 | 40 | 0 | 0 | 3041 | 1645 | **45.9** |
| 6 | 0.40 | 0 | 6 | 25 | 1278 | 511 | **60.0** |
| 7 | 0.35 | 0 | 0 | 0 | 3491 | 2708 | **22.4** |
| 8 | 0.40 | 0 | 0 | 0 | 3561 | 3229 | **9.3** |
| 9 | 0.35 | 0 | 0 | 25 | 1873 | 1723 | **8.0** |
| 10 | 0.35 | 25 | 0 | 25 | 2025 | 1271 | **37.3** |

Plain concrete (No. 8) with w/b of 0.4 has the highest RCP value after 56 days of curing. The plain concrete (No. 7) with water-binder ratio of 0.35 also showed a relatively high Coulomb value after 56 days of curing.

5.4.2.1 28-day RCP Value of HPC: Figure 5.3 shows that the rapid chloride permeability of concrete with different binder combinations increases dramatically with an increase in the water-binder ratio. It is apparent that low water-binder ratio is needed for achievement of low chloride permeability of concrete.

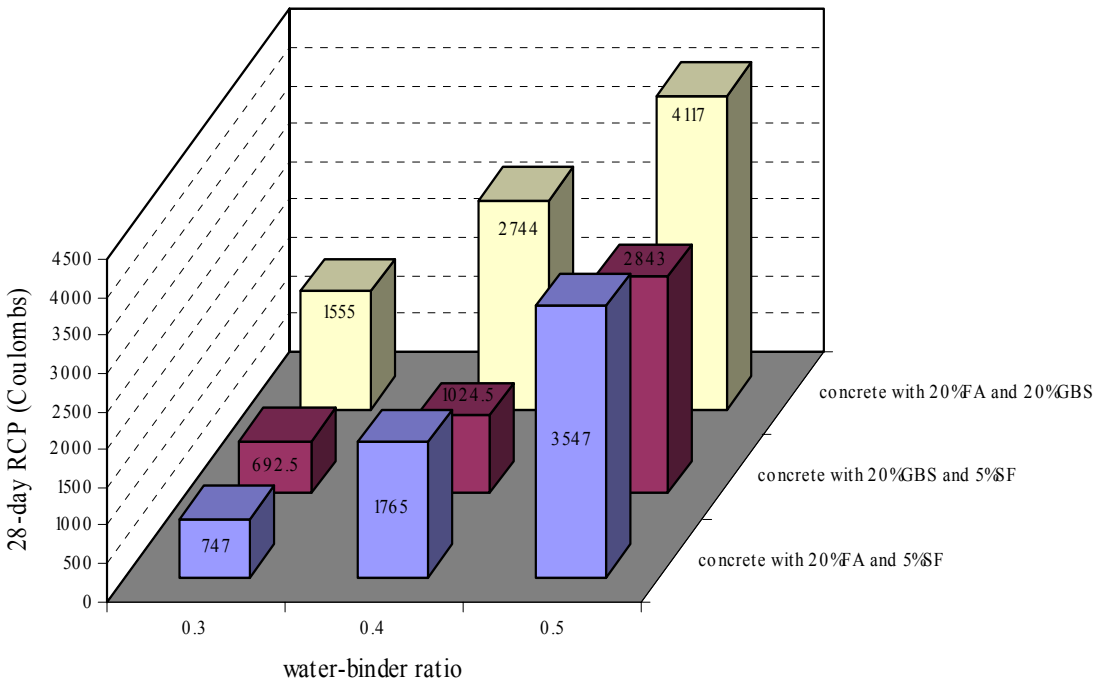


Figure 5.3: Effects of Water-binder Ratio on 28-day RCP of Concrete

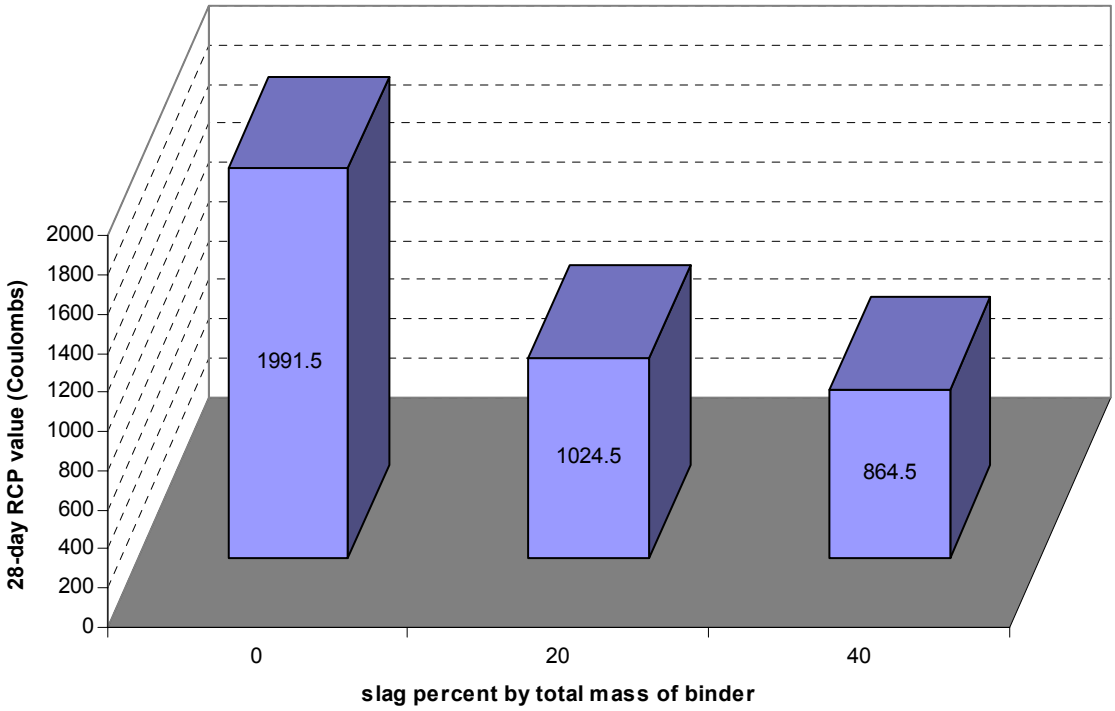


Figure 5.4: Effects of slag on 28-day RCP value of concrete

According to Figure 5.4, the rapid chloride permeability of concrete with 5% SF at 0.40 w/b decreases with an increase in the amount of slag. Especially for the first 20% addition of slag, a 50% reduction of the charge passed is observed. Addition of extra 20% slag does not contribute significantly to the decrease in RCP values at 28 days. As the pozzolanic reaction continues in concrete, more improvement in impermeability in the mixtures with higher amount of slag can be expected at later ages.

It is apparent that fly ash does not contribute to the chloride impermeability of concrete at 28 days, as shown in Figure 5.5. When fly ash was added to the concrete, the RCP value increased. However, it can be expected that there will be an enhancement of impermeability of concrete by the addition of fly ash at later age due to the pozzolanic reaction between the silica in fly ash and calcium hydroxide.

5.4.2.2 56-day RCP Value of HPC: As shown in Table 5.13 and in Figure 5.6, all concrete mixtures showed a decrease in RCP value at 56 days, as compared to 28 day RCP value. In general, the addition of fly ash or slag to concrete really helped to decrease the RCP value at 56 days. However, No. 3 concrete with 40% fly ash and 6% silica fume showed only limited decrease in 56-day RCP value. No. 6 concrete with 25% slag and 6% silica fume achieved the steepest decrease in 56-day RCP among all 10 concrete mixtures. For this mixture, decrease was up to 60% compared to the 28-day RCP value. This mixture also showed the lowest coulomb value at 56 days (about 500 Coulombs). No. 2 and No. 10 concrete also have low coulomb values at 56 days. Although No. 4 concrete with 25% fly ash at 0.40 w/b showed the highest 28-day RCP value, 56-day RCP value for No. 4 concrete was even lower than that of No. 7 control mixture with 0.35 w/b, which means the enhancement of the impermeability due to fly ash addition really showed only after 28 days. Compared to other concrete mixtures from Phase II of this study, mixtures No. 8 and No. 7 achieved the highest 56-day RCP value.

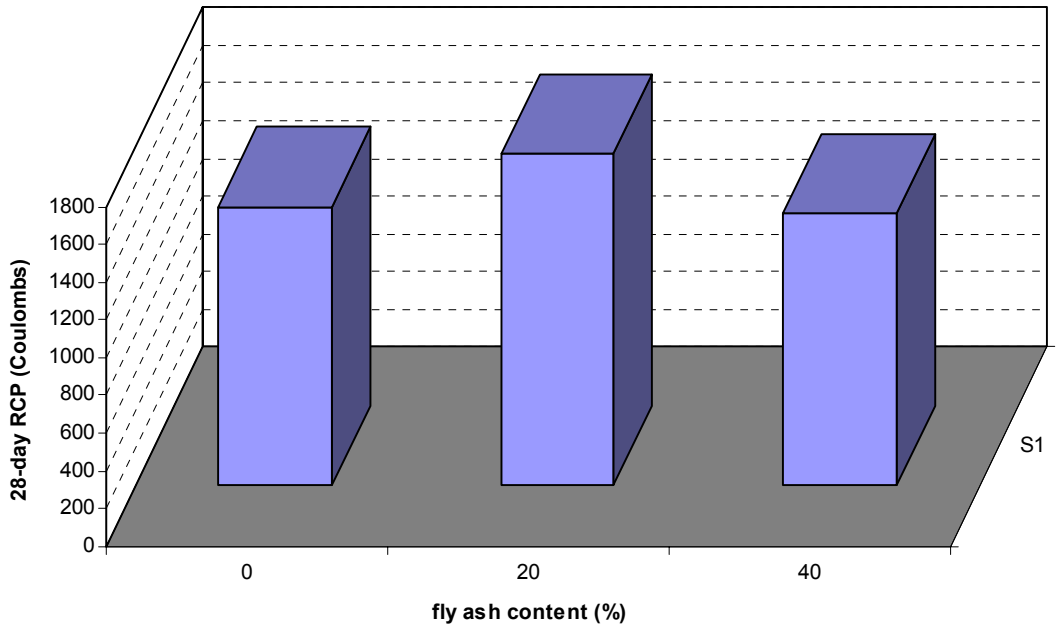


Figure 5.5: Effects of Fly Ash on 28-day RCP of Concrete

Water-binder ratio in concrete is a very important factor influencing 56-day RCP value. Only when pozzolanic materials are properly added in concrete, high resistance to chloride permeability can be expected at 56 days. Silica fume is effective in the reduction of RCP value at 56 days, and combination of silica fume with fly ash also contributes to the reduction of 56-day RCP value significantly. Combination of silica fume with slag resulted in the lowest RCP value. As shown in Figure 5.6, No. 6 mixture had a RCP value of only about 500 Coulombs at 56 days.

This is only about half of the RCP value for mixture No. 1, which contained 6% silica fume but did not have slag addition.

5.4.2.3 Long-term RCP Value of HPC: Figure 5.7 shows the development of RCP value of concrete mixtures with time. After 180 days of curing, mixtures No. 2, No. 3, No .5, No. 6 and No. 10 developed almost the same RCP value, (less than 1000 Coulombs). These five concrete mixtures can be divided into two groups, one group containing silica fume (No. 2, No. 3, and No. 6), and the other one without silica fume (No. 5 and No. 10). No. 2, No. 3 and No. 6 mixtures have the same water-binder ratio (0.40); however, mixtures No. 5 and No. 10 required lower water-binder ratio (0.35) to achieve 1000 Coulombs at 180 days.

For silica fume concrete (such as No. 1), only limited decrease in RCP value has been observed from 56 days to 180 days. From all 10 concrete mixtures, No. 8 and No. 7 have the two highest RCP value after 180 days of curing. Comparing No. 2 with No. 6, it can be stated that slag reduced the RCP value more significantly than fly ash at relatively early ages such as 28 or 56 days. However, as shown in Figure 5.7, these two concrete mixtures had similar RCP values after 180 days of curing.

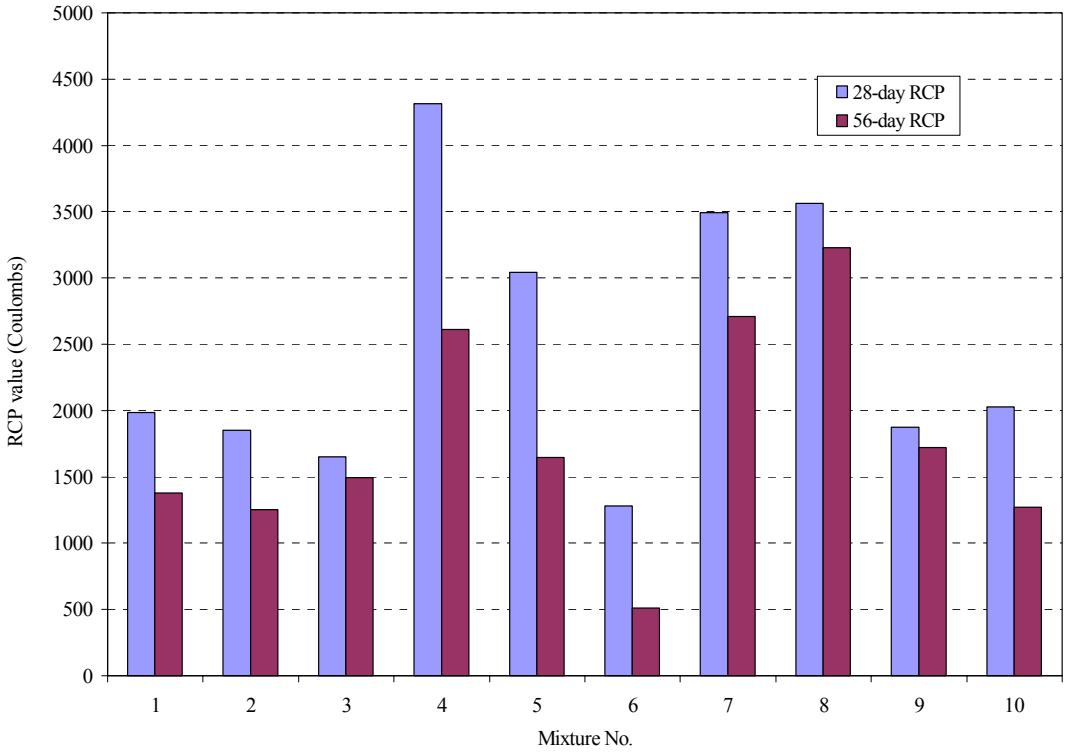


Figure 5.6: Comparison of 56-day RCP and 28-day RCP Values of 10 Concrete Mixtures

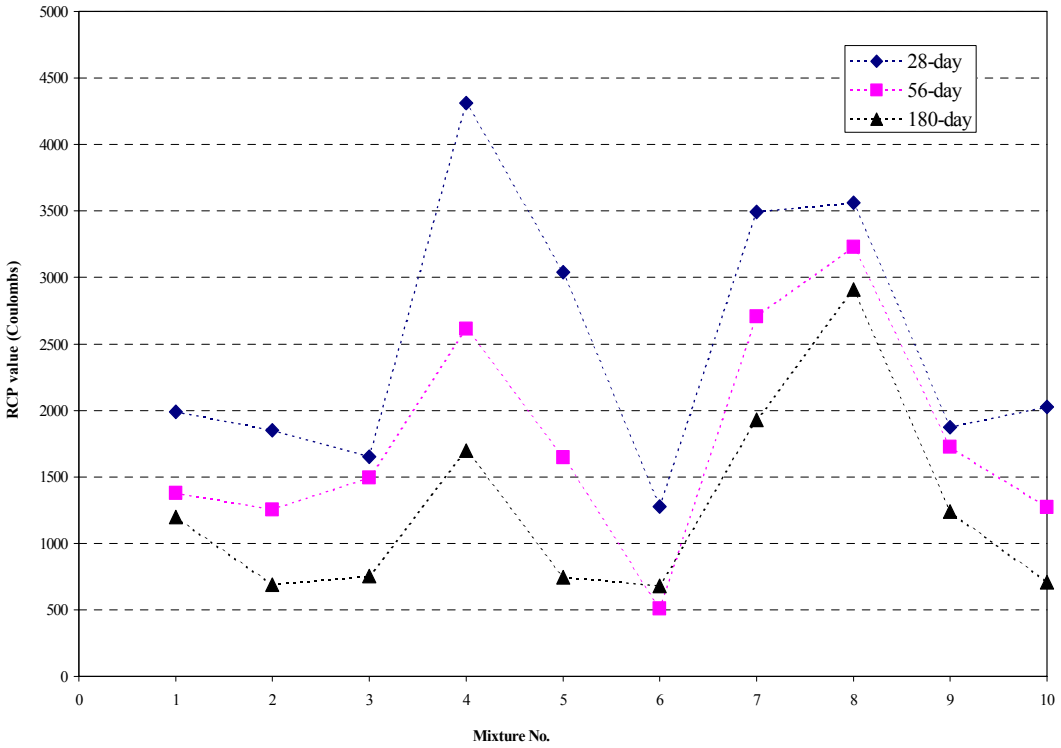


Figure 5.7: Change of RCP Value with Time

5.4.2.4. Verification of RCP Models: based on RCP values of 45 concrete mixtures from three different binder systems tested in the laboratory, statistically best-fitting quadratic models were developed for each binder system.

For Portland cement/fly ash/silica fume binder system, the best-fitting model for RCP is:

RCP value (Coulombs) at 28 days = 2131.2 – 236.1*(SF – 5) + 11582*(w/b – 0.40) – 2.223 *(FA – 20)$^2$ – 382.1 *(FA –20)*(w/b – 40)……..……..(5.9)

RCP value (Coulombs) at 56 days = 1258.9 – 16.3 * (FA – 20) – 197.4 * (SF – 5) + 8369.4 * (w/b – 0.40) + 20.8 * (SF – 5) $^2$ – 425.1 * (FA – 20) * (w/b – 0.40)…....…...(5.10)

Assuming the variables are continuous in the model for 56-day RCP value, the rate of change of RCP value with the addition of SF can be expressed as the differential equation:

$$\frac{\partial RCP}{\partial SF} = -197.4 + 41.6 \times (SF - 5) \quad \text{.....(5.11)}$$

Mathematically, when the dosage of SF added in the concrete is less than 10%, $\partial$ RCP/$\partial$ SF < 0, which means that addition of SF will help to reduce 56-day RCP value of concrete. The lower addition of SF in concrete is more effective in reduction of RCP value than higher addition. If 6% SF is added in the concrete mixture, every percentage of SF will cause a decrease of 150 Coulombs in 56-day RCP value.

The rate of RCP value change with the change of w/b can be expressed according to the following equation:

$$\frac{\partial RCP}{\partial w/b} = 8369.4 - 425.1 \times (FA - 20) \quad \text{.....(5.12)}$$

Mathematically, when FA addition in the concrete is less than 40%, $\partial$ RCP/$\partial$ w/b > 0, which means that increase of water-binder ratio in concrete mixtures will cause dramatic increase of 56-day RCP value, especially for concrete

without addition of FA. For example, when water-binder ratio of the plain concrete mixture increases from 0.30 to 0.40, 56 day RCP value is expected to increase about 1700 Coulombs. Addition of fly ash in the concrete drives the prediction to be more complex because of the pozzolanic reaction between fly ash particles and calcium hydroxide at later ages, especially when fly ash dosage in the concrete is so high that the effect of fly ash on reduction of permeability offsets the effect of water-binder ratio. However, this is not true in practice. Therefore, the model used here overestimates the effects of high addition of fly ash on the reduction of RCP value at 56 days.

The rate of change of RCP value with the addition of FA in concrete can be expressed according to the following equation:

$$\frac{\partial RCP}{\partial FA} = -16.3 - 425.1 \times (\frac{w}{b} - 0.40) \quad \text{.....(5.13)}$$

Mathematically, when water-binder ratio in the concrete is less than 0.40, ∂ RCP/∂ FA < 0. Every percentage of fly ash added in the concrete will cause a reduction of about 16 or more Coulombs in the 56-day RCP value. Especially for concrete with higher water-binder ratio, the effects of fly ash on impermeability of concrete will become much more significant. It means that fly ash will contribute to the improvement of the pore structure, and also the pozzolanic reaction of fly ash at later ages will keep on enhancing impermeability of concrete. However, when water-binder ratio is lower than 0.40, addition of fly ash in concrete will become ineffective in the reduction of permeability at 56 days, and even produce opposite effects at 0.35 water-binder ratio. This does not match the laboratory results in this research, which means that this model underestimates the effects of fly ash on the reduction of RCP value of concrete at low water-binder ratio at later age.

For Portland cement/slag/silica fume binder system, the best-fitting model for RCP is:

RCP value (Coulombs) at 28 days = 1206.9 – 22.3 * (slag – 20) – 240.8 * (SF – 5) + 9099.4 * (w/b – 0.40) + 34.7 * (SF – 5)$^2$ + 49589 * (w/b – 0.40)$^2$ – 1370.5 * (SF – 5) * (w/b – 0.40)……(5.14)

RCP value (Coulombs) at 56 days = 604.3 – 21.5 * (slag – 20) – 200.9 * (SF – 5) + 7707 * (w/b – 0.40) + 0.89 * (slag – 20)$^2$ + 36.3 * (SF – 5)$^2$ + 81046 * (w/b –0.40)$^2$ + 4.8 * (slag – 20)* (SF – 5) – 1209 * (SF – 5) * (w/b – 0.40)……....(5.15)

Assuming the variables are continuous in the model for 56-day RCP value, the change in 56-day RCP value with the addition of SF can be expressed according to the differential equation:

$$\frac{\partial RCP}{\partial SF} = -200.9 + 72.6 \times (SF - 5) + 4.8 \times (slag - 20) - 1209 \times (\frac{w}{b} - 0.40) \quad \text{……...…....(5.16)}$$

For slag content lower than 40% and water-binder ratio higher than 0.35, Equation (5.16) will yield negative values when SF content is below 5%. That means that for this range of parameters, adding silica fume will be very effective in reducing 56-day RCP, (about 200 Coulombs reduction for each percent of SF added). When SF is added to the same system in higher percentage, the reduction in RCP is smaller (about 120 Coulombs per every percentage added). In summary, the effectiveness of SF in reducing RCP value is high for concretes with relatively high water-binder ratio and low slag content.

The change in 56-day RCP value with the change of w/b can be expressed according to the following equation:

$$\frac{\partial RCP}{\partial w/b} = 7707 + 162092 \times (\frac{w}{b} - 0.40) - 1209 \times (SF - 5) \quad \text{……..(5.17)}$$

Mathematically, when water-binder ratio is higher than 0.40 and SF content is lower than 10%, ∂ RCP/∂ w-b >> 0, which means that an increase in water-binder ratio of concrete mixtures will cause a dramatic increase of the 56-day RCP value. For example, when water-binder ratio of the plain concrete mixture increases from 0.40 to 0.45, 56-day

RCP value is expected to increase by about 1100 Coulombs. However, this does not match experimental observation. This means the model overestimates effects of water-binder ratio on permeability.

The change in 56-day RCP value with the addition of slag in concrete can be expressed as the following equation:

$$\frac{\partial RCP}{\partial slag} = -21.5 + 1.78 \times (slag - 20) + 4.8 \times (SF - 5) \quad \text{.....(5.18)}$$

Mathematically, when slag content in the concrete is less than 30% and SF is less than 5%, $\partial$ RCP/$\partial$ slag < 0, addition of slag to concrete will cause reduction on the 56-day RCP value, especially for concrete with lower SF content (less than 5%). If the slag content in concrete is lower than 20%, every percentage of slag added in the concrete will lower the 56-day RCP value by about 20 Coulombs.

For Portland cement/ fly ash/ slag binder system, the best fitting models for RCP is:

RCP value (Coulombs) at 28 days = 2636.3 – 13.1 * (FA – 20) – 62.4 * (Slag – 20) + 17048 * (w/b – 0.40) + 1.54 * (FA – 20)$^2$ + 3.68 * (Slag – 20)$^2$…….…….(5.19)

RCP value (Coulombs) at 56 days = 1472.1 – 34.9 * (FA – 20) – 39.9 * (slag – 20) + 8013.8 * (w/b – 0.40) + 2.1 * (FA – 20)$^2$ + 2.44 * (Slag – 20)$^2$ + 1.05 * (FA – 20)* (Slag – 20)……...……...(5.20)

The best-fitting models applied to simulate RCP values of concrete mixtures are shown in Table 5.14. Depending on the binder system in the concrete mixture, different models will be used. For example, in order to predict RCP value of No. 1 concrete mixture, models developed from both Portland cement/fly ash/silica fume binder system and from Portland cement/slag/silica fume binder system can be employed, and two predicted RCP values can be achieved from these models for each curing period (28 days, or 56 days). The two predicted values for the 56-day curing period were 1407 and 1131 Coulombs, and a result of 1378 Coulombs was obtained from the laboratory. It is obviously clear that FASF model can predict 56-day RCP value of No. 1 concrete more accurately.

Table 5.14 shows the summary of predicted RCP values through models developed from three binder systems for each concrete mixture. In general, the predicted 56 day-RCP values matched the values obtained from laboratory tests much better than that of predicted 28-day RCP values. The RCP values of control mixtures (No. 7 & 8) (Portland cement as the only binder in the mixture) are predicted quite well by the models for slag-silica fume binder system. When used for plain concrete mixture, models for fly ash-slag binder system in general provide much higher predicted RCP values than other models. It is suggested that models for fly ash-slag binder system are only valid for those concrete mixtures that include both fly ash and slag.

Table 5.14: Summary of Predicted RCP Values for 10 Concrete Mixtures

| Mix No. | W/B | Binder | | | Actual value | | Predicted Value | | | | | |
|---|---|---|---|---|---|---|---|---|---|---|---|---|
| | | FA | SF | Slag | RCPT(Coulomb) | | FASF model | | GBSF model | | FAGBS model | |
| | | % | % | % | 28days | 56days | 28days | 56days | 28days | 56days | 28days | 56days |
| 1 | 0.4 | 0 | 6 | 0 | 1987 | 1378 | 1005 | 1407 | 1447 | 1131 | ---- | ---- |
| 2 | 0.4 | 25 | 6 | 0 | 1851 | 1252 | 1839 | 1001 | ---- | ---- | ---- | ---- |
| 3 | 0.4 | 40 | 6 | 0 | 1651 | 1494 | 1006 | 757 | ---- | ---- | ---- | ---- |
| 4 | 0.4 | 25 | 0 | 0 | 4313 | 2612 | 3256 | 2686 | ---- | ---- | 5330 | 3020 |
| 5 | 0.35 | 40 | 0 | 0 | 3041 | 1645 | 2226 | 2449 | ---- | ---- | 4858 | 2569 |
| 6 | 0.4 | 0 | 6 | 25 | 1278 | 511 | ---- | ---- | 889 | 378 | ---- | ---- |
| 7 | 0.35 | 0 | 0 | 0 | 3491 | 2708 | 1461 | 2249 | 3053 | 3298 | 5383 | 4802 |
| 8 | 0.4 | 0 | 0 | 0 | 3561 | 3229 | 2423 | 3092 | 3726 | 3783 | 6235 | 5202 |
| 9 | 0.35 | 0 | 0 | 25 | 1873 | 1723 | ---- | ---- | 2494 | 1828 | 2442 | 2366 |
| 10 | 0.35 | 25 | 0 | 25 | 2025 | 1271 | ---- | ---- | ---- | ---- | 1536 | 837 |

Although only one model could be utilized to predict RCP value of concrete mixtures such as No. 2 (25% FA and 6% SF), No. 6 (25% slag and 6% SF) and No. 10 (25% FA and 25% slag), all the predicted values matched very well with the results from laboratory at both 28 days and 56 days. These three concrete mixtures were recommended for further study in Phase II of the research, based on the models and contour maps constructed for each binder system. The good match with experimental results further proved that the models and contour maps constructed for each binder system worked well.

5.4.2.5 Factors Affecting RCP Value of HPC

*Effect of mineral admixtures*: Silica fume has significant effect on the 56-day RCP value of concrete. Concrete with 7.5% SF at 0.35 water-binder ratio showed much lower RCP values than concrete with 2.5% SF at the same w/b. Other materials also influence the effects of silica fume on permeability. At low SF contents (2.5%), the reduction of RCP value resulting from the use of slag is higher than that resulting from the use of fly ash. The rate of reduction with the addition of the slag and fly ash also is influenced by the dosage added in the concrete. The higher the content of slag, the lower the 56-day RCP value. As shown in Figure 5.8, when the slag content increases from 10% to 30%, a decrease of about 300 Coulombs was observed. However, for concrete with fly ash, the decrease of RCP values was only about 100 Coulombs when fly ash content increased from 10% to 30% in the concrete. At higher SF content (7.5%), the increase of slag content in the concrete resulted in only a slight reduction of RCP value. However, the increase in the content of fly ash from 10% to 30% did not lead to a reduction of RCP value at 56 days any more. Concrete with a combination of 5-6% SF and other mineral admixtures at 0.35 w/b is expected to have RCP value lower than 1000 Coulombs at 56 days.

As shown in Figure 5.9, at 0.40 w/b, for a concrete mixture with 20% slag, the initial addition of 5% silica fume by mass of the total binder led to a decrease of the 56-day RCP value from 2600 to 800 Coulombs. Further increase of SF content from 5% to 7% results in only limited decrease of 56-day RCP value. Based on the results achieved during this study, continued increase of SF from 7% to 10% in concrete did not cause the additional decrease in the 56-day RCP value. Therefore, the addition of less than 7% of SF in the concrete mixture with 20% slag should be both effective and economical.

For concrete with 20% fly ash at 0.40 w/b, the addition of 5% silica fume led to a decrease of 1600 Coulombs in the 56-day RCP value, as shown in Figure 5.10. Further increase of SF from 5% to 10% did not have any significant

effect. on the 56-day RCP value. This points out that silica fume enhances the impermeability of concrete more effectively at lower content than at higher content. Considering that the market price of silica fume is about 8 times that of cement, higher content of silica fume will increase the price of concrete dramatically. Therefore, the addition of SF content for the concrete mixture with 20% fly ash should be about 6% from the point of economy.

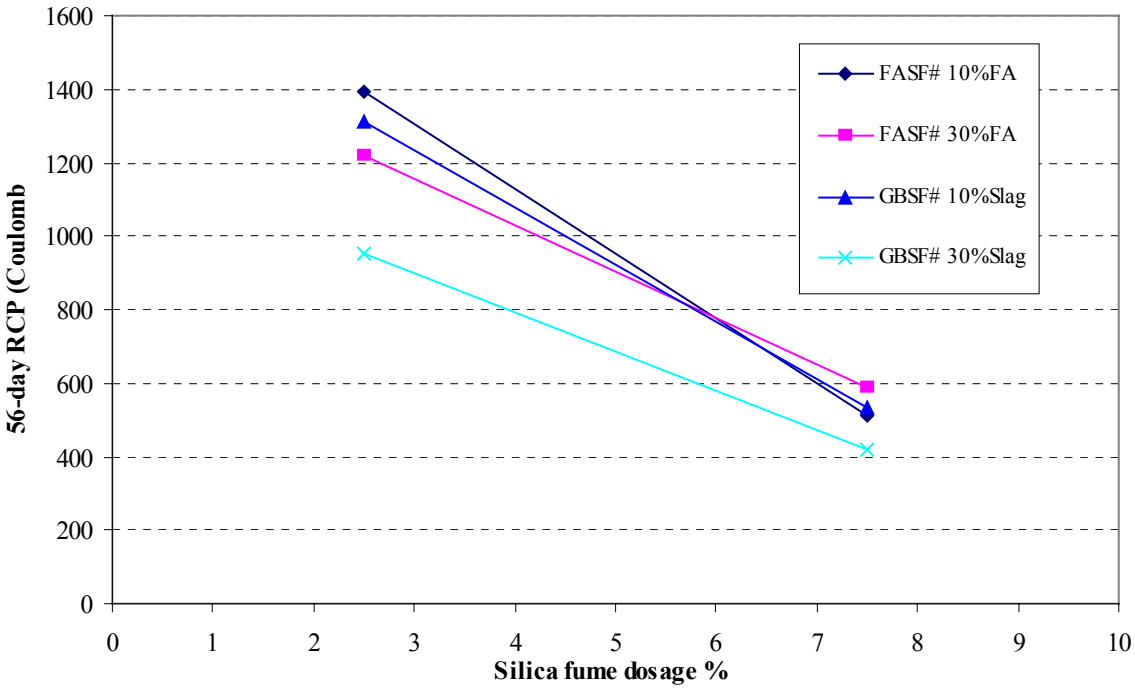


Figure 5.8: Effect of Silica Fume on 56-day RCP Value of Concrete at w/b=0.35

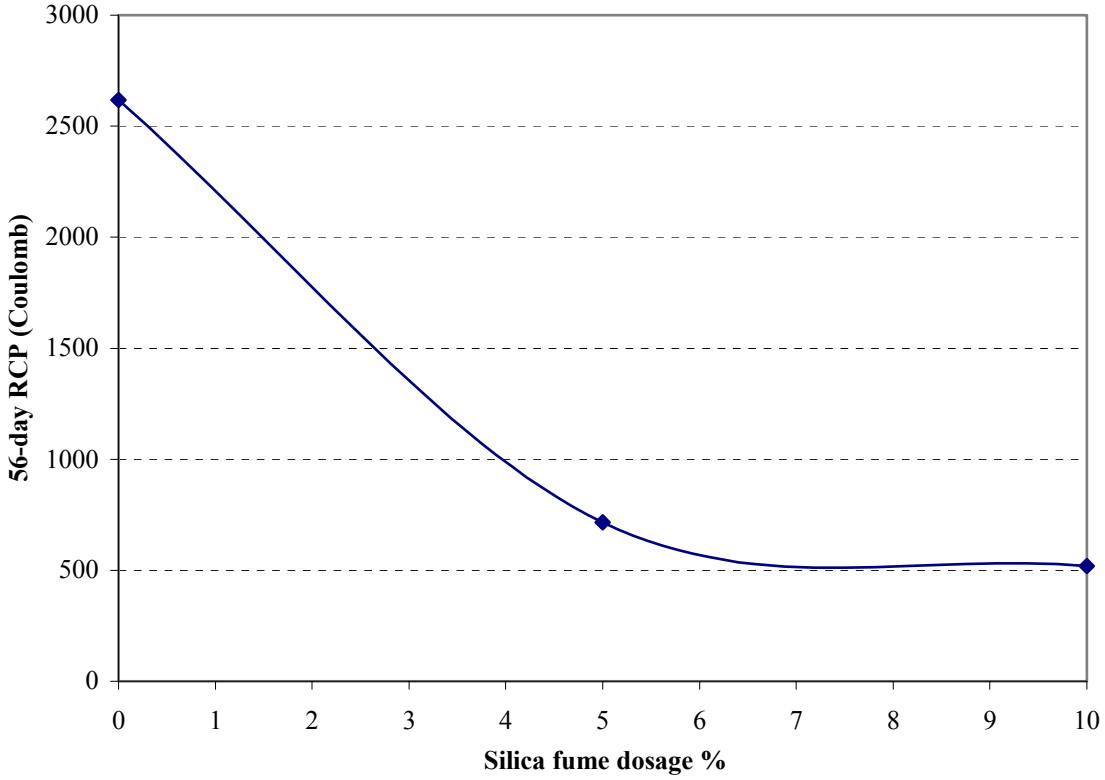


Figure 5.9: Effect of Silica Fume on 56-day RCP Value of Concrete Mixture Containing 20% Slag at w/b=0.40

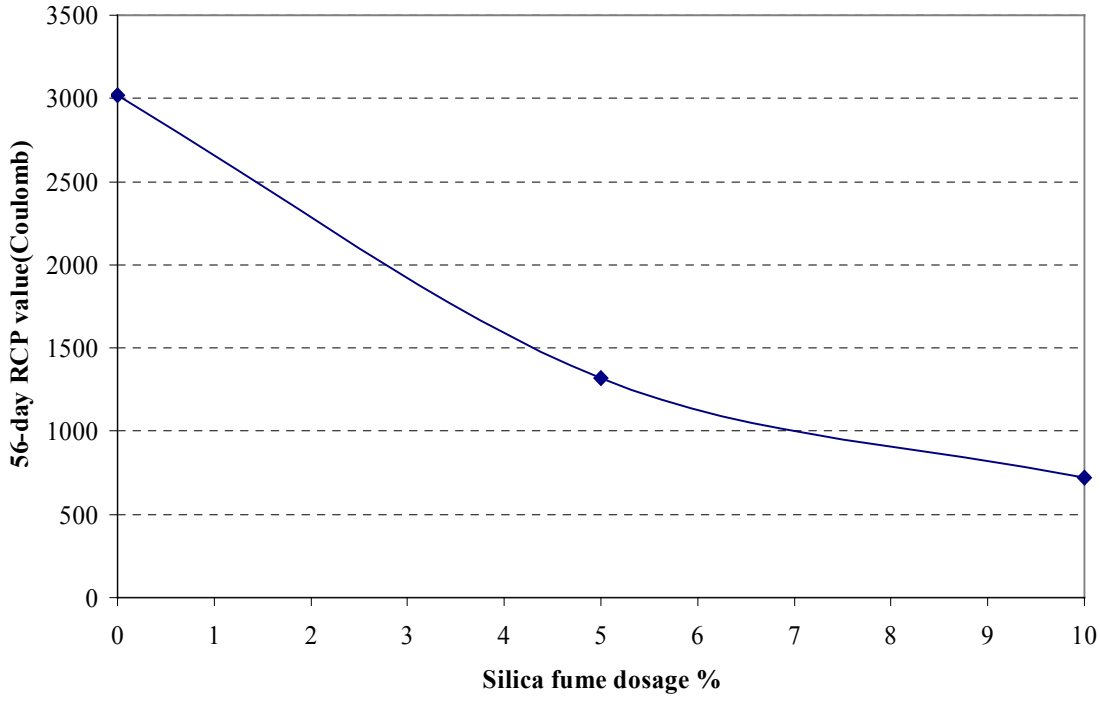


Figure 5.10: Effect of Silica Fume on 56 days RCP Value of Concrete Mixture Containing 20% FA at w/b=0.40

For concrete with 0.45 w/b, effects of SF are significant with respect to the enhancement of impermeability of concrete. Concrete with 7.5% SF showed much lower RCP values than concrete with 2.5% SF at the same w/b, as shown in Figure 5.11. A 50% decrease in 56-day RCP value was observed except for the concrete with 10% fly ash. For the concrete with 10% slag, the decrease of 56-day RCP was up to 70%. Other supplementary materials also showed strong influence on permeability of concrete. The enhancement of impermeability due to slag or fly ash is affected by their dosage in the concrete, as shown in Figure 5.11. As slag content increases from 10% to 30%, with a combination of 2.5% SF in concrete, a decrease of about 1000 Coulombs in the RCP value was observed. However, the effect of increase of slag content in the concrete on improving the impermeability of concrete is limited at higher SF content (such as 7.5%). For concrete with fly ash, a significant decrease of RCP values, of about 1000 Coulombs, was observed when fly ash content was increased from 10% to 30% in the concrete at both low and high SF contents.

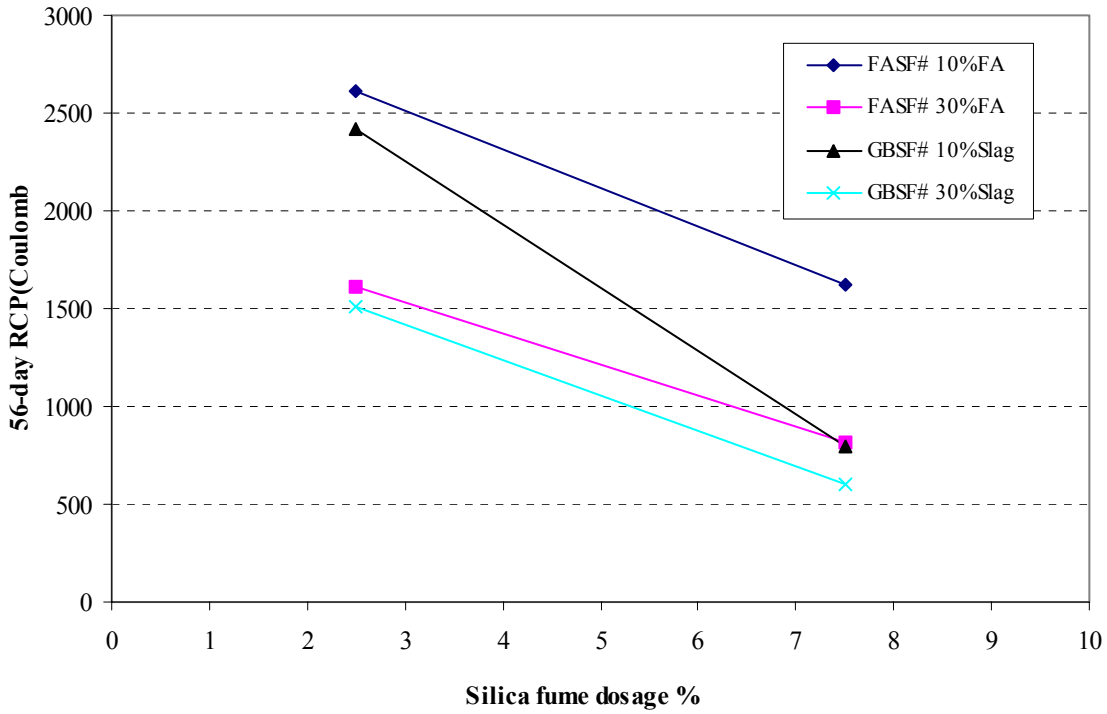


Figure 5.11: Effect of Silica Fume on 56-day RCP Value of Concrete Mixture at w/b=0.45

### 5.4.3 Summary of Results

Based on 10 concrete mixtures tested in this study, mixtures No. 7 and No. 8 maintained the highest RCP value at 56 days and 180 days of curing. These two mixtures were plain Portland cement concrete with water-binder ratio 0.35 and 0.40, respectively. Although reducing the water-binder ratio helps to enhance the impermeability of concrete, the mixture No. 7 (w/b=0.35) still had a high RCP value at 56 days (larger than 2500 Coulombs). No. 6 mixture with 25% slag and 6% silica fume achieved the most promising RCP results at all test ages.

Silica fume is very effective in reducing the RCP value of concrete, especially at early ages (up to 28 days). However, at later ages, the effect of other cementitious materials such as fly ash or slag is also significant on the reduction of RCP value of concrete.

Combination of silica fume with fly ash or slag produces concrete with higher resistance to chloride ion penetration than can be achieved in concrete containing silica fume only. In such system, the enhancement of the chloride penetration resistance by using ternary binders is more obvious at later ages such as 56 days or 180 days.

Compared with fly ash, slag was relatively more effective in the reduction of RCP value at 28 and 56 days, especially at 28 days. However, the effect of slag on RCP value of concrete is quite similar to that of fly ash at 180 days. Concrete with fly ash and slag (No. 10) also shows low RCP value after 28, 56 and 180 days of curing.

In general, the models built in Phase I of this study worked well. With respect to predicting the RCP value, however, it should be stated that different models based on different binder systems have varying accuracy of prediction. Models work much better if concrete mixture proportions are closer to the center point shown in 3-factor central experimental design (seen in Figure 3.1).

### 5.5 Chloride Diffusion Coefficient from the Electrical Migration Test

Table 5.15 shows summary of the results of the diffusion coefficients for Phase II concrete mixtures. No. 6 achieved the lowest value of diffusion coefficient among all the mixtures. For 28 days old concrete mixtures, mixture No. 1 and No. 2 also achieved low values, indicating high resistance to chloride penetration. Among all the concrete mixtures with water-binder ratio of 0.40, No. 4 with 25% fly ash and No. 8 (plain Portland cement concrete) have the highest value of diffusion coefficient. Addition of silica fume or the combination of silica fume and other cementitious materials significantly helps to enhance the resistance of chloride penetration into the concrete after 28 days, as shown by the results for mixtures No. 2, No. 3 and No. 6. Decreasing the water-binder ratio of concrete mixtures also enhances the resistance to chloride penetration, as evidenced by comparing the results for mixtures No. 7 and No. 8.

Table 5.15: Summary of Chloride Diffusion Coefficients (from Migration Test) for Phase II Mixtures

| Mix No. | W/B | Binder | | | Diffusion coefficient ($x10^{-12}$ $m^2/s$) | | |
|---|---|---|---|---|---|---|---|
| | | FA | SF | Slag | | | |
| | | % | % | % | 28 days | 56days | 180 days |
| 1 | 0.4 | 0 | 6 | 0 | 6.77 | 6.25 | 5.06 |
| 2 | 0.4 | 25 | 6 | 0 | 6.57 | 4.72 | 4.07 |
| 3 | 0.4 | 40 | 6 | 0 | 8.53 | 7.92 | 3.34 |
| 4 | 0.4 | 25 | 0 | 0 | 11.62 | 9.00 | 5.60 |
| 5 | 0.35 | 40 | 0 | 0 | 9.79 | 6.44 | 3.39 |
| 6 | 0.4 | 0 | 6 | 25 | 5.48 | 4.68 | 3.05 |
| 7 | 0.35 | 0 | 0 | 0 | 9.99 | 8.76 | 6.59 |
| 8 | 0.4 | 0 | 0 | 0 | 11.05 | 10.85 | 8.30 |
| 9 | 0.35 | 0 | 0 | 25 | 7.10 | 6.26 | 5.98 |
| 10 | 0.35 | 25 | 0 | 25 | 10.26 | 4.85 | 2.84 |

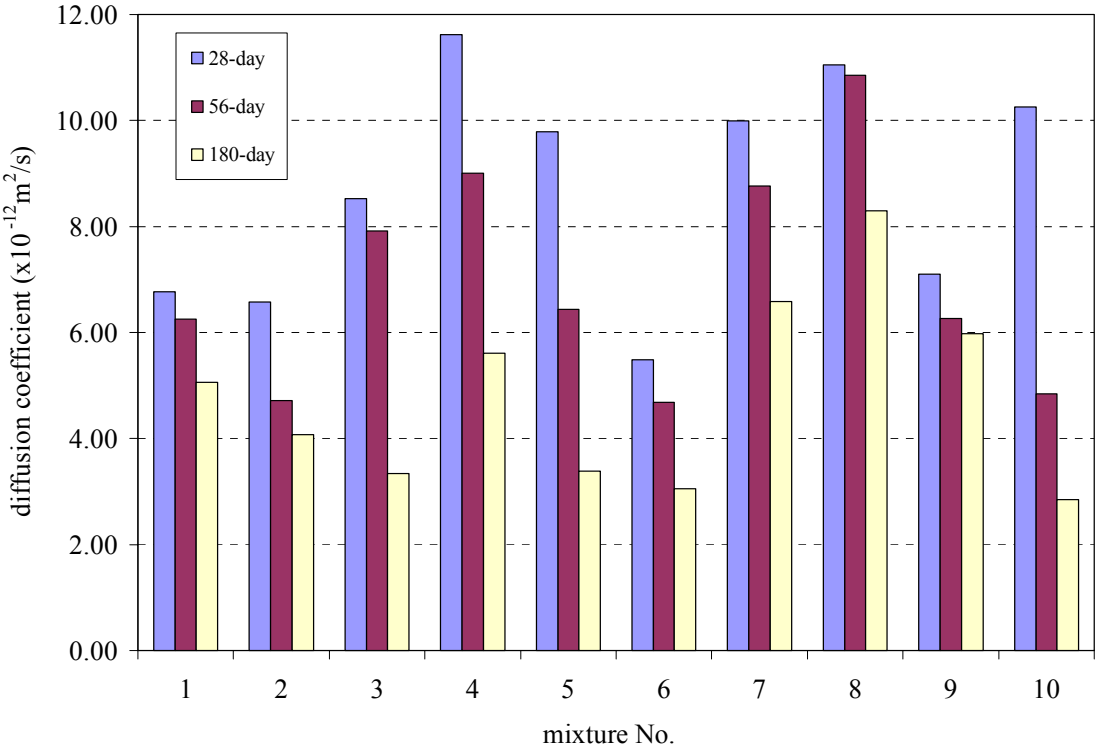


Figure 5.12: Diffusion Coefficient of Concrete Mixtures with Time

As shown in Figure 5.12, most of the diffusion coefficients decrease significantly with the increase in the curing age. The degree of reduction in diffusion coefficient value depends on the characteristics of the concrete mixture. Concrete containing fly ash or slag, achieved relatively higher amounts of reduction in 56-day diffusion coefficient value compared to the 28-day value. No. 10 concrete showed the highest (almost 60%) amount of reduction in diffusion coefficient value, when the curing time was extended from 28 to 56 days. Mixtures No. 2, No. 6 and No. 10 achieved similar diffusion coefficient value (~ 4.7 x $10^{-12}$ $m^2$/s) at 56 days.

Mixture No. 10 with 25% fly ash and 25% slag has the lowest diffusion coefficient at 180 days, which is 2.84 x $10^{-12}$ $m^2$/s. No. 3 concrete has the highest amount of reduction in diffusion coefficient between 56 days and 180 days. However, mixture No. 3 showed limited reduction in diffusion coefficient during the curing period from 28 days to 56 days. Mixture No. 8 (plain Portland cement concrete) had the highest value of diffusion coefficient at both 56 and 180 days. Although mixture No. 4 has the highest value of diffusion coefficient at 28 days, it also had a significant reduction with time. At 56 days, this mixture had a diffusion coefficient similar to the diffusion coefficient of mixture No. 7. (w/b = 0.35). At 180 days, the diffusion coefficient of mixture No. 4 was much lower than that of No. 7.

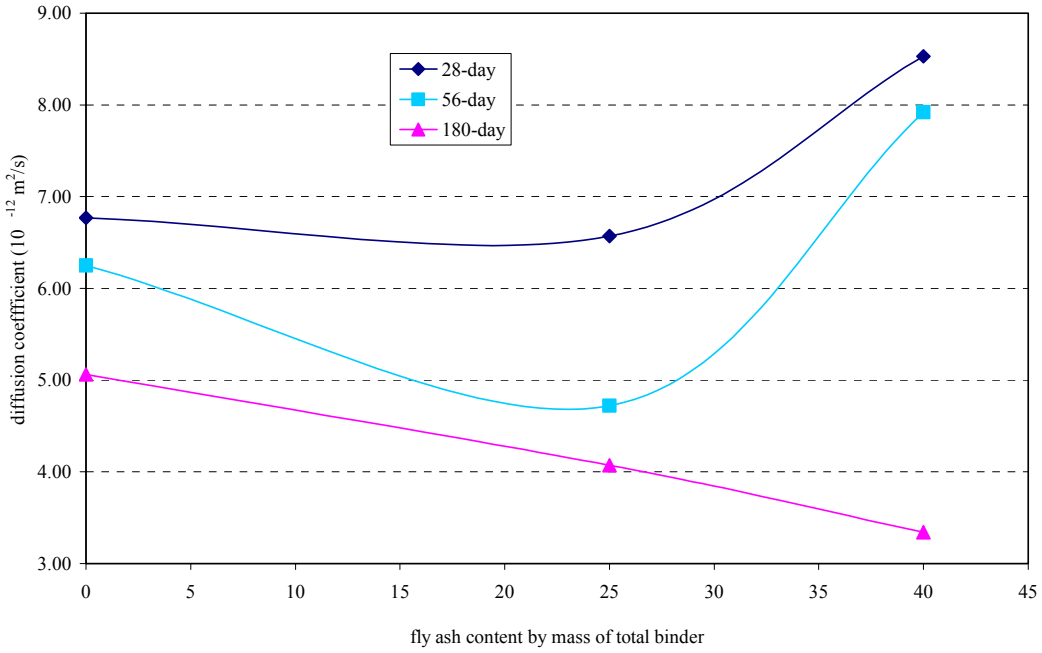


Figure 5.13: Effects of Fly Ash on Diffusion Coefficient Value of Concrete with 6% SF

Figure 5.13 shows the change of diffusion coefficient value of concrete mixtures containing 6% silica fume at 0.40 water-binder ratio as a function of fly ash content. At 28 days, the addition of fly ash does not help to enhance the resistance of chloride penetration into concrete, and a high percentage of fly ash (40%) actually reduces the resistance of concrete.

However, at the age of 180 days, addition of fly ash significantly contributes to the reduction of diffusion coefficient, and the resistance to penetration increases with an increase in the fly ash content. The results obtained in this study clearly indicate that 25% fly ash content by mass of total binder improves the resistance of mixture to chloride diffusion based on 56-day properties of concrete, and this trend coincides with the results that have been achieved in Phase I of this study.

As shown in Table 5.15, the diffusion coefficient of mixture No. 10 is much higher than that of No. 9, even though these two concrete mixtures have the same water-binder (0.35). Although mixture No. 9 has 25% fly ash added, it appears that fly ash does not help to enhance the 28-day resistance to chloride penetration. However, the 56-day resistance to chloride penetration of concrete containing 25% fly ash and 25% slag improved significantly, which is manifested by the fact that 56-day diffusion coefficient of No. 10 is much lower than that of No. 9 mixture.

The comparison of 28-day or 56-day diffusion coefficient of mixture No. 6 with mixture No. 1 shows that addition of 25% slag enhances the resistance to chloride penetration into concrete not only at later age (56 days) but also at 28 days. Both mixture No. 6 and mixture No. 1 have the same water-binder ratio (0.40) and contain 6% silica fume. The enhancing effect of slag with respect to the resistance to chloride penetration can also be observed by comparing concrete mixtures No. 7 and No. 9. These two mixtures have the same water-binder ratio (0.35), but No. 7 is a plain concrete mixture. The diffusion coefficient of mixture No. 9 is about 30% lower than that of No. 7 at both 28 and 56 days. Based on the results achieved in this study, it can be concluded that the addition of slag used in this study leads to the higher resistance to chloride penetration into the concrete at both 28 and 56 days. As expected, further reduction in diffusion coefficient takes place at later ages.

Water-binder ratio has important effect on the chloride diffusion coefficient value, as shown by comparing the results for mixture No. 7 (w/b = 0.35) and 8 (w/b = 0.40). At each age, mixture No. 7 had consistently (w/b=0.35) lower diffusion coefficient value than No. 8 (w/b=0.40).

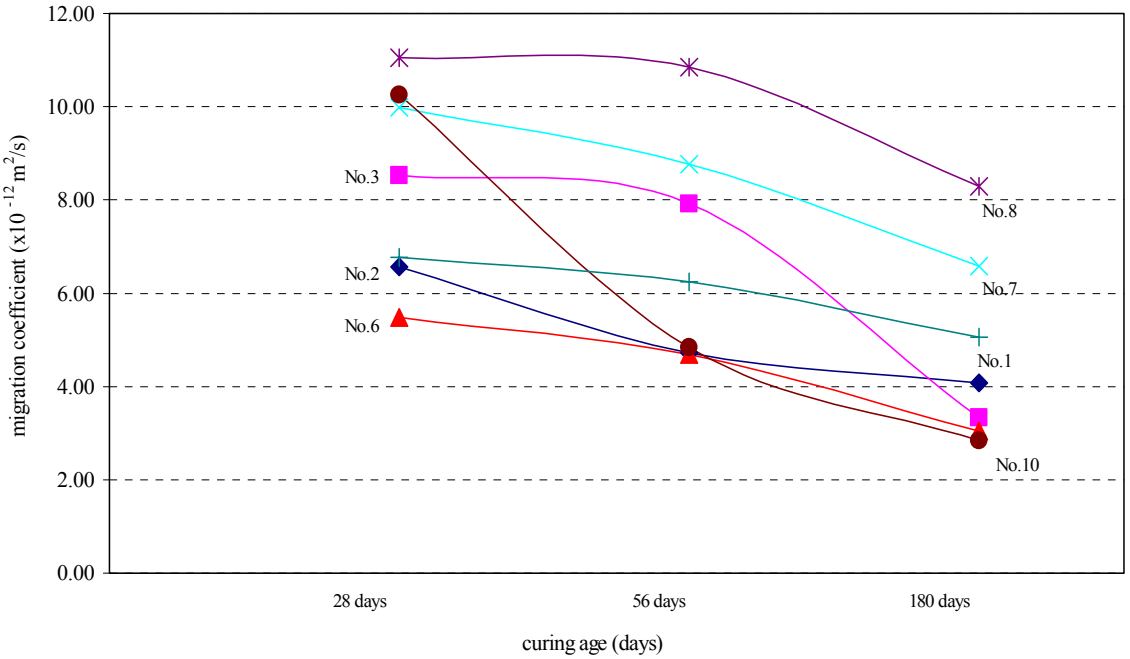


Figure 5.14: Effects of Curing Time on Chloride Diffusion Coefficient of Concrete

Figure 5.14 shows the effects of curing time on the diffusion coefficient value of Phase II concrete mixtures. Three testing ages were chosen in this study: 28, 56 and 180 days. The increase in the resistance of chloride penetration with longer curing time can be observed for all mixtures shown in the figure. However, the development rate of the resistance depends on the proportions of the given mixture. In general, concrete mixtures containing fly ash or slag show higher rate of enhancement in the resistance. Also, mixtures with higher amount of pozzolanic materials show greater reduction in diffusion coefficient values as the curing time increases. In this study, No. 10 concrete mixture with 25% fly ash and 25% slag had the largest amount of enhancement in the resistance to chloride penetration after 180 days of moist curing (when compared to 28-day values), and about 80% reduction in the diffusion coefficient was observed.

### 5.5.1 Summary of Results

CTH electrical migration test [Tang et al., 1995] can be applied to determine the chloride diffusion coefficient of concrete mixtures. Based on the results achieved in this study, Class C fly ash used in this research provides enhancement to the resistance to chloride penetration only at 56 days. No reduction in chloride diffusion coefficient was observed in concrete cured for 28 days.

Silica fume has significant effects on the reduction of chloride diffusion coefficient. As the curing age increases, all the concrete mixtures developed an increased resistance to chloride penetration. The higher the amount of fly ash or slag in the concrete, the larger the degree of the reduction of the chloride diffusion coefficient at later ages (compared to results at 28 days).

Mixture No. 2, No. 6 and No. 10 achieved the lower value of chloride diffusion coefficient at 56 days than the other mixtures in the 10 mixtures in Phase II.

## 5.6 Chloride Conductivity of HPC

### 5.6.1 Introduction

Chloride conductivity test developed by Streicher and Alexander [1995] was selected as one of the tests to measure the permeability of concrete to chloride ions in this study. This test method was applied to select the optimized binder combinations for concrete mixtures in Phase I of this study. It was also used as one of the permeability-related tests for the 10 concrete mixtures in Phase II of this study. Effects of water-binder ratio, and different type and content of cementitious materials on the chloride conductivity of concrete are repeated in this section.

### 5.6.2 Theoretical Background

The development of chloride conductivity test is based on the ionic distribution that develops during steady state transport conduction. Diffusivity and conductivity are two properties that can be easily measured and calculated under steady state conditions. However, in pure diffusion tests, a long period of time is needed before steady state conditions are achieved in the concrete specimens of certain thickness. The ionic concentration gradient is the driving force for the diffusion.

For conduction, the driving force is the electric field. When the specimens are saturated in a 5M NaCl solution before testing, steady state conduction under electric field can be easily achieved in a short time. To avoid the dilution of the chloride solution inside the concrete during saturation, specimens are dried before immersion. After the specific potential difference (2, 5, 10 or 12 V DC) is applied on the specimen, the electrical current through the specimens is recorded.

Usually, the following three factors determine the conductivity of concrete: water content in the concrete, the concentration of ions in the pore fluid, and the connectivity of the pore network existing in the concrete. During the test method suggested by Streicher and Alexander [1995], all the concrete specimens are immersed in a 5M NaCl solution, and the specimens are saturated under vacuum before immersion. As a result, the contribution of other ions to the conductivity can be ignored and the test effectively measures the connectivity of the pore structure of concrete.

The Nernst-Planck equation can be written as follows:

$$\frac{D}{D_0} = \frac{\sigma}{\sigma_0} \quad \text{.....(5.21)}$$

where:
D is the diffusivity of the ion through the porous material;
$D_0$ is the diffusivity of the ion through the pore solution;
$\sigma$ is the conductivity of the porous material;

$\sigma_0$ is the conductivity of the pore solution.

Using the Equation 5.21, it is possible to determine the chloride diffusivity of a porous medium by conductivity measurements. By measuring the conductivity of the porous medium and the conductivity of its pore fluid, the diffusivity ratio can be obtained. The diffusivity of the porous medium can be calculated through the ratio and the chloride diffusivity of the pore solution can also be determined.

Based on the research by Streicher and Alexander [1995], the conductivity, as shown in Figure 5.15, is dependent on the concentration of NaCl solution and other ions in the solution.

As shown in Figure 5.15, the conductivity ratio remains relatively stable and constant at higher chloride concentrations regardless of the concentration levels of KOH in the pore solution, and this is the reason that a 5 M NaCl is used during the test.

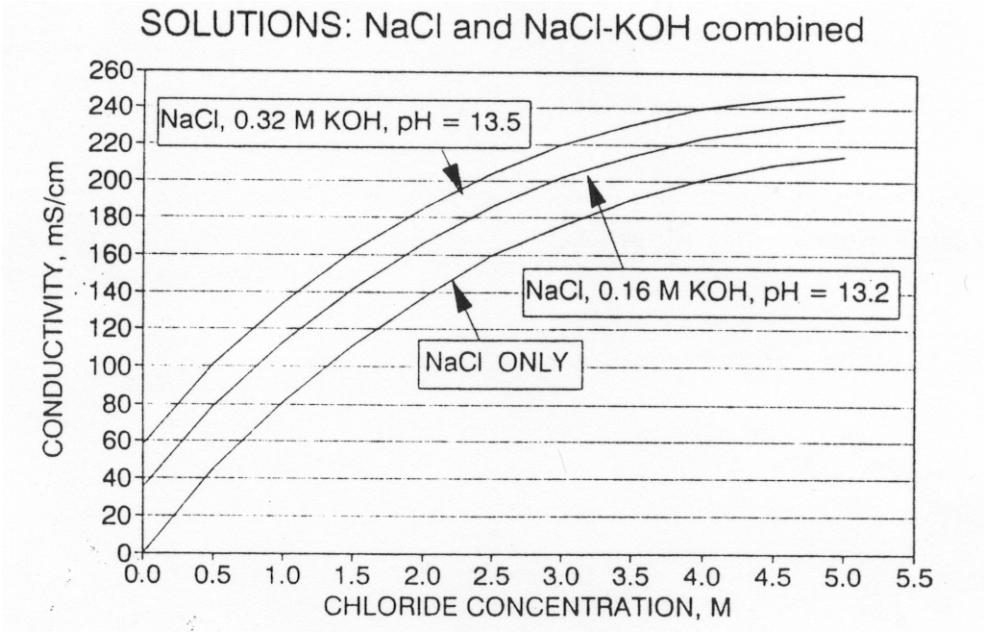


Figure 5.15: Conductivity versus Chloride Concentration
[Streicher and Alexander, 1995]

### 5.6.3 Results and Discussion

This section presents the results for chloride conductivity obtained from both Phase I and Phase II concrete mixtures. Phase I concrete mixtures were non-entrained and Phase II mixtures were air-entrained (6.5% total air content).

5.6.3.1 Conductivity Results – Phase I Mixtures

*Concrete containing slag and silica fume:* Figure 5.16 shows the effects of slag content on the chloride conductivity of concrete mixtures containing 5% silica fume at a water-binder ratio of 0.40. It is obvious that the addition of slag reduces the chloride conductivity of concrete significantly at both 28 days and 56 days. About 50% reduction in the conductivity can be seen when the content of slag in concrete increases from 0 to 20%. However, as the content of slag increases from 20 to 40%, the chloride conductivity of concrete shows slight increase. Figure 5.16 indicates that there is an optimum slag content, which leads to the lowest chloride conductivity. The influence of slag content on chloride conductivity is similar for both 28 days and 56 days, as seen from the two parallel curves.

Figure 5.17 shows the effects of water-binder ratio on the chloride conductivity of concrete containing 20% slag and 5% silica fume. As the water-binder ratio decreases from 0.50 to 0.40, the chloride conductivity of concrete decreases by more than 60%.

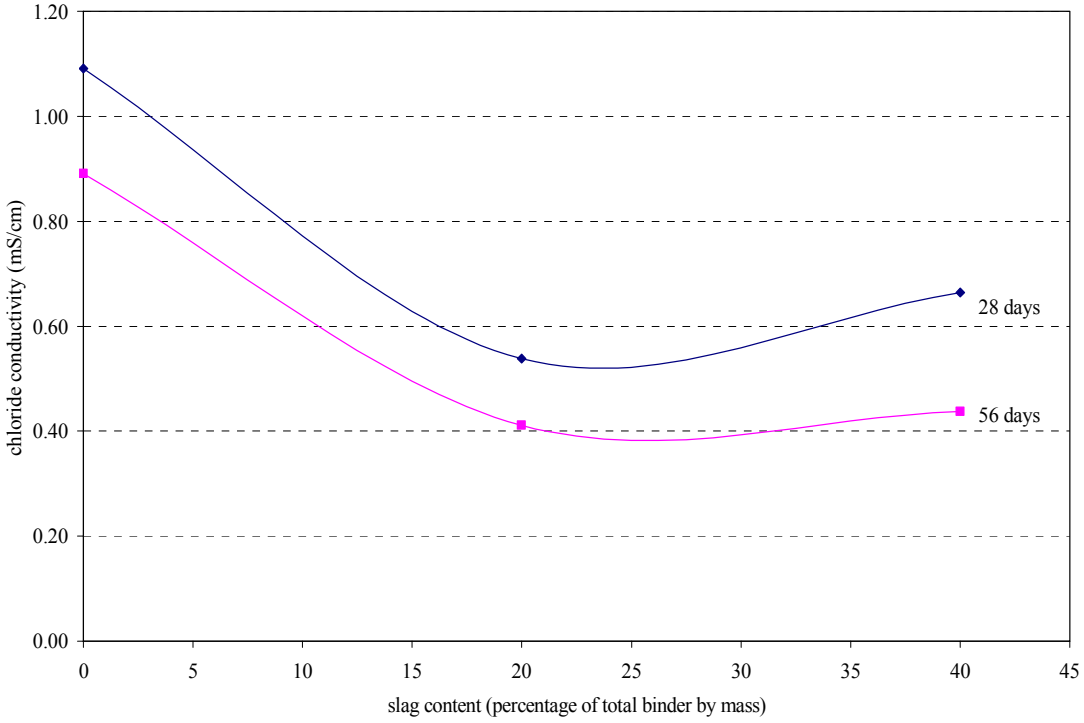


Figure 5.16: Effects of Slag on Chloride Conductivity of Concrete with w/b 0.40 and 5% Silica Fume

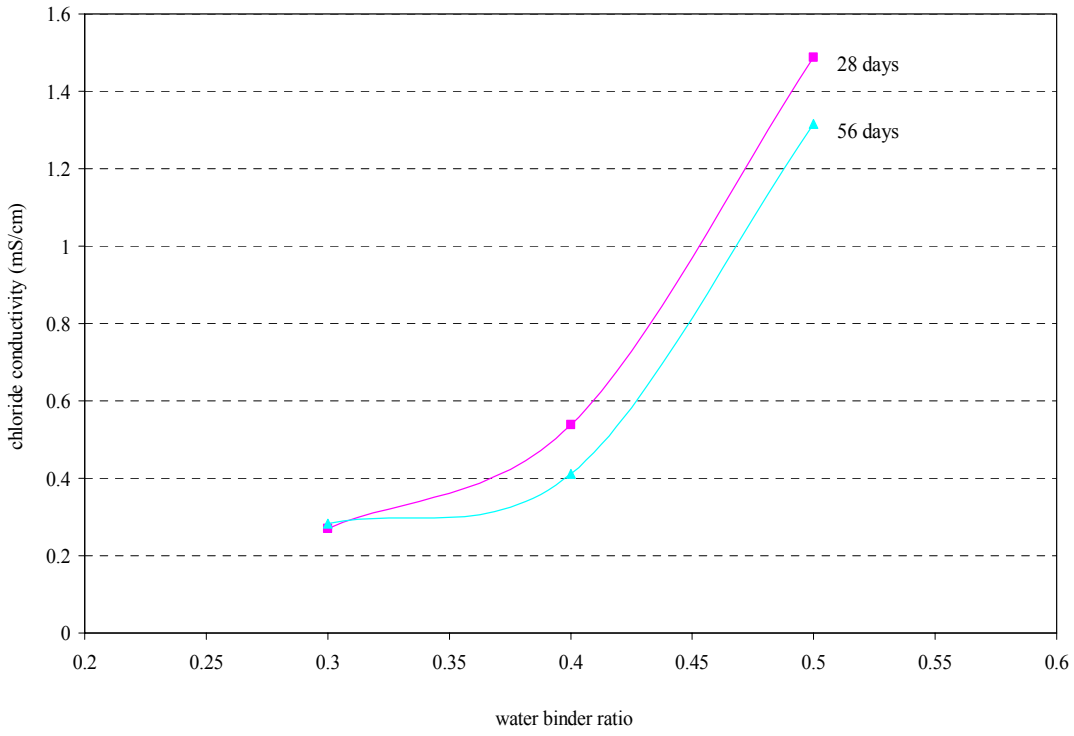


Figure 5.17: Effects of Water-binder ratio on Chloride Conductivity of Concrete Containing 20% Slag and 5% Silica Fume

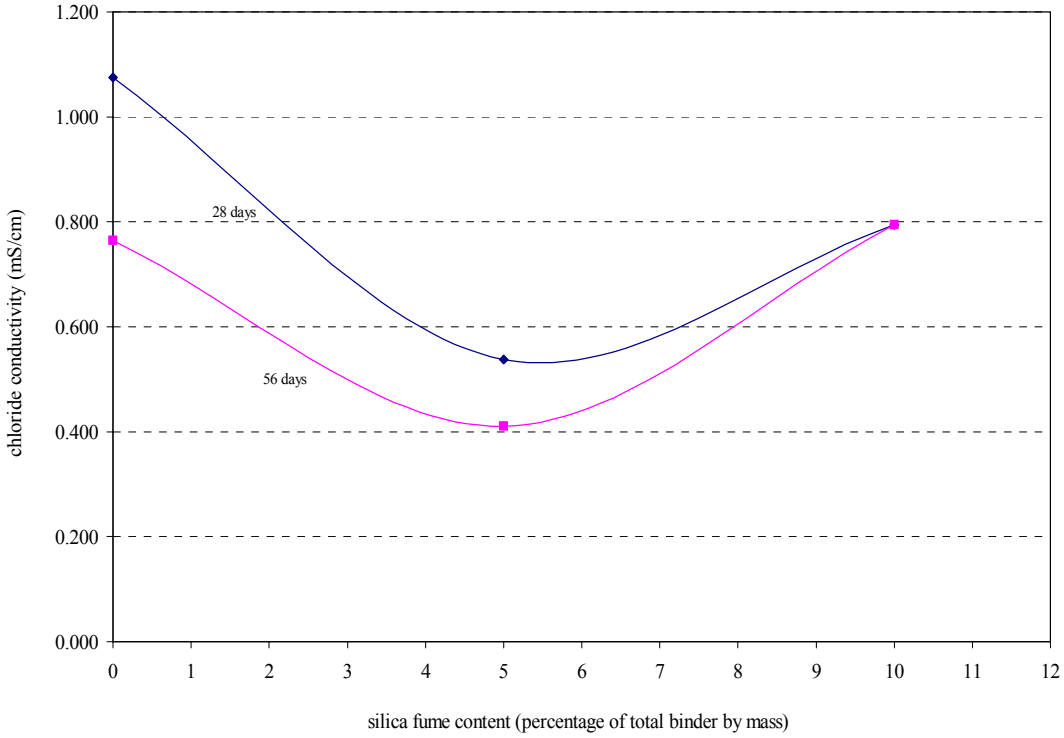


Figure 5.18: Effects of Silica Fume on Chloride Conductivity of Concrete Containing 20% Slag at 0.40 w/b

As the water-binder ratio continues to decrease, the rate of reduction of chloride conductivity decreases, especially for 56-day chloride conductivity values. As shown in Figure 5.17, the chloride conductivity values for concrete with water-binder ratio of 0.30 were the same for 28 and 56 days old concrete.

Figure 5.18 shows the effects of silica fume content on chloride conductivity of concrete containing 20% slag and at 0.40 water-binder ratio. The shape of curves indicated that there is an optimum content of silica fume that produces the lowest chloride conductivity for the concrete mixture containing 20% slag. The optimum content of silica fume is close to 5% of total binder content by mass.

*Concrete containing fly ash and slag:* Figure 5.19 shows the effects of water-binder ratio on chloride conductivity value of concrete containing 20% fly ash and 20% slag. Decreases in water-binder ratio of concrete mixture will dramatically reduce the chloride conductivity of hardened concrete, especially at high water-binder ratio. From Figure 5.19, the rate of reduction in conductivity at 56 days is different than the rate observed at 28 days, and varies with the water-binder ratio. Specifically, it can be shown that the relative difference between chloride conductivity values measured at 28 days and 56 days becomes greater as the water-binder ratio of concrete decreases. Figure 5.19 also shows that concrete containing fly ash and slag requires relatively low water binder ratio to achieve low chloride conductivity value, and at high water-binder ratio, even prolonged curing will not help too much in reducing the chloride conductivity.

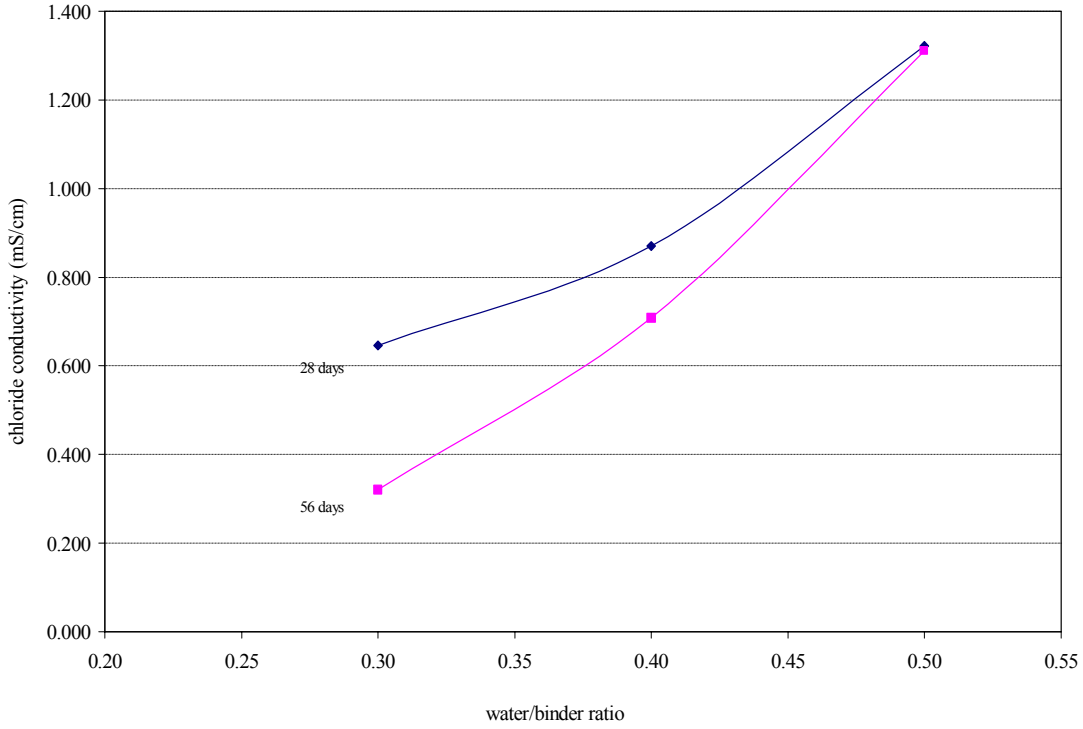


Figure 5.19: Effects of Water-binder Ratio on Chloride Conductivity of Concrete Containing 20% Fly Ash and 20% Slag

5.6.3.2 Conductivity Results – Phase II Mixtures

*Air-entrained concrete mixtures in Phase II mixtures*: The data from Table 5.16 indicate that chloride conductivity of concrete mixtures decreases as the water-binder ratio decreases from 0.40 to 0.35. At 0.35 water-binder ratio, concrete containing pozzolanic materials shows chloride conductivity values 30 - 50% lower than plain concrete at the same water-binder ratio. For concrete mixtures with a water-binder ratio of 0.40, concrete containing pozzolanic materials achieved lower conductivity than the plain concrete (No. 8) at both 28 days and 56 days. Compared to plain concrete, about 30% reduction in 56-day chloride conductivity of concrete containing pozzolanic materials can be observed.

Concrete with 25% slag and 6% silica fume also achieved low chloride conductivity. Although this concrete has water-binder ratio of 0.40, its conductivity values were similar to the binary or ternary concrete with lower water-binder ratio (0.35).

Reduction in conductivity can be observed with the addition of 25% fly ash to concrete at a water-binder ratio of 0.40. However, the reduction is not significant. Effects of silica fume on conductivity of concrete mixtures are also not significant, as shown in Figure 5.18. Only a limited reduction in chloride conductivity of silica fume concrete over plain concrete was observed, and the combination of fly ash with silica fume does not decrease chloride conductivity of the concrete. However, the combination of slag with silica fume helped to decrease chloride conductivity in the concrete. This can be seen from Figure 5.18, by comparing the results of mixture No. 1 with the results of mixture No. 6.

As shown in Figure 5.20, all chloride conductivity values of concrete at 56 days are lower than that at 28 days, which indicates the resistance to ionic movement in concrete increases with age.

Based on the results achieved in this study, fly ash contributes little to the decrease of chloride conductivity of concrete as can be seen by comparing results for mixture No. 6 and 8. Furthermore, conductivity of mixtures containing both silica fume and fly ash, was similar to concrete containing silica fume only.

Comparing No. 9 and No. 7, it can be seen that concrete with 25% slag achieved much lower chloride conductivity than plain concrete of the same water-binder ratio (0.35).

Table 5.16: Chloride Conductivity of Concrete Mixtures in Phase II

| Mix No. | W/B | Binder | | | Conductivity (mS/cm) | |
|---|---|---|---|---|---|---|
| | | FA | SF | Slag | | |
| | | % | % | % | 28 days | 56 days |
| 1 | 0.4 | 0 | 6 | 0 | 1.045 | 0.907 |
| 2 | 0.4 | 25 | 6 | 0 | 1.040 | 0.921 |
| 3 | 0.4 | 40 | 6 | 0 | 1.074 | 0.953 |
| 4 | 0.4 | 25 | 0 | 0 | 1.173 | 1.170 |
| 5 | 0.35 | 40 | 0 | 0 | 0.874 | 0.602 |
| 6 | 0.4 | 0 | 6 | 25 | 0.787 | 0.645 |
| 7 | 0.35 | 0 | 0 | 0 | 0.948 | 0.926 |
| 8 | 0.4 | 0 | 0 | 0 | 1.299 | 1.270 |
| 9 | 0.35 | 0 | 0 | 25 | 0.618 | 0.608 |
| 10 | 0.35 | 25 | 0 | 25 | 0.654 | 0.486 |

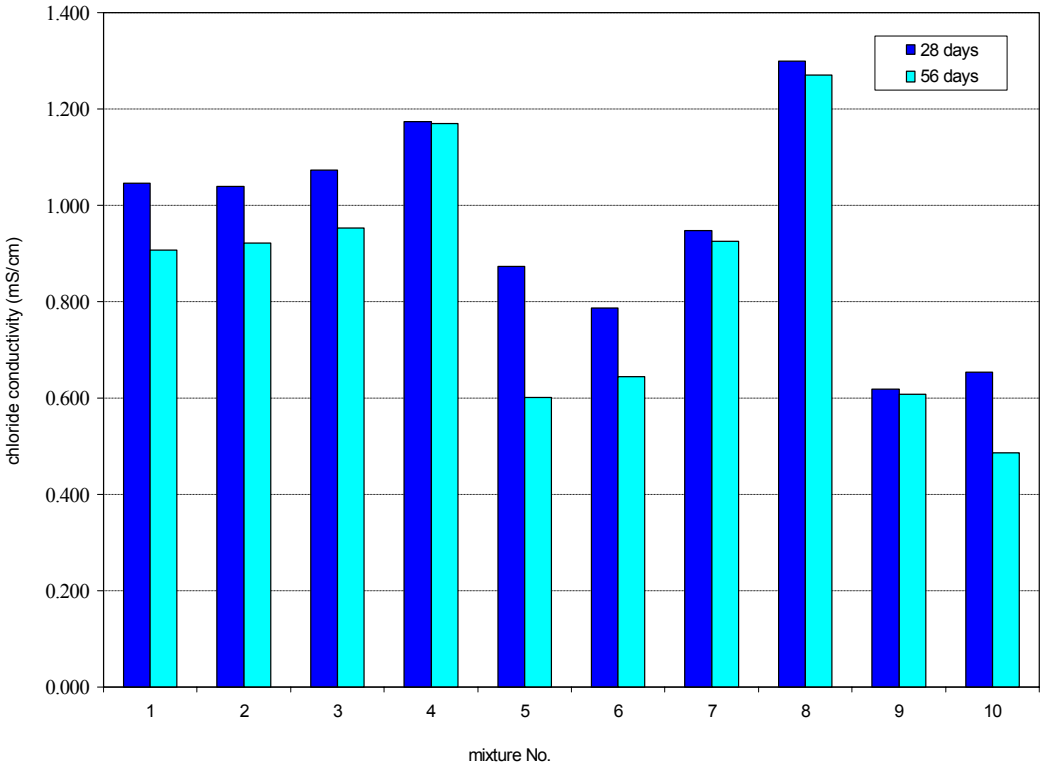


Figure 5.20: Chloride Conductivity of Phase II Concrete Mixtures

### 5.6.4 Summary of Results

Chloride conductivity test can be used during the trial stage of concrete mixture proportioning to evaluate the relative resistance of concrete to chloride ion penetration.

The advantage offered by this test over the rapid chloride permeability test is the ability to eliminate the influence of different types and concentration of ions in the concrete pore solution on the test results. In addition, it also eliminates the effect of the temperature rise during the test. However, the test was not sensitive to the effects of combination of fly ash and silica fume and indicated that silica fume has limited impact on the improvement of pore structure. In addition, some of the results were contradictory. For example, some 56-day conductivity values were the same or even higher than corresponding 28-day values. This would imply that the pore structure of concrete stored in a moist room for 56 days is more permeable than the pore structure of concrete that have been stored for 28 days only.

## 5.7 Analysis of Air Void system in Hardened Concrete

### 5.7.1 Introduction

The presence of the air voids initially suspended in the fresh concrete influences not only the workability and yield of the fresh concrete, but also the strength and frost resistance of the hardened concrete. The effects of air voids on the frost resistance of concrete depend on not only the total volume of the air voids in the concrete, but also the size distribution of air voids and their distribution in the concrete. To effectively provide frost resistance of concrete, the air void system in the hardened concrete must have a total volume of air voids that at least equals the volume of water not accommodated by empty space in the capillary pore system [STP 169C, 1994]. The air voids must be dispersed through the cement paste so that all the paste is within the protective shell of one or more air voids.

Air entraining agent was used in Phase II concrete mixtures, in order to obtain the uniform distribution of small air voids in the concrete and enough total air content, to improve the frost resistance of concrete. Since the air voids could become larger or smaller or coalesce during the transportation, placement, and consolidation procedures when concrete is at the plastic state, characteristics of the air voids in the fresh concrete are different from that of hardened concrete. Therefore, it is necessary to determine the characteristics of air voids in the hardened concrete.

### 5.7.2 Test Procedure

Microscopic Analysis of air void system was conducted on concrete slabs prepared by slicing concrete cylinders to determine the air content in the hardened concrete. The analysis was conducted in accordance with ASTM C 457 (Standard Practice for Microscopical Determination of Air-Void Content and Parameters of the Air-Void System in Hardened concrete). Modified point count method was used to determine the parameters of air void system in Phase II mixtures during this study. Determination of air void content and parameters of air voids system in Phase II hardened concrete was done in INDOT M&T Division, Indianapolis.

### 5.7.3 Results and Analysis

Since the air voids in the fresh concrete can become larger or smaller, or be removed from the concrete completely during the mixing, casting, consolidation and finishing of concrete, it is important to realize that characteristics of the air voids in the fresh concrete still keep on changing with time.

Table 5.17 provides the comparison between the measured values of air content in the fresh concrete and hardened concrete. As shown in Table 5.17, it is apparent that the air content in the hardened concrete is less than that in the fresh concrete, which indicates that some air lost from concrete during the procedure of casting, consolidation, and finishing. The difference in air content between fresh and hardened concrete varied from 0.8 to 2.4%, depending on the mixture proportioning. Concrete No. 9 had the highest difference in air content between fresh and hardened concrete (2.4%). Concrete No. 10 had the lowest difference in air content between fresh and hardened concrete (0.8%).

Table 5.17: Comparison of Measured Values of Air Content in Fresh and Hardened Concrete

| Mix No. | w/b | Binder | | | Air content | |
|---|---|---|---|---|---|---|
| | | FA(%) | SF(%) | Slag(%) | Fresh concrete (Pressure Meter) | Hardened concrete (ASTM C 457) |
| 1 | 0.40 | 0 | 6 | 0 | 6.5 | 4.9 |
| 2 | 0.40 | 25 | 6 | 0 | 6.3 | 4.1 |
| 3 | 0.40 | 40 | 6 | 0 | 6.4 | 5.1 |
| 4 | 0.40 | 25 | 0 | 0 | 6.1 | 5.6 |
| 5 | 0.35 | 40 | 0 | 0 | 6.5 | 4.5 |
| 6 | 0.40 | 0 | 6 | 25 | 6.2 | 5.2 |
| 7 | 0.35 | 0 | 0 | 0 | 6.5 | 5.3 |
| 8 | 0.40 | 0 | 0 | 0 | 6.3 | 5.1 |
| 9 | 0.35 | 0 | 0 | 25 | 6.4 | 4.0 |
| 10 | 0.35 | 25 | 0 | 25 | 6.3 | 5.5 |

Table 5.18 shows the parameters of air void system in Phase II hardened concrete. As shown in Table 5.18, the air content in the specimens varied from 4.0 to 5.6 % of the total volume of concrete. Except for concrete No.2 and 3, other concrete mixtures had higher spacing factor than 0.008 inch, which is the recommended value for the frost-resistant concrete [ACI 212.3R-91]. As shown in Table 5.18, the spacing factor of concrete No. 7 had 0.016 inches, which is twice the recommended spacing factor.

Table 5.18: Parameters of Air Void systems for Phase II Hardened Concrete

| Mix No. | Air content A, % | Air voids per inch of transverse VPI | Specific surface $\alpha$ ($in^2/in^3$) | Spacing factor L (inch) |
|---|---|---|---|---|
| # | 4.9 | 4.5 | 366 | 0.014 |
| 2# | 4.1 | 7.4 | 717 | 0.007 |
| 3# | 5.1 | 8.2 | 647 | 0.007 |
| 4# | 5.6 | 5.5 | 391 | 0.012 |
| 5# | 4.5 | 5.9 | 520 | 0.010 |
| 6# | 4.9 | 6.0 | 493 | 0.009 |
| 6# | 5.5 | 5.7 | 422 | 0.011 |
| 7# | 5.3 | 4.0 | 298 | 0.016 |
| 8# | 5.1 | 7.1 | 562 | 0.009 |
| 9# | 4.0 | 3.7 | 377 | 0.014 |
| 10# | 5.5 | 5.2 | 377 | 0.013 |

## 5.8 Resistance to Freezing and Thawing

### 5.8.1 Introduction

There are two main causes of deterioration of concrete bridge decks in Indiana. One is related to chloride-induced corrosion of steel bars in the concrete, and the other is the damage of concrete due to freezing and thawing. To protect concrete from freezing and thawing, a proper entrained air void system should be provided in the concrete.

There are some uncertainties about the resistance of concrete containing pozzolanic materials to freezing and thawing attack, especially for concrete containing relatively high content of pozzolanic materials.

### 5.8.2 Experimental Procedure

5.8.2.1 Freezing and thawing test: Set-up of test for freezing and thawing of concrete is shown in Figure 5.21. Freezing and thawing test was carried out according to ASTM C 666 (Standard Test Method for Resistance of Concrete to Rapid Freezing and Thawing), procedure A. After 27 days immersion in lime-saturated water, the fundamental transverse frequency of vibration, and weight of the prismatic specimens were measured at a temperature of 0°C. These concrete specimens were then placed into the chamber of a freezing and thawing instrument, and the freezing and thawing cycles were started. Five mixtures were chosen for freezing and thawing and the mixture proportions are shown in Table 5.17. For each concrete mixture, two beams (3" x 4" x 15") were prepared for testing.

During the freezing and thawing, fundamental transverse frequency of vibration and mass of the specimens were measured periodically, in order to monitor the resistance of concrete specimens to freezing and thawing. The measurement was taken every 30 freezing and thawing cycles. The testing was continued until the specimens were subjected to 300 freezing and thawing cycles, or until their relative dynamic modulus of elasticity reached 60% of the initial modulus, whichever occurred first.


Figure 5.21: Set-up of Freezing and Thawing Test

5.8.2.2 Change in Relative Dynamic Modulus of Elasticity: The dynamic modulus of elasticity of concrete specimens was measured by the resonant frequency method-ASTM E 1876-99 (Standard Method for Dynamic Young's Modulus, Shear Modulus, and Poisson's Ratio by Impulse Excitation of Vibration).

Relative dynamic modulus of elasticity of the concrete specimens can be calculated using the following equation:

$$P_N = (\frac{n_1}{n})^2 x100 \quad \text{.....(5.22)}$$

where:
$P_N$ = relative dynamic modulus of elasticity, after N cycles of freezing and thawing, percent;
n = fundamental transverse frequency at 0 cycles of freezing and thawing, and
$n_1$ = fundamental transverse frequency after N cycles of freezing and thawing.

Durability factor of the specimen is calculated by the following equation:

$$DF = \frac{PN}{M} \quad \text{.....(5.23)}$$

where:
DF = durability factor of concrete specimen;
P = relative dynamic modulus of elasticity at N cycles, %;
N = number of cycles at which P reaches the specified minimum value for discontinuing the test or the specified number of cycles at which the exposure is terminated, whichever is less, and;
M = specified number of cycles at which the exposure is terminated.

### 5.8.3 Results and Discussion

As shown in Table 5.19, concrete No. 2 and No. 3 achieved the higher value of durability factor than the other concrete mixtures tested in this study. As shown in Tables 5.18 and 5.19, concrete with 25% slag and 6% silica fume after 28 days' water curing failed during the test before 300 freezing and thawing cycles, and its durability factor was less than 60%. No. 10 concrete with 25% fly ash and 25% slag after 28 days' water curing also failed before 300 cycles of freezing and thawing, and its durability factor was less than 60%. As shown in Table 5.18, concrete No. 2 and No. 3 had the lowest spacing factor among all the concrete specimens tested in this study (0.007 inch), which is lower than the maximum spacing factor (0.008 in) recommended for frost resistant concrete. As shown in Figure 5.22, low spacing factor of air voids in the concrete helped to increase the resistance of concrete to freezing and thawing attack. As also seen in Table 5.19, No. 2 and No. 3 concrete both achieved relatively high durability factor (0.81) after 300 cycles of freezing and thawing. However, concrete No. 10 and No. 6 had high spacing factor of air voids (larger than 0.008 in), therefore, the durability factors of these concrete were less than 60%. However, plain concrete (No. 8) had a durability factor of only 73% after 300 cycles of freezing and thawing, even the spacing factor was lower than 0.008 in. As mentioned early, 28 days of immersion in water for the specimens was used during the first series test.

Additional testing for the resistance to freezing and thawing of concrete has been carried out, and two different curing regimes were used: one of them was 14 days curing in the lime-water, and the other was 14 days water immersion, followed by 14 days drying at the temperature of 20°C and relative humidity of 50%.

As shown in Table 5.19, concrete specimens after 14 days' water curing achieved higher value of durability factor than that after 28 days' water curing, which indicated that longer water curing decreased the frost resistance of concrete. The decrease in the durability factor may be related to the fact that longer water curing increased the degree of saturation of water in concrete specimens. Concrete No. 10 and No. 3 had relatively lower durability factor, which may be related to the limited scaling during freezing and thawing test.

Due to the limited capacity of the freezing and thawing machine (the maximum number of prisms tested each time is 16), second series concrete specimens (total of 20 prisms) were divided into two groups. Concrete mixtures No. 8 and 10 were tested first, and followed by concrete mixtures No. 2, 3, and 6. Therefore, testing of the resistance of

three concrete mixtures (after 14 days' water curing, followed by 14 days' drying) to freezing and thawing is till under way. All the results will be available until July 15th, 2001. Based on the durability factors of two mixtures (No. 8, and No. 10) achieved now, concrete specimens with 14 days' drying had higher durability factor than that without 14 days' drying. As shown in Table 5.19, the increase of 7% and 10% in the average durability factor was observed for concrete No. 8 and 10 separately. The results achieved so far indicated that the drying procedure increased the resistance of concrete to freezing and thawing.

Table 5.19: Summary of Durability Factors for Phase II Mixtures

| Mix No. | W/B | Binder | | | Durability Factor for First Series | | | |
|---|---|---|---|---|---|---|---|---|
| | | FA | SF | Slag | after 28 days' water curing | | | |
| | | (%) | (%) | (%) | Specimen 1 | Specimen 2 | Average | Cycles |
| 2 | 0.4 | 25 | 6 | 0 | 79 | 83 | 81 | 300 |
| 3 | 0.4 | 40 | 6 | 0 | 87 | 74 | 81 | 300 |
| 6 | 0.4 | 0 | 6 | 25 | 62 | 55 | 58 | 270 |
| 8 | 0.4 | 0 | 0 | 0 | 79 | 68 | 73 | 300 |
| 10 | 0.35 | 25 | 0 | 25 | 54 | 55 | 54 | 255 |

Table 5.19: Summary of Durability Factors for Phase II Mixtures (Continuation)

| Mix No. | Durability factor for Second Series | | | | | | | |
|---|---|---|---|---|---|---|---|---|
| | after 14 days' water curing | | | | after 14 days' water curing +14 days' drying | | | |
| | Specimen 1 | Specimen 2 | Average | Cycles | Specimen 1 | Specimen 2 | Average | Cycles |
| 2 | 91 | 88 | 90 | 300 | ---- | ---- | ---- | ---- |
| 3 | 83 | 87 | 85 | 300 | ---- | ---- | ---- | ---- |
| 6 | 88 | 85 | 87 | 300 | ---- | ---- | ---- | ---- |
| 8 | 88 | 85 | 87 | 318 | 95 | 93 | 94 | 300 |
| 10 | 85 | 81 | 83 | 318 | 91 | 95 | 93 | 300 |

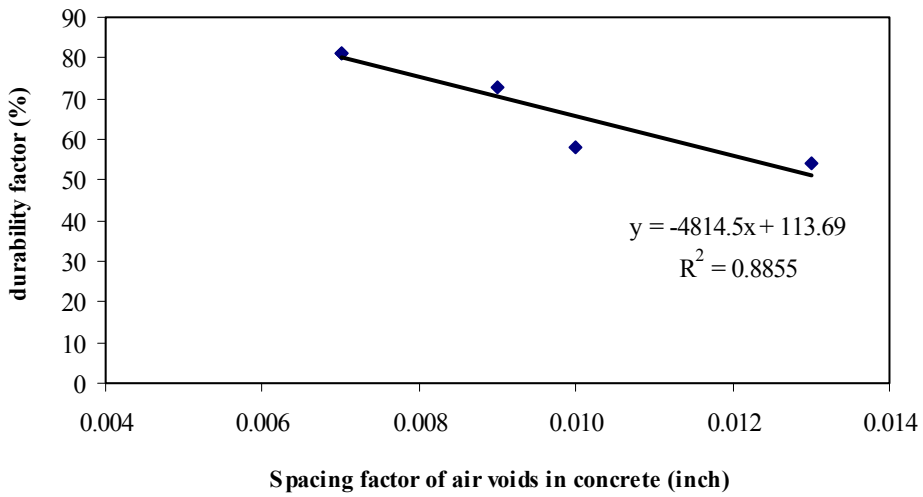


Figure 5.22: Durability Factor of Specimens (First Series) versus Spacing Factor of Air Void System in the Hardened Concrete

## 5.9 Scaling Resistance

### 5.9.1 Introduction

The frequent use of deicing salts during cold weather to remove ice from pavements is one of the main causes to the deterioration of many concrete structures. The use of deicing salts increases the risk of corrosion of reinforcing steel in concrete as well as the damage due to freezing and thawing.

In the early 1960s, it became apparent that the increased use of de-icing chemicals as part of a bare pavement policy adopted for the nation's highways was being reflected in widespread surface scaling of pavement and bridge decks [ASTM STP 169C]. Based on the performance characteristics selected in Phase I of this study, four optimized concrete mixtures were chosen for further testing, and all these concrete mixtures are ternary concrete (containing three types of binder). The objective of this test is to understand the resistance of these optimized concrete mixtures to the attack by deicing chemicals during freezing and thawing.

The ASTM C 672 method was followed in this study to determine the scaling resistance of the 10 concrete mixtures chosen in Phase II.

### 5.9.2 Scaling Test

ASTM C 672 covers determination of the resistance to scaling of a horizontal concrete surface subjected to freezing and thawing cycles in the presence of deicing chemicals. The size of slabs exposed to 3% sodium chloride solution is 10 x 7.5 inches, and the thickness of the slab is 3 inches. Two slabs were prepared for each concrete mixture, and the slab surface was covered with plastic membrane after casting until demolding. Six concrete mixtures were chosen for scaling test. All the slabs were stored in the moist room for 14 days after demolding, and then removed from the moist room to the drying room, at the temperature of 20 °C and relative humidity of 50% RH, for 14 days, before the start of freezing and thawing cycles. After the completion of curing, the flat surface of the slabs was covered with approximately ¼ inch height of the solution of 4% calcium chloride by mass.

The specimens were stored in a chamber, where the temperature was alternately lowered to 17.8 °C and maintained for 16 hours and then raised up to 23 °C and maintained for 6 hours. Water was added in between the cycles, in

order to maintain the proper depth of solution. The cycle was repeated daily and the solution was flushed after every five cycles. Visual evaluation of the exposed surface was done after every five cycles, after this, the solution was replaced and the test continued until 50 cycles. Figure 5.23 shows the set-up of test for the evaluation of scaling resistance of concrete surface to the attack by deicing salts during freezing and thawing.


Figure 5.23: Set-up of the Test for Scaling Resistance to Deicing Salts

### 5.9.3 Visual Evaluation of Surface Condition of Concrete

Visual rating of the surface of slabs after 5,10, 15, 25, 30, 35, 40, 45, 50 cycles was attributed in accordance with the following scale:

Table 5.20: Reference Criteria for Visual Evaluation of Surface Condition [ASTM C 672]

| Rating | Condition of surface |
|---|---|
| 0 | No scaling |
| 1 | Very slight scaling (1/8 inch depth max, no coarse aggregate visible) |
| 2 | Slight to moderate scaling |
| 3 | Moderate scaling (some coarse aggregate visible) |
| 4 | Moderate to severe scaling |
| 5 | Severe scaling (coarse aggregate visible over entire surface) |

### 5.9.4 Results and Discussion

Table 5.21 shows the summary of the results of visual evaluation for Phase II concrete mixtures. Except for No. 3 concrete containing 40% fly ash and 6% silica fume, the other five concrete mixtures had excellent scaling resistance to deicing chemicals, and no scaling was found in these five concrete mixtures. No. 3 concrete with 40% fly ash showed slight scaling after 50 cycles, however, the scaling of concrete surface occurred at the first 10 cycles of freezing and thawing. No. 10 concrete with 25% fly ash and 25% slag showed a good scaling resistance, and it did not show any attack by deicing salt after up to 50 cycles of freezing and thawing. However, No. 3 concrete with 0.40 showed a little scaling during the first 10 cycles of freezing and thawing, and this concrete had 40% fly ash and 6% silica fume. Comparing the scaling resistance of No. 3 with No. 10, the difference in the scaling resistance is caused by the difference in water-binder ratio.

Table 5.21: Resistance of Concrete Surface to the Attack by Deicing Salts after F/T Cycles

| Mix No. | W/B | Binder | | | Scaling Resistance of Concrete Mixtures in Phase II | | | | | | | | | |
|---|---|---|---|---|---|---|---|---|---|---|---|---|---|---|
| | | FA (%) | SF (%) | Slag (%) | Visual rating of the concrete surface after the following F/T cycles | | | | | | | | | |
| | | | | | 5 | 10 | 15 | 20 | 25 | 30 | 35 | 40 | 45 | 50 |
| 2 | 0.4 | 25 | 6 | 0 | 0 | 0 | 0 | 0 | 0 | 0 | 0 | 0 | 0 | 0 |
| 3 | 0.4 | 40 | 6 | 0 | 0 | 1 | 1 | 1 | 1 | 1 | 1 | 1 | 1 | 1 |
| 6 | 0.4 | 0 | 6 | 25 | 0 | 0 | 0 | 0 | 0 | 0 | 0 | 0 | 0 | 0 |
| 7 | 0.35 | 0 | 0 | 0 | 0 | 0 | 0 | 0 | 0 | 0 | 0 | 0 | 0 | 0 |
| 8 | 0.4 | 0 | 0 | 0 | 0 | 0 | 0 | 0 | 0 | 0 | 0 | 0 | 0 | 0 |
| 10 | 0.35 | 25 | 0 | 25 | 0 | 0 | 0 | 0 | 0 | 0 | 0 | 0 | 0 | 0 |

## 5.10 Drying Shrinkage of HPC

As was mentioned in the definition of high performance concrete, one of the most important characteristics of high performance concrete is its dimensional stability. Several types of volume changes occur in concrete in response to environmental effects, such as, drying and wetting, freezing and thawing, heating and cooling, and also chemical attack, such as, carbon dioxide, alkali aggregate reaction, or sulfate attack. In this section, drying shrinkage of concrete is investigated.

### 5.10.1 Introduction

In general, a concrete structure is subjected to certain restraints, due to steel reinforcement, sub-grade friction or other foundation. This could cause volume changes in concrete, which could have a deleterious effect on the concrete. External cracking will provide the shortest way for water, chemical fluids or gases to attack the concrete or reinforcing bar in the concrete, and this will shorten the service life of concrete structure significantly, although the cracking in the concrete may be not influence the integrity of the concrete structure itself.

As discussed in Phase I of this study, three concrete mixtures with ternary binders show the most promising properties, and two contain 25% fly ash (or slag) and 6% silica fume at 0.40 water-binder ratio. Concrete mixture with 25% fly ash and 25% slag also showed good properties at 0.35 water-binder ratio. In general, these three concrete mixtures have normal water-binder ratio, and the total binder content (390 $kg/m^3$) is also in the normal range. Therefore, autogenous shrinkage of these concrete mixtures is expected to be similar to plain concrete (No. 8).

Two test methods for measuring the shrinkage of cement-based materials are described ASTM C 157 (Standard Test Method for Length Change of Hardened Hydraulic Cement, Mortar and Concrete); and ASTM C 596 (Standard Test Method for Drying Shrinkage of Mortar Containing Portland Cement). ASTM C 157 provides a method for potential volumetric expansion or contraction of mortar or concrete due to various causes other than applied stress or temperature change. This method is particularly useful for comparative evaluation of potential expansion or shrinkage in different hydraulic cement mortar or concrete mixtures [STP 169C, 1994]. For this study, ASTM C 157 was followed to determine the drying shrinkage of the 10 concrete mixtures under a standard laboratory environment (at the temperature of 20°C and relative humidity of 50%). ASTM C 596 covers the determination of the effects of Portland cement on the drying shrinkage of a graded standard sand mortar subjected to certain environment. However, the drying shrinkage of concrete would be quite different from that of mortar with the same cement content and the same exposure condition, depending on the type and content of aggregate and water content in the concrete mixtures. Therefore, people doubt the validity of extrapolating the data of mortar shrinkage to concrete shrinkage.

### 5.10.2 Sample Preparation

Since the maximum size of coarse aggregate used in this study was 1 inch, concrete prisms with the size of 3" x 3" x 11.25" were prepared in accordance with ASTM C 157. Three prisms were prepared for each test condition, and the average results from three specimens are reported as the drying shrinkage of concrete after each drying period.

After casting, the concrete specimens were covered by a plastic membrane, followed by wet burlap, in order to prevent the water loss from the concrete surface and also prevent the external water from dripping onto the concrete before the final setting of concrete.

### 5.10.3 Test Procedure

After the specimens are moved into the drying room, the length change of concrete prisms is measured by a comparator and weight change is measured by a balance at 1, 3, 7, 28, 56, 90, and 180 days from the start of drying. At each measurement of specimen length, a standard reference bar is used to check and zero the comparator before and after the reading. If difference between the two readings is larger than 0.0001 in, the measurement should be repeated. During each length measurement of the specimens, the reference bar and the specimens should be placed along the same direction into the comparator.

### 5.10.4 Results and Discussion

Table 5.22 shows the drying shrinkage for Phase II concrete mixtures as a function of drying time. A negative value in Table 5.22 means a shrinkage of specimens, and the positive number means an expansion of specimens. At 180 days of drying, the drying shrinkage for all the 10 mixtures in Phase II ranged from 360 to 450 microstrains. Concrete with 25% fly ash and 6% silica fume obtained the lowest drying shrinkage, which was about 360 microstrains at 180-day drying, and plain concrete No. 8 achieved the highest amount of drying shrinkage, which was 450 microstrains. Based on the results achieved in this test, concrete containing fly ash, slag or silica fume does not show any potential of higher drying shrinkage than plain concrete at the same water-binder ratio. Comparing the drying shrinkage of two plain concrete mixtures, concrete with water-binder ratio of 0.35 had much lower shrinkage than that with water-binder ratio of 0.40. These two mixtures had the same amount of Portland cement, and similar aggregate contents.

Table 5.22: Summary of Drying Shrinkage for Phase II Concrete

| Mix No. | Drying shrinkage (microstrain) | | | | | | | | |
|---|---|---|---|---|---|---|---|---|---|
| | 28days in water | 1 day | 3 days | 7 days | 28 days | 56 days | 90 days | 180 days | Rank |
| 1 | 6.67E+01 | 1.00E+01 | -5.67E+01 | -1.27E+02 | -2.87E+02 | -3.33E+02 | -3.57E+02 | -3.73E+02 | 4th |
| 2 | 7.00E+01 | -6.67E+00 | -7.00E+01 | -1.73E+02 | -2.87E+02 | -3.33E+02 | -3.43E+02 | -3.57E+02 | 1st |
| 3 | 4.67E+01 | -4.67E+01 | -1.47E+02 | -2.37E+02 | -3.63E+02 | -4.03E+02 | -4.27E+02 | -4.33E+02 | 7th |
| 4 | 5.67E+01 | -3.00E+01 | -9.67E+01 | -1.93E+02 | -3.53E+02 | -4.07E+02 | -4.30E+02 | -4.50E+02 | 9th |
| 5 | 5.33E+01 | -1.33E+01 | -1.00E+02 | -2.00E+02 | -3.43E+02 | -3.83E+02 | -4.10E+02 | -4.37E+02 | 8th |
| 6 | 6.00E+01 | -3.33E+00 | -5.33E+01 | -1.13E+02 | -2.63E+02 | -3.10E+02 | -3.47E+02 | -3.93E+02 | 5th |
| 7 | 8.00E+01 | 1.33E+01 | -7.67E+01 | -1.33E+02 | -2.63E+02 | -3.17E+02 | -3.37E+02 | -3.60E+02 | 2nd |
| 8 | 4.00E+01 | -2.00E+01 | -1.07E+02 | -1.83E+02 | -3.20E+02 | -4.10E+02 | -4.20E+02 | -4.50E+02 | 9th |
| 9 | 3.00E+01 | -8.67E+01 | -8.67E+01 | -1.47E+02 | -3.13E+02 | -3.43E+02 | -3.93E+02 | -4.00E+02 | 6th |
| 10 | 7.67E+01 | -2.33E+01 | -8.00E+01 | -1.37E+02 | -2.80E+02 | -3.03E+02 | -3.37E+02 | -3.70E+02 | 3rd |

Notes:
ASTM C 157 was followed to test the drying shrinkage of Phase II concrete mixturtes;
Three specimens were used for each concrete mixture(3"x3"x111/4" prism)
Rank is based on the shrinkage of specimens after 180 days of drying (3"x3"x111/4")

As shown in Table 5.22, all the concrete mixtures show a limited amount of expansion after 27 days immersion in lime-saturated water, ranging from 30 to 80 microstrains. Figure 5.24 shows the relationship between 27-day expansion in lime-saturated water and the 180-day drying shrinkage of concrete. From the statistical point of view, the higher the 28-day expansion of specimen in water, the higher the amount of 180-day drying shrinkage. The $R^2$ for the linear relationship is 0.79.

Table 5.23: Development Rate of Drying Shrinkage of Concrete with Time

| Mix No. | development rate percentage of drying shrinkage | | | | | | | |
|---|---|---|---|---|---|---|---|---|
| | 28days in water | 1 day | 3 days | 7 days | 28 days | 56 days | 90 days | 180 days |
| 1 | -17.9 | -2.7 | 15.2 | 33.9 | 76.8 | 89.3 | 95.5 | 100.0 |
| 2 | -19.6 | 1.9 | 19.6 | 48.6 | 80.4 | 93.5 | 96.3 | 100.0 |
| 3 | -10.8 | 10.8 | 33.8 | 54.6 | 83.8 | 93.1 | 98.5 | 100.0 |
| 4 | -12.6 | 6.7 | 21.5 | 43.0 | 78.5 | 90.4 | 95.6 | 100.0 |
| 5 | -12.2 | 3.1 | 22.9 | 45.8 | 78.6 | 87.8 | 93.9 | 100.0 |
| 6 | -15.3 | 0.8 | 13.6 | 28.8 | 66.9 | 78.8 | 88.1 | 100.0 |
| 7 | -22.2 | -3.7 | 21.3 | 37.0 | 73.1 | 88.0 | 93.5 | 100.0 |
| 8 | -8.9 | 4.4 | 23.7 | 40.7 | 71.1 | 91.1 | 93.3 | 100.0 |
| 9 | -7.5 | 21.7 | 21.7 | 36.7 | 78.3 | 85.8 | 98.3 | 100.0 |
| 10 | -20.7 | 6.3 | 21.6 | 36.9 | 75.7 | 82.0 | 91.0 | 100.0 |

Table 5.23 shows the percentage of drying shrinkage of concrete at different drying times, compared to drying shrinkage at 180 days. As shown in Table 5.23, 7-day drying shrinkage of concrete was about 1/3 of 180-day drying shrinkage. Concrete after 28-day drying achieved about 70% of the 180-day drying shrinkage, which indicates that most of the drying shrinkage of concrete takes place during the early ages of drying. After 56 days of drying, the development rate of the shrinkage of concrete dropped. This trend exists in all the 10 concrete mixtures.

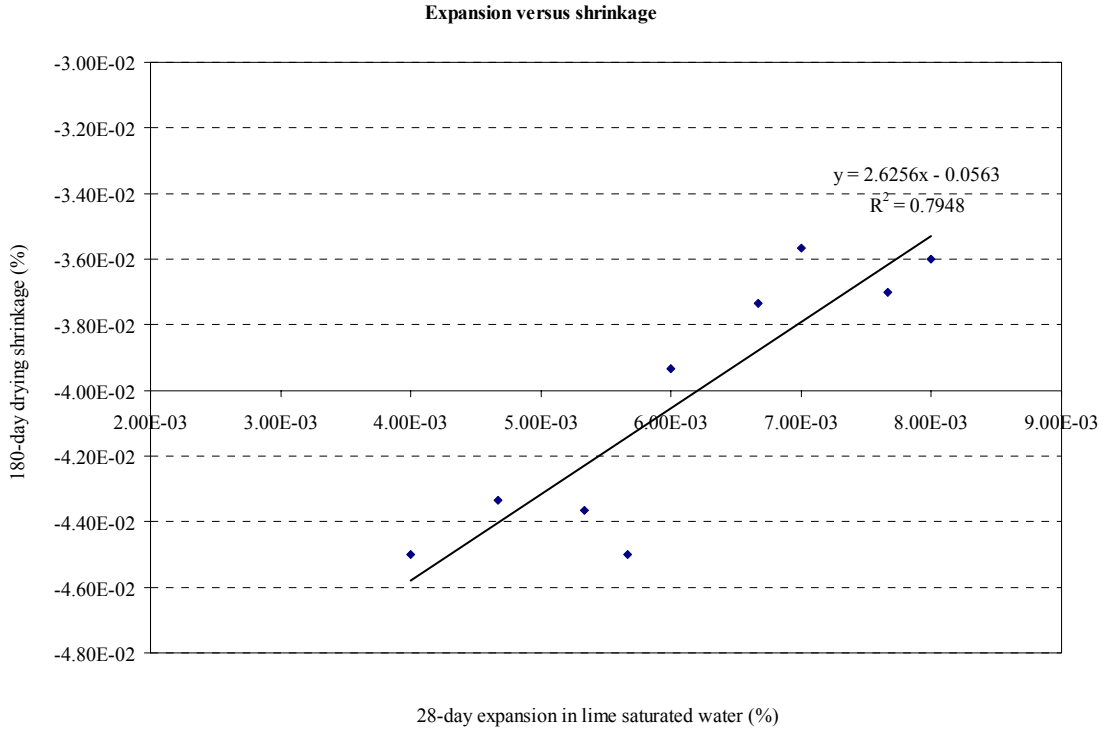


Figure 5.24: Expansion versus Drying Shrinkage of Concrete

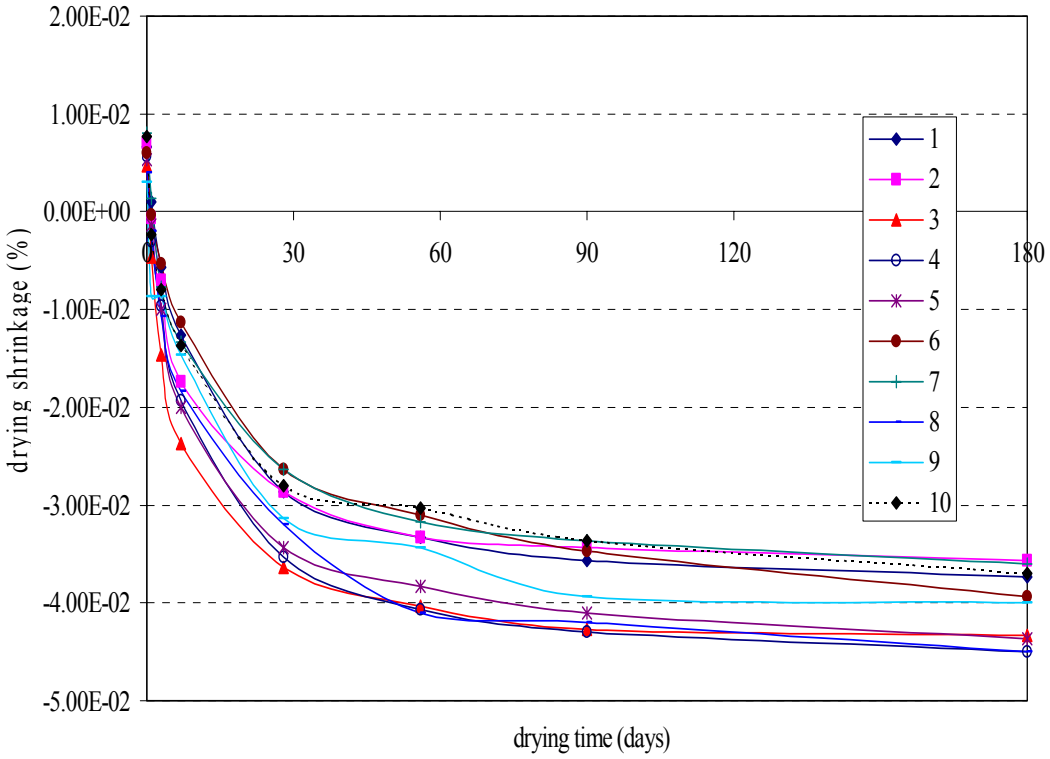


Figure 5.25: Development of Drying Shrinkage of Concrete with Drying Time

As shown in Figure 5.25, the drying shrinkage of specimens developed quickly during the early drying periods, especially during the first 28 days of drying. The figure shows that all the shrinkage curves drop steeply during the early ages, and then become flat. A limited amount of drying shrinkage of concrete was observed from 90 days drying to 180 days drying. Compared to plain concrete, concrete containing fly ash, slag or silica fume did not show any higher potential of drying shrinkage at the same water-binder ratio.

Concrete is made up of two components: cement paste and aggregate. The former shrinks and the latter restrains the shrinkage. The effectiveness of the aggregate restraint to shrinkage of cement paste is related to the stiffness of the aggregate (elastic modulus). The effects of different type of aggregate on the drying shrinkage were not investigated in this study. Obviously, as the amount of aggregate used in concrete increases, the amount of drying shrinkage occurring in the concrete will decrease.

For the cement paste in concrete, the most important factor contributing to drying shrinkage is water content for a given cement content. As higher amount of water is added to the concrete, higher drying shrinkage of concrete can be expected. This is due to the presence of more water available for removal from concrete with higher water-binder ratio than that with lower water-binder ratio. As shown in Table 5.22, mixture No. 7 (w/b = 0.35) showed lower drying shrinkage at all drying ages than mixture No. 8 (w/b = 0.40), although both concrete contained the same amount of coarse aggregate.

Diffusion of the absorbed water and the water held by the capillary tension in small pores of the hydrated cement paste to large capillary pores within the concrete or to the atmosphere is a slow time-dependent process. Figure 5.26 shows the relationship between the weight loss and length change of concrete containing 25% fly ash and 6% silica fume during the drying period. According to the high coefficient of determination ($R^2$ = 0.97) between the weight loss and length change of the specimen, a strong linear relationship exists between the weight loss and the length change of the concrete prisms during drying shrinkage testing. The higher the weight loss of specimens observed,

the higher the magnitude of drying shrinkage that can be expected. As shown in Figure 5.26, the regression line does not pass through the origin (0, 0), which may be related to some shrinkage caused by other mechanism during the drying period. Other concrete mixtures also showed similar trends between weight loss and length change.

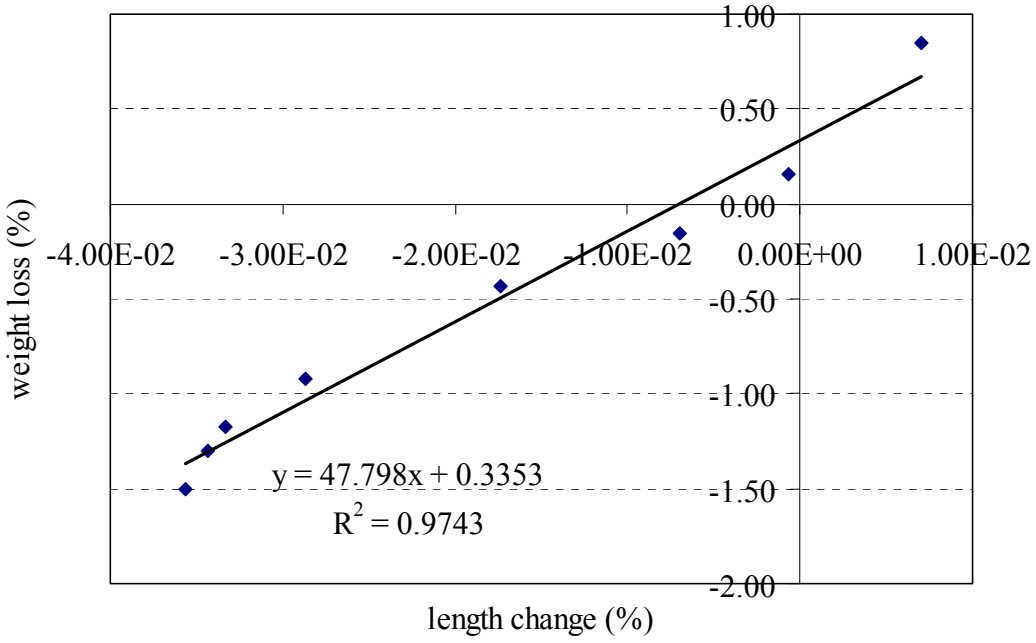


Figure 5.26: Relationship between Length Changes of Concrete Specimen with Weight Loss during the Drying Period

### 5.10.5 Conclusion

ASTM C 157 standard test method was followed to evaluate the drying shrinkage of Phase II air entrained concrete mixtures. All the concrete mixtures tested in this section showed that the magnitude of 180-day drying shrinkage varied from 350 to 450 microstrains, and concrete with 25% fly ash and 6% silica fume obtained the lowest amount of drying shrinkage among the 10 concrete mixtures, which was 357 microstrains. Plain concrete No. 8 (w/b = 0.40) had the highest magnitude of 180-day drying shrinkage.

Based on the results achieved in this study, concrete mixtures containing fly ash, slag or silica fume did not show higher potential of drying shrinkage than plain Portland cement concrete at the same water-binder ratio and aggregate content. Concrete mixtures recommended in Phase I (No. 2, No. 6, and No. 10) had relatively low amount of 180-day drying shrinkage.

All the 10 concrete mixtures were subjected to a small amount of expansion after 27-day immersion in lime saturated water, and the value of expansion was in the range of 30 to 80 microstrains. The regression analysis between the expansion value and the 180-day drying shrinkage of concrete specimens showed that there is a statistical trend. The expansion after 27-day immersion in water was linearly related to the 180-day drying shrinkage.

During the drying period, the weight loss of the concrete prisms showed a strong linear relationship with the drying shrinkage, and the coefficient of determination for the regression line was 0.97. The regression line is close to the origin (0,0), which indicates that magnitude of shrinkage caused by other mechanism did not contribute to the total shrinkage very much.

## 5.11 Absorption of HPC

### 5.11.1 Introduction

The volume of pore space in concrete can be measured by absorption. However, only the volume of permeable pore can be effectively measured during absorption test. Absorption of concrete is generally measured by the following procedure: First the specimen is oven-dried to a constant weight, and then, immersed in water. Finally, the increased weight is obtained after the immersion for certain time in water. A wide variety of absorption tests on concrete are available [STP 169C, 1994]. These tests measure the weight gain of a specimen, or the volume of water entering the specimen, or the depth of water penetration.

The total porosity of concrete has a very important effect not only on the mechanical properties such as compressive strength, but also on the impermeability of the material to water or other liquids. Therefore, water absorption characteristics of concrete are particularly interesting and of practical significance. It is known that the moisture content in concrete before immersion affects the test results significantly, and their drying at ordinary temperature may be ineffective in removing water from a specimen. However, drying at high temperature may remove some combined water, and also cause damage to the concrete during drying. It can be expected that high quality or more impermeable concrete will suffer more damage than poor concrete during a high temperature drying process.

### 5.11.2 Sample Preparation

Cement concrete cylinders (4" x 8") were cast for the 10 concrete mixtures and all these concrete achieved total 6 - 7% air content at fresh state. Three cylinders were cast for each mixture. The cylinders were stored in a moist room (RH = 100%, temperature: 23 °C) for 56 days. Concrete slices with a thickness of 2 ± 1/8" from the top of each cylinder were used for the absorption test.

### 5.11.3 Test Procedure

Absorption studies of HPC were conducted according to ASTM C 642-90 (Standard Test Method for Specific Gravity, Absorption, and Voids in Hardened Concrete). The following procedure was followed during the absorption test:

1. The specimens were oven-dried to the constant weight;
2. The saturated weight after 72 hours' immersion was recorded;
3. Saturated weight after 5-hour boiling was recorded;
4. Weight of specimens immersed in water was recorded;

### 5.11.4 Results and Discussion

The following characteristics of concrete were calculated by using the weights measured in the test procedure described in Section 5.11.3:

Absorption after immersion (%) =
(Saturated weight after 72 hour immersion – Dry weight)/ Dry weight *100
Absorption after immersion and 5-hour boiling (%) =
(Saturated weight after 5-hour boiling – Dry weight)/ Dry weight *100

Table 5.24: Absorption value for Phase II concrete mixtures

| Mix No. | Absorption values for PART TWO concrete mixtures | | | | | | | |
|---|---|---|---|---|---|---|---|---|
| | Absorption % (after immersion) | | | | Absorption % (after boiling) | | | |
| | Sample 1 | Sample 2 | Sample 3 | **Mean** | Sample 1 | Sample 2 | Sample 3 | **Mean** |
| 1 | 6.3 | 6.7 | 6.6 | **6.5** | 8.2 | 8.6 | 8.6 | **8.5** |
| 2 | 6.4 | 6.7 | 6.5 | **6.5** | 8.4 | 8.8 | 8.5 | **8.6** |
| 3 | 6.2 | 6.0 | 6.1 | **6.1** | 8.4 | 8.4 | 8.4 | **8.4** |
| 4 | 6.1 | 6.2 | 6.4 | **6.2** | 8.1 | 8.1 | 8.5 | **8.2** |
| 5 | 5.3 | 5.5 | 5.3 | **5.4** | 7.5 | 7.7 | 7.3 | **7.5** |
| 6 | 5.2 | 6.0 | 6.0 | **5.7** | 6.9 | 7.8 | 7.7 | **7.5** |
| 7 | 5.4 | 5.6 | 5.6 | **5.5** | 7.0 | 7.1 | 7.1 | **7.1** |
| 8 | 5.9 | 6.3 | 6.2 | **6.1** | 7.7 | 8.3 | 8.2 | **8.1** |
| 10 | 4.7 | 5.1 | 5.0 | **4.9** | 6.5 | 6.9 | 6.8 | **6.7** |

As shown in Table 5.24, concrete mixtures with 0.35 water-binder ratio had lower absorption value than that with 0.40 water-binder ratio. Less water was added in the concrete mixture with lower water-binder ratio during mixing, and thus a lower volume of capillary pores existed in the hardened concrete. Among concrete mixtures with water-binder ratio of 0.35, concrete No. 10 had the lowest absorption value either under immersion or 5 hours boiling, which indicates that the lowest volume of permeable pore in concrete exists in this concrete. Among concrete mixtures with water-binder ratio of 0.40, concrete No. 6 showed the lowest water absorption value. It is expected that silica fume will enhance the impermeability of concrete. However, plain concrete had a lower water absorption value than silica fume concrete (No. 1), which may have been due to the damage of concrete during the oven drying process. This trend can also be observed in fly ash concrete, which shows a relatively higher water absorption value than plain concrete.

## 5.12 Electrical Resistance at 60 Volts (DC)

Electrical resistance of concrete influences the progress of corrosion of steel bar in concrete. During the corrosion process of steel, ion exchange takes place between anode and cathode and drives the corrosion of steel. The magnitude of the electrical resistance of concrete indicates the degree of difficulty of the ionic movement in the concrete, whose value is related not only to the concentration and type of ions in pore fluid, but also to the pore structure of the hardened concrete.

### 5.12.1 Introduction

As water is added to cement, the electrical properties of fresh mixtures start to change significantly. With the hydration of Portland cement, more and more amounts of water are involved with the chemical reaction and converted to chemically combined water. The electrical property of water drops significantly as free water is converted to chemical combined water. As cement starts to hydrate, and the hydration products of cement fill the space that was initially filled by water, a discontinuity of pore structure started to form in the concrete system. The amount of free water and the degree of the discontinuity of pore structure in concrete can be represented by the electrical property of concrete. The influence of the concentration and types of ions in the pore fluid on the electrical properties of hardened concrete is not investigated in this research, although these variations in the pore fluid are important to the electrical property of concrete.

### 5.12.2 Sample Preparation

Three concrete cylinders (4" x 8") were prepared for each mixture. Before casting of concrete, three holes were punched in the side of plastic cylinder mold with a diameter of ¼ inch. Three copper rods (1/4 in diameter and 3 inch long) were inserted through the holes into the molds to the depth of 2 inch and were secured to the side of the mold. The rods were located 2 in apart with the first rod being placed 2 inch from the top of the sample as shown in Figure 5.27. The mold was then filled with concrete and covered with plastic cap. At the age of 24 hours, the cylinders were removed from the molds, and transferred to the moist room where they were stored until test time.

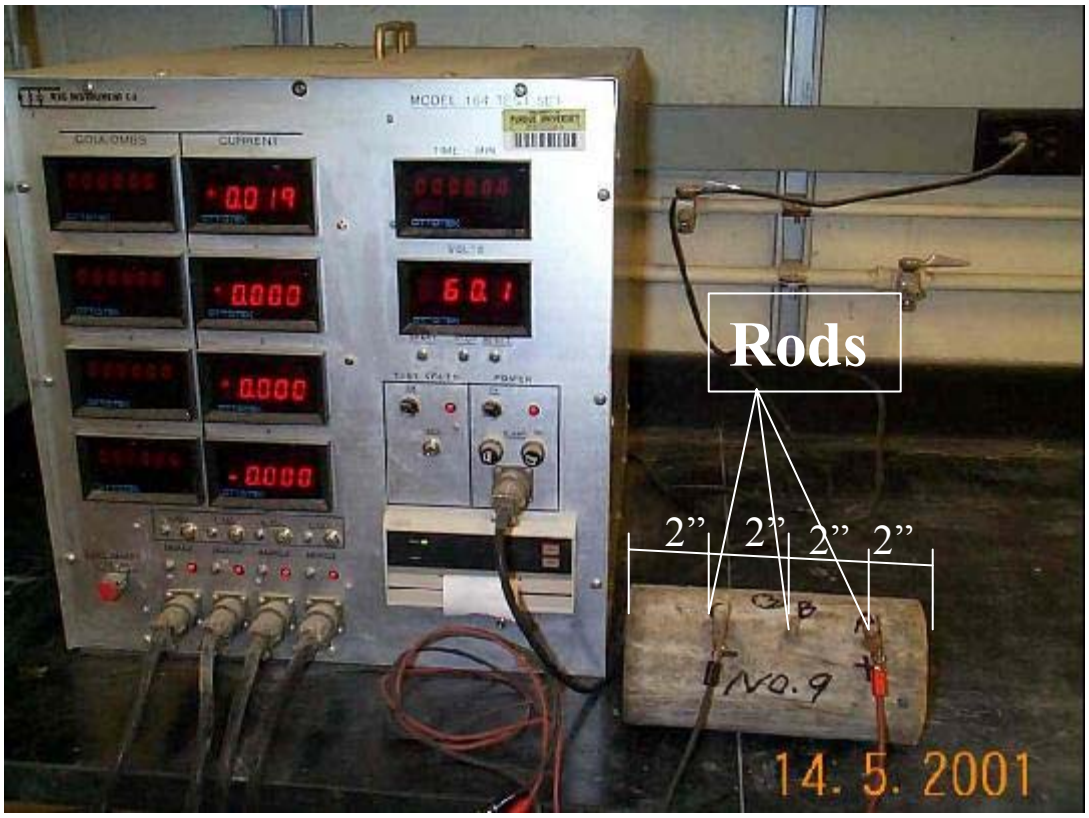


Figure 5.27: Set-up of DC Electrical Resistance Test

### 5.12.3 Test Procedure

At the prescribed test age, the specimens were removed from the curing room, and two of the rods were hooked up to the 60 V DC power source. The 60 V potential was then applied to two of the rods, and the resulting current was recorded. Initially, the measurements were conducted using pairs of rods located with either 2 or 4 inches apart. However, the data indicated that 2 in distance between the rods was too small compared to maximum size of the aggregate and led to inconsistent results. To avoid this problem, all results presented in this report were collected from rods located 4 in apart. Three specimens were tested for each mixture. Specimens were tested at 1, 3, 7, 14, 28, 42, 56, 90, and 180 days after casting.

### 5.12.4 Results and Discussion

Table 5.25 and Figure 5.28 show the changes in the electrical current through the copper rods under 60 DC volts with the curing ages. The distance between the rods was 4 inches. As seen in Table 5.25, at ages later than 14 days, the magnitude of electrical current was lowest in concrete No. 6, which contained 25% slag and 6%. This indicates that concrete No. 6 offered the highest resistance to the movement of electrical ions. Similar trends can be observed while analyzing the rapid chloride permeability data (see Figure 5.7) and diffusion coefficient data (Table 6.5). These confirm that measurement of concrete electrical current (resistance) can provide a good indication of its ability to resist the transport of ions.

Table 5.25: Summary of the Electrical Currents of Concrete under 60 Volts DC

| Mix No. | DC current under 60 volts (A) | | | | | | | | | |
|---|---|---|---|---|---|---|---|---|---|---|
| | 1 day | 3 days | 7 days | 14 days | 21 days | 28 days | 42 days | 56 days | 90 days | 180 days |
| 1 | 0.0910 | 0.0513 | 0.0437 | 0.0273 | 0.0213 | 0.0187 | 0.0153 | 0.0133 | 0.0123 | 0.0107 |
| 2 | 0.1450 | 0.0810 | 0.0620 | 0.0373 | 0.0280 | 0.0217 | 0.0160 | 0.0133 | 0.0103 | 0.0070 |
| 3 | 0.1603 | 0.1027 | 0.0750 | 0.0410 | 0.0283 | 0.0213 | 0.0163 | 0.0127 | 0.0097 | 0.0067 |
| 4 | 0.1347 | 0.0770 | 0.0550 | 0.0420 | 0.0367 | 0.0310 | 0.0287 | 0.0257 | 0.0250 | 0.0160 |
| 5 | 0.1397 | 0.0793 | 0.0567 | 0.0377 | 0.0347 | 0.0310 | 0.0262 | 0.0213 | 0.0140 | 0.0087 |
| 6 | 0.1267 | 0.0753 | 0.0443 | 0.0233 | 0.0157 | 0.0130 | 0.0090 | 0.0083 | 0.0067 | 0.0057 |
| 7 | 0.0837 | 0.0493 | 0.0420 | 0.0387 | 0.0350 | 0.0317 | 0.0290 | 0.0273 | 0.0237 | 0.0193 |
| 8 | 0.0847 | 0.0530 | 0.0463 | 0.0427 | 0.0400 | 0.0390 | 0.0343 | 0.0323 | 0.0290 | 0.0220 |
| 9 | 0.1180 | 0.0727 | 0.0507 | 0.0403 | 0.0327 | 0.0293 | 0.0263 | 0.0237 | 0.0190 | 0.0163 |
| 10 | 0.1497 | 0.0883 | 0.0647 | 0.0413 | 0.0317 | 0.0260 | 0.0220 | 0.0170 | 0.0127 | 0.0087 |

The two plain concrete mixtures (No. 7 and 8) and concrete No. 1 showed much lower magnitude of electrical current 7 days after casting than the others. This indicates that the discontinuity of pore structure in these three concrete occurred earlier than other concrete mixtures containing fly ash or slag. However, plain concrete No. 7 with water-binder ratio of 0.35 obtained the highest magnitude of the electrical current at the age of 180 days, and plain concrete No. 8 with 0.40 w/b had the highest amount of electrical current at the age of 14 days or later.

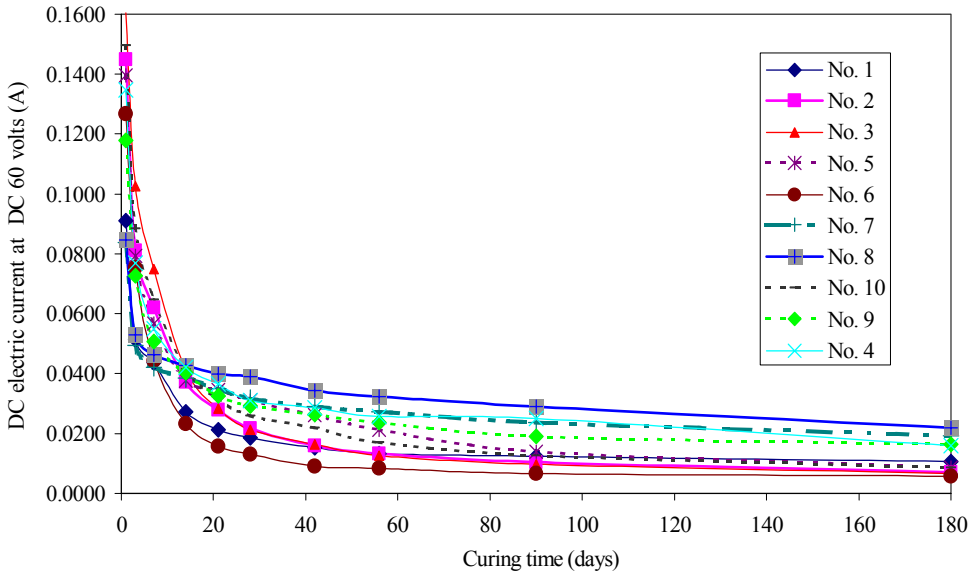


Figure 5.28: Development of Electrical Current of Concrete with Age

5.12.4.1 Effects of silica fume on electrical resistance of concrete: As shown in Figure 5.29, (No. 8 was plain concrete with w/b of 0.40, and No. 1 was silica fume concrete with w/b of 0.40), the increase of the electrical resistance of concrete by the addition of silica fume occurred only 3 days later after mixing. Silica fume concrete achieved a higher electrical current than plain concrete in the first 3 days. However, from 7 to 21 days after mixing, the electrical current for silica fume concrete reduced more than 50% and plain concrete showed only a reduction of 15% in the electrical current. From 7 to 14 days, the reduction is about 40% for silica fume concrete, compared to 10% for plain concrete. After 21 days of moist curing, the electrical current for silica fume concrete decreased to only half of plain concrete. This suggests that the effects of silica fume on the reduction of electrical current passing through concrete is significant after 7 days, especially between 7 and 21 days. The effects of silica fume on the reduction in electrical current of concrete before the age of three days was not found in this study.

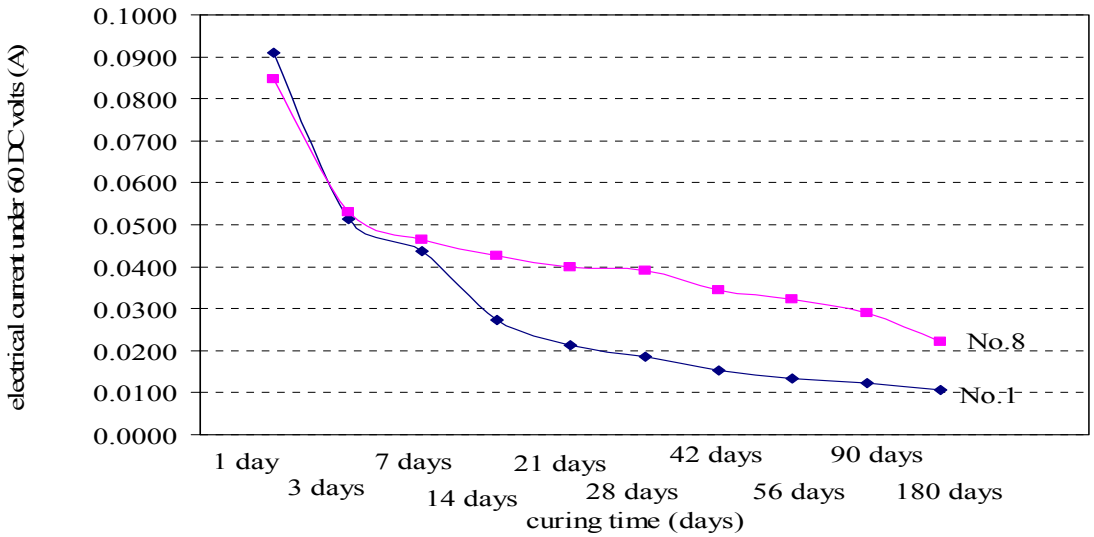


Figure 5.29: Effects of Silica Fume on the Electrical Property of Concrete

5.12.4.2 Effects of fly ash on the electrical resistance of concrete: Figure 5.29 shows the electrical current passing through four concrete mixtures containing fly ash and/or silica fume with time. Two concrete with a combination of fly ash and silica fume achieved similar electrical current at the age of 21 days after casting. Before 21 days, concrete No. 2 with 25% FA and 6% SF obtained lower electrical current than concrete No.3 with 40% FA and 6% SF. Therefore, the higher addition of fly ash did not contribute to the enhancement of the electrical resistance of the early age concrete. The higher the amount of fly ash added in the concrete, the more serious the delay in enhancement in electrical resistance. However, after 21 days of curing, both concrete mixtures (No. 2 and 3) achieved good results, and no significant difference in the electrical resistance was observed.

Comparing ternary concrete with only silica fume concrete, the addition of fly ash in ternary concrete weakened the electrical resistance of concrete at early ages, and this weakening was obvious during the initial 28 days after mixing. As the pozzolanic reaction started to take place, lower electrical current values in ternary binder concrete were observed at 90 days or later, than in silica fume concrete. After 90 days of moist curing, both ternary binder concrete mixtures showed lower electrical current than only silica fume concrete.

As shown in Figure 5.30, for concrete No. 4 (containing only 25% fly ash), the enhancement by fly ash could be observed 14 days after casting, compared to plain concrete No. 8. However, the enhancement in the electrical resistance of concrete is a slow time-dependent process. As shown in Figure 5.30, the curve for fly ash concrete is almost flat after 14 days. Even at 180 days, higher electrical current was observed in fly ash concrete (No. 4) than in silica fume concrete (No. 1), which indicates that 6% silica fume did contribute to more enhancement in the electrical resistance than 25% fly ash.

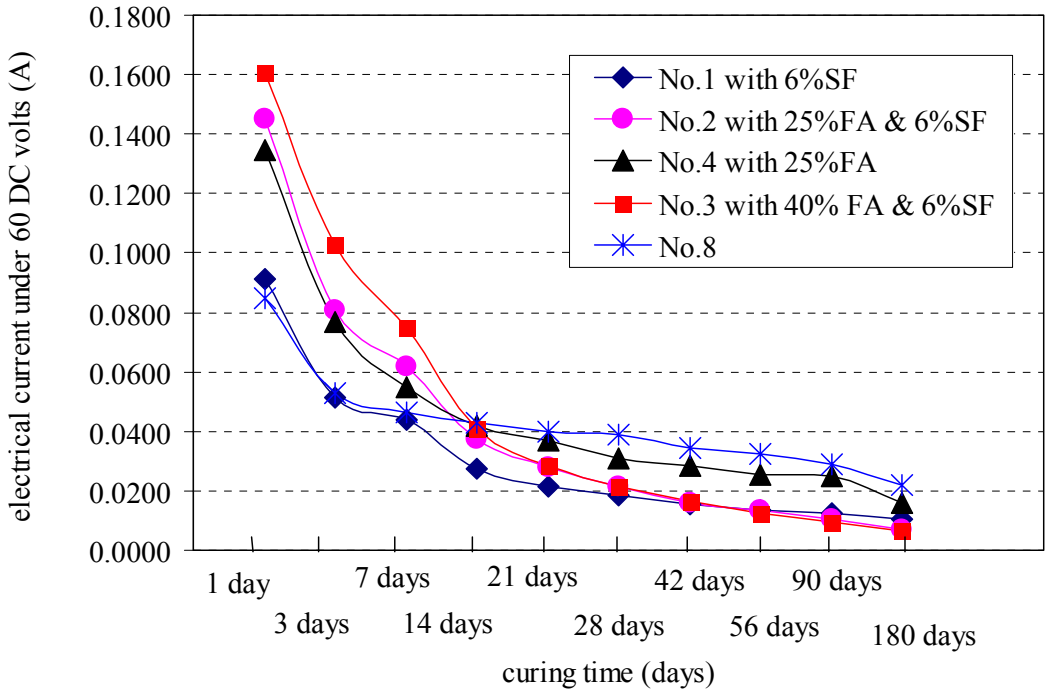


Figure 5.30: Effects of Fly Ash on Electrical Current of Concrete

5.12.4.3 Effects of slag on the electrical resistance of concrete: As shown in Table 5.24, concrete No. 9 with 25% slag showed lower electrical current than plain concrete No. 7 only at the age of 21 days or later. This suggests that the addition of slag lowered the electrical resistance of concrete before the age of 21 days, while enhancing it at later ages. However, when slag and silica fume were both added into concrete, the enhancement in the electrical

resistance due to slag can be observed as early as 14 days after mixing. Concrete with the combination of slag and silica fume achieved lower electrical current at the age of 14 days or later than concrete containing silica fume only.

As seen clearly from Figure 5.28, all the concrete mixtures showed a decrease of electrical current with age. However, the reduction rate of electrical current with age was different for different concrete mixtures. For instance, the slopes of the curves for plain concrete (No. 7 and 8) and silica fume concrete (No. 1) were steep before 7 days, and then, the curves stabilized gradually, and the electrical current showed little decrease after 28 days. However, concrete containing fly ash showed the lower reduction rate of the electrical current at 7 days or earlier than plain concrete; but from 7 days to 90 days, fly ash concrete showed a significant reduction in electrical current.

### 5.12.5. Conclusion

The electrical resistance of concrete was tested by the application of 60 volts DC, and measuring the current passing through the concrete. All the concrete mixtures, which were cured in the standard moist room, showed a decrease of the electrical current with time.

Based on the results obtained in this test, mixture No. 6 with 25% slag and 6% silica achieved the lowest electrical current 14 days or later after casting among all the concrete mixtures tested in this study. At the age of 180 days, its electrical current was only half of mixture No. 1 with 6% silica fume, and only about one third of plain concrete No. 7, and one-fourth of plain concrete No. 8.

Plain concrete No. 8 with water-binder ratio of 0.40 obtained the highest magnitude of electrical current at 14 days or later after casting among all 10 concrete mixtures.

Silica fume showed a significant enhancement on the electrical resistance of concrete after 7 days.

The effects of slag or fly ash on the enhancement of electrical resistance were also observed in this study, and the enhancement by slag occurred about 21 days or later after mixing. The enhancement by fly ash could be observed after 28 days or later. When silica fume was added in concrete, the enhancement from fly ash or slag was seen much earlier than concrete without silica fume. At 90 days or later, concrete containing both fly ash (or slag) and silica fume showed much higher electrical resistance than binary concrete containing one of these materials (slag, fly ash or silica fume).

All the optimized concrete mixtures recommended in Phase I (No. 2, No. 6 and No. 10) showed low electrical current at 90 days or later compared with other concrete mixtures.

## 5.13 Estimation of Early Age Strength of Concrete by Maturity Method

### 5.13.1 Introduction

The development of compressive strength of concrete after proper placing, consolidating and curing is a function of the degree of cement hydration and pozzolanic reactions in concrete. In the early 1950s[STP 169C, 1994], the combined effects of time and temperature were accounted for by using a maturity function to convert the temperature history to a maturity index that would be indicative of strength development. Maturity method was built based on the above idea. Maturity was defined as the product of time and temperature above the datum temperature of -10 °C (14 °F). After a relationship is established between the strength development and the temperature history for a specific concrete, the strength of concrete can be estimated by this relationship and its temperature history.

Maturity functions are mathematical expressions to convert the temperature history of concrete to an index indicative of its strength development. There are two basic types of maturity functions. The first produced a temperature-time index having units of degree-time, and this method assumes that the hydration rate is a linear faction of temperature. The other produces an equivalent age index having units of time, and this one assumes that the hydration rate obeys the exponential Arrhenius equation.

The Nurse-Saul maturity function is as follows:

$$M(t) = \Sigma(T_a - T_0)\Delta t \quad \text{.....(5.24)}$$

where:
M(t) = the temperature-time factor at age t, degree hours;
Δ(t) = a time interval, hours;
$T_a$ = average concrete temperature during time interval, Δt, °C; and;
$T_0$ = datum temperature, °C.

However, the above function does not accurately represent time-temperature effects, because this function is based on the assumption that the rate of strength development is a linear function of temperature. Therefore, the rate of cement hydration is assumed to be constant. Compared to the above function, an equivalent–age index can be computed at a specified temperature as follows (which is based on the Arrhenius equation):

$$t_e = \Sigma e^{-[Q((1/T_a)-(1/T_s))]}\Delta t \quad \text{.....(5.25)}$$

where:
t= equivalent age at a specified temperature $T_s$, hours;
Q = activation energy divided by the gas constant, K, J/(mol K).
Ta = average temperature of concrete during time interval Δt, K;
Ts = specified temperature. K; and
Δt = time interval, hours;
E = activation energy, J/mol.

6 concrete mixtures were selected for the maturity test and these concrete were: concrete No. 2, 3, 6, 7, 8, and No. 10. The proportions of all these concrete mixtures were shown in Table 5.3. The Nurse-Saul maturity function was used to calculate the maturity index in this study. The datum temperature for the Nurse-Saul function was taken as a traditional value of – 10 °C.

### 5.13.2 Sample Preparation

The maturity of concrete was determined in accordance with ASTM C 1074 (Standard Practice for Estimating Concrete Strength by the maturity Method). Concrete cylinders with a size of 100 mm x 200 mm were used for this test. One thermocouple was placed in the cylinder. In addition, three concrete cylinders for the determination of compressive strength at each test age were also cast during this test, three early ages were selected for this test: 1 day, 3 days, and 7 days.

### 5.13.3 Test Procedure

5.13.3.1 Determination of Compressive strength: After casting, concrete cylinders were covered with plastic caps immediately. After demolding, the concrete cylinders were removed into the standard moist curing room until the test age (1 day, 3 days and 7 days). Compressive strength of concrete specimens were determined in accordance with ASTM C 39 (Standard Test Method for Compressive Strength of Cylindrical Concrete Specimens).

5.13.3.2 Temperature measurement: One thermocouple was placed in the mid-depth of each cylinder for the temperature measurement. The temperature history of the cylinders was recorded from the time of concrete placement until an age of 7 days. The temperature history of all the concrete specimens was recorded using a Campbell Scientific, Inc. CR10X Measurement and Control System. The system was programmed to measure the temperature at each thermocouple every minute and record the average temperature every 10 minutes.

### 5.13.4 Results and Discussion

5.13.4.1 Early age compressive strength

Table 5.26 shows the summary of early age compressive strength of concrete up to 7 days. Concrete No. 7 achieved the highest amount of early age compressive strength at the age of 1 day, 3 days and 7 days. Concrete No. 3 had the lowest compressive strength at 1 day, 3 days and 7 days.

Table 5.26: Summary of Early Age Compressive Strength of Concrete

| Mix No. | W/B | Binder | | | Compressive strength (psi) | | |
|---|---|---|---|---|---|---|---|
| | | FA | SF | Slag | | | |
| | | % | % | % | 1 day | 3 days | 7 days |
| 2 | 0.4 | 25 | 6 | 0 | **1976** | **3767** | **5000** |
| 3 | 0.4 | 40 | 6 | 0 | **1141** | **2639** | **4178** |
| 6 | 0.4 | 0 | 6 | 25 | **2122** | **3952** | **5504** |
| 7 | 0.35 | 0 | 0 | 0 | **2958** | **5305** | **6512** |
| 8 | 0.4 | 0 | 0 | 0 | **2241** | **3952** | **4602** |
| 10 | 0.35 | 25 | 0 | 25 | **1432** | **3767** | **5504** |

5.13.4.2 Measurement of Maturity of Concrete

The temperature history was recorded by the thermocouple placed in the concrete cylinders, and Figure 5.31 shows the temperature history of concrete No.2, no. 7 and No.10. The temperature history was used to calculate the cumulative temperature-time factor using the Nurse-Saul function (Equation 5.24) with a datum temperature of –10 °C. The results of cumulative temperature-time factors were shown in Table 2. As shown in Table 5.27, Concrete No. 7 had the highest amount of temperature–time factor, and Concrete No. 3 had the lowest value.

Table 5.27: Maturity Indexes of Concrete

| Mix. No. | Average temeraptuer-time factor (°C-hr) | | |
|---|---|---|---|
| | 1 days | 3 days | 7 days |
| No. 2 | 863 | 2319 | 5208 |
| No.3 | 867 | 2325 | 5200 |
| No.6 | 858 | 2303 | 5142 |
| No.7 | 894 | 2523 | 5478 |
| No.8 | 871 | 2316 | 5185 |
| No.10 | 858 | 2464 | 5430 |

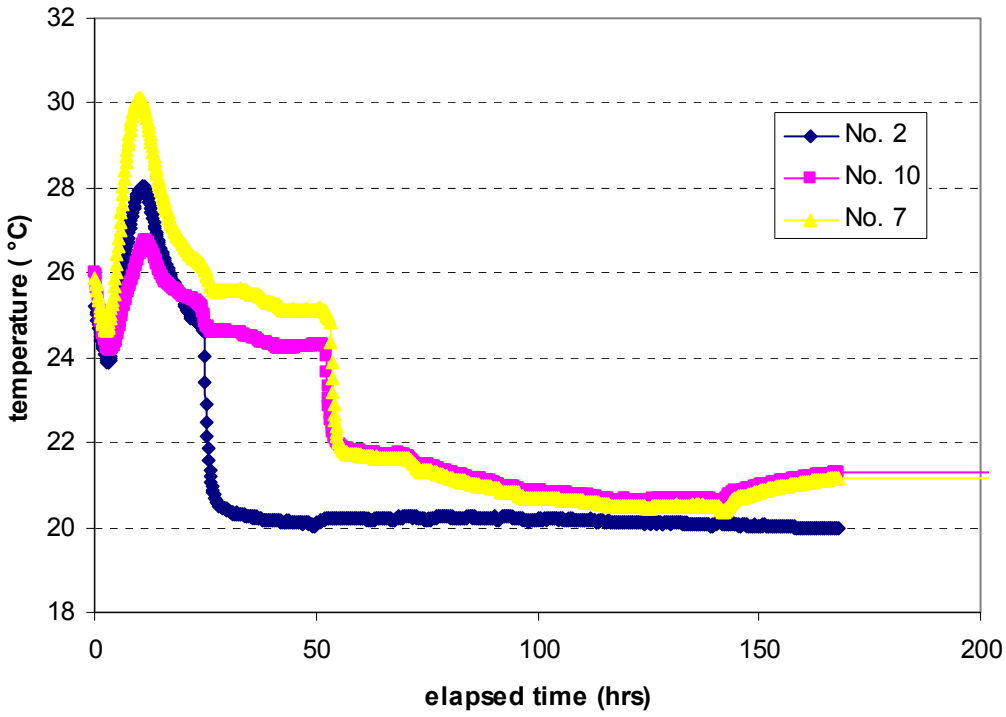


Figure 5.31: Temperature History of Concrete with Elapsed Time

15.13.4.3 Relationship between the Maturity Index and the Development of Strength

The relationship between the strength and maturity was determined from the maturity indexes and the average compressive strength. There are many forms of the strength-maturity relationship, however, this following semi-logarithmic function can be used to link the maturity indexes with compressive strength [STP 169C, 1994]. This is generally a reasonable approximation for strength development between one day and 28 days under standard room temperature curing:

$$S_m = a + b \log M \quad \text{.....(5.26)}$$

where:
Sm = compressive strength at M;
M = maturity index;
a,b = regression constant;

The relationships between the compressive strength of concrete and maturity index are shown in Figures 5.32 to 5.37. As shown in these figures, all corresponding coefficients for determination ($R^2$) value for each relationship are very high (close to 1.0), which indicates that form of the strength-maturity relationship (shown in Equation 5.26) worked well in this study. Through these relationships between strength and maturity built here, compressive strength of these concrete can be estimated by measuring the temperature history.

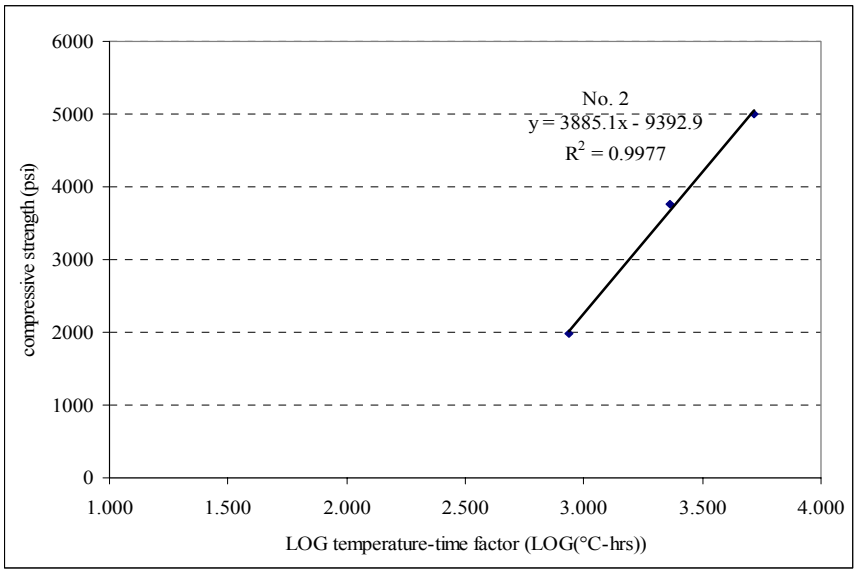


Figure 5.32: Compressive Strength of Concrete No. 2 versus LOG(temperature-time factor)

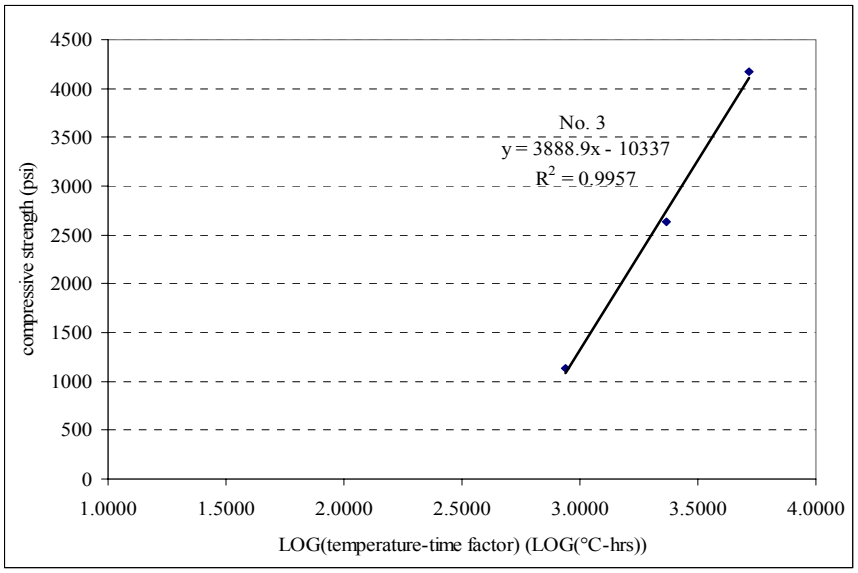


Figure 5.33: Compressive Strength of Concrete No. 3 versus LOG(temperature-time factor)

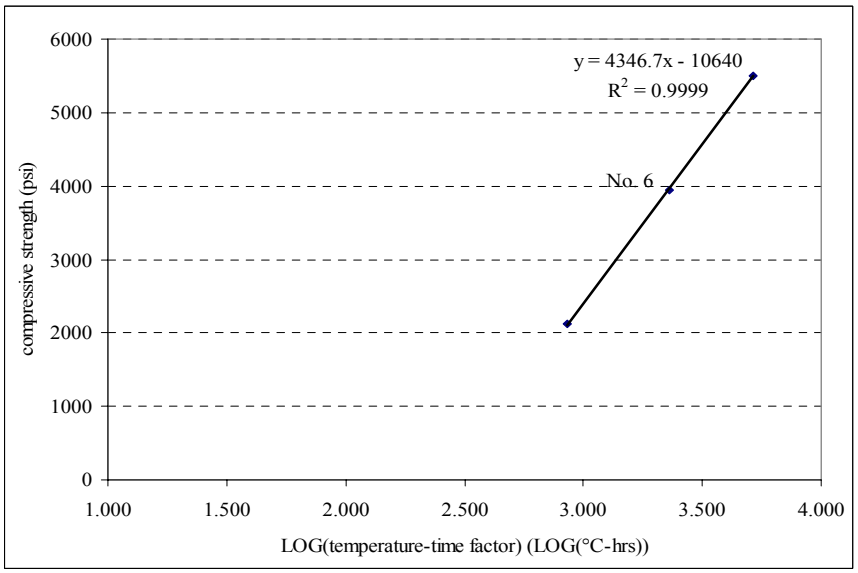


Figure 5.34: Compressive Strength of Concrete No. 6 versus LOG(temperature-time factor)

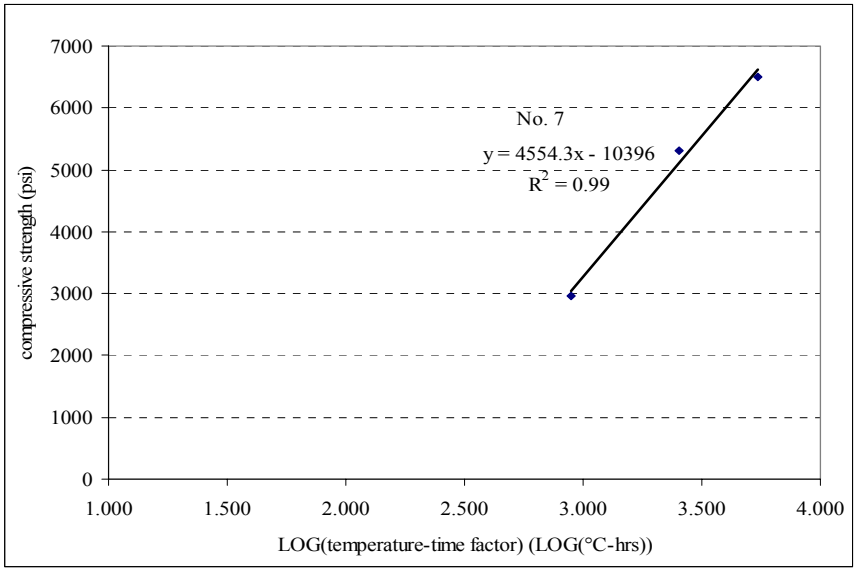


Figure 5.35: Compressive Strength of Concrete No. 7 versus LOG(temperature-time factor)

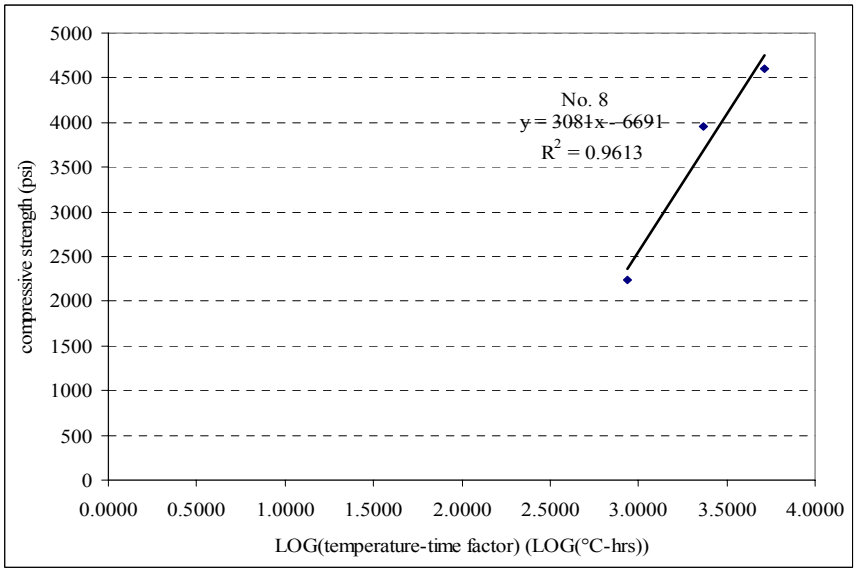


Figure 5.36: Compressive Strength of Concrete No. 8 versus LOG(temperature-time factor)

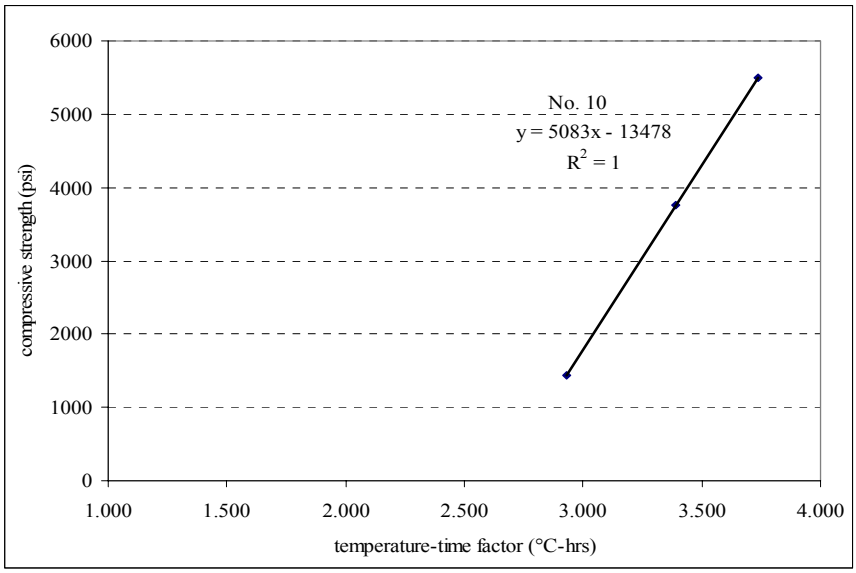


Figure 5.37: Compressive Strength of Concrete No. 10 versus LOG(temperature-time factor)

## 5.14 Effects of Curing on the Properties of HPC

### 5.14.1 Introduction

Curing is the critical process to achieve the designed properties of concrete during concrete construction process. The function of proper curing is to ensure that cement can get enough water to hydrate as much as possible during curing period, and the second function is to reduce the shrinkage of the concrete structure to avoid cracking caused by too much of plastic shrinkage, drying shrinkage or other type of shrinkage.

In general, three common types of shrinkage often occur in high performance concrete structure: plastic shrinkage because of the use of supplementary materials and low water/binder ratio; autogenious shrinkage caused by cement hydration; drying shrinkage caused by water loss of concrete structure.

Proper curing should be chosen for the concrete mixture containing optimized binder combinations during Phase II of the study, in order to achieve the enhanced properties of hardened concrete. Current curing procedures are specified for normal concrete, however, as high performance concrete mixtures are recommended in this study, proper curing procedure will be developed in order to prevent plastic shrinkage cracking and early age cracking and also to ensure the achievement of the designed properties of concrete.

To evaluate the effects of curing on the properties of HPC, the following parameters were evaluated:

- Rapid chloride ion permeability (ASTM C 1202);
- Drying shrinkage (ASTM C 157);
- Resistance to potential early age cracking (AASHTO PP34);

During this study, the restrained shrinkage cracking behavior of optimized concrete mixtures (concrete mixtures: No. 2, No. 6, No. 10 and control mixture No. 7) was examined experimentally.

### 5.14.2 Sample Preparation

The mixture proportions by weight of the selected four concrete are shown in Table 5.28.

Table 5.28: Proportion Parameters of Concrete Mixtures (by Weight)

| Mix No. | W/B | Binder | | | | | | | | Aggregate | | |
|---|---|---|---|---|---|---|---|---|---|---|---|---|
| | | FA (%) | SF (%) | Slag (%) | FA (kg/m$^3$) | SF (kg/m$^3$) | Slag (kg/m$^3$) | Portland cement (kg/m$^3$) | Total binder (kg/m$^3$) | Coarse (kg/m$^3$) | Fine (kg/m$^3$) | water (kg/m$^3$) |
| 2 | 0.4 | 25 | 6 | 0 | 97.5 | 23.4 | 0 | 269 | 390 | 1049 | 669 | 156 |
| 6 | 0.4 | 0 | 6 | 25 | 0 | 23.4 | 97.5 | 269 | 390 | 1049 | 677 | 156 |
| 7 | 0.35 | 0 | 0 | 0 | 0 | 0 | 0 | 390 | 390 | 1049 | 743 | 137 |
| 10 | 0.35 | 25 | 0 | 25 | 97.5 | 0 | 97.5 | 195 | 390 | 1049 | 723 | 137 |

Type I Portland cement was used in all the mixtures, crushed limestone with a maximum size of 1.0 inch was used as coarse aggregate, and natural river sand was used. The amount of coarse aggregate was kept the same as 1049 kg/m$^3$ in all air-entrained concrete mixtures. The total designed air content is 6.5% by volume of concrete. As supplementary materials were added in concrete to replace the same amount of Portland cement by weight, the amount of sands by weight was adjusted to achieve the same yield of concrete after the replacement of Portland cement by supplementary materials. Densified silica fume (produced by W. R. Grace & Co.) was used, and American fly ash (Class C) was also used in this study. High range water reducer (DARACEM 19) and air–entraining agent (DARAVAIR 1400) were used, and these two products are manufactured by W. R. Grace & Co.

All concrete mixtures were mixed in the vertical axis mixer. The surface of the mixer was wetted before mixing to ensure the accurate water-binder ratio value in the mixture as desired. First coarse aggregate and sand were placed into the mixer, and then cement and other mineral admixtures. All these materials were mixed 5 minutes before any water was added in the mixer. Water, along with the whole air-entraining agent was added in the mixture, and then half of the water was added in the following step, and high range water reducer was also added with the left water to achieve the 5 – 7 inches slump, and 6 - 7% air content of concrete. All the specimens were cast in two layers, (three metal rings for restrained shrinkage, 6 cylinders for rapid chloride permeability). The specimens were covered with the membrane sheet using wet burlap on the top of the membrane after finishing until demolding.

### 5.14.3. Experimental Procedure

5.14.3.1. Resistance to Potential Early Age Cracking of HPC: For the restrained shrinkage-cracking test, a ring type of specimen was used in this study, and AASHTO PP34-98 (Standard Practice for Estimating the Crack Tendency of Concrete) was followed during the test with modification related to sealing of the outer side of the specimen as described in the next paragraph. During this test, measurement of the strain was taken in the inside of steel ring as a surrounding concrete ring shrinks. The objective of this test was to determine the effects of different curing duration and also concrete mixtures containing pozzolanic materials on the relative likelihood of early age cracking tendency. Only concrete mixtures with less possibility to crack would be selected as an optimized concrete in terms of cracking tendency.

A PVC tube was used as an outer mold. The steel ring and the PVC ring were placed concentrically on a wooded base with membrane sheet on the top. Four uniformly distributed strain gages were bonded in the mid-height location on the interior side of the steel ring. The outside form of concrete rings is removed at the age of 24 hours, and the ring was slid slightly to break the specimen free from the base form support. Aluminum tape was also used to seal the outer circumferential surface of the concrete and the top and bottom surface were kept exposed to the air environmental condition, in order to achieve the uniform drying strain along the height of the concrete specimen. After the wet burlap-curing period ended, concrete rings were moved into the drying chamber room at the temperature of 20°C and relative humidity 50% (RH). Three different curing periods were studied: no curing after demolding, 2-day wet burlap curing after demolding, and 6-day wet burlap curing after demolding. The initial strain

reading was recorded immediately after the concrete rings were moved into the drying room. In the following testing days, Switch and Balance units were used to acquire the strain value from each strain gage until concrete was 28 days old. Simple visual inspection was made to locate any cracking if occurred. Figure 5.38 shows the set-up of the concrete ring test.


Figure 5.38: Set-up of Concrete Ring Test

5.14.3.2. Rapid Chloride Ion Permeability at 28 Days: Two cylinder specimens (4" dia. x 8" high) were cast for rapid chloride ion permeability test per each curing condition. Three different curing periods were studied: no curing after demolding, 2-day wet burlap curing after demolding, and 6-day wet burlap curing after demolding. When the curing ended, specimens were moved into the drying room at the temperature of 20°C and relative humidity of 50 % (RH) until 28 days.

5.14.3.3. Drying shrinkage: Two prismatic specimens (3" x 3" x 111/4") were prepared for the measuring drying shrinkage of concrete mixture per each curing condition. When the curing ended, the specimens were moved into the drying room at the temperature of 20 °C and relative humidity of 50% (RH).

### 5.14.4 Results and Discussion

Table 5.29 shows the summary results of 28-day RCP values of concrete subjected to different curing regimes. No. 2 and No. 6 showed that moist curing after demolding is necessary to achieve the desired RCP value at 28 days. Longer moisture curing continuously enhances the reduction of RCP value at 28 days. As for the No.10 mixture, the results showed that an additional 2 days moisture curing after demolding is still not sufficient to ensure that the mixture achieves the desired RCP value, and a little longer time is needed compared with the No. 2 and No. 6 mixtures. The RCP value of No.10 after 7 days curing was much lower than those after 3 days curing period, which means 7 days or longer curing is necessary for No.10 mixture. After 3 days or 7 days moist curing, No. 2, No. 6, and No.10 concrete showed much lower RCP values at 28 days than No. 7 concrete. For concrete No. 7, the longer moisture curing did not greatly help to reduce the RCP value.

Table 5.29: Summary Results of RCP Values of Concrete after Different Curing Time

| Mix No. | W/B | Binder | | | RCP value (Coulombs) | | | RCP value at 28 days | | |
|---|---|---|---|---|---|---|---|---|---|---|
| | | FA | SF | Slag | Moist curing unitl testing | | | Wet burlap curing time | | |
| | | % | % | % | 28days | 56days | 180 days | 0 day | 2 days | 6 days |
| 2 | 0.4 | 25 | 6 | 0 | 1851 | 1252 | 689 | 3396 | 2228 | 1380 |
| 6 | 0.4 | 0 | 6 | 25 | 1278 | 511 | 679 | 1416 | 1282 | 1069 |
| 7 | 0.35 | 0 | 0 | 0 | 3491 | 2708 | 1931 | 4222 | 4152 | 3579 |
| 10 | 0.35 | 25 | 0 | 25 | 2025 | 1271 | 709 | 5502 | 3159 | 2519 |

Table 5.30 shows the summary results of drying shrinkage of concrete mixtures after three different moist curing times before the start of drying. The drying shrinkage of concrete mixtures decreased as the moist curing time increased. Compared to the drying shrinkage value after 2 days' moist curing, the reduction in 56-day drying shrinkage after 27 days' moist curing is about 40 to 50% for the optimum mixtures. As the moist curing time increased from 2 days to 6 days, the drying shrinkage of specimens after 56 days' drying period decreased about 55 to 110 microstrain. In order to achieve low value of drying shrinkage, the long moist curing time is needed.

Table 5.30: Summary of Drying Shrinkage of Concrete Mixtures after Different Curing Time

| Mix No. | Drying shrinkage (microstrain) | | | | | |
|---|---|---|---|---|---|---|
| | 28days in water | 1 day | 3 days | 7 days | 28 days | 56 days |
| No.2-3 | 40 | -140 | -240 | -390 | -570 | -620 |
| No.2-7 | 45 | -115 | -235 | -365 | -495 | -525 |
| No.2-28 | 70 | -7 | -70 | -173 | -287 | -333 |
| No.6-3 | 40 | -105 | -265 | -385 | -545 | -570 |
| No.6-7 | 30 | -85 | -185 | -290 | -440 | -460 |
| No.6-28 | 60 | -3 | -53 | -113 | -263 | -310 |
| No.10-3 | 40 | -60 | -150 | -290 | -475 | -535 |
| No.10-7 | 60 | -40 | -140 | -280 | -430 | -480 |
| No.10-28 | 77 | -23 | -80 | -137 | -280 | -303 |

Summary results of restrained drying shrinkage of concrete mixtures after different moist curing time are shown in Figure 5.39. Since the size of concrete ring specimens is different from that for free shrinkage, the value measured from concrete ring is different from free shrinkage. As shown in Figure 5.39 and Table 5.30, the restrained drying shrinkage is much lower than that from free drying shrinkage, for the concrete in the ring test was restrained from metal during the drying procedure. During the test for the determination of potential early age cracking, daily observation of the concrete ring was made to find whether there is any cracking or not on the concrete surface. In all the concrete ring specimens from mixtures (No. 7. No. 10, No. 2 and No. 6), no cracking was found during the test after demolding until the age of 40 days. The restrained drying shrinkage of concrete mixtures No. 7 and No. 10 is shown in Figure 5.40. As shown in Figure 5.39 and Figure 5.40, the restrained drying shrinkage of concrete specimens decreased with the moist curing time increased. For concrete No. 6, compared to the restrained shrinkage after the curing of one day, the value after 3 days' moisture curing decreased about 30 microstrains. It should be stated that the longer curing not only helps to reduce the drying shrinkage of concrete exposed to the drying environmental condition, but also to prevent concrete from the early age cracking due to the drying process.

Based on the research [Weiss, et al., 2001], the residual stressed developed in the concrete could be calculated in terms of the size of the metal ring and concrete specimen, modulus of elasticity of steel and the restrained drying shrinkage. The summary of residue stressed calculated are shown in Figure 5.41 to 5.37, and the split tensile strength is also shown for each concrete. As shown in Figure 5.41, longer moist curing than 3 days is needed to avoid the cracking of concrete No. 2 due to the restrained drying shrinkage. As shown in 5.35, moist curing is required for concrete No. 6 after demloding, and 3 days or longer moist curing can prevent the cracking due to restrained drying shrinkage. As shown in Figure 5.43, 3 days or longer moist curing is needed to prevent the cracking due to the restrained drying shrinkage for concrete No. 10. Based on the results of ring test, moist curing is not required to avoid the cracking due to the restrained drying shrinkage.

In order to ensure the achievement of low permeability, and low drying shrinkage, and avoiding the early age cracking of concrete due to the restrained drying shrinkage, moist curing is needed for these four concrete: 3 days or longer moist curing is needed for concrete mixtures No. 2, No. 6; and 7 days or longer moist curing is needed for concrete No. 10. As to concrete No. 7, RCP value at 28 days after 7 days' moist curing was still very high (higher than 3500 Coulombs), although the result of restrained ring test did not show any moist curing required to avoid the cracking.

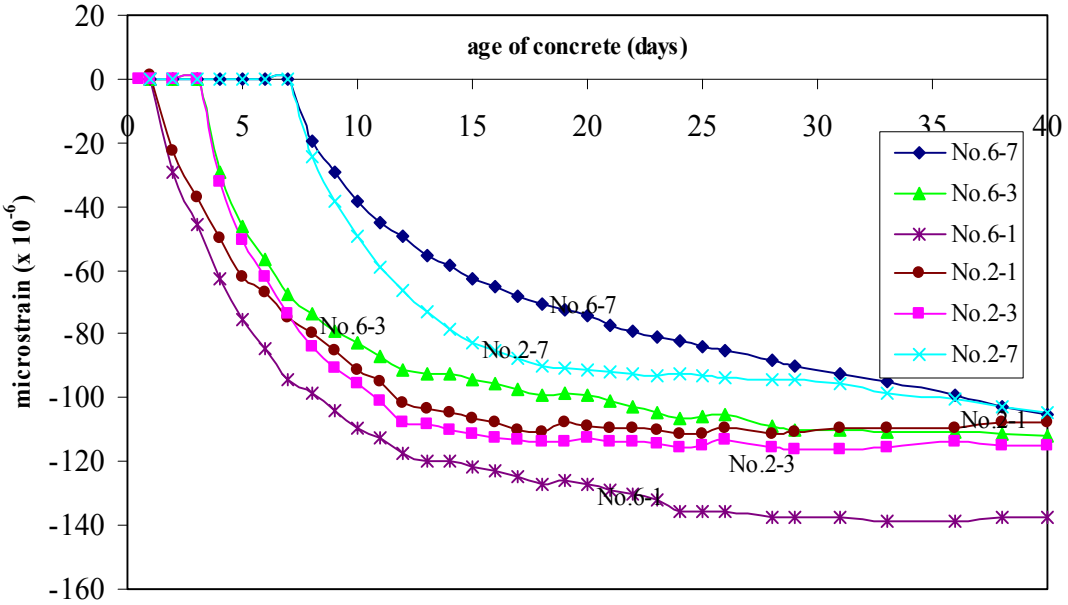


Figure 5.39: Restrained Drying Shrinkage of Mixtures No. 2 and No. 6 after Different Moist Curing Time

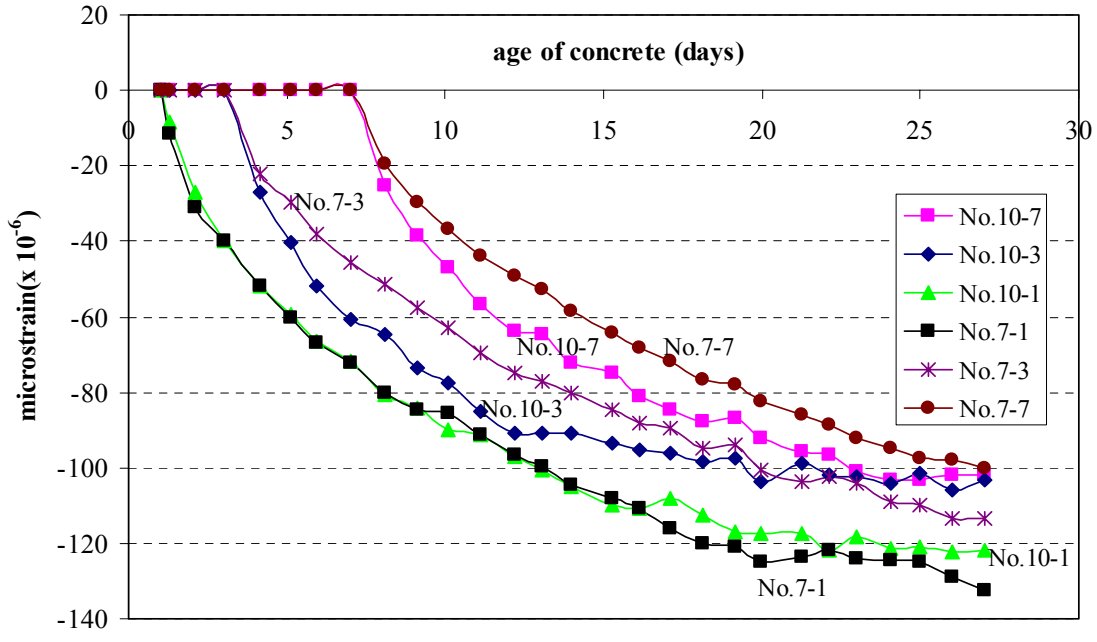


Figure 5.40: Restrained Drying Shrinkage of Mixtures No. 7 and No. 10 after Different Moist Curing Time

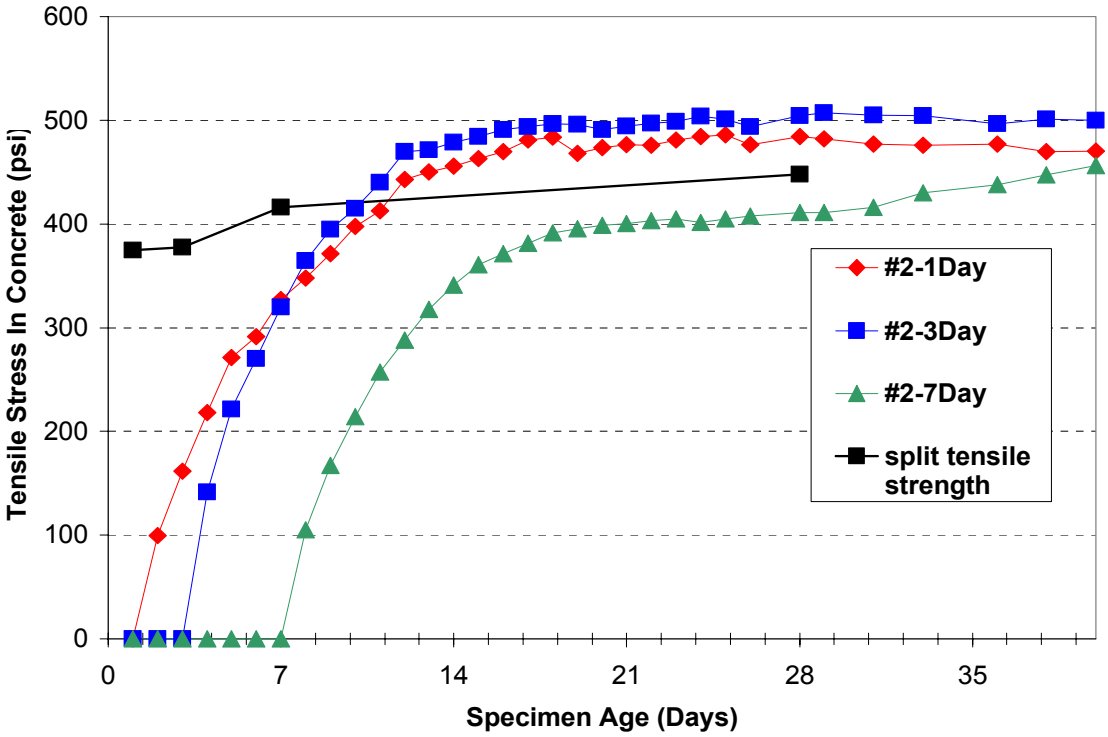


Figure 5.41: Residual Stress Developed in Concrete No. 2 with Ages

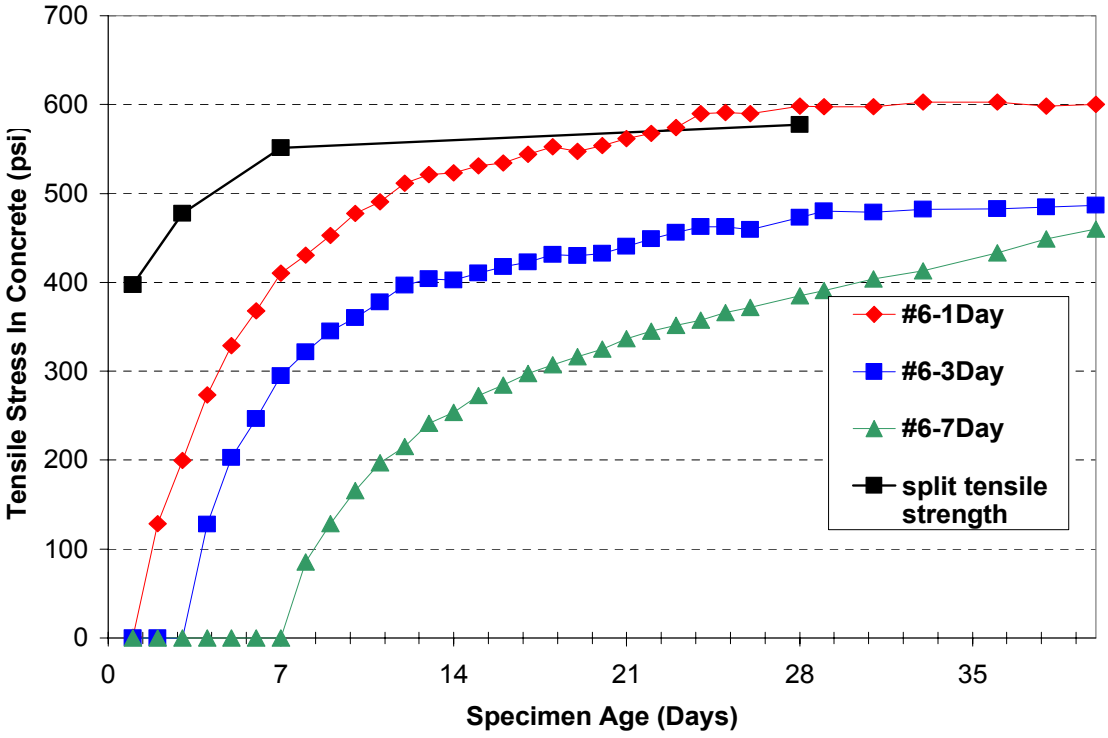


Figure 5.42: Residual Stress Developed in Concrete No. 6 with Ages

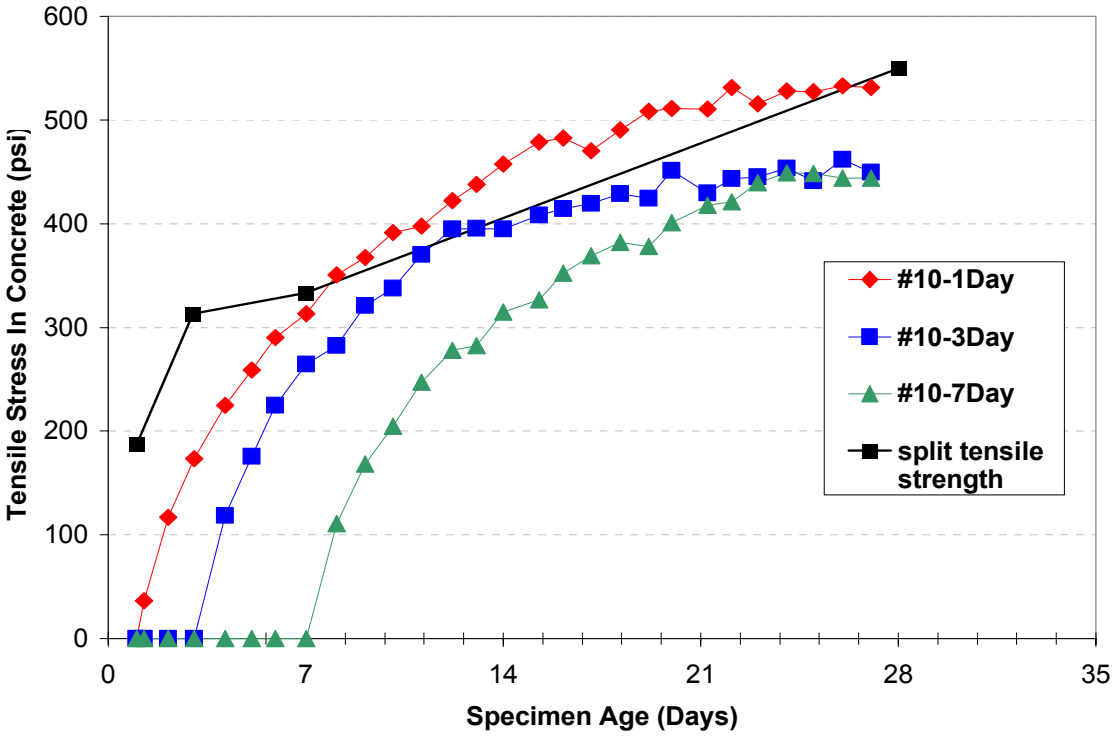


Figure 5.43: Residual Stress Developed in Concrete No. 10 with Ages

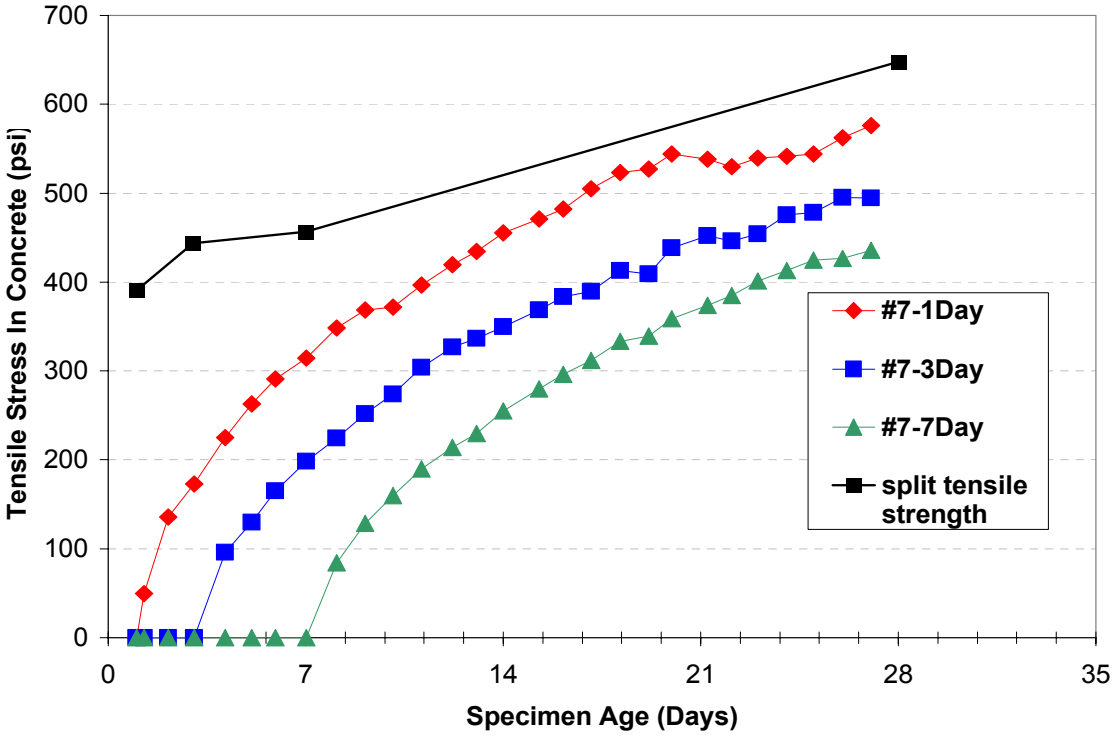


Figure 5.44: Residual Stress Developed in Concrete No. 7 with Ages

# 6 EVALUATION OF DIFFUSION COEFFICIENT OF HPC

## 6.1 Evaluation of Diffusion Coefficient from Ponding Test

### 6.1.1 Introduction

One of the common methods to delay the corrosion of steel bar is the application of high performance concrete in bridge decks. Due to the low permeability of high performance concrete, the chloride ions from external sources take a long time to arrive at the steel bar so that the initiation of the corrosion is postponed significantly. Other methods can be also used to increase the service life of the reinforced structure, such as the use of corrosion inhibitors, epoxy coated steel, cathodic protection, or non-ferrous reinforcement (fiber or glass reinforcement), membranes to protect the exposed surface of concrete structure, and so on. However, for concrete bridge decks, improvement of the permeability of concrete is one of the most effective means to prevent or postpone the corrosion of steel bar in concrete. In this study, high performance concrete with enhanced properties is applied in the construction of bridge decks, in order to extend the service life of bridge decks.

The concrete cover provides a physical and chemical barrier to corrosion. The chemical barrier means the high alkalinity of the concrete pore solution, which has pH value of about 13. A permanent protective passivating film forms on the surface of steel, and this film is maintained in the alkaline environment condition. This high alkalinity provides thus a good protection of the steel in concrete to chloride attack. The physical barrier is the impermeability of the concrete cover, which not only limits the diffusion of external chloride ions into concrete, but also limits the diffusion of oxygen toward the steel, which slows down the corrosion rate even after the initiation of corrosion of steel in concrete.

The corrosion process of the steel in concrete actually involves two separate chemical reactions, which take place simultaneously at two different sites on the steel surface. These two sites are called the anode and cathode. Corrosion of steel takes place only when an electrical current exists between the cathode and anode. The electric current contains two parts; one part is the ionic current passing through the concrete, the other is the electronic current through the steel. The electric current must flow in a closed loop between the two sites, as indicated in Figure 6.1 [Bentur et al., 1997].

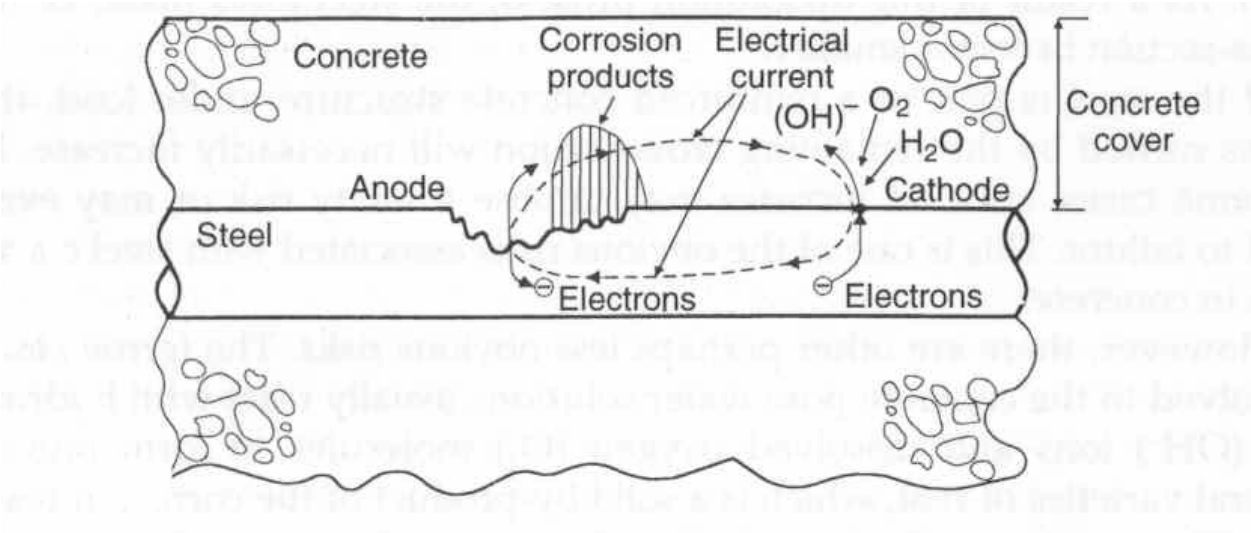


Figure 6.1. Corrosion Processes on the Surface of Steel [Bentur et al., 1997]

There are two reactions in the corrosion processes, which are known as anodic and cathodic reactions:

Anodic reaction:

$2\,Fe^{0}$ — 4 electrons $\rightarrow$ $2Fe^{2+}$ ……(6.1)

metallic atoms at the steel surface — ions dissolved in solution

Cathodic reaction:

$O_2 + 2\,H_2O + 4$ electrons $\rightarrow$ $4(OH^-)$ ……..(6.2)

Dissolved oxygen molecules — ions dissolved in solution

The ferrous ($Fe^{2+}$) and hydroxide ($OH^-$) ions flow towards one another. When they meet, they react to form ferrous hydroxide, $Fe(OH)_2$, and also produce, $Fe(OH)_3$. In general, the volume of rust produced in a corrosion reaction is at least twice the volume of the dissolved steel [Bentur et al., 1997]. Therefore, rust formation involves a substantial volume increase, which will generate an expansive stress in concrete, and this stress can be high enough to cause cracking in the concrete cover. Because of the dissolution of the steel, the cross section of reinforced steel decreases during the corrosion, which weakens the load capacity of concrete structures rapidly.

### 6.1.2 Research Need and Objectives

The penetration of chloride ions into concrete takes place only through the aqueous solution within the concrete pores. In order to estimate the resistance of concrete to chloride penetration quantitatively, AASHTO T 259 and 260 are used to determine the diffusion coefficient of chloride ions in concrete structures. Ten air-entrained concrete mixtures have been tested in this study, and the effects of mineral admixtures such as fly ash, slag and silica fume on the diffusion coefficient of concrete are investigated. Efforts are also made to develop correlations between the diffusion coefficient from ponding test and the diffusion coefficient from migration test, so that the diffusion coefficient of concrete can be evaluated from the diffusion coefficient from migration test.

### 6.1.3 Sample Preparation

The resistance to chloride ion penetration of concrete was evaluated in accordance with AASHTO T 259 (Standard Method of Test for Resistance of Concrete to Chloride Ion Penetration). Two concrete slabs (10 x 15 x 3 in) were used for each concrete mixture, and total of 20 slabs were prepared in this study. After 14 days of the moist curing, the specimens were stored for another 14 days in the drying room at a temperature of 20°C and relative humidity of 50%. At the age of 29 days, the slab surfaces were abraded using a steel brush. After the abrasion process, all the slabs were returned back to the drying room for an additional 13 days (until the age of 42 days). Rubber was used around the side surface of the slabs to build the embankment for holding the solution on the exposed surface of slabs.

Concrete slabs were ponded by a 3% sodium chloride solution by mass for 90 days. In order to retard the evaporation of solution, glass plates were used to cover the top of the concrete. Additional solution was added periodically during the 90 days ponding period, in order to maintain a height of 13 mm. After 90 days of ponding, the solution was removed from the slab surface, the slabs were dried, and a steel brush was used to remove any visible salt crystals on the ponded surface of the slabs.

### 6.1.4 Test Procedure

After 90-day ponding, a cylinder with the diameter of 2 inches was cored from the center of the slab, and total of 20 cylinders were obtained from testing. All the cylinders were oven-dried at a temperature of 105°C for 72 hours before slicing. Air-cooled plate was used to slice the cylinders. The thickness of each slice was about half an inch, and five or six slices were cut per cylinder.

All the concrete slices were pulverized until the powder sample passed the No. 50 sieve. Potentiometric titration method was used to determine acid soluble chloride ion content in this study. INDOT Materials and Testing Division helped to complete the analysis for chloride ion content of powder samples.

### 6.1.5 Chloride Ion Concentration Profile

Table 6.1 shows the chloride ion concentration profile with depth after 90 days ponding for 10 concrete mixtures. About one tenth of an inch was abraded from the ponding surface before slicing. As shown in Table 6.1, chloride ion content for the top layer varied from 8.83 to 18.81 $kg/m^3$ of concrete. Chloride content in the other layers dropped quickly, and reached baseline content at the depth of one inch or more. During this study, the average of the chloride ion contents for $4^{th}$, $5^{th}$ and bottom layer from the same sample was treated as the baseline chloride ion content for concrete mixtures. As shown in Table 6.1, chloride ion content at the bottom layer from No.10 concrete was unusually high, which was probably caused by the leakage of salt solution from the side of the slab during the ponding test. Since the depth of each slice was different from the others, and chloride ion content in concrete changes with depth significantly, it was difficult to compare the chloride content for one concrete with others directly.

The procedures, described in section 6.1.6, were used in this study to determine the diffusion coefficient of concrete mixtures and surface concentration of chloride ions in the ponded slabs.

Table 6.1: Chloride Ion Content Profile for Phase II 10 Mixtures

| Mix No. | | | Top layer | 2nd layer | Third layer | 4th layer | 5th layer | bottom layer |
|---|---|---|---|---|---|---|---|---|
| No.1 | Slab 1 | Thickness * | 0.43 | 0.52 | 0.58 | 0.46 | 0.53 | 0.58 |
| | | Depth to center point ** | 0.215 | 0.69 | 1.24 | 1.76 | 2.255 | 2.81 |
| | | Chloride content *** | 15.02 | 0.6 | 0.45 | 0.48 | 0.44 | 0.48 |
| | Slab 2 | Thickness | 0.52 | 0.37 | 0.51 | 0.47 | 0.68 | 0.55 |
| | | Depth to center point ** | 0.26 | 0.705 | 1.145 | 1.635 | 2.21 | 2.825 |
| | | Chloride content *** | 13.76 | 1.51 | 0.44 | 0.42 | 0.5 | 0.46 |
| No.2 | Slab 1 | Thickness | 0.48 | 0.54 | 0.48 | 0.52 | 0.5 | 0.56 |
| | | Depth to center point ** | 0.24 | 0.75 | 1.26 | 1.76 | 2.27 | 2.8 |
| | | Chloride content *** | 14.75 | 0.91 | 0.4 | 0.43 | 0.44 | 0.46 |
| | Slab 2 | Thickness | 0.52 | 0.53 | 0.52 | 0.58 | 0.5 | 0.5 |
| | | Depth to center point ** | 0.26 | 0.785 | 1.31 | 1.86 | 2.4 | 2.9 |
| | | Chloride content *** | 15.35 | 1.12 | 0.57 | 0.46 | 0.45 | 0.59 |
| No.3 | Slab 1 | Thickness | 0.34 | 0.27 | 0.34 | 0.28 | 0.58 | |
| | | Depth to center point ** | 0.17 | 0.475 | 0.78 | 1.09 | 1.52 | |
| | | Chloride content *** | 13.66 | 4.13 | 1.48 | 0.48 | 0.41 | |
| | Slab 2 | Thickness | 0.29 | 0.29 | 0.29 | 0.22 | 0.4 | |
| | | Depth to center point ** | 0.145 | 0.435 | 0.725 | 0.98 | 1.29 | |
| | | Chloride content *** | 18.81 | 5.76 | 1.01 | 0.47 | 0.5 | |
| No.4 | Slab 1 | Thickness | 0.37 | 0.34 | 0.23 | 0.4 | 0.46 | |
| | | Depth to center point ** | 0.185 | 0.54 | 0.825 | 1.14 | 1.57 | |
| | | Chloride content *** | 14.55 | 2.74 | 0.55 | 0.53 | 0.35 | |
| | Slab 2 | Thickness | 0.33 | 0.23 | 0.26 | 0.36 | 0.35 | |
| | | Depth to center point ** | 0.165 | 0.445 | 0.69 | 1 | 1.355 | |
| | | Chloride content *** | 15.39 | 5.68 | 4.12 | 1.07 | 0.45 | |
| No.5 | Slab 1 | Thickness | 0.3 | 0.29 | 0.31 | 0.26 | 0.49 | |
| | | Depth to center point ** | 0.15 | 0.445 | 0.745 | 1.03 | 1.405 | |
| | | Chloride content *** | 9.81 | 2.85 | 1.37 | 0.41 | 0.47 | |
| | Slab 2 | Thickness | 0.39 | 0.36 | 0.29 | 0.4 | 0.44 | |
| | | Depth to center point ** | 0.195 | 0.57 | 0.895 | 1.24 | 1.66 | |
| | | Chloride content *** | 14.09 | 3.61 | 0.65 | 0.41 | 0.4 | |
| No.6 | Slab 1 | Thickness | 0.51 | 0.46 | 0.45 | 0.5 | 0.5 | 0.46 |
| | | Depth to center point ** | 0.255 | 0.74 | 1.195 | 1.67 | 2.17 | 2.65 |
| | | Chloride content *** | 10.21 | 1.28 | 0.43 | 0.43 | 0.49 | 0.43 |
| | Slab 2 | Thickness | 0.47 | 0.5 | 0.39 | 0.62 | 0.6 | 0.49 |
| | | Depth to center point ** | 0.235 | 0.72 | 1.165 | 1.67 | 2.28 | 2.825 |
| | | Chloride content *** | 14.73 | 0.56 | 0.4 | 0.43 | 0.45 | 0.45 |
| No.7 | Slab 1 | Thickness | 0.53 | 0.46 | 0.45 | 0.55 | 0.57 | 0.5 |
| | | Depth to center point ** | 0.265 | 0.76 | 1.215 | 1.715 | 2.275 | 2.81 |
| | | Chloride content *** | 13.59 | 2.03 | 0.42 | 0.4 | 0.44 | 0.48 |
| | Slab 2 | Thickness | 0.43 | 0.46 | 0.59 | 0.57 | 0.51 | 0.5 |
| | | Depth to center point ** | 0.215 | 0.66 | 1.185 | 1.765 | 2.305 | 2.81 |
| | | Chloride content *** | 13.93 | 1.91 | 0.47 | 0.42 | 0.55 | 0.47 |
| No.8 | Slab 1 | Thickness | 0.61 | 0.56 | 0.5 | 0.47 | 0.5 | 0.43 |
| | | Depth to center point ** | 0.305 | 0.89 | 1.42 | 1.905 | 2.39 | 2.855 |
| | | Chloride content *** | 11.46 | 2.3 | 0.45 | 0.37 | 0.44 | 0.41 |
| | Slab 2 | Thickness | 0.45 | 0.46 | 0.37 | 0.55 | 0.53 | 0.64 |
| | | Depth to center point ** | 0.225 | 0.68 | 1.095 | 1.555 | 2.095 | 2.68 |
| | | Chloride content *** | 8.83 | 2.54 | 0.55 | 0.45 | 0.4 | 0.43 |
| No.9 | Slab 1 | Thickness | 0.19 | 0.34 | 0.28 | 0.5 | 0.31 | |
| | | Depth to center point ** | 0.095 | 0.36 | 0.67 | 1.06 | 1.465 | |
| | | Chloride content *** | 17.29 | 4.54 | 1.01 | 0.43 | 0.43 | |
| | Slab 2 | Thickness | 0.26 | 0.37 | 0.33 | 0.34 | 0.51 | |
| | | Depth to center point ** | 0.13 | 0.445 | 0.795 | 1.13 | 1.555 | |
| | | Chloride content *** | 12.8 | 4.43 | 0.61 | 0.43 | 0.39 | |
| No.10 | Slab 1 | Thickness | 0.56 | 0.52 | 0.44 | 0.49 | 0.5 | 0.58 |
| | | Depth to center point ** | 0.28 | 0.82 | 1.3 | 1.765 | 2.26 | 2.8 |
| | | Chloride content *** | 9.94 | 0.79 | 0.39 | 0.42 | 0.46 | 0.88 |
| | Slab 2 | Thickness | 0.35 | 0.41 | 0.58 | 0.49 | 0.6 | 0.58 |
| | | Depth to center point ** | 0.175 | 0.555 | 1.05 | 1.585 | 2.13 | 2.72 |
| | | Chloride content *** | 14.99 | 3.12 | 1.13 | 0.62 | 0.54 | 1.08 |

* The unit of thickness of the samples in Table 6.1 is inch;

** Depth to center point is the distance from the top surface of slab to the center point of each layer, in inches;

*** The unit for chloride content is kg/m$^3$ concrete (1 lb/yd$^3$ = 0.59 kg/m$^3$).

### 6.1.6 Determination of Diffusion Coefficient

Fick's second law was used to describe the diffusion of chloride ions into concrete with time, as shown in the following equation:

$$\frac{dc}{dt} = D\frac{d^2c}{d^2x} \quad \text{.....(6.3)}$$

where:
c is the concentration of chloride at a distance x from the surface at time t;
D is the diffusion coefficient of the concrete.

When the concentration of the chloride on the external surface is constant, and the concentration C(x,t) within the concrete at a distance x, after time t can be expressed by:

$$C(x,t) = C_0 \times (1 - erf\frac{x}{2\sqrt{Dt}}) \quad \text{.....(6.4)}$$

where:
C(x, t) = the chloride content at depth x and time t, kg/m$^3$;
$C_0$ = the chloride content at the boundary surface, kg/m$^3$;
D = diffusion coefficient of concrete, m$^2$/s;
t = exposure time of concrete to chloride source, s;
x = the depth from the surface, m;
erf = the error function.

As shown in Table 6.1, each concrete slab has at least two points, where the concentration of chloride with depth is not equal to the baseline chloride content. Since the concentration of chloride on the external surface ($C_0$) is unknown in the study, Equation. (6.4) cannot be directly used to solve D value based on the concentration of chloride at one depth. A modified method was used to calculate D value and $C_0$ for each concrete slab in this test and one example for this method is shown below:

For the first slab from concrete mixture No. 2:

$$x_1 = 0.24 \quad (inch), \qquad C_1(x_1,t) = 14.75 \quad (kg/m^3) \quad \text{.....(6.5)}$$

$$x_2 = 0.75 \quad (inch), \qquad C_2(x_2,t) = 0.91 \quad (kg/m^3) \quad \text{.....(6.6)}$$

Baseline chloride content of the slab = (0.43+0.44+0.46)/3 = 0.44 (kg/m$^3$), and t = 7776000 s.

Discounting the baseline chloride content, the corrected chloride content for the above two points are:

$$C'_1(x_1,t) = 14.75 - 0.44 = 14.31 \quad (kg/m^3) \quad \text{.....(6.7)}$$

$$C'_2(x_2,t) = 0.91 - 0.44 = 0.47 \quad (kg/m^3) \quad \text{.....(6.8)}$$

Equation. (6.5), (6.6), (6.7) and (6.8) are inserted into Eq. 6.4:

$$C'_1(x_1,t) = C_0(1 - erf\frac{x_1}{2\sqrt{Dt}}) \quad \text{.....(6.9)}$$

$$C'_2(x_2,t) = C_0(1 - erf\frac{x_2}{2\sqrt{Dt}}) \quad \text{.....(6.10)}$$

Both sides of Equation. (6.9) are divided by that of Equation. 6.10:

$$\frac{C'_1(x_1,t)}{C'_2(x_2,t)} = \frac{1 - erf\dfrac{x_1}{2\sqrt{Dt}}}{1 - erf\dfrac{x_2}{2\sqrt{Dt}}} \quad \text{.....(6.11)}$$

$$\frac{14.31}{0.47}(= 30.447) = \frac{1 - erf\dfrac{0.24 \times 2.54 \times 10^{-2}}{2\sqrt{D \times 7.776 \times 10^{6}}}}{1 - erf\dfrac{0.75 \times 2.54 \times 10^{-2}}{2\sqrt{D \times 7.776 \times 10^{6}}}} \quad \text{.....(6.12)}$$

- Step 1: Assuming D = 4 x $10^{-12}$ $m^2/s$;

Based on the table of error function, the right side of Equation (6.12) is equal to 27.841.

- Step 2: Assuming D = 3.5 x $10^{-12}$ $m^2/s$, the right side of Equation (6.12) is equal to 41.076.
- Step 3: Assuming D = 3.75 x $10^{-12}$ $m^2/s$, the right side of Equation (6.12) is equal to 33.1438.
- Step 4: Assuming D = 3.85 x $10^{-12}$ $m^2/s$, the right side of Equation (6.12) is equal to 30.505.

Thus, using an iterative process to solve for D, a value of 3.85 x $10^{-12}$ $m^2/s$ is obtained.

Using this D-value in Equation (6.9), and $C_0$ = 33.297 $kg/m^3$.

Diffusion coefficient and surface concentration of chloride content for other concrete mixtures can be also calculated using the above method. Results of diffusion coefficient and surface chloride concentration for Phase II mixtures are summarized in Table 6.2. The binder combinations for 10 concrete mixtures in Phase II are shown in Table 6.3.

Table 6.2: Summary of Diffusion Coefficient and Surface Concentration of Chloride Content for Phase II Mixtures

| Mix No. | Slab No. | D-value($m^2/s$) | $C_0$ ($kg/m^3$) | $C_0$ (average) | D (average) |
|---|---|---|---|---|---|
| No.1 | No.1-1 | 2.3E-12* | 40.30 | 35.58 | 4.63E-12 |
| | No.1-2 | 4.63E-12 | 30.85 | | |
| No.2 | No.2-1 | 3.85E-12 | 33.30 | 33.50 | 4.30E-12 |
| | No.2-2 | 4.75E-12 | 33.70 | | |
| No.3 | No.3-1 | 5.13E-12 | 21.07 | 24.37 | 4.89E-12 |
| | No.3-2 | 4.65E-12 | 27.67 | | |
| No.4 | No.4-1 | 4.90E-12 | 20.44 | 21.60 | 5.30E-12 |
| | No.4-2 | 5.70E-12 | 22.76 | | |
| No.5 | No.5-1 | 4.25E-12 | 14.65 | 18.42 | 5.28E-12 |
| | No.5-2 | 6.30E-12 | 22.19 | | |
| No.6 | No.6-1 | 5.43E-12* | 20.31 | 31.70 | 2.43E-12 |
| | No.6-2 | 2.43E-12 | 43.08 | | |
| No.7 | No.7-1 | 6.90E-12 | 25.49 | 25.32 | 5.95E-12 |
| | No.7-2 | 5.00E-12 | 25.15 | | |
| No.8 | No.8-1 | 1.20E-11 | 19.35 | 16.20 | 1.09E-11 |
| | No.8-2 | 9.80E-12 | 13.05 | | |
| No.9 | No.9-1 | 2.90E-12 | 23.43 | 20.17 | 4.45E-12 |
| | No.9-2 | 6.00E-12 | 16.91 | | |
| No.10 | No.10-1 | 4.80E-12 | 21.18 | 22.39 | 4.85E-12 |
| | No.10-2 | 4.90E-12 | 23.59 | | |

* Not used in calculating D-average.

Table 6.3: Binder Combination for Phase II Concrete Mixtures

| Mix No. | W/B | Binder | | |
|---|---|---|---|---|
| | | FA | SF | Slag |
| | | % | % | % |
| 1 | 0.4 | 0 | 6 | 0 |
| 2 | 0.4 | 25 | 6 | 0 |
| 3 | 0.4 | 40 | 6 | 0 |
| 4 | 0.4 | 25 | 0 | 0 |
| 5 | 0.35 | 40 | 0 | 0 |
| 6 | 0.4 | 0 | 6 | 25 |
| 7 | 0.35 | 0 | 0 | 0 |
| 8 | 0.4 | 0 | 0 | 0 |
| 9 | 0.35 | 0 | 0 | 25 |
| 10 | 0.35 | 25 | 0 | 25 |

As shown in Table 6.2 and 6.3, plain concrete with 0.40 w/b (No. 8) had the highest value of diffusion coefficient, which is at least twice the D-values for other concrete mixtures. All the concrete mixtures containing pozzolanic materials have lower diffusion coefficient values than plain concrete with 0.35 w/b (No. 7), which indicates that the addition of pozzolanic materials in concrete mixtures increases the resistance of concrete to the diffusion of chloride ions. Among all the 10 mixtures, concrete with 6% silica fume achieved the lowest diffusion coefficient value. While, combination of fly ash with silica fume did not show the enhancement of the resistance of concrete to the diffusion of chloride ion from ponding test, combining silica fume and slag reduced the average diffusion coefficient by 50% as compared to the system containing silica fume alone.

Based on the diffusion coefficient and surface concentration of chlorides for each mixture, prediction of the chloride concentration at any depth at exposure time, t, can be made. As an example, Figure 6.2 shows the predicted concentration of chlorides with depth for concrete No. 2 with 25% fly ash and 6% silica fume.

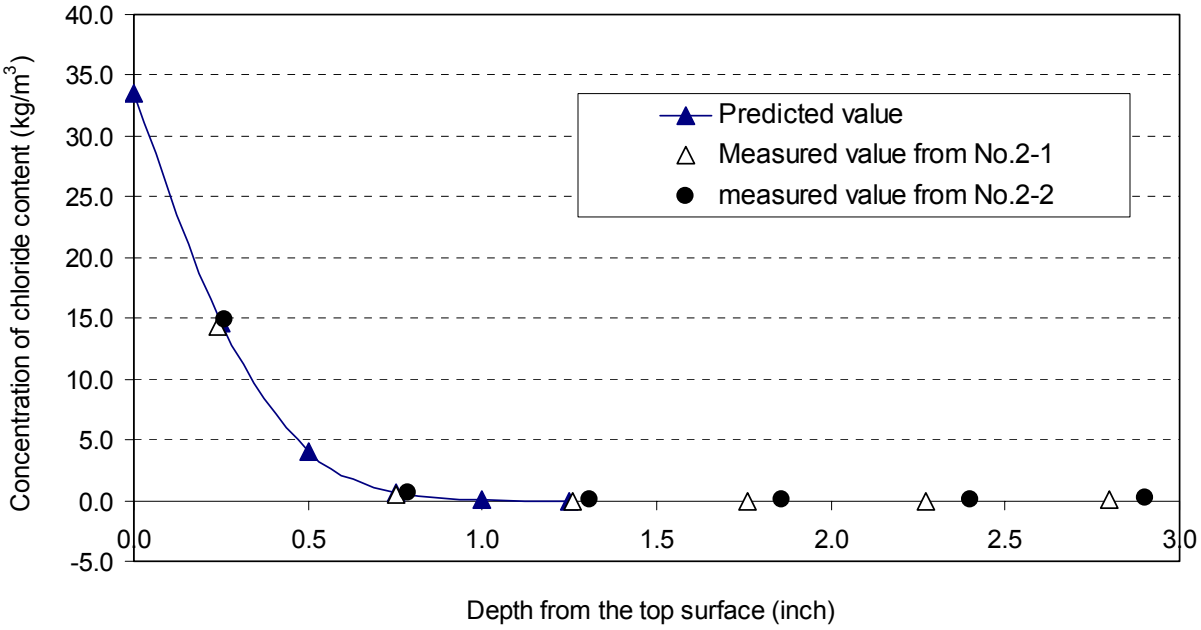


Figure 6.2: Predicted Concentration of Chloride with Depth for No. 2 Concrete (25% Fly Ash and 6% Silica Fume)

As shown in Figure 6.2, the measured and predicted concentration of chlorides with depth almost lie on the same curve, which indicates that the method used in the calculation of diffusion coefficient and surface concentration of chlorides is effective. This similar result was also found in the other 9 concrete mixtures.

### 6.2 Review of Existing Models for Predicting D-value of Concrete

The ultimate goal of the present study is to develop materials and procedures that will yield bridge structures of improved and predictable performance. To satisfy this goal, an attempt was made to develop mathematical models that could utilize actual properties of the tested material for the purposes of predicting service life and life-cycle cost of the structure. As a first step in this process, the ability of some of the existing models to predict the performance of some of the concrete bridges in Indiana was evaluated.

The model utilized for this purpose was "Life-365" model that was developed jointly by the W. R. Grace & Co. and University of Toronto. This model is currently tested and evaluated under the patronage of the existing ACI Committee 365 on Service Life Prediction. This model was used to predict the chloride profiles in two of the

existing Indiana bridges for which the actual field data were available. The two existing bridges used in the evaluation were:

Structure 27-A WB
Structure 2563 - both southbound (SB) and northbound (NB) directions.

Both structures were constructed in central Indiana more than 10 years ago. Unfortunately, the original contract information has been destroyed and the actual information on mix composition was not available. In order to be able to run the model, it was therefore necessary to assume the value for w-c ratio. That value was assumed to be 0.443, which is the maximum value for w/c allowed for Indiana bridges under INDOT specifications. The SB lane of structure 2563 was an experimental structure build with DCI corrosion inhibitor.

Figure 6.3 shows both the actual and the predicted chloride profiles (chloride content vs. depth) for bridge 27-A WB. It can be seen that the estimated amount of chloride in concrete by the model matched the actual chloride content quite well for all four exposure times.

Figure 6.4 shows chloride content profile vs. depth for the SB lanes of Bridge 2563. It appears that for this particular structure the model underestimates the amount of chlorides for all of the exposure periods evaluated. However, he maximum differences between the estimated and measured chloride content are less than 2 lbs/yd$^3$ for all measured depth. When running the model for this bridge, it was assumed that maximum surface chloride concentration would not change and that it will be equal to the actual surface chloride concentration determined on this bridge after three years of exposure. This assumption was not entirely correct, since, as can be seen from the figure, the actual surface concentration of chlorides fluctuates with exposure time.

An attempt was made to evaluate the influence of the constant surface chloride concentration assumption on the values of model-predicted chloride content when running the model for NB lanes of the same bridge (see Figure 6.5). Initially, the model was run assuming that the surface chloride concentration was about 10 lb/yd$^3$ (the actual value measured after 3 years of exposure) and that it remained constant. As can be seen from Fig.6 5, the model estimated the actual concentrations at all depths for all exposure times well.

### 6.3 Modeling Construction for Predicting D-value of HPC

As shown in Figure 6.6, R-square for the linear regression model between RCP value and diffusion coefficient value fore Phase II mixtures is 0.8241, which indicates that RCP value for Phase II mixtures has very good relationship with predicted diffusion coefficient modified by m-value from diffusion coefficient from migration test (the definition of m-value is shown in section 6.3). Figure 6.6 shows that D-value at 56 days can be expressed as a function of RCP value at 56 days, and the function can be written as the following:

$$\text{D-value at 56 days} = 2E\text{-}15 * RCP + 4E\text{-}13 \quad \text{.....(6.13)}$$

Models for predicting RCP value of concrete mixtures have been developed in Phase I of this study, and the mathematical expression of those constructed models are described in Equation (5.10), (5.15) and (5.20) in section 5.5.4. Based on w/b and the content of pozzolanic materials in concrete, 56-day RCP value of concrete can be predicted. The relationship between the best predicted RCP values and measured RCP for Phase II mixtures is shown in Figure 6.7. Since the R-square for the linear regression line is 0.8833 in Figure 6.7, it can be stated that the models developed for the prediction of RCP value of concrete predicted RCP value of Phase II mixtures well.

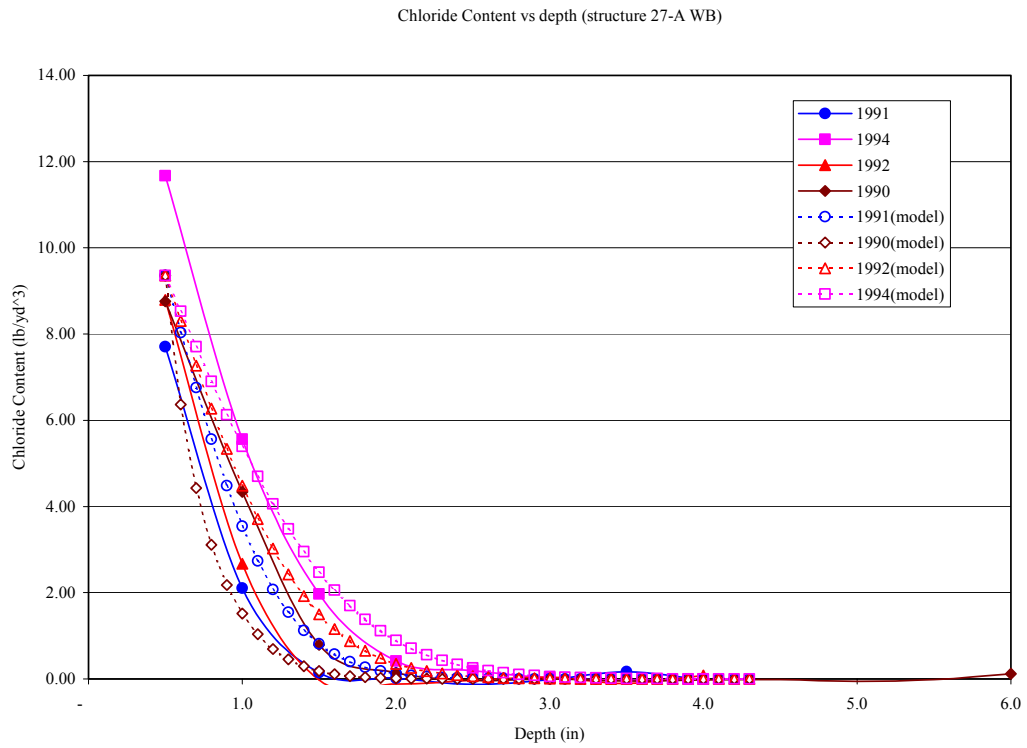


Figure 6.3: Chloride Content versus Depth for Structure 27-A WB

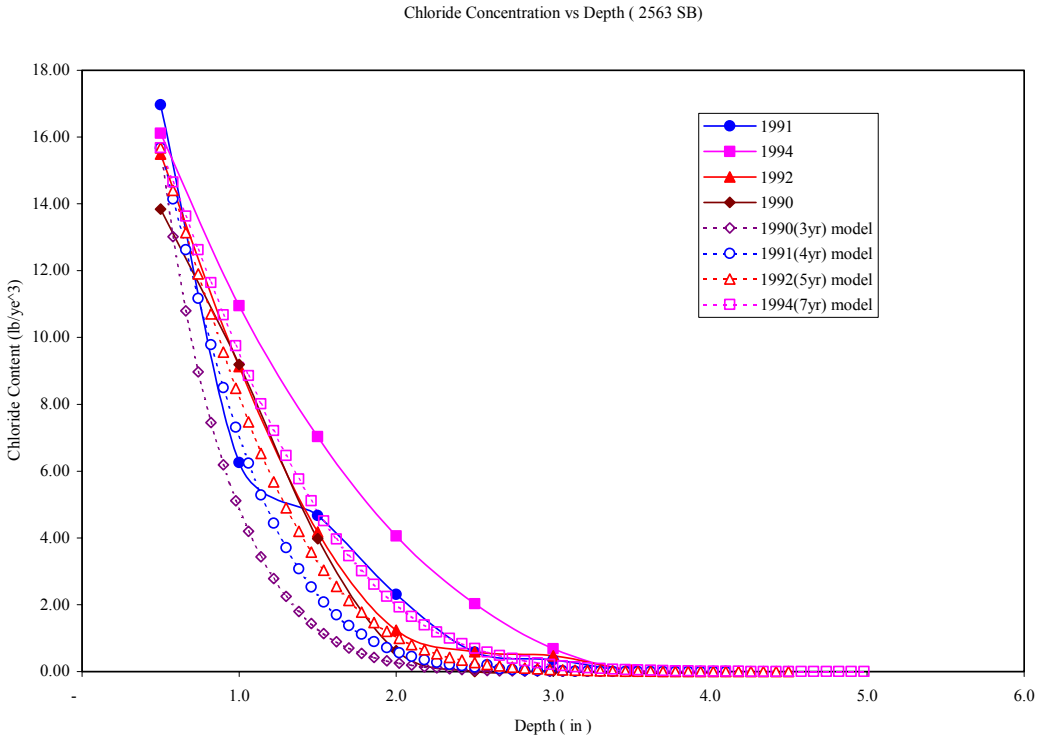


Figure 6.4: Chloride Content versus Depth for SB of Bridge 2563

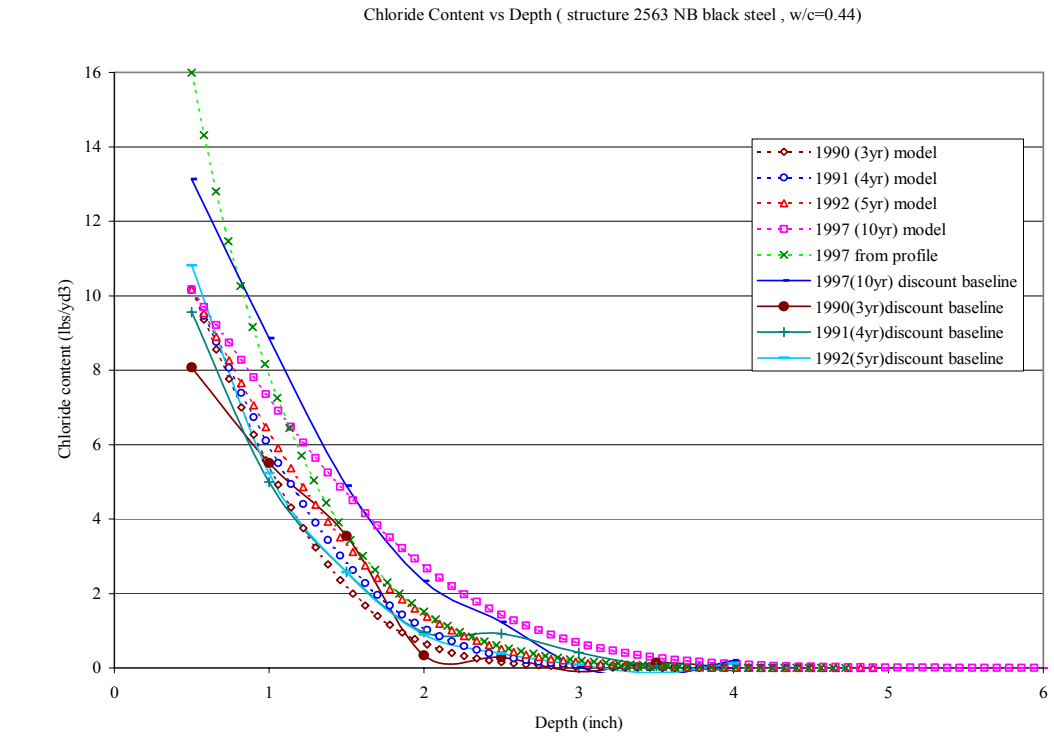


Figure 6.5: Chloride Content versus Depth for NB Lanes of Bridge 2563

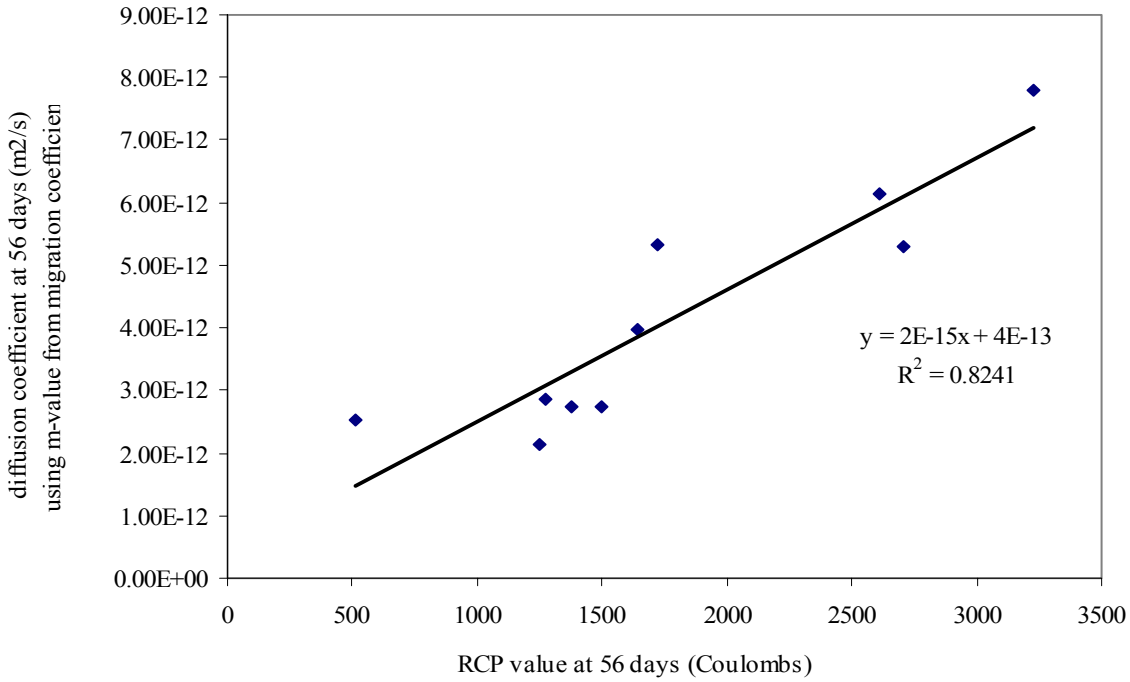


Figure 6.6: 56-day RCP Value versus Predicted Diffusion Coefficient Using the m-value from Migration Test for Phase II Mixtures

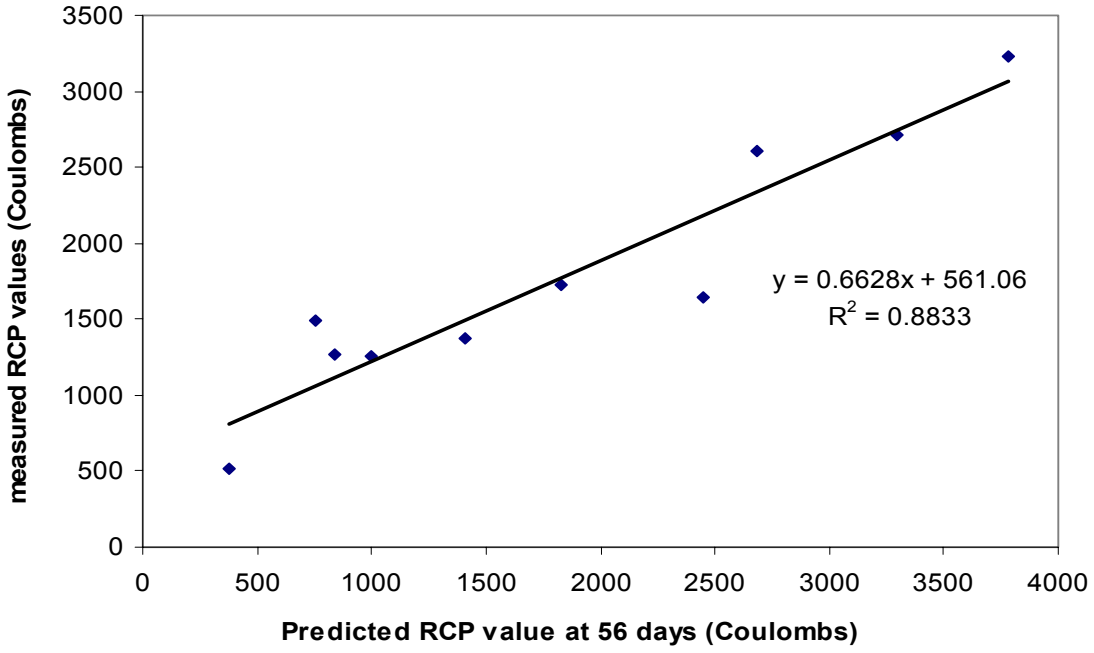


Figure 6.7: Predicted RCP Value versus Measured RCP Value for Phase II Mixtures

Table 6.4: Summary Results of Predicted Diffusion Coefficient at 56 days from Predicted RCP Value

| Mix. No. | Measured RCP value (Coulombs) | Predicted RCP value (Coulombs) | Predicted diffusion coefficient from RCP ($m^2/s$) | Predicted diffusion coefficient using m-value from migration ($m^2/s$) |
|---|---|---|---|---|
| 1#(6%SF 0.40w/b) | 1378 | 1407 | 3.21E-12 | 2.73E-12 |
| 2#(25%FA6%SF0.40w/b) | 1252 | 1001 | 2.40E-12 | 2.13E-12 |
| 3#(40%FA6%SF0.40w/b) | 1494 | 757 | 1.91E-12 | 2.75E-12 |
| 4#(25%FA0.40w/b) | 2612 | 2686 | 5.77E-12 | 6.15E-12 |
| 5#(40%FA0.35w/b) | 1645 | 2449 | 5.30E-12 | 3.97E-12 |
| 6#(25%Slag6%SF0.40w/b) | 511 | 378 | 1.16E-12 | 2.53E-12 |
| 7#(plain0.35w/b) | 2708 | 3298 | 7.00E-12 | 5.29E-12 |
| 8#(plain0.40w/b) | 3229 | 3783 | 7.97E-12 | 7.80E-12 |
| 9#(25%slag0.35w/b) | 1723 | 1828 | 4.06E-12 | 5.32E-12 |
| 10#(25%FA25%slag0.35w/b) | 1271 | 837 | 2.07E-12 | 2.85E-12 |

It can be seen from Table 6.4 that, in general, the predicted diffusion coefficient at 56 days is close to the diffusion coefficient from Life-365 model. However, the high variance in the prediction of RCP value of concrete mixture at 56 days will always lead to a high variance in the predicted diffusion coefficient.

### 6.4 Correlation Between Diffusion Coefficients from Life-365, Ponding and Migration

Table 6.5 shows the summary results of diffusion coefficient from migration test, and diffusion coefficient predicted from Life-365, and diffusion coefficient from ponding test for Phase II concrete mixtures. Life-365 model uses 28

days as the reference time in calculations. In order to calculate the diffusion coefficient of concrete mixtures at other times, m-value is input in Life-365 model (shown in Equation 6.14).

Table 6.5: Summary of Diffusion Coefficient from Migration Test and Diffusion Coefficient from Life-365 and Ponding Test

| Mix No. | D-value from migration test($m^2/s$) | | | D-value from Toronto model ($m^2/s$) | | | D-value from ponding ($m^2/s$) |
|---|---|---|---|---|---|---|---|
| | 28 days | 56 days | 180 days | 28 days | 56 days | 180 days | |
| 1 | 6.77E-12 | 6.25E-12 | 5.06E-12 | 2.96E-12 | 2.58E-12 | 2.04E-12 | 4.63E-12 |
| 2 | 6.57E-12 | 4.72E-12 | 4.07E-12 | 2.96E-12 | 2.24E-12 | 1.41E-12 | 4.30E-12 |
| 3 | 8.53E-12 | 7.92E-12 | 3.34E-12 | 2.96E-12 | 2.06E-12 | 1.12E-12 | 4.89E-12 |
| 4 | 1.16E-11 | 9.00E-12 | 5.60E-12 | 7.94E-12 | 6.02E-12 | 3.77E-12 | 5.30E-12 |
| 5 | 9.79E-12 | 6.44E-12 | 3.39E-12 | 6.03E-12 | 4.21E-12 | 2.29E-12 | 5.28E-12 |
| 6 | 5.48E-12 | 4.68E-12 | 3.05E-12 | 2.96E-12 | 2.34E-12 | 1.57E-12 | 2.43E-12 |
| 7 | 9.99E-12 | 8.76E-12 | 6.59E-12 | 6.03E-12 | 5.25E-12 | 4.16E-12 | 5.95E-12 |
| 8 | 1.11E-11 | 1.08E-11 | 8.30E-12 | 7.94E-12 | 6.91E-12 | 5.47E-12 | 1.09E-11 |
| 9 | 7.10E-12 | 6.26E-12 | 5.98E-12 | 6.03E-12 | 4.76E-12 | 3.20E-12 | 4.45E-12 |
| 10 | 1.03E-11 | 4.85E-12 | 2.84E-12 | 6.03E-12 | 4.15E-12 | 2.21E-12 | 4.85E-12 |

### 6.4.1 Correlation between Diffusion Coefficient from Migration Test and D-value from Life-365 Model

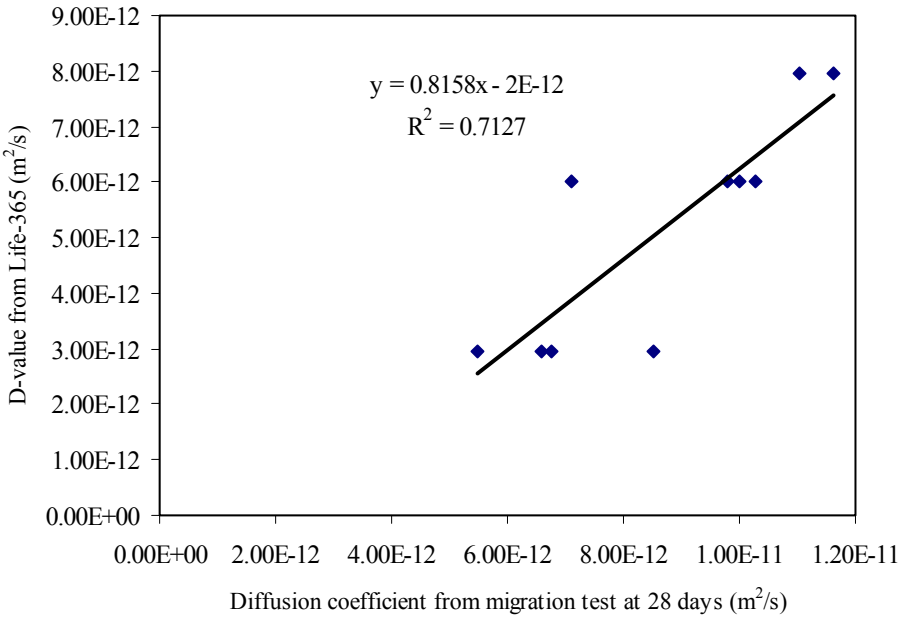


Figure 6.8: D-value from Life-365 versus Diffusion Coefficient from Migration Test for Phase II Mixtures at 28 Days

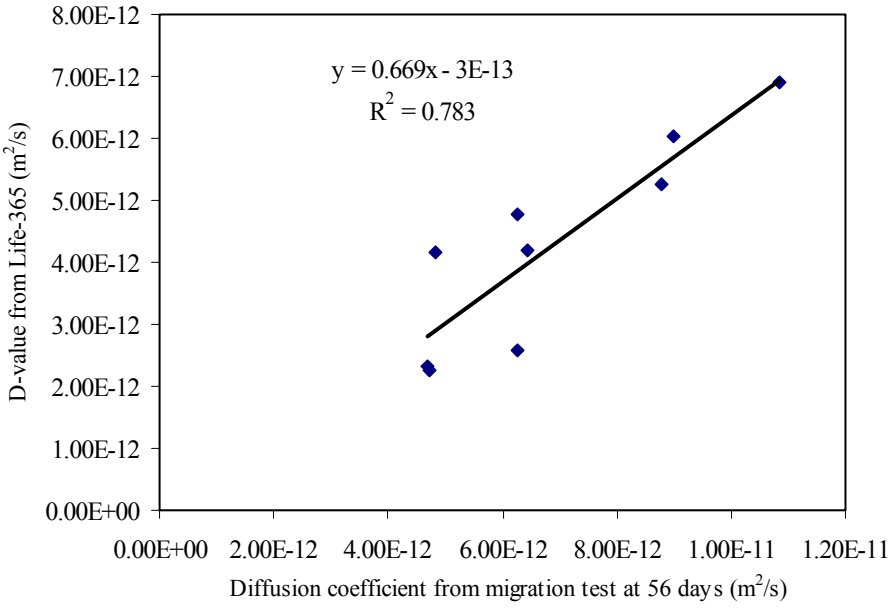


Figure 6.9: D-value from Life-365 versus Diffusion Coefficient from Migration Test for Phase II Mixtures at 56 Days

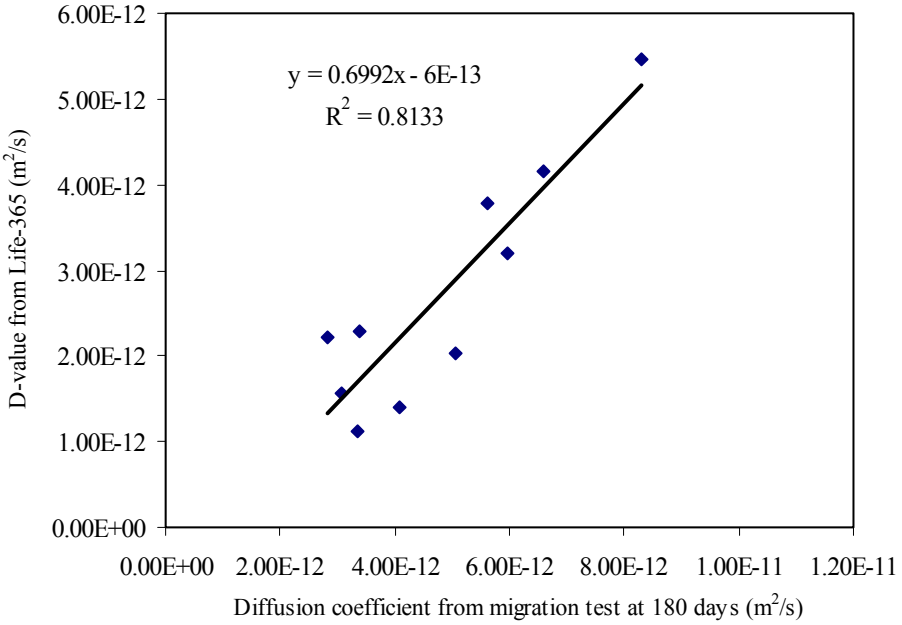


Figure 6.10: D-value from Life-365 vs. Diffusion Coefficient from Migration Test for Phase II Mixtures at 180 Days

As shown in Figures 6.8 through 6.10, diffusion coefficient predicted from Life-365 showed a good correlation with diffusion coefficient from migration test for Phase II mixtures at 28 days to 180 days, and the $R^2$ for the linear regression model, as shown in each figure, is higher than 0.70. The $R^2$ value increases at later ages. As shown in Table 6.5, for each concrete mixture in Phase II, the value of diffusion coefficient from migration test at 28 days is always higher than diffusion coefficient predicted from Life-365. For the results at 56 days or 180 days, the same conclusion can also be made.

### 6.4.2 Correlation between Diffusion Coefficient from Migration Test and D-value from Ponding Test

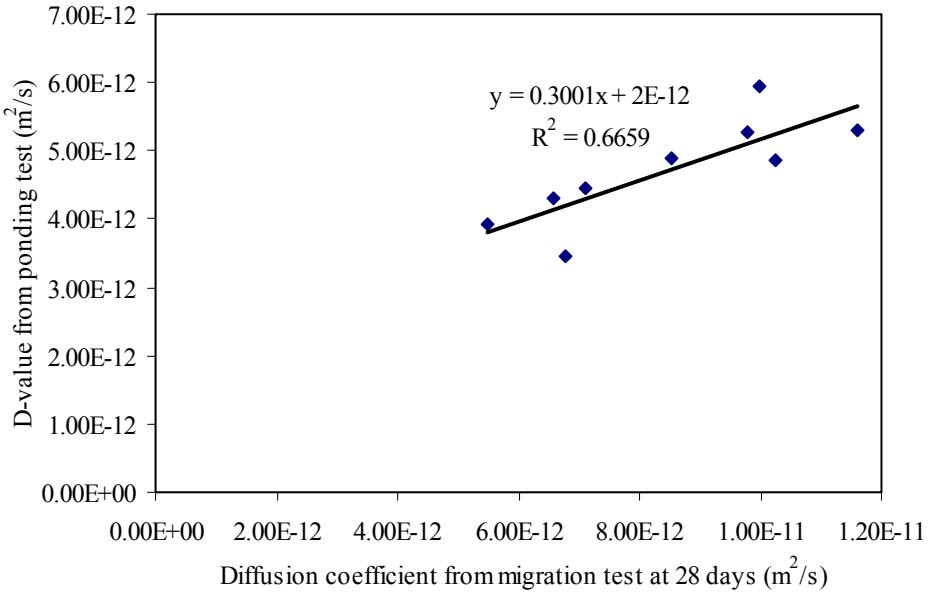


Figure 6.11: Diffusion Coefficient from Migration Test at 28 Days versus Diffusion Coefficient from Ponding Test for Phase II Mixtures

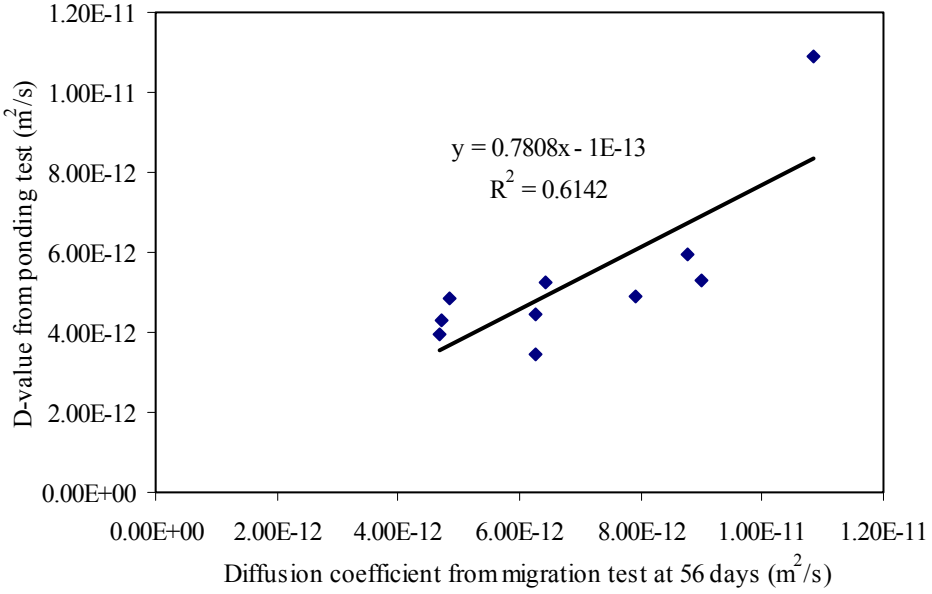


Figure 6.12: Diffusion Coefficient from Migration Test at 56 Days versus Diffusion Coefficient from Ponding Test for Phase II Mixtures

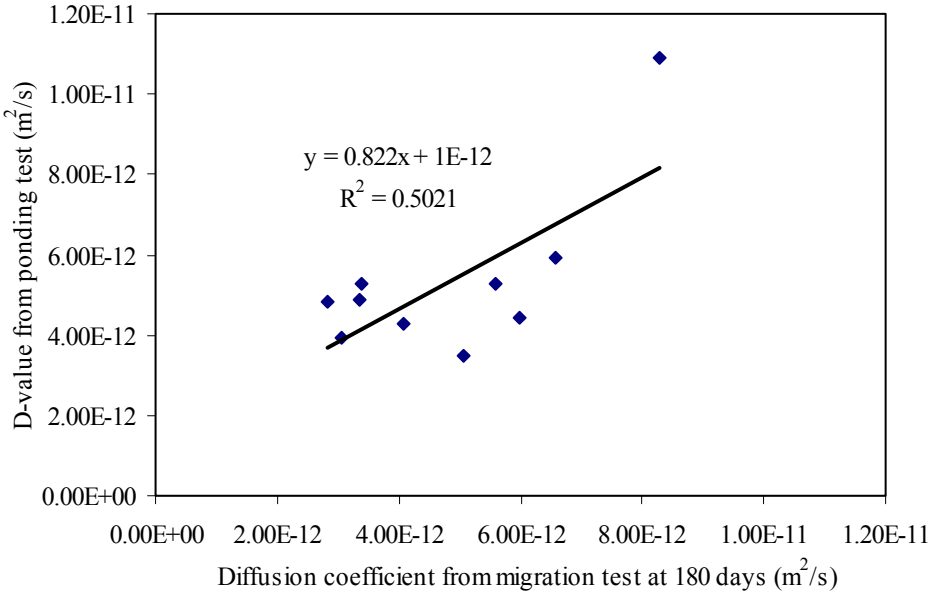


Figure 6.13: Diffusion Coefficient from Migration Test at 180 Days versus Diffusion Coefficient from Ponding Test for Phase II Mixtures

As shown in Figures 6.1 through 6.13, diffusion coefficient determined from ponding test showed a poor relationship with diffusion coefficient from migration test at 28, 56 and 180 days. The $R^2$ value decreased as the test age increased.

### 6.4.3 Correlation between Diffusion Coefficient Predicted from Life-365 and Determined from Ponding Test

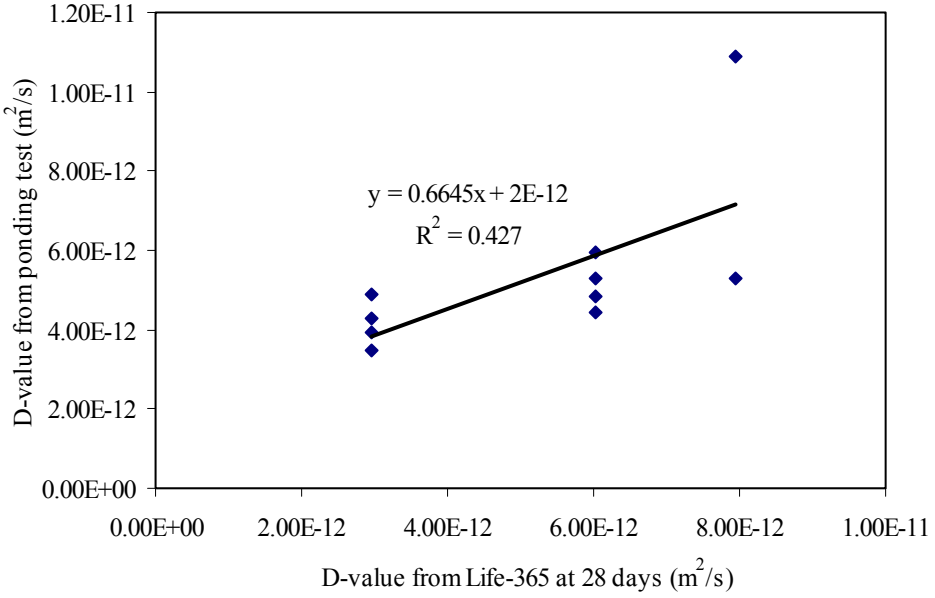


Figure 6.14: 28-day Diffusion Coefficient Predicted from Life-365 Model versus D-value from Ponding Test for Phase II Mixtures

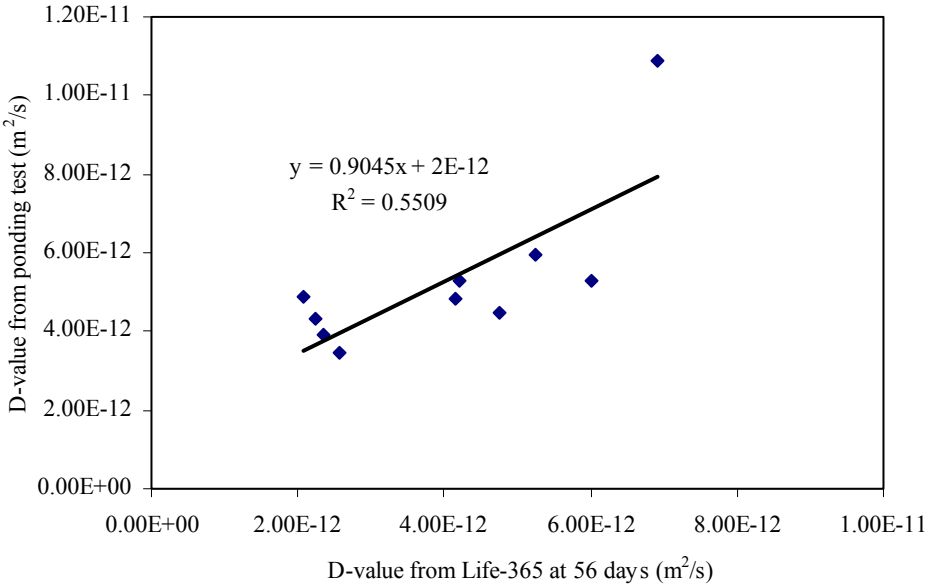


Figure 6.15: 56-day Diffusion Coefficient Predicted from Life-365 Model versus D-value from Ponding Test for Phase II Mixtures

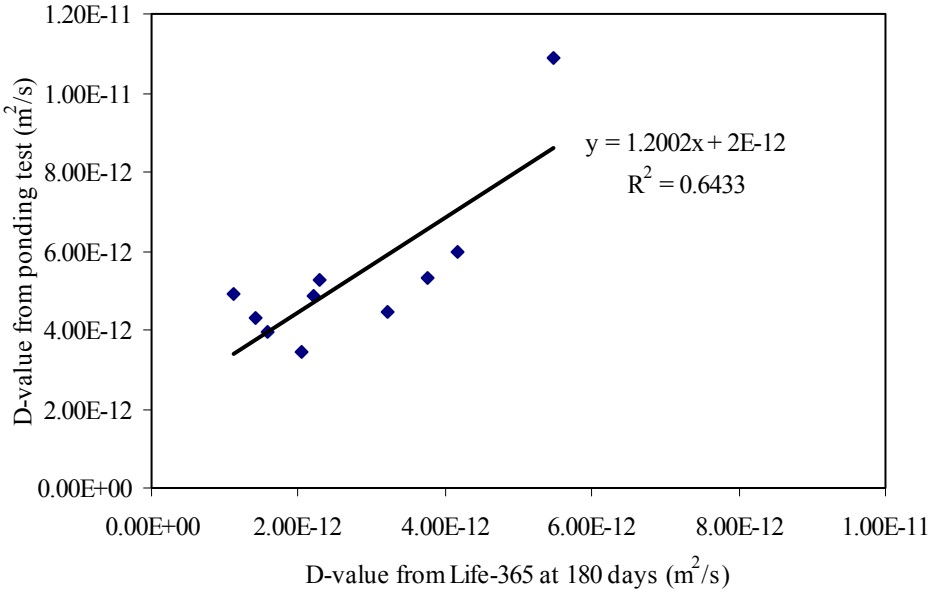


Figure 6.16: 180-day Diffusion Coefficient Predicted from Life-365 Model versus D-value from Ponding Test for Phase II Mixtures

As shown in Figures 6.14 through 6.16, diffusion coefficient predicted from Life-365 did not show a good relationship with diffusion coefficient determined from ponding test. The R-squares for the regression models, as shown in Figures 6.14 through 6.16, are lower than 0.65. For these models, the $R^2$ value increased as the test age increased.

In the Life-365 model, the chloride diffusion coefficient is defined as a function of both time and temperature. The effect of time on the change of diffusion coefficient is described by the following equation [Life-365, 2000]:

$$D(t) = D_{ref}(\frac{t_{ref}}{t})^m \quad \text{.....(6.14)}$$

where:
D(t) = diffusion coefficient at time t;
$D_{ref}$ = diffusion coefficient at 28 days (the reference time in Life-365);
m = constant (depending on mix proportions).

Through Equation (6.14), 56-day and 180-day diffusion coefficients can be calculated from 28-day diffusion coefficient and m-value related to specific concrete mixture proportions. These diffusion coefficient values at different ages are shown in Table 6.3.

Equation (6.14) is used in this study to calculate the time effect on the migration coefficient of Phase II mixtures. Migration coefficient at 28 days is regarded as the reference of migration coefficient. Since 56-day and 180-day migration coefficients of Phase II mixtures are determined in this study, the m-value for each mixture can be calculated by solving Equation (6.13). The results of m-values for Phase II mixtures are shown in Table 6.6.

Table 6.6: Summary Results of m-values from Life-365 and Migration Test for Phase II Mixtures

| Mix. No. | m-value from Life-365 model | m-value from migration test | |
|---|---|---|---|
| | | 56 days | 180 days |
| 1#(6%SF 0.40w/b) | 0.20 | 0.12 | 0.16 |
| 2#(25%FA6%SF0.40w/b) | 0.40 | 0.48 | 0.26 |
| 3#(40%FA6%SF0.40w/b) | 0.52 | 0.11 | 0.50 |
| 4#(25%FA0.40w/b) | 0.40 | 0.37 | 0.39 |
| 5#(40%FA0.35w/b) | 0.52 | 0.60 | 0.57 |
| 6#(25%Slag6%SF0.40w/b) | 0.34 | 0.23 | 0.31 |
| 7#(plain0.35w/b) | 0.20 | 0.19 | 0.22 |
| 8#(plain0.40w/b) | 0.20 | 0.03 | 0.15 |
| 9#(25%slag0.35w/b) | 0.34 | 0.18 | 0.09 |
| 10#(25%FA25%slag0.35w/b) | 0.54 | 1.08 | 0.69 |

As shown in Table 6.6, m-values calculated from migration test are different at different ages for the same mixture, and the difference between m-value for 56 days and m-value for 180 days is related to the mixture proportion of concrete. The m-value for silica fume concrete (No. 1) is similar to that of plain concrete (No. 8) at 180 days. Concrete with fly ash and slag always has relatively higher m-value than plain concrete. Concretes with higher amount of these supplementary materials have higher m-values.

Based on 28-day chloride diffusion coefficients predicted from Life-365, and m-value for migration test for Phase II mixtures, 56-day and 180-day chloride diffusion coefficients can be calculated from Equation 6.14. The results for 56-day and 180-day diffusion coefficients are shown in Table 6.7.

Table 6.7: Predicted Diffusion Coefficient Using 28-day D-value from Life-365 and m-value from Migration Test for Phase II Mixtures

| Mix. No. | Diffusion coefficient using m-value from migration coefficient | | |
|---|---|---|---|
| | 28 days | 56 days | 180 days |
| 1#(6%SF 0.40w/b) | 2.96E-12 | 2.73E-12 | 2.21E-12 |
| 2#(25%FA6%SF0.40w/b) | 2.96E-12 | 2.13E-12 | 1.83E-12 |
| 3#(40%FA6%SF0.40w/b) | 2.96E-12 | 2.75E-12 | 1.16E-12 |
| 4#(25%FA0.40w/b) | 7.94E-12 | 6.15E-12 | 3.83E-12 |
| 5#(40%FA0.35w/b) | 6.03E-12 | 3.97E-12 | 2.09E-12 |
| 6#(25%Slag6%SF0.40w/b) | 2.96E-12 | 2.53E-12 | 1.65E-12 |
| 7#(plain0.35w/b) | 6.03E-12 | 5.29E-12 | 3.98E-12 |
| 8#(plain0.40w/b) | 7.94E-12 | 7.80E-12 | 5.96E-12 |
| 9#(25%slag0.35w/b) | 6.03E-12 | 5.32E-12 | 5.08E-12 |
| 10#(25%FA25%slag0.35w/b) | 6.03E-12 | 2.85E-12 | 1.67E-12 |

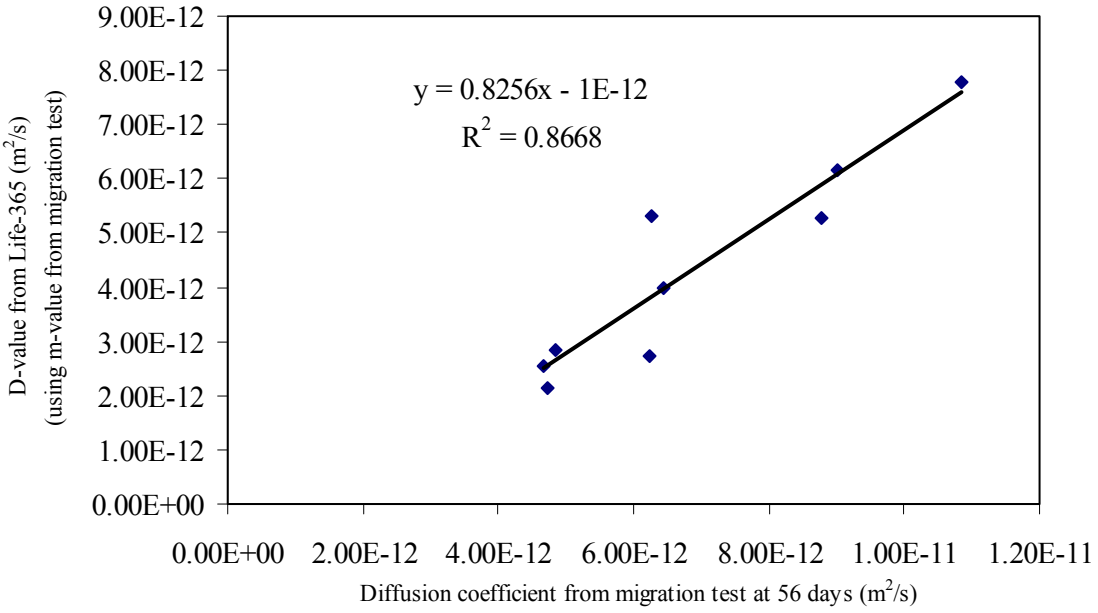


Figure 6.17: Diffusion Coefficient from Migration Test at 56 Days versus Diffusion Coefficient Using 28-day D-value from Life-365 and m-value from Migration Test

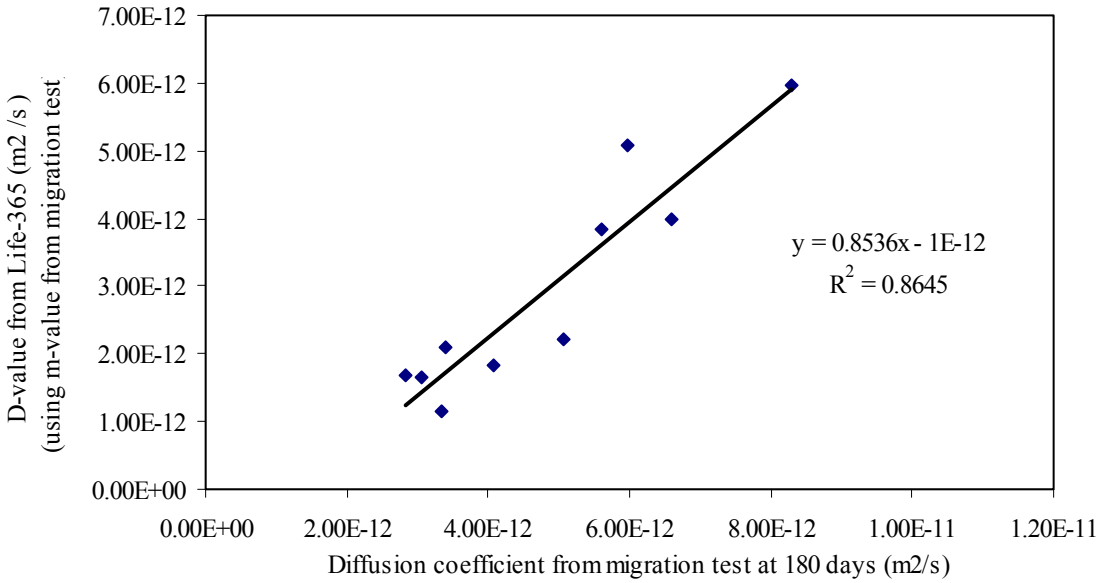


Figure 6.18: Diffusion Coefficient from Migration Test at 180 Days versus Diffusion Coefficient Using 28-day D-value from Life-365 and m-value from Migration Test

Comparing Figure 6.9 with Figure 6.17, 56-day diffusion coefficient modified by the m-value obtained from the migration test had a better relationship with diffusion coefficient from migration test than diffusion coefficient modified by m-value from Life-365. This is shown by the higher $R^2$ in Figure 6.17 than in Figure 6.9. Similarly, 180-day diffusion coefficient modified by m-value from migration test also showed a better linear relationship with diffusion coefficient from migration test than the 180-day diffusion coefficient modified by m-value from Life-365. Therefore, m-value (time factor) calculated from migration test of Phase II mixtures helped to strengthen the relationship between diffusion coefficients from Life-365 with diffusion coefficient from migration test of concrete mixtures.

### 6.5 Correlation Between D-Value and Other Permeability-Related Characteristics

Based on the average ranking for Phase II mixtures shown in Table 6.8, No. 6 mixture ranked first among all the 10 mixtures. This high ranking indicates that mixture No. 6 achieved the best properties at 56 days. Mixture No. 2 with 25% fly ash and 6% silica fume ranked second. Mixture No. 8 achieved the lowest ranking, which indicates No. 8 had the worst properties at 56 days.

Correlation between D-value and other properties of concrete can be seen from the fact that the ranking of concrete mixtures based on D-value from ponding test is similar to the average ranking of concrete mixtures. Since other properties such as RCP, electric current, diffusion coefficient from migration) are easier to determine than D-value from ponding test, these properties could be used to rank the concrete instead of diffusion coefficient from ponding test.

As shown in Table 6.2, the difference in diffusion coefficient between two samples from concrete No. 1 and No. 6 is quite big. The individual diffusion coefficient from concrete slab was used in the ranking. As shown in Table 6.8, Concrete No. 1 and 6 had two different ranking in D-value based on the different D-value used. One was ranked based on the average D-value from two concrete slabs, and the other was based on the individual D-value for one concrete slab. However, the average ranking based on individual D-value still kept the same as that based on the average D-value used in the ranking.

Table 6.8: Summarization of Ranking of Properties of Phase II Mixtures

| Mix No. | W/B | Binder | | | Ranks for each mixture in Phase II based on properties tested at Lab | | | | | | | | | | | |
|---|---|---|---|---|---|---|---|---|---|---|---|---|---|---|---|---|
| | | FA (%) | SF (%) | Slag (%) | RCP Value | | Diffusion coefficient from migration | | Conductivity | | Electric Current | | D-value from ponding | | Average | (Rank) |
| | | | | | 56-day (Coulomb) | Rank | 56 days ($m^2/s$) | Rank | 56 days (mS/cm) | Rank | 56 Current (A) | Rank | D-value ($m^2/s$) | Rank | | |
| 1 | 0.4 | 0 | 6 | 0 | 1378 | ***4th*** | 6.25 | ***4th*** | 0.907 | ***5th*** | 0.0133 | ***4th*** | 3.46E-12 | ***1st*** | **3.6** | **4th** |
| 1* | 0.4 | 0 | 6 | 0 | 1378 | ***4th*** | 6.25 | ***4th*** | 0.907 | ***5th*** | 0.0133 | ***4th*** | 4.63E-12 | ***4th*** | **4.2** | ***4th*** |
| 2 | 0.4 | 25 | 6 | 0 | 1252 | ***2nd*** | 4.72 | ***2nd*** | 0.921 | ***6th*** | 0.0133 | ***3rd*** | 4.30E-12 | ***3rd*** | **3.2** | **2nd** |
| 3 | 0.4 | 40 | 6 | 0 | 1494 | ***5th*** | 7.92 | ***7th*** | 0.953 | ***8th*** | 0.0127 | ***2nd*** | 4.89E-12 | ***6th*** | **5.60** | **7th** |
| 4 | 0.4 | 25 | 0 | 0 | 2612 | ***8th*** | 9.00 | ***9th*** | 1.170 | ***9th*** | 0.0257 | ***8th*** | 5.30E-12 | ***8th*** | **8.4** | **8th** |
| 5 | 0.35 | 40 | 0 | 0 | 1645 | ***6th*** | 6.44 | ***6th*** | 0.602 | ***2nd*** | 0.0213 | ***6th*** | 5.28E-12 | ***7th*** | **5.4** | **6th** |
| 6 | 0.4 | 0 | 6 | 25 | 511 | ***1 st*** | 4.68 | ***1st*** | 0.645 | ***4th*** | 0.008 | ***1st*** | 3.93E-12 | ***2nd*** | **1.8** | **1st** |
| 6* | 0.4 | 0 | 6 | 25 | 511 | ***1 st*** | 4.68 | ***1st*** | 0.645 | ***4th*** | 0.008 | ***1st*** | 2.43E-12 | ***1st*** | **1.6** | ***1st*** |
| 7 | 0.35 | 0 | 0 | 0 | 2708 | ***9th*** | 8.76 | ***8th*** | 0.926 | ***7th*** | 0.0273 | ***9th*** | 5.95E-12 | ***9th*** | **8.4** | **8th** |
| 8 | 0.4 | 0 | 0 | 0 | 3229 | ***10th*** | 10.85 | ***10th*** | 1.270 | ***10th*** | 0.032 | ***10th*** | 1.09E-11 | ***10th*** | **10** | **10th** |
| 9 | 0.35 | 0 | 0 | 25 | 1723 | ***7th*** | 6.26 | ***5th*** | 0.608 | ***3rd*** | 0.024 | ***7th*** | 4.45E-12 | ***4th*** | **5.20** | **5th** |
| 10 | 0.35 | 25 | 0 | 25 | 1271 | ***3rd*** | 4.85 | ***3rd*** | 0.486 | ***1st*** | 0.0170 | ***5th*** | 4.85E-12 | ***5th*** | **3.4** | **3rd** |

* The individual value of diffusion coefficient of concrete mixtures No. 1 and 6 was used during the ranking for D-value of these two concrete.

# 7 SUMMARY OF FINDINGS

## 7.1 Phase I: Identification of Optimum Mixes in Terms of Performance

1) In order to identify the optimum mixtures whose performance may be influenced by several composition-related variables, 3-factor central composite experimental design approach was adopted in the current research.

2) 45 concrete mixes designed using the above-mentioned statistical experimental approach have been made in the laboratory during the Phase I of this research. For each mix, four concrete properties have been tested: compressive strength, static modulus of elasticity, rapid chloride penetration, and chloride conductivity.

3) Using multiple regression analysis, and utilizing the laboratory test results, a total of 27 mathematical models have been developed for prediction of the four parameters that were evaluated for these mixes. Based on these models, a total of 81 contour maps that related binder and mix composition to concrete properties have been obtained.

4) The contour maps have been used to identify 10 mixes with optimum composition (in terms of the previously mentioned performance parameters) for more in-depth evaluation in Phase II of the study.

## 7.2 Phase II: Evaluation of Performance of the Optimum Mixtures

1. The required dosages of superplasticizer and air-entraining admixture for the 10 concrete mixtures have been determined using a series of trial mixes for which slump and air content have been monitored and checked against target values.

2. Overall properties of the 10 mixtures have been tested in Phase II. Among all the 10 mixtures, four mixtures are the optimized mixtures, which are recognized in Phase I. Other concrete mixtures are the mixtures, which may be normally defined HPC concrete and plain concrete. The tested properties in Phase II mixtures contained properties of concrete both in fresh state and in hardened state. The following properties of concrete in fresh state have been tested: slump value and air content, slump loss and air loss. The mechanical properties of concrete at hardened state tested are: compressive strength, modulus of elasticity, dynamic modulus of elasticity, and flexural strength. The durability-related properties of concrete tested in Phase II contain: rapid chloride permeability, chloride conductivity, DC resistance, diffusion coefficient from migration test, diffusion coefficient from ponding test, drying shrinkage, absorption, resistance to early age cracking, resistance to freezing and thawing, and resistance to scaling.

3. Based on test results achieved at this study, the optimized mixtures (No. 2: 25% flyash and 6% silica fume, No. 6 with 25%slag and 6% silica fume, and No. 10 with 25% fly ash and 25% slag) got the most promising properties, such as low RCP value, diffusion coefficient from migration test, diffusion coefficient from ponding, and conductivity.

4. Since there is a very good relationship between the RCP value at 56 days and diffusion coefficient at 56 days, models for predicting diffusion coefficient of concrete have been constructed using RCP value at 56 days. The input for the model is the binder composition and water-binder ratio in concrete mixtures. The 56-day diffusion coefficient can be evaluated using the above models and the proportion characteristics of concrete mixtures.

5. Since RCP value at 56 days can be directly used to predict the diffusion coefficient of concrete mixtures, RCP test at worksite can be used not only as quality control, but also for the estimation of life-cycle cost of the concrete structures as-built.

## 7.3 Suggested Procedure for Selecting Composition of HPC Mixtures with Desired Characteristics

As stated in the Phase 1 of this study (sections 3.4.1 – 3.4.3), 45 mixtures of different binder combinations were prepared as a part of the design matrix. The strength and RCP values data resulting from these 81 mixtures were used to generate 81 contour maps showing the variation in strength and RCP values, corresponding to variations in

binder composition as a function of w/b ratio. From these contour maps, ranges of binder compositions were selected, which yielded high performance characteristics in the concrete mixtures. The ranges of binder composition chosen were as follows:
For concrete containing fly ash and silica fume: fly ash (25 – 30 %) and silica fume (5 – 7 %);
For concrete containing slag and silica fume: slag (25-30 %) and silica fume (5 – 7 %);
For concrete containing fly ash and slag: fly ash (20-30 %) and slag (20-30 %).

In Phase II of this study, binder combinations falling within these ranges were chosen to prepare 10 new concrete mixtures in Phase II and several mechanical and durability parameters of these mixtures were measured. Based on these data, mathematical models were constructed that allow for the prediction of strength, rapid chloride permeability and chloride diffusion coefficient values based on the binder composition of the mixture.

The data generated by these models for the previously described ranges of binder composition have been arranged in an Excel sheet, which allows the user to input desired minimum and maximum values of strength (at 28 days) and/or RCP values (at 56 days) and obtain binder combinations which yield/satisfy the desired input values. Binder system 1 refers to mixtures, which contain PC, SF and GGBS. Binder system 2 refers to mixtures, which contain PC, SF and FA. Binder system 3 refers to mixtures, which contain PC, GGBS and FA. The percentage increments of SF represented in the Excel worksheet are 0, 5 and 7.5 %. The percentage increments of FA and GGBS represented are 0, 20, 25 and 30 %.

A regression equation was developed to represent the relationship between the measured values of RCP and diffusion coefficient measured at 56 days (Phase II). This relation was linear and had an $R^2$-value of 0.8241 A relationship between strength at 28 days and binder composition was also obtained (Phase I) for each of the 3 binder systems. These relationships were quadratic with $R^2$-values of 0.963, 0.915 and 0.950, respectively.

The Excel file that can be used to select the composition of HPC mixtures with desired performance characteristics is composed of three worksheets.

The first worksheet titled “Specify Strength & RCP, shown in Figure 7.1, allows the user to input minimum and maximum compressive strength (in psi) and RCP (in Coulombs) values in the input cells (shaded blue), corresponding to each binder system. The table immediately below the input cells automatically shows values of strength and RCP values for mixtures that satisfy *either* the strength or the RCP criteria. The D-values are corresponding to the RCP values are also shown in the third row. If input criteria are not met, the cell displays “N/A”, indicating that the binder combination does not produce a mix that satisfies the desired criteria.

If the user wishes to specify only the strength values, the second worksheet titled “Specify Strength” (Figure 7.2), may be used. In this case, on the minimum and maximum strength values need to be input in the blue-shaded cells. Strength values of mixtures that satisfy these upper and lower strength limits are displayed, along with their corresponding RCP and D-values.

Similarly, if the user wishes to specify only the RCP values, the third worksheet titled “Specify RCP” (Figure 7.3) may be used. Once the desired minimum and maximum RCP values are input in the blue-shaded cells, the tables display the RCP values for mixes which satisfy the minimum and maximum values. The corresponding D-values and compressive strength is also displayed.

### 7.4 Suggested Testing Procedures for Use with QA/QC Specification

Test procedures selected to measure the properties of concrete should be timely, economical, non-destructive, reliable and reproducible, if possible. As shown in Table 6.8 of this study (summarization of ranking for Phase II mixtures), except the ranking based on the chloride conductivity of concrete was quite different from the overall ranking of concrete mixtures, ranking based on other properties of concrete matched the overall ranking very well. This indicated that all these tests except for chloride conductivity test could be used to measure the properties of concrete with good accuracy. However, since ponding test is time and effort consuming, it is not a suitable test for QA/QC purposes.

Test for rapid chloride ion permeability (RCPT) and electric current measurement under DC volts show suitable for use as routine control tests for QA/QC purposes, since these two tests are both easy to set up and operate. Models for 56-day RCP value of concrete had been developed, and they can provide a good prediction of 56-day RCP based on the mixture proportion of concrete. Therefore, the available models for predicting 56-day RCP value of concrete further support RCPT to be used as a suitable test in the purpose of QA/QC. As discussed in section 6.3, 56-day RCP value of concrete had a good relationship with diffusion coefficient at 56 days predicted from Life-365 model, which directly connects RCP value with long-term performance of concrete.

As to the test for determination of electric current under DC power (DC resistance test), this is a non-destructive test, and can be set up in situ. The set-up of DC resistance test is very easy, and the cost for the set-up of this test is also low. Therefore, it shows lots of benefits that can be achieved from this test if used in QC/QA specification. However, further improvement on this test should be done before used in the worksite, because this test does not need any preconditioning of concrete specimens, which means the moisture state in concrete is not controlled during the test. Since the state of moisture in concrete affects the electric properties of concrete, careful control of moisture state prior to and during test is necessary to obtain acceptable levels of precision. The following method is suggested to ensure the moisture state of concrete before testing: wet burlap, (followed by plastic membrane) is used to cover the concrete surface for 24 hours before testing. In order to make this test more suitable in the worksite, the modification of this test is encouraged: the replacement of copper rods by stainless plate is recommended.

The most common of test methods on hardened concrete is the compressive strength test, because it is easy to perform, and many of the desirable characteristics of concrete are qualitatively related to its strength. Test for compressive strength is also suggested for use as a routine test for the purposes in QC/QA.

### 7.5 Suggested Guidelines for Mixing, Sampling, and Consolidation of HPC

The suggested mixing procedure for the production of HPC was as follows:

- The inner surface of the mixer is wetted;
- Sand and coarse aggregate are added into the mixer for 3 minutes. If needed, a small of water is added into the aggregate to keep it in the saturated-surface dry state;
- All cementitious materials are added into the mixer, and mixed for 5 minutes to ensure uniform distribution of supplementary materials in the mixture;
- The air-entraining admixture diluted with some portion of mixing water is added into the mixer and all ingredients are mixed for about 2 minutes;
- Half of the mixing water is added into the mixture and all ingredients are mixed for 2 minutes;
- High range water reducer (diluted with mixing water) and the remaining portion of the mixing water are added into the mixture;
- All the ingredients are mixed for 3 minutes after all the water is added into the mixture;
- The mixer is stopped for 3 minutes;
- Mixing is resumed for additional 2 minutes;

Suggested guidelines for sampling of HPC are presented below:

- Before obtaining the sample, remixing by trowel or shovel is needed;
- Start tests for slump or air content, or both as soon as possible after the concrete sample is available;
- Start molding specimens for strength tests or other tests as soon as possible after fabricating the composite sample;
- Keep the elapsed time between obtaining and using the sample as short as possible;
- Protect the sample from the sun, wind, and other sources of rapid evaporation, and from contamination;

The following consolidation procedures are suggested for the production of HPC:
Based on the slump value of fresh concrete, different consolidation methods should be selected. Rodding is required for concrete with a slump greater than 3 inches. Rodding or vibration method can be selected for consolidating concrete with a slump in the range of 1 to 3 inches. If the slump of concrete is less than 1 inch, vibration is required to consolidate the concrete.

Since the slump of concrete produced in this study is much higher than 3 inches, rodding is used to consolidate the concrete. The procedures for consolidating concrete with a slump greater than 3 inches are provided below:

- Place the concrete in the mold, in the required number of layers of approximately equal volume;
- Rod each layer with the rounded end of the rod, and the required number of strokes (the number of strokes and size of rod are specified in ASTM C 192 (Table 2), and distribute the strokes uniformly over the cross section of the mold;
- Rod the bottom layer through the depth of mold, and for each upper later allow the rod to penetrate about ½ inch into the underlying layer when the depth of layer is less than 4 inches;
- After each layer is rodded, tap the outsides of the mold lightly 10 to 15 times with the mallet to close any holes left by rodding, and to release any larger air entrapped in the concrete;
- After tapping, spade the concrete along the sides and ends of beam and prism molds with a trowel.

### 7.6 Selection of Other Performance Related Parameters

High performance concrete should possess a certain level of dimensional stability. Properties such as high elastic modulus, low drying shrinkage and creep, and low thermal strain are the important factors contribute to the high dimensional stability of concrete structure. These properties are essential for counteracting any undesirable stress effects produced as a result of volume changes under restraint conditions.

Although high strength is not necessary for high performance concrete, most of high performance concretes show high strength, for high performance concrete has low porosity in hardened state.

### 7.7 LCC of Phase II Mixtures

The strength and chloride diffusion coefficient values determined for the 10 concrete mixtures tested in Phase II of the study were used as input values for the LCC model described in Vol. 1 of this report. The LCC model was run for a single, simply supported span and the results are summarized in Figure 7.4. This figure also shows the LCC of the three field mixtures. It can be seen that LCC for all laboratory mixtures was lower than the LCC for standard INDOT class C concrete mixture (No. 8). It can also be seen that the LCC of the actual field mixtures was slightly higher than the LCC of No. 8 mixture.

**THIS WORKSHEET REQUIRES STRENGTH AND RCP INPUT VALUES**

**Binder System 1 -- PC/SF/GGBS**

Min. 28 day strength, psi = 7000 Min. RCP value at 56 days = 1500
Max. 28 day strength, psi = 10000 Max. RCP value at 56 days = 2500

| w/b | | 0.35 | | | 0.40 | | | 0.45 | | |
|---|---|---|---|---|---|---|---|---|---|---|
| SF % | | 0 | 5 | 7.5 | 0 | 5 | 7.5 | 0 | 5 | 7.5 |
| GGBS % | Property | | | | | | | | | |
| 0 | Strength | N/A | N/A | N/A | N/A | N/A | N/A | N/A | 7911 | N/A |
| | RCPT | N/A | N/A | N/A | N/A | N/A | N/A | N/A | 1980 | N/A |
| | D - value | N/A | N/A | N/A | N/A | N/A | N/A | N/A | 4.36E-12 | N/A |
| 20 | Strength | 9220 | N/A | N/A | N/A | N/A | N/A | N/A | N/A | N/A |
| | RCPT | 2033 | N/A | N/A | N/A | N/A | N/A | N/A | N/A | N/A |
| | D - value | 4.47E-12 | N/A | N/A | N/A | N/A | N/A | N/A | N/A | N/A |
| 25 | Strength | 9341 | N/A | N/A | 7813 | N/A | N/A | N/A | N/A | N/A |
| | RCPT | 1828 | N/A | N/A | 2313 | N/A | N/A | N/A | N/A | N/A |
| | D - value | 4.06E-12 | N/A | N/A | 5.03E-12 | N/A | N/A | N/A | N/A | N/A |
| 30 | Strength | 9463 | N/A | N/A | 7934 | N/A | N/A | N/A | N/A | N/A |
| | RCPT | 1668 | N/A | N/A | 2153 | N/A | N/A | N/A | N/A | N/A |
| | D - value | 3.74E-12 | N/A | N/A | 4.71E-12 | N/A | N/A | N/A | N/A | N/A |

**Binder System 2 -- PC/FA/SF**

Min. 28 day strength, psi = 7000 Min. RCP value at 56 days, Coulombs = 1500
Max. 28 day strength, psi = 10000 Max. RCP value at 56 days, Coulombs = 2500

| w/b | | 0.35 | | | 0.40 | | | 0.5 | | |
|---|---|---|---|---|---|---|---|---|---|---|
| SF % | | 0 | 5 | 7.5 | 0 | 5 | 7.5 | 0 | 5 | 7.5 |
| FA % | Property | | | | | | | | | |
| 0 | Strength | N/A | N/A | N/A | N/A | 9622 | N/A | N/A | 8088 | 8793 |
| | RCPT | N/A | N/A | N/A | N/A | 1584 | N/A | N/A | 2428 | 2064 |
| | D - value | N/A | N/A | N/A | N/A | 3.57E-12 | N/A | N/A | 5.26E-12 | 4.53E-12 |
| 20 | Strength | N/A | N/A | N/A | N/A | N/A | N/A | N/A | 8540 | N/A |
| | RCPT | N/A | N/A | N/A | N/A | N/A | N/A | N/A | 1677 | N/A |
| | D - value | N/A | N/A | N/A | N/A | N/A | N/A | N/A | 3.75E-12 | N/A |
| 25 | Strength | N/A | N/A | N/A | N/A | N/A | N/A | N/A | N/A | N/A |
| | RCPT | N/A | N/A | N/A | N/A | N/A | N/A | N/A | N/A | N/A |
| | D - value | N/A | N/A | N/A | N/A | N/A | N/A | N/A | N/A | N/A |
| 30 | Strength | N/A | N/A | N/A | N/A | N/A | N/A | N/A | N/A | N/A |
| | RCPT | N/A | N/A | N/A | N/A | N/A | N/A | N/A | N/A | N/A |
| | D - value | N/A | N/A | N/A | N/A | N/A | N/A | N/A | N/A | N/A |

**Binder System 3 -- PC/FA/GGBS**

Min. 28 day strength, psi = 7000 Min. RCP value at 56 days, Coulombs = 1500
Max. 28 day strength, psi = 10000 Max. RCP value at 56 days, Coulombs = 2500

| w/b | | 0.35 | | | | 0.40 | | | | 0.45 | | | |
|---|---|---|---|---|---|---|---|---|---|---|---|---|---|
| FA % | | 0 | 20 | 25 | 30 | 0 | 20 | 25 | 30 | 0 | 20 | 25 | 30 |
| GGBS % | Property | | | | | | | | | | | | |
| 0 | Strength | N/A | N/A | N/A | 8060 | N/A | N/A | N/A | N/A | N/A | N/A | N/A | N/A |
| | RCPT | N/A | N/A | N/A | 2497 | N/A | N/A | N/A | N/A | N/A | N/A | N/A | N/A |
| | D - value | N/A | N/A | N/A | 5.39E-12 | N/A | N/A | N/A | N/A | N/A | N/A | N/A | N/A |
| 20 | Strength | N/A | N/A | N/A | N/A | N/A | N/A | N/A | N/A | N/A | 7980 | 8059 | 8139 |
| | RCPT | N/A | N/A | N/A | N/A | N/A | N/A | N/A | N/A | N/A | 1873 | 1751 | 1734 |
| | D - value | N/A | N/A | N/A | N/A | N/A | N/A | N/A | N/A | N/A | 4.15E-12 | 3.90E-12 | 3.87E-12 |
| 25 | Strength | N/A | N/A | N/A | N/A | N/A | N/A | N/A | N/A | N/A | 7693 | 7772 | 7852 |
| | RCPT | N/A | N/A | N/A | N/A | N/A | N/A | N/A | N/A | N/A | 1734 | 1638 | 1647 |
| | D - value | N/A | N/A | N/A | N/A | N/A | N/A | N/A | N/A | N/A | 3.87E-12 | 3.68E-12 | 3.69E-12 |
| 30 | Strength | N/A | N/A | N/A | N/A | N/A | N/A | N/A | N/A | N/A | 7303 | 7383 | 7462 |
| | RCPT | N/A | N/A | N/A | N/A | N/A | N/A | N/A | N/A | N/A | 1718 | 1648 | 1683 |
| | D - value | N/A | N/A | N/A | N/A | N/A | N/A | N/A | N/A | N/A | 3.84E-12 | 3.70E-12 | 3.77E-12 |

Figure 7.1: First worksheet titled, “Specify Strength & RCP”

**THIS WORKSHEET REQUIRES STRENGTH INPUT VALUES**

**Binder System 1 -- PC/SF/GGBS**

Min. 28 day strength, psi = 7000
Max. 28 day strength, psi = 10000

| w/b | | 0.35 | | | 0.40 | | | 0.45 | | |
|---|---|---|---|---|---|---|---|---|---|---|
| SF % | | 0 | 5 | 7.5 | 0 | 5 | 7.5 | 0 | 5 | 7.5 |
| GGBS % | Property | | | | | | | | | |
| 0 | Strength | 8735 | N/A | N/A | 7207 | 9439 | 9513 | N/A | 7911 | 7985 |
| | RCPT | 3298 | N/A | N/A | 3783 | 1392 | 878 | N/A | 1980 | 1315 |
| | D - value | 7.00E-12 | N/A | N/A | 7.97E-12 | 3.18E-12 | 2.16E-12 | N/A | 4.36E-12 | 3.03E-12 |
| 20 | Strength | 9220 | N/A | N/A | 7692 | 9924 | 9998 | N/A | 8395 | 8470 |
| | RCPT | 2033 | N/A | N/A | 2518 | 604 | 329 | N/A | 1192 | 766 |
| | D - value | 4.47E-12 | N/A | N/A | 5.44E-12 | 1.61E-12 | 1.06E-12 | N/A | 2.78E-12 | 1.93E-12 |
| 25 | Strength | 9341 | N/A | N/A | 7813 | N/A | N/A | N/A | 8517 | 8591 |
| | RCPT | 1828 | N/A | N/A | 2313 | N/A | N/A | N/A | 1107 | 741 |
| | D - value | 4.06E-12 | N/A | N/A | 5.03E-12 | N/A | N/A | N/A | 2.61E-12 | 1.88E-12 |
| 30 | Strength | 9463 | N/A | N/A | 7934 | N/A | N/A | N/A | 8638 | 8712 |
| | RCPT | 1668 | N/A | N/A | 2153 | N/A | N/A | N/A | 1066 | 760 |
| | D - value | 3.74E-12 | N/A | N/A | 4.71E-12 | N/A | N/A | N/A | 2.53E-12 | 1.92E-12 |

**Binder System 2 -- PC/FA/SF**

Min. 28 day strength, psi = 7000
Max. 28 day strength, psi = 10000

| w/b | | 0.35 | | | 0.40 | | | 0.5 | | |
|---|---|---|---|---|---|---|---|---|---|---|
| SF % | | 0 | 5 | 7.5 | 0 | 5 | 7.5 | 0 | 5 | 7.5 |
| FA % | Property | | | | | | | | | |
| 0 | Strength | N/A | N/A | N/A | 8212 | 9622 | N/A | N/A | 8088 | 8793 |
| | RCPT | N/A | N/A | N/A | 3092 | 1584 | N/A | N/A | 2428 | 2064 |
| | D - value | N/A | N/A | N/A | 6.58E-12 | 3.57E-12 | N/A | N/A | 5.26E-12 | 4.53E-12 |
| 20 | Strength | N/A | N/A | N/A | 9156 | 9622 | 9854 | 8075 | 8540 | 8773 |
| | RCPT | N/A | N/A | N/A | 2767 | 1259 | 896 | 3186 | 1677 | 1314 |
| | D - value | N/A | N/A | N/A | 5.93E-12 | 2.92E-12 | 2.19E-12 | 6.77E-12 | 3.75E-12 | 3.03E-12 |
| 25 | Strength | N/A | N/A | N/A | 9393 | 9622 | 9736 | 8425 | 8654 | 8768 |
| | RCPT | N/A | N/A | N/A | 2686 | 1178 | 814 | 2998 | 1490 | 1127 |
| | D - value | N/A | N/A | N/A | 5.77E-12 | 2.76E-12 | 2.03E-12 | 6.40E-12 | 3.38E-12 | 2.65E-12 |
| 30 | Strength | N/A | N/A | N/A | 9629 | 9622 | 9618 | 8774 | 8767 | 8763 |
| | RCPT | N/A | N/A | N/A | 2604 | 1096 | 733 | 2810 | 1302 | 939 |
| | D - value | N/A | N/A | N/A | 5.61E-12 | 2.59E-12 | 1.87E-12 | 6.02E-12 | 3.00E-12 | 2.28E-12 |

**Binder System 3 -- PC/FA/GGBS**

Min. 28 day strength, psi = 7000
Max. 28 day strength, psi = 10000

| w/b | | 0.35 | | | | 0.40 | | | | 0.45 | | | |
|---|---|---|---|---|---|---|---|---|---|---|---|---|---|
| FA % | | 0 | 20 | 25 | 30 | 0 | 20 | 25 | 30 | 0 | 20 | 25 | 30 |
| GGBS % | Property | | | | | | | | | | | | |
| 0 | Strength | 8537 | 8219 | 8140 | 8060 | 7737 | 7737 | 7737 | 7737 | 7792 | 8110 | 8189 | 8269 |
| | RCPT | 4.80E+03 | 2846 | 2619 | 2497 | 5203 | 3246 | 3020 | 2898 | 5604 | 3647 | 3420 | 3299 |
| | D - value | 1.00E-11 | 6.09E-12 | 5.64E-12 | 5.39E-12 | 1.08E-11 | 6.89E-12 | 6.44E-12 | 6.20E-12 | 1.16E-11 | 7.69E-12 | 7.24E-12 | 7.00E-12 |
| 20 | Strength | N/A | 9979 | 9900 | 9820 | 8551 | 8551 | 8551 | 8551 | 7662 | 7980 | 8059 | 8139 |
| | RCPT | N/A | 1071 | 949 | 932 | 3010 | 1472 | 1350 | 1333 | 3411 | 1873 | 1751 | 1734 |
| | D - value | N/A | 2.54E-12 | 2.30E-12 | 2.26E-12 | 6.42E-12 | 3.34E-12 | 3.10E-12 | 3.07E-12 | 7.22E-12 | 4.15E-12 | 3.90E-12 | 3.87E-12 |
| 25 | Strength | N/A | N/A | N/A | N/A | 8500 | 8500 | 8500 | 8500 | 7375 | 7693 | 7772 | 7852 |
| | RCPT | N/A | N/A | N/A | N/A | 2767 | 1334 | 1238 | 1247 | 3167 | 1734 | 1638 | 1647 |
| | D - value | N/A | N/A | N/A | N/A | 5.93E-12 | 3.07E-12 | 2.88E-12 | 2.89E-12 | 6.73E-12 | 3.87E-12 | 3.68E-12 | 3.69E-12 |
| 30 | Strength | N/A | N/A | N/A | N/A | 8348 | 8348 | 8348 | 8348 | N/A | 7303 | 7383 | 7462 |
| | RCPT | N/A | N/A | N/A | N/A | 2646 | 1317 | 1247 | 1283 | N/A | 1718 | 1648 | 1683 |
| | D - value | N/A | N/A | N/A | N/A | 5.69E-12 | 3.03E-12 | 2.89E-12 | 2.97E-12 | N/A | 3.84E-12 | 3.70E-12 | 3.77E-12 |

Figure 7.2: Second Worksheet Titled, “Specify Strength”

**THIS WORKSHEET REQUIRES RCP INPUT VALUES**

**Binder System 1 -- PC/SF/GGBS**

Min. RCP value at 56 days, Coulombs = 1500
Max. RCP value at 56 days, Coulombs = 2500

| w/b | | 0.35 | | | 0.40 | | | 0.45 | | |
|---|---|---|---|---|---|---|---|---|---|---|
| SF % | | 0 | 5 | 7.5 | 0 | 5 | 7.5 | 0 | 5 | 7.5 |
| GGBS % | Property | | | | | | | | | |
| 0 | Strength | N/A | N/A | N/A | N/A | N/A | N/A | N/A | 7911 | N/A |
| | RCPT | N/A | N/A | N/A | N/A | N/A | N/A | N/A | 1980 | N/A |
| | D - value | N/A | N/A | N/A | N/A | N/A | N/A | N/A | 4.36E-12 | N/A |
| 20 | Strength | 9220 | N/A | N/A | N/A | N/A | N/A | N/A | N/A | N/A |
| | RCPT | 2033 | N/A | N/A | N/A | N/A | N/A | N/A | N/A | N/A |
| | D - value | 4.47E-12 | N/A | N/A | N/A | N/A | N/A | N/A | N/A | N/A |
| 25 | Strength | 9341 | N/A | N/A | 7813 | N/A | N/A | N/A | N/A | N/A |
| | RCPT | 1828 | N/A | N/A | 2313 | N/A | N/A | N/A | N/A | N/A |
| | D - value | 4.06E-12 | N/A | N/A | 5.03E-12 | N/A | N/A | N/A | N/A | N/A |
| 30 | Strength | 9463 | N/A | N/A | 7934 | N/A | N/A | N/A | N/A | N/A |
| | RCPT | 1668 | N/A | N/A | 2153 | N/A | N/A | N/A | N/A | N/A |
| | D - value | 3.74E-12 | N/A | N/A | 4.71E-12 | N/A | N/A | N/A | N/A | N/A |

**Binder System 2 -- PC/FA/SF**

Min. RCP value at 56 days, Coulombs = 1500
Max. RCP value at 56 days, Coulombs = 2500

| w/b | | 0.35 | | | 0.40 | | | 0.5 | | |
|---|---|---|---|---|---|---|---|---|---|---|
| SF % | | 0 | 5 | 7.5 | 0 | 5 | 7.5 | 0 | 5 | 7.5 |
| FA % | Property | | | | | | | | | |
| 0 | Strength | 10460 | N/A | N/A | N/A | 9622 | N/A | N/A | 8088 | 8793 |
| | RCPT | 2249 | N/A | N/A | N/A | 1584 | N/A | N/A | 2428 | 2064 |
| | D - value | 4.90E-12 | N/A | N/A | N/A | 3.57E-12 | N/A | N/A | 5.26E-12 | 4.53E-12 |
| 20 | Strength | 10953 | N/A | N/A | N/A | N/A | N/A | N/A | 8540 | N/A |
| | RCPT | 2349 | N/A | N/A | N/A | N/A | N/A | N/A | 1677 | N/A |
| | D - value | 5.10E-12 | N/A | N/A | N/A | N/A | N/A | N/A | 3.75E-12 | N/A |
| 25 | Strength | 11076 | N/A | N/A | N/A | N/A | N/A | N/A | N/A | N/A |
| | RCPT | 2374 | N/A | N/A | N/A | N/A | N/A | N/A | N/A | N/A |
| | D - value | 5.15E-12 | N/A | N/A | N/A | N/A | N/A | N/A | N/A | N/A |
| 30 | Strength | 11199 | N/A | N/A | N/A | N/A | N/A | N/A | N/A | N/A |
| | RCPT | 2399 | N/A | N/A | N/A | N/A | N/A | N/A | N/A | N/A |
| | D - value | 5.20E-12 | N/A | N/A | N/A | N/A | N/A | N/A | N/A | N/A |

**Binder System 3 -- PC/FA/GGBS**

Min. RCP value at 56 days, Coulombs = 1500
Max. RCP value at 56 days, Coulombs = 2500

| w/b | | 0.35 | | | | 0.40 | | | | 0.45 | | | |
|---|---|---|---|---|---|---|---|---|---|---|---|---|---|
| FA % | | 0 | 20 | 25 | 30 | 0 | 20 | 25 | 30 | 0 | 20 | 25 | 30 |
| GGBS % | Property | | | | | | | | | | | | |
| 0 | Strength | N/A | N/A | N/A | 8060 | N/A | N/A | N/A | N/A | N/A | N/A | N/A | N/A |
| | RCPT | N/A | N/A | N/A | 2497 | N/A | N/A | N/A | N/A | N/A | N/A | N/A | N/A |
| | D - value | N/A | N/A | N/A | 5.39E-12 | N/A | N/A | N/A | N/A | N/A | N/A | N/A | N/A |
| 20 | Strength | N/A | N/A | N/A | N/A | N/A | N/A | N/A | N/A | N/A | 7980 | 8059 | 8139 |
| | RCPT | N/A | N/A | N/A | N/A | N/A | N/A | N/A | N/A | N/A | 1873 | 1751 | 1734 |
| | D - value | N/A | N/A | N/A | N/A | N/A | N/A | N/A | N/A | N/A | 4.15E-12 | 3.90E-12 | 3.87E-12 |
| 25 | Strength | 10483 | N/A | N/A | N/A | N/A | N/A | N/A | N/A | N/A | 7693 | 7772 | 7852 |
| | RCPT | 2366 | N/A | N/A | N/A | N/A | N/A | N/A | N/A | N/A | 1734 | 1638 | 1647 |
| | D - value | 5.13E-12 | N/A | N/A | N/A | N/A | N/A | N/A | N/A | N/A | 3.87E-12 | 3.68E-12 | 3.69E-12 |
| 30 | Strength | 10566 | N/A | N/A | N/A | N/A | N/A | N/A | N/A | N/A | 7303 | 7383 | 7462 |
| | RCPT | 2245 | N/A | N/A | N/A | N/A | N/A | N/A | N/A | N/A | 1718 | 1648 | 1683 |
| | D - value | 4.89E-12 | N/A | N/A | N/A | N/A | N/A | N/A | N/A | N/A | 3.84E-12 | 3.70E-12 | 3.77E-12 |

Figure 7.3: Third Worksheet Titled, “Specify RCP”

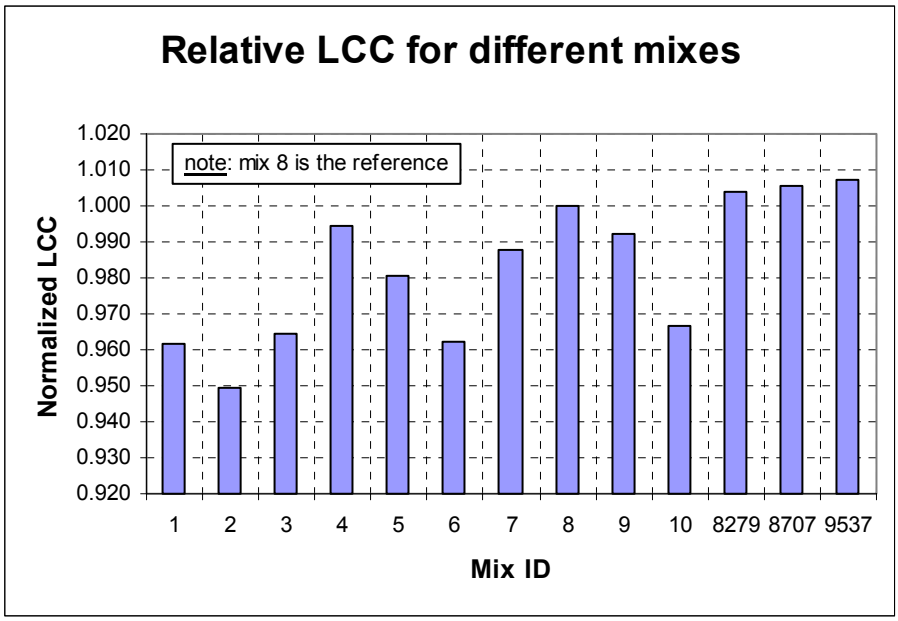


Figure 7.4: Comparison of LCC of the 10 Phase II Mixtures (1 – 10) and Three Field Mixtures (8279, 8707, 9537)

## 8 REFERENCES


AASHTO PP34-98: Standard Practice for Estimating the Crack Tendency of Concrete.

AASHTO T 259-80: Standard Method of Test for Resistance of Concrete to Chloride Ion Penetration, pp. 924-925.

AASHTO T277-86: Rapid Determination of the Chloride Permeability of Concrete. American Association of States Highway and Transportation Officials, Standard Specifications – Part II, Tests, Washington D.C.

ACI 308: Standard Practice for Curing Concrete, *American Concrete Institute*, Detroit, 1981, 11pp.

ACI 318-89: Building Code Requirements for Reinforced Concrete and Commentary, *American Concrete Institute*, Detroit, 1989, 353pp.

ACI 363R-92, "Sate of the Art Report on High Strength Concrete", *ACI Manual of concrete practice*, Part 1, American Concrete Institute, Detroit, 1993.

ACI Committee 363, "State-of –the-Art Report on High Strength Concrete", *ACI Journal*, Proceedings Vol. 81, No. 4, July-Aug., 1984, pp. 364-411.

Aitcin, P.C., High Performance Concrete, Modern Concrete Technology 5. Published by E & FN Spon, London, 1998.

[+] Aitcin, P.-C. and Lessard, M, "Canadian Experience with Air-entrained High-performance Concrete", *Concrete International*, Vol.16, No.10, Oct., 1994, pp. 35-38.

[+] Aitcin, P. C. and Neville, A., "High-performance Concrete Demystified", *Concrete International: Design & Construction*, Vol.15, No.1, Jan., 1993, pp. 21-26.

Alexander, M.G., and Magee, B.J., "Durability Performance of Concrete Containing Condensed Silica Fume", *Cement and Concrete Research*, Vol.29, No.6, 1999, pp. 917-922.

Al-Khaiat H., and Haque M.N.,: "Effect of Curing on Concrete in Hot Exposure Conditions", *Magazine of Concrete Research*, No. 4, 1999, pp. 269-274.

Armaghani, J., Romano, D., Bergin M., and Moxley, J., "High Performance Concrete in Florida Bridges", *ACI SP-140-1*, Detroit, MI, 1993.

Armaghani, J.M. and Bloomquist, D.G., "Development of Concrete Durability Specification and Ratings in Florida", *Transportation Research Record 1458*, Transportation Research Board, Washington, DC, 1998, pp. 8-13.

Aster, R., "SAA Foundations from Installation to Operation", Windcrest /McGraw-Hill, ISBN 0-8306-4316-8, 1994.

[+] Ahmad, S.H., Zia, P., Leming, M. and Hansen, M.R., "Mechanical Properties of High Performance Concretes", *Proceedings of Engineering Mechanics*, Published by ASCE, New York, NY, USA, pp. 864-867.

American Society for Testing and Materials: ASTM C 666-92: Standard Test Method for Resistance of Concrete to Rapid Freezing and Thawing.

American Society for Testing and Materials: ASTM C 672-92: Standard Test Method for Scaling Resistance of Concrete Surfaces Exposed to De-icing Chemicals.

[+] Anon. "High-performance Concrete Speeds Reconstruction for McDonald's", *Concrete International*, Vol.16, No.9, Sept. 1994, pp. 47-50.

[+] Baalbaki, W. Baalbaki, M. Benmokrane, B. and Aitcin, P.-C., "Influence of Specimen Size on Compressive Strength and Elastic Modulus of High-performance Concrete", *Cement, Concrete & Aggregates*, Vol.14, No.2, 1992, pp. 113-117.

[+] Baalbaki, W., Benmokrane, B., Chaallal, O. and Aitcin, P.-C., "Influence of Coarse Aggregate on Elastic Properties of High-performance Concrete", *ACI Materials Journal*. Vol. 88, No. 5, Sep-Oct, 1991, pp. 499-503.

Bajorski, P., Streeter, D.A. and Perry, R.J., "Applying Statistical Methods for Further Improvement of High-performance Concrete for New York State Bridge Decks", *Transportation Research Record*, No.1574, Nov., 1996, pp. 71-79.

Blais, F.A., Dallaire, E., Lessard, M. and Aitcin, P.C., "The Reconstruction of the Bridge Deck of the Jacques Cartier Bridge in Sherbrooke, Using High-performance Concrete", *30th Annual Meeting of the Canadian Society for Civil Engineering*, Edmonton, Alberta, May, 1996, pp. 501-507.

[+] Bowser, J.D., Krause, G.L. and Tadros, M.K., "Freeze-thaw Durability of High-performance Concrete Masonry Units", *ACI Materials Journal*, Vol.93, No.4, Jul-Aug, 1996, pp. 386-394.

Boddy, A., Bentz, E., Thomas, M. D.A., and Hooton, R.D., "An Overview and Sensitivity Study of a Multimechanistic Chloride Transport Model," *Cement and Concrete Research*, vol. 29, 1999, pp. 827-837.

*Book of Standard Specifications*, Indiana Department of Transportation, 1999.

Cetin, A., and Carrasquillo, R. L., "High Performance Concrete: Influence of Coarse Aggregates on Mechanical Properties", *ACI Materials Journal*, Vol.95, No.3, May-June 1998, pp. 252-261.

Chamberlin, W.P., "NCHRP Synthesis 212: Performance Related Specifications for Highway Construction and Rehabilitation", *TRB*, National Research Council, National Academy Press, Washington, D.C., 1995.

CONCRETE SOCIETY, "Developments in Durability Design and Performance-based Specification of Soncrete", *Concrete Society Special Publication CS 109,* 1996.

Collepardi, M., Marcialis, A., and Turriziani, R., "Kinetics of Penetration of Chloride Ions into the Concrete", *II Cemento*, No.4, Oct. 1970, pp. 157-164.

Coppola, L., Erali, E., Troli, R., and Collepardi, M., "Blending of Acrylic Superplasticizer with Napthalene, Melamine or Lignosulfate-based Polymers", *Fifth CANMET/ACI*, 1997, SP 173, pp.203-223.

[+] Dallaire, E., Lessard, M. and Aitcin, P.C., "Ten-year Performance of a High Performance Concrete Used to Build Two Experimental Columns", *World-wide Advances in Structural Concrete and Masonry Structures Congress – Proceedings*, ASCE, New York, NY, USA, 1996, pp. 375-384.

Darter, M.I., Hoerner, T.E., Smith, K.D., Okamoto, P.A. and Kopac, P.A, "Development of Prototype Performance-related Specifications for Concrete Pavements", *Transportation Research Record 1544*, Transportation Research Board, Washington, DC, 1996.

[+] De Larrard, F. and Sedran, T., "Optimization of Ultra-high-performance Concrete by the Use of a Packing Model", *Cement & Concrete Research*, Vol.24, No.6, 1994, pp. 997-1009.

[+] De Larrard, F., Belloc, A., Renwez, S. and Boulay, C., "Is the Cube Test Suitable for High Performance Concrete?", *Materials & Structures*, Vol.27, No.174, Dec., 1994, pp. 580-583.

[+] De Larrard, F., Bosc, F., Catherine, C. and Deflorenne, F., "AFREM Method for the Mix-design of High Performance Concrete", *Materials & Structures,* Vol.30, No.201, Aug-Sep., 1997, pp. 439-446.

Dehuai, W., Zhaoyuan, C. and Weizu, Q, "Computerized Mix Proportioning for HPC", *Concrete International*. Vol.19, No.9, Sep., 1997, pp. 42-45.

[+] Detwiler, G., "High-performance Concrete Production Creates New Challenge", *Concrete Construction*, Vol.37, No.5, May 1992, pp. 359-362.

[+] Dilger, W.H., Rao, S. and Krishna, M., "High Performance Concrete Mixtures for Spun-cast c
Concrete Poles", PCI *Journal*, Vol.42, No.4, Jul-Aug., 1997, pp. 82-96.

[+] Do, M.T., Chaallal, O. and Aitcin, P.C., "Fatigue Behavior of High-performance Concrete", *Journal of Materials in Civil Engineering*, Vol.5, No.1, Feb., 1993, pp. 96-111.

[+] Domone, P. and His-wen, C., "Testing of Binders for High Performance Concrete", *Cement & Concrete Research*, Vol.27, No.8, Aug., 1997, pp. 1141-1147.

[+] Dunaszegi, L., "High-performance Concrete in the Confederation Bridge", *Concrete International*, Vol.20, No.4, Apr., 1998, pp. 66-68.

Elliot, R.P., "Quality Assurance: Top Management's Tool for Construction Quality*", Transportation Research Record 1310*, TRB, National Research council, National academy Press, 1991, pp. 17-19.

ElSakhawy, N.R., El-Dien, H.S., Ahmed, M.E., and Bendary K. A., " Influence of Curing on Durability Performance of Concrete", *Magazine of Concrete Research*, No. 5, 1999, pp. 309-318.

Elsen, J.L., Vyncke, N., Aarre, T.Q., Smolej, D., and Source, V., "Quality Assurance and Quality Control of Air Entrained Concrete", *Cement & Concrete Research*, Vol. 24, No. 7, 1994, pp. 1267-1276.

[+] El-dieb, A.S. and Hooton, R.D., "Water-permeability Measurement of High Performance Concrete Using a High-pressure Triaxial Cell", *Cement & Concrete Research*, Vol.25, No.6, Aug., 1995, pp. 1199-1208.

[+] El-dies, A.S. and Hooton, R.D., "High Pressure Triaxial Cell with Improved Measurement Sensitivity for Saturated Water Permeability of High-performance Concrete", *Cement & Concrete Research*, Vol.24, No.5, 1994, pp. 854-862.

[+] Eymael, M. and Cornelissen, H.A.W., "Processed Pulverized Fuel Ash for High-performance Concrete", *Waste Management*, Vol.16, No.1-3, 1996, pp. 237-242.

FEDERAL HIGHWAY ADMINISTRATION: Performance-related Specifications (PRS), A Cooperative Effort to Improve Pavement Quality, FHWA-SA-97-098, 1998.

[+] Ferraris, C.F. and Lobo, C.L., "Processing of HPC", *Concrete International*, Vol.20, No.4, Apr., 1998, pp. 61-64.

[+] Forster, S.W., "High-performance Concrete - Stretching the Paradigm", *Concrete International*, Vol.16, No.10, Oct., 1994, pp. 33-34.

Ford, S.J., Shane, J.D., and Mason, T.O., "Assignment of Features in Impedance Spectra of the Cement-Paste/Steel system", *Cement and Concrete Research*, Vol. 28, No.12, 1998, pp. 1737-1751.

French, C., Eppers, L., Le, Q., and Hajjar, J. F., "Transverse Cracking in Concrete Bridge Decks", *Transport Research Record*, Journal of the Transportation Research Board, No. 1688, pp. 21-29.

NCHRP Report 380, "Transverse Cracking in Newly Constructed Bridge Decks", *Transportation Research Board*, National Research Council, pp. 26-30.

[+] Gerwick, B.C. Jr., "High-performance Concrete", *Concrete Construction*, Vol.37, No.5, May 1992, pp. 355-357.

[+] Goodspeed, C.H., Vanikar. and Cook, R.A., "High-performance Concrete Defined for Highway Structures", *Concrete International*, Vol.18, No.2, Feb., 1996, pp. 62-67.

Gutierrez, P.A. and Canovas, M.F., "High-performance Concrete: Requirements for Constituent Materials and Mix Proportioning", *ACI Materials Journal*, Vol.93, No.3, May-June, 1996, pp. 233-241.

Gene, C.W., "Designing Corrosion Resistance into Reinforced Concrete", *Materials Performance*, Vol. 34, No. 9, Sept. 1995, pp. 54-58.

Harrison, T.A., "Performance Testing of Concrete for Durability", *Concrete*, November / December 1997, pp. 14-15.

HILSDORF, H.K., "Durability of Concrete – a Measurable Quantity?", *In proceedings of IABSE symposium*, Lisbon, Vol.1, 1989, pp. 111-123, 198.

[+] Hindy, E.E., Miao, B., Chaallal, O. and Aitcin, P.C., "Drying Shrinkage of Ready-mixed High-performance Concrete", *ACI Materials Journal*, Vol.91, No.3, May-Jun, 1994, pp. 300-305.

HO, D.W.S. AND LEWIS, R.K., "The Specification of Concrete for Reinforcement Protection - performance Criteria and Compliance by Strength", *Cement and Concrete Research*, Vol.18, 1988, pp. 584-594.

[+] Hu, C., De Larrard, F., "Rheology of Fresh High-performance Concrete", *Cement & Concrete Research*, Vol.26, No.2, Feb., 1996, pp. 283-294.

[+] Hwang, C.L. and Lee, L.-SH., "Future Research Trends in High-performance Concrete: Cost-effective Considerations", *Transportation Research Record*, No.1574, Nov., 1996, pp.49-55.

[+] Iravani, S., "Mechanical Properties of High-performance Concrete", *ACI Materials Journal,* Vol.93, No.5, Sep-Oct, 1996, pp. 416-426.

Jones, M.R., Dhir, R.K. and Magee, B.J., "Concrete Containing Ternary Binders: Resistance to Chloride Ingress and Carbonation", *Cement and Concrete Research*, Vol.27, No.6, 1997, pp. 825-831.

[+] Khatri, R P. Sirivivatnanon, V. and Gross, W., "Effect of Different Supplementary Cementitious Materials on Mechanical Properties of High Performance Concrete", *Cement & Concrete Research*, Vol.25, No.1, Jan., 1995, pp. 209-220.

[+] Kjellsen, K O., Wallevik, O H. and Fjallberg, L., "Microstructure and Microchemistry of the Paste-aggregate Interfacial Transition Zone of High-performance Concrete", *Advances in Cement Research*, Vol.10, No.1, Jan., 1998, pp. 33-40.

[+] Kjellsen, K.O., "Heat Curing and Post-heat Curing Regimes of High-performance Concrete: Influence on Microstructure and C-S-H Composition", *Cement & Concrete Research*, Vol. 26, No.2, Feb., 1996, pp. 295-307.

[+] Konin, A., Francois, R. and Arligue, G., "Analysis of Progressive Damage to Reinforced Ordinary and HPC in Relation to Loading", *Materials & Structures*, Vol.31, No.205, Jan-Feb., 1998, pp. 27-35.

[+] Kucharska, L. and Moczko, M., "Influence of Silica Fume on the Rheological Properties of the Matrices of High-Performance Concretes", *Advances in Cement Research*, Vol.6, No.24, Oct., 1994, pp. 139-145.

Khatri, R.P., Sirivivatnanon, V., and Gross, W., "Effect of Different Supplementary Cementitious Materials on Mechanical Properties of High Performance Concrete", *Cement & Concrete Research*, Vol.25, No.1, Jan. 1995, pp. 209-220.

Klieger, P., and Lamond, J.F., Significance of Tests and Properties of Concrete and Concrete-Making Materials, STP, 169C, 1994.

Lamond, J.F., "Designing for Durability", *Concrete International*, Vol. 19, No. 11, Nov. 1997, pp. 34-36.

+ Lachemi, M. and Aitcin, P.C., "Influence of Ambient and Fresh Concrete Temperatures on the Maximum Temperature and Thermal Gradient in a High-performance Concrete Structure", *ACI Materials Journal*, Vol.94, No.2, Mar-Apr, 1997, pp. 102-110.

+ Lafraugh, R.W., "High-performance Concrete Meets Stringent Requirements", *Concrete Construction*, Vol.37, No.5, May 1992, pp. 371-372.

+ Leshchinsky, A. and Pattison, J., "High-performance Concrete for Australian Freeways", *Concrete International*, October, 1994, pp.45-48.

+ Lessard, M., Dallaire, E., Blouin, D. and Aitcin, P.C., "High-performance Concrete. Construction Specifier", Vol.48, No.8, Aug., 1995, pp. 58-64.

+ Lewis, R., "Silica Fume for High-performance Concrete", *Concrete (London*), Vol.32, No.5, May, 1998, pp. 19-20, 22.

Maage, M., Helland, S., Poulsen, E., Vennesland, O. and Carlsen, J.E., "Service Life Prediction of Existing Concrete Structures Exposed to Marine Environment", *ACI Materials Journal*, Vol.93, No.6, Nov.-Dec., 1996, pp. 602-608.

Macgregor J., Reinforced Concrete, Third Edition, Prentice Hall Inc, 1997.

+ Macgregor, J.G., "Canadian Network of Centres of Excellence on High-performance Concrete", *Concrete International: Design & Construction*, Vol.15, No.2, Feb., 1993, pp. 60-61.

Mason, L.M., Gunst, R.F. and Hess, J.L., *Statistical Design and Analysis of Experiments: With Applications to Engineering and Science*. John Wiley & Sons, Inc., 1989.

Matthew, P., "Design & Maintenace for Serviceability and Durability", *Concrete (London)*, Vol.32, No. 4, Apr. 1998, pp. 12-13.

Matsushima M., Seki H., AND Matsui K., "Reliability Approach to Landing Pier Optimum Repair Level", *ACI Materials Journal*, Vol. 95, No. 3, 1998, pp. 218-225.

Manning, M., "A Rational Approach to Corrosion Protection of the Concrete Components of Highway Bridges", *ACI*, SP 100-77, 1987, pp. 1527-1547.

Mailvaganam, N.P., and Litvan, G.G., "Long Term Durability of Concrete Structures: Basic Issues", *Indian Concrete Journal*, Vol. 70, No. 9, Sep. 1996, pp. 471-475.

+ Mehta, K., "High-performance concrete durability affected by many factors", *Concrete Construction*, Vol.37, No.5, May, 1992, pp. 367-370.

Mehta P.K, and Aitcin, P.C., "Effect of Coarse Aggregates Characteristics on Mechanical Properties of High Strength Concrete", *ACI Materials Journal*, 1990, March, pp.103-107.

+ Mehta, P.K. and Aitcin, P.C., "Principles Underlying Production of High-performance Concrete", *Cement, Concrete & Aggregates*, Vol.12, No.2, 1990, pp. 70-78.

Mehta, P.K., "High Performance Concrete Durability by Many Factors", *Concrete Construction*, Vol. 37, n 5, May 1992, pp. 363-365.

Mehta, P.K., Aitcin, P.C., "Principles Underlying Production of High Performance Concrete," *Cement, Concrete and Aggregate*, Vol.16, No.2, Dec. 1994, pp. 115-124.

[+] Mor, A., "High-performance Concrete Becoming a Practical Option", *Concrete Construction*, Vol.37, No.5, May, 1992, pp. 351-353.

[+] Mor, A., "High-performance Concrete Quality Control Tests Challenge Labs", *Concrete Construction*, Vol.37, No.5, May, 1992, pp. 363-365.

[+] Moreno, J., "High-performance Concrete: Economic Considerations", *Concrete International*, Vol.20, No.3, Mar., 1998, pp. 68-70.

Mobasher, B., and Mitchell, T.M., "Laboratory Experience with the Rapid Chloride Permeability Test", *Permeability of Concrete*, SP-108, American Concrete Institute, Detroit, Michigan, 1988, pp. 117-144.

Naik, T.R.S., Shiw, S.H., and Mohammad, M., " Properties of High Performance Concrete Systems Incorporating Large Amounts of High lime Fly Ash", *Construction & Building Materials*, Vol. 9, No. 4, Aug. 1995, pp. 195-204.

[+] Nawy, E G. and CHEN, B., "Deformational Behaviour of High Performance Concrete Continuous Composite Beams Reinforced with Prestressed Prisms and Instrumented with Bragg Grating Fibber Optic Sensors", *ACI Structural Journal*, Vol.95, No.1, Jan-Feb, 1998, pp. 51-60.

Neter, J., Kutner, M.H., Nachtsheim, C.J., and Wasserman, W., "Applied Linear Statistical Models", 4th edition, ISBN 0-256-11736-5, 1996.

NEW CIVIL ENGINEER: Hong Kong Countdown. Published by Emap Construct Ltd., London, 9 Feb 1995.

Neville, A.M., Properties of Concrete, Fourth Edition, Published by Longman Group Limited, Essex, England, 1995.

NTBuild 443, Approved 1995-11. Concrete, hardened: Accelerated Chloride Penetration.

[+] Okamura, H.,"Self-compacting High-performance Concrete", *Concrete International*, Vol.19, No.7, July, 1997, pp. 50-54.

[+] Ozyildirim, C., "High-performance Concrete for Transportation Structures", *Concrete International: Design & Construction*, Vol.15, No.1, Jan., 1993, pp. 33-38.

Ozyildirim, C., "Permeability Specifications for High-performance Concrete Decks", *Transportation Research Record 1610*, Transportation Research Board, Washington, DC, 1998, pp. 1-5.

[+] Ozyildirim, C. and Gomez, J., "High-performance Concrete in Bridge Structures in Virginia", *Materials for the New Millennium Proceedings of the Materials Engineering Conference*, Vol.2, ASCE, New York, NY, USA, 1996, pp. 1357-1366.

[+] Ozyildirim, C., Gomez, J. and Elnahai, M., "High-performance Concrete Applications in Bridge Structures in Virginia", *World-wide Advances in Structural Concrete and Masonry Structures Congress - Proceedings*, ASCE, New York, NY, USA, 1996, pp. 153-163.

Parrott, L.J., "Simplified Methods of Predicting the Deformation of Structural Concrete", Development Report No.3, *Cement and Concrete Association*, Oct. 1979.

Paul, Z., and Hansen, M.R., "Durability of High Performance Concrete", *Publ. By ASCE*, New York, NY, USA, 1993, pp. 398-404.

Pauw, A., "Static Modulus of Concrete as Affected by Density", *ACI Journal*, Proceedings, Vol. 57, No. 6, Dec. 1960, pp. 679-688.

Priest, A., “Concrete Durability Design and Performance Testing”, *Concrete*, January / February, 1995, pp. 32-33.

+ Persson, B., “Hydration and Strength of High Performance Concrete”, *Advanced Cement Based Materials*. Vol.3, No.3-4, Apr-May., 1996, pp. 107-123.

+ Persson, B., “Quasi-instantaneous and Long-term Deformations of High Performance Concrete with Sealed Curing”, *Advanced Cement Based Materials*, Vol.8, No.1, Jul., 1998, pp. 1-16.

+ Phelan, W.S., “Admixtures and HPC: A Happy Marriage”, *Concrete International*, Vol.20, No.4, Apr., 1998, pp. 27-30.

+ Plean, R., Pigeon, M., Lamontagne, A. and Lessard, M., “Influence of Pumping on Characteristics of Air-void System of High-performance Concrete”, *Transportation Research Record*, No.1478, 1995, pp. 30-36.

PORTLAND CEMENT INSTITUTE: Fulton’s Concrete Technology, Seventh (revised) edition, *Portland cement institute*, Midrand, South Africa, 1994.

Ramirez, J.A., Frosch, J.F. and Olek, J., Performance-Related Specifications for Concrete Bridge Superstructures Interim Report (Literature Review and Future Directions) to Joint Transportation Research Program. Project No. SPR-2325, File No. 7-4-48, School of Civil Engineering, Purdue University, February 1999, 120p.

Ramirez, J.A., Frosch, J.F. and Olek, J. Research Project Proposal – Performance-Related Design Specifications for Concrete Bridge Superstructures. Joint Transportation Research Program, Project No. C-36-56WW, School of Civil Engineering, Purdue University, 1998.

Russel, H.G., “ACI Defines High Performance Concrete”, *Concrete International*, Feb. 1999.

+ Russell, H.G., “High-performance Concrete - From Buildings to Bridges”, *Concrete International*, Vol.19, No.8, Aug., 1997, pp. 62-63.

Russel, H.G., "ACI Defines High-Performance Concrete," *Concrete International*, Vol.21, No.2, Feb. 1999, pp. 56-57.

+ Ralls, M.L., “San Angelo High Performance Concrete Bridge in Texas”, *World-wide Advances in Structural Concrete and Masonry Structures Congress - Proceedings*, ASCE, New York, NY, USA, 1996, pp. 164-175.

+ Ralls, M.L., “Texas High-performance Concrete Bridges - How Much Do They Cost?”, *Concrete International*, Vol.20, No.3, Mar., 1998, pp. 71-74.

Rangaraju, P., “Mixture Proportioning and Microstructural Aspects of High-Performance Concrete”, Doctoral Thesis, Department of Civil Engineering, Purdue University, December, 1997, pp. 45-58.

+ Reddi, S.A., “Use of HSC/HPC for Road Bridges in India”, *Indian Concrete Journal*, Vol.70, No.12, Dec., 1996, pp. 661-673.

RILEM: Report 12 - Performance Criteria for Concrete Durability, (Edited by Kropp, J. and Hilsdorf, H.K.). Published by E & FN Spon, London, 1995.

+ Rivera-Villarreal, R., “Draft State-of-the-art Report on Admixtures in High-performance Concrete - Part 1”, *Materials & Structures*, Vol.30, Mar., 1997, pp. 47-53.

+ Rougeron, P. and Aitcin, P.-C., “Optimization of the Composition of a High-performance Concrete”, *Cement, Concrete & Aggregates*, Vol.16, No.2, Dec., 1994, pp. 115-124.

Roy, D.M., Silsbee, M.R., Sabol, S. and Scheetz, B.E., “Superior Microstructure of High-performance Concrete for Long-term Durability”, *Transportation Research Record 1478*, 1998, pp. 11-19.

Sarkar, S.L., Baalbaki, M., and Aitcin, P.C., "Microstructural Development in a High Strength Concrete Containing a Ternary Cementitous System," *ASTM Cement, Concrete, and Aggregate*, Vol. 13(2), Winter, 1991, pp. 81-87.

Shane, J.D., and Mason, T.O., " Fundamentals of Transport Properties and Impedance Spectroscopy in Cement-based Materials", *sixth international Purdue Conference on Concrete Pavement Design and Materials for High Performance*, Nov. 18-21, 1997, pp. 177-194.

Simon, M. J., Lagergren, E.S., and Wathne, L.G., "Optimizing High Performance Concrete Mixtures Using statistical Response Surface Methods", *5th International symposium on Utilization of High Strength/High Performance Concrete*, June, 1999, Sandefjord, Norway.

Simon, M.J., Lagergren, E.S., and Wathne, L.G., "Optimizing High-Performance Concrete Mixtures Using Statistical Response Surface Methods," *Proceedings of 5th International Symposium on Utilization of High Strength/High Performance Concrete*, I. Holand and E.J. Sellevold, ed., Sandefjord, Norway, 1999, pp. 1311-1321.

Simon,M.J., Lagergren, E.S., and Snyder, K.A., " Concrete Mixture Optimization Using Statistical Mixture Design Method", *Proceeding of the PCI/FHWA, International Symposium on High Performance Concrete*, New Orleans, Louisiana, Oct. 1997, pp. 230-244.

Sri Ravindrarajah, R., Mercer, C.M., and Toth, J., " Moisture Induced Volume Changes in High Strength Concrete", *Proceedings of ACI International Conference on High Performance Concrete*, SP-149, ACI, Farmington Hills, MI, 1994, pp. 475-490.

+ Streeter, D.A., "Developing High-performance Concrete Mix for New York State Bridge Decks", *Transportation Research Record*, No.1532, Sep., 1996, pp. 60-65.

Streicher, P.E., and Alexander, M.G., "A Chloride Conduction Test for Concrete", *Cement and Concrete Research*, Vol. 25, No.6, 1995, pp. 1284-1294.

Streeter, P.E. and ALEXANDER, M.G., "A Critical Evaluation of Chloride Diffusion Test Methods for Concrete", *Proceedings 3rd CANMET/ACI International Conference on Concrete Durability*, ACI, Detroit, 1994, pp. 517-530.

Shi, C., Stegemann, J.A. and Caldwell, R.J., "Effect of Supplementary Cementing Materials on the Specific Conductivity of Pore Solution and Its Implications on the Rapid Chloride Permeability Test (AASHTO T277 and ASTM C1202) results", *ACI Materials Journal*, Vol.95, No.4, July-August, 1998.

+ SHRP: High-performance concrete bridge showcase, March 25-27, 1996, Houston, Texas.

+ SHRP: High-performance concrete regional showcase, November 18-20, 1996, Omaha, Nebraska.

Schell, H.C., Berszakiewicz, B. and IP, A.K.C., "Developing High Performance Concrete Specifications for Highway Bridge Construction - Experience of the Ontario Ministry of Transportation", *Proceedings of the PCI/FHWA International Symposium on High Performance Concrete*, New Orleans, Louisiana, October 20-22, 1997, pp. 328-342.

SMITH, G.R., "Synthesis of Highway Practice 263, State DOT Management Techniques for Materials and Construction Acceptance", *National Cooperative Highway Research Program*. National Academy Press, Washington D.C, 1998.

+ Sprimkel, M.M. and Ozyildirim, C., "Shrinkage of High-performance Concrete Overlays on Route 60 in Virginia", *Transportation Research Record 1610*, Concrete in Construction, National Academy Press, Washington, D.C., 1988, pp. 15-19.

+ Strand, G.W. "High-performance Concrete in All-weather Deck Pours", *Cold Regions Engineering Sixth Int. Cold Reg. Eng*. Published by ASCE, New York, NY, USA, pp. 210-229.

Tang, L., and Nilsson, L., "Rapid Determination of the Chloride Diffusivity in Concrete by Applying an Electrical Field", *ACI Materials Journal*, Vol. 89, No. 1, Jan-Feb. 1992, pp. 49-53.

Tang. L., "Electrically Accelerated Methods for Determining Chloride Diffusivity in Concrete-Current Development", *Magazine of Concrete Research*, Vol.48, No.176, Sep. 1996, pp. 173-179.

[+] Tamimi, A K., "High-performance Concrete Mix for an Optimum Protection in Acidic Conditions", *Materials & Structures*, Vol.30, No.197, Apr., 1997, pp. 188-191.

[+] Tighiouart, B., Benmokrane, B. and Baalbaki, W., "Mechanical Characteristics and Modulus of Elasticity of High Performance Concretes Made with Various Types of Coarse Aggregate", *Materials & Structures*, Vol.27, No.168, May, 1994, pp. 211-221.

[+] Tumidajski, P.J. and Chan, G W., "Durability of high performance concrete in magnesium brine", *Cement & Concrete Research*, Vol.26, No.4, Apr.1996, pp. 557-565.

Vincensten, L.J. and Henrikson, K.R., "The Great Belt Link – Built to Last", *Concrete International*, Vol.14, No.25, 1992, pp. 30-33.

[+] Vivekandam, K. and Patnaikuni, I., "Transition Zone in High Performance Concrete During Hydration", *Cement & Concrete Research*, Vol.27, No.6, Jun., 1997, pp. 817-823.

Weiss, W. J, Yang, W., and Shah, S. P., (2000). "Influence of Specimen Size and Geometry on Shrinkage Cracking." J. of Engrg. Mechanics Div., ASCE, 126(1), 93-101

Weiss, W. J., and Furgeson, S., "Restrained Shrinkage Testing: The Impact of Specimen Geometry on Quality Control Testing for Material Performance Assessment," To be presented at Concreep-6 August 200

Whiting, D., "Permeability of Selected Concretes", *Permeability of Concrete*, SP-108, American Concrete Institute, Detroit, Michigan, 1988, pp. 195-222.

Whiting, D., "Rapid Determination of the Chloride Permeability of Concrete", Final Report No.: FHWA/RD-81/119, Federal Highway Administration, Aug. 1981, NTIS No.: PB 82140724.

Wilson, M.A., Carter, M.A., and Hoff, W.D., "British Standard and RILEM Water Absorption Tests: A Critical Evaluation", *Materials and Structures*, vol. 32, No. 222, Oct. 1999, pp. 571-578.

[+] Weber, S. and Reinhardt, H.W., "New Generation of High Performance Concrete: Concrete with Autogeneous Curing", *Advanced Cement Based Materials*, Vol.6, No.2, Aug., 1997, pp. 59-68.

Zhang, T., and Gjorv, O.E., "Electrochemical Method for Accelerated Testing of Chloride Diffusivity in Concrete", *Cement and Concrete Research*, Vol. 24, No. 8, 1994, pp. 1534-1548.

Zia, P., and Hansen, M.R., "Durability of High Performance Concrete," *Proceedings of the ASCE 3rd International Conference on Applications of Advanced Technologies in Transportation Engineering,* Pacific Rim Trans Tech Conference, Seattle, WA, USA., Publ. by ASCE, New York, NY, USA. 1993. pp. 398-404.

[+] Zhou, F.P., Lydon, F.D. and Barr, B., "Effect of Coarse Aggregate on Elastic Modulus and Compressive Strength of High Performance Concrete", *Cement & Concrete Research*, Vol.25, No.1, Jan., 1995, pp. 177-186.